

Implications of nanoparticles in the aquatic environment

Ilona Velzeboer

Thesis committee

Promotor

Prof. Dr A.A. Koelmans
Personal chair at Aquatic Ecology and Water Quality Management
Wageningen University

Other members

Prof. Dr A.J. Murk, Wageningen University
Prof. Dr A.P. van Wezel, Utrecht University
Prof. Dr W.J.G.M. Peijnenburg, RIVM, Bilthoven / Leiden University
Prof. Dr R.N.J. Comans, Wageningen University

This research was conducted under the auspices of the Graduate School for Socio-Economic and Natural Sciences of the Environment (SENSE)

Implications of nanoparticles in the aquatic environment

Ilona Velzeboer

Thesis

submitted in fulfilment of the requirements for the degree of doctor
at Wageningen University
by the authority of the Rector Magnificus
Prof. Dr M.J. Kropff,
in the presence of the
Thesis Committee appointed by the Academic Board
to be defended in public
on Wednesday 18 June 2014
at 1.30 p.m. in the Aula.

Ilona Velzeboer
Implications of nanoparticles in the aquatic environment,
254 pages.

PhD thesis, Wageningen University, Wageningen, NL (2014)
With references, with summaries in Dutch and English

ISBN 978-94-6173-950-6

Contents

Chapter 1

General introduction 7

Chapter 2

Heteroaggregation and sedimentation rates for nanomaterials in natural waters ... 19

Chapter 3

Rapid settling of nanoparticles due to heteroaggregation with suspended sediment 57

Chapter 4

Sorption of perfluorooctane sulfonate to carbon nanotubes in aquatic sediments .. 93

Chapter 5

Strong sorption of PCBs to nanoplastics, microplastics, carbon nanotubes and fullerenes 109

Chapter 6

Aquatic ecotoxicity tests of some nanomaterials 155

Chapter 7

Community effects of carbon nanotubes in aquatic environments 171

Chapter 8

Multiwalled carbon nanotubes at environmentally relevant concentrations affect the composition of benthic communities 187

Chapter 9

Implications of nanoparticles for the aquatic environment – general discussion .. 217

Addendum

Summary 240

Samenvatting 243

Dankwoord 246

Curriculum vitae 249

List of publications 250

SENSE certificate 252

Chapter 1



TiO₂ C₆₀ ZrO₂ CeO₂ SWCNTs C₆₀ Al₂O₃
CNTs PMMA Al₂O₃ PFOS PVP-Ag MWCNTs PVP-Ag SWCNTs
nano-PS C₆₀ micro-PE PVP-Ag CeO₂ MWCNTs SiO₂-Ag TiO₂ SiO₂-Ag
ZrO₂ SiO₂-Ag MWCNTs PVP-Ag C₆₀ CeO₂ PVP-Ag C₆₀
SWCNTs PMMA PVP-Ag nano-PS C₆₀ MWCNTs PFOS micro-PE
SiO₂-Ag micro-PE PMMA MWCNTs CeO₂ micro-PE CeO₂ Al₂O₃
SiO₂-Ag PVP-Ag C₆₀ PVP-Ag nano-PS Al₂O₃ MWCNTs TiO₂
CNTs C₆₀ nano-PS MWCNTs PVP-Ag TiO₂ PFOS
micro-PE PCBs MWCNTs CeO₂ CeO₂ ZrO₂ PVP-Ag TiO₂
nano-PS Al₂O₃ CeO₂ PCBs CeO₂ SWCNTs C₆₀ PMMA MWCNTs
SWCNTs PCBs PFOS MWCNTs nano-PS ZrO₂ MWCNTs SiO₂-Ag PMMA
ZrO₂ Ag SiO₂-Ag PFOS SiO₂-Ag nano-PS PMMA Al₂O₃ MWCNTs ZrO₂
PCBs SiO₂-Ag PVP-Ag PMMA PVP-Ag PCBs TiO₂
TiO₂ PCBs SiO₂-Ag MWCNTs TiO₂ PVP-Ag ZrO₂ C₆₀
ZrO₂ micro-PE CeO₂ PFOS MWCNTs MWCNTs ZrO₂ C₆₀
MWCNTs PCBs SWCNTs micro-PE SiO₂-Ag PMMA
SiO₂-Ag SWCNTs PFOS ZrO₂ CeO₂ MWCNTs
micro-PE nano-PS PMMA C₆₀ C₆₀ PFOS PVP-Ag
MWCNTs Al₂O₃ PFOS PVP-Ag C₆₀ TiO₂ CeO₂
PCBs micro-PE ZrO₂ C₆₀ SWCNTs PMMA nano-PS

General introduction



TiO₂ MWCNTs ZrO₂ TiO₂ CeO₂ MWCNTs CeO₂ SWCNTs SiO₂-Ag
SWCNTs PMMA Al₂O₃ PFOS PVP-Ag CeO₂ MWCNTs PVP-Ag SWCNTs
nano-PS C₆₀ micro-PE C₆₀ SiO₂-Ag TiO₂ C₆₀
Al₂O₃ SiO₂-Ag MWCNTs PVP-Ag CeO₂ PVP-Ag C₆₀ MWCNTs PFOS micro-PE
SiO₂-Ag PMMA PVP-Ag nano-PS C₆₀ MWCNTs PFOS micro-PE
PVP-Ag C₆₀ PMMA MWCNTs CeO₂ micro-PE CeO₂ Al₂O₃
PCBs SiO₂-Ag CeO₂ Al₂O₃ PVP-Ag nano-PS Al₂O₃ MWCNTs MWCNTs
MWCNTs C₆₀ nano-PS PVP-Ag nano-PS Al₂O₃ MWCNTs TiO₂ PFOS
micro-PE PCBs MWCNTs CeO₂ CeO₂ ZrO₂ PVP-Ag C₆₀ PMMA MWCNTs
nano-PS Al₂O₃ CeO₂ PCBs CeO₂ SWCNTs nano-PS MWCNTs
SiO₂-Ag ZrO₂ C₆₀ MWCNTs ZrO₂ micro-PE SiO₂-Ag PMMA
C₆₀ PCBs SiO₂-Ag PFOS SiO₂-Ag PMMA Al₂O₃ MWCNTs ZrO₂
ZrO₂ TiO₂ PCBs SiO₂-Ag PVP-Ag PMMA Al₂O₃ MWCNTs TiO₂
ZrO₂ C₆₀ MWCNTs TiO₂ PVP-Ag PCBs TiO₂ C₆₀
CeO₂ MWCNTs PCBs SWCNTs ZrO₂ PFOS MWCNTs ZrO₂ C₆₀
micro-PE SiO₂-Ag nano-PS PFOS SiO₂-Ag MWCNTs
SiO₂-Ag SWCNTs PFOS ZrO₂ CeO₂ C₆₀ PFOS PMMA PVP-Ag
MWCNTs PCBs nano-PS Al₂O₃ PFOS PMMA PVP-Ag TiO₂ CeO₂
TiO₂ MWCNTs micro-PE Al₂O₃ PFOS PVP-Ag SWCNTs PMMA nano-PS
PCBs micro-PE Al₂O₃ PFOS ZrO₂ C₆₀ SWCNTs PMMA nano-PS

General introduction

Nanoparticles

The concept of nanotechnology was first introduced in 1959 by Richard Feynman in his presentation “There’s plenty of room at the bottom” [1]. In 1986 Eric K. Drexler introduced in his book “The Engines of Creation: The Coming Era of Nanotechnology” nanotechnology as a new paradigm for manipulating atoms and molecules in the atomic level to produce desirable substances or molecular-sized machines (nanomachines) [2]. With nanotechnology, nanoparticles are involved. Following the latest Recommendation on the definition of a nanomaterial of the European Commission [3], nanomaterials are defined as:

“A natural, incidental or manufactured material containing particles, in an unbound state or as an aggregate or as an agglomerate and where, for 50% or more of the particles in the number size distribution, one or more external dimensions is in the size range of 1 - 100 nm.”

Nanoparticles can be divided in two groups [4]. *Unintentionally* or incidentally produced nanoparticles like atmospheric ultrafine dust (PM_{0.1} i.e. soot, black carbon; BC) originate from incomplete combustion of biomass and fossil fuels [5]. *Intentionally* produced, engineered or manufactured nanoparticles originate from industrial activities (e.g. production of resins, pigments and cosmetics) [6]. The engineered nanoparticles (ENPs) include carbon-based ENPs, such as fullerenes, single- and multiwalled carbon nanotubes, nano-polystyrene and polymethylmethacrylate, and inorganic ENPs like cerium oxides, silver, titanium dioxide, zirconium oxide and aluminium oxide [7] (Table 1.1).

ENPs are being used in a broad range of products such as in cosmetics (i.e. sunscreens), electronics, pharmaceuticals, textiles (i.e. socks), food (i.e. coffee creamer), in sports materials (i.e. rackets) or tyres to increase material strength, in coating (i.e. paints) and in energy (i.e. solar cells), catalytic, environmental (i.e. remediation) and sustainability applications [8]. The number of products containing ENPs is still increasing and is expected to keep growing in the next decades [9].

With the increasing production and use of ENPs, emissions to the environment are expected [7, 10]. ENPs are transported to receiving waters through atmospheric deposition, surface run-off, wastewater treatments plants and direct input. Eventually, aquatic systems and especially the sediments will form the most important sink for ENPs [4, 6, 7]. Studies measuring environmental concentrations are still scarce because it is difficult to determine the low levels of ENPs in environmental matrices. Gottschalk et al. [11] reviewed a handful of measured environmental concentrations, such as 1 to 10 µg L⁻¹ for nano-TiO₂ in surface waters and 1 to 6 µg g⁻¹ Ti in sediment. Because of the analytical difficulties, many studies provide model predicted concentrations of ENPs in the environment [4, 6, 7, 11]. Concentrations of 10⁻⁵ to 10¹ µg L⁻¹ ENPs were

estimated for surface waters and concentrations of 10^{-2} to 10^4 $\mu\text{g kg}^{-1}$ were estimated for aquatic sediments, but given predicted future emissions, these concentrations are expected to increase [4, 11-13].

ENP properties may deviate from their bulk material as the surface area per unit mass of ENPs is relatively large compared to the bulk material. This implies that surface reactions are much more important for ENPs than for the bulk material. At the lower nanometer scale *quantum effects* can affect the electrical, magnetic and optical behaviour and dominate the characteristics of the ENPs [14, 15]. When materials are build up by grains, the interface area within the material will increase with reducing the grain size to the nanoscale, resulting in an enhancement of the strength of the material [15]. The specific physico-chemical properties related to their increased surface area to volume ratio contributed to the increasing interest for ENPs. As an intermediate state they constitute a bridge between bulk material and atomic or molecular material [16]. Because of these unique physico-chemical properties, a good understanding of the fate, bioavailability and toxicity is essential for a suitable risk assessment of ENPs.

Table 1.1 ENPs used for experiments in this thesis

Name	Abbreviation	Type of particles
Fullerenes	C ₆₀	Carbon
Singlewalled carbon nanotubes	SWCNTs	Carbon
Multiwalled carbon nanotubes	MWCNTs	Carbon
Ceriumdioxide	CeO ₂	Metal
Silica coated silver	SiO ₂ -Ag	Metal
Polyvinylpyrrolidone coated silver	PVP-Ag	Metal
Titaniumdioxide	TiO ₂	Metal
Zirconiumdioxide	ZrO ₂	Metal
Aluminiumoxide	Al ₂ O ₃	Metal
Polymethylmethacrylate	PMMA	Plastic
Micro-polyethylene	PE	Plastic
Nano-polystyrene	PS	Plastic

Fate of ENPs in the aquatic environment

Given the increasing levels of ENPs in the environment, a thorough understanding of the behaviour of ENPs in the aquatic environment is essential. The aquatic fate of ENPs governs the potential transport and subsequent ecotoxicity in the aquatic environment. Whereas the distribution of conventional hydrophobic organic contaminants is mainly based on equilibrium partitioning phenomena, other approaches may be needed for ENPs [17]. Understanding the fate of ENPs requires the concepts of colloid chemistry, as ENPs are comparable to colloidal systems. By definition, ENPs fit within the range of colloids, which are defined as particles with a diameter between 1 and 1000 nm [6, 14, 18]. Aggregation and sedimentation are two important colloid chemical

processes driving the behaviour and transport of ENPs. The formation of aggregates is dependent on the attachment efficiency and the collision frequency. The attachment efficiency describes the chance that particles will attach and form an aggregate when they collide, and is related to several factors, such as electrostatic and Van der Waals forces, steric hindrance, magnetic and hydration forces [19]. The collision frequency between particles is dependent on Brownian motion, fluid motion and differential settling [14]. ENPs may aggregate with other ENPs (homoaggregation), but may also associate or aggregate with organic matter or other particles present in the water, like natural colloids (NC), suspended solids and dissolved compounds (heteroaggregation) [14]. Depending on the attachment efficiency and collision frequency, larger aggregates can be formed, which can lead to sedimentation. Furthermore, chemical transformations of ENPs are possible, including oxidation/reduction, dissolution, hydrolysis and biological degradation [6]. These transformations are highly dependent on the composition of the ENP. Furthermore, the type of the receiving water body will influence the fate of ENPs, because of the differences in the composition of substances in water (e.g. natural organic matter (NOM), NC, dissolved molecules, pollutants), pH, turbulence (e.g. deep or shallow lake or river) and salinity (fresh vs. marine water).

Fate models for ENPs are important within the framework of prognostic risk assessment but also because of the limited empirical data available and because of the present challenges in analysing ENPs in complex systems. In order to predict ENP behaviour it is important to account for several ENP specific processes, like sedimentation and dissolution. Quantification of these processes differs from that for more conventional pollutant categories like heavy metals or organic micropollutants [20-22]. To improve input parameters for ENP fate models, experimental data for aggregation and sedimentation of ENPs are urgently needed [22, 23]. More specifically, there is a great lack of sedimentation and heteroaggregation rate data of ENPs for natural waters over a range of geochemical conditions.

Because the available analytical methods usually cannot make a distinction between pristine ENPs, natural nanoparticles or bulk or combustion generated nanoparticles, measured concentrations are expected to be higher than the predicted concentrations, because most fate model predictions are based on the engineered part of the total nano-sized fraction [11]. Therefore, improvements of analytical methods for complex environmental matrices will contribute to a better understanding of the fate and transport of ENPs and will improve the quantification of exposure concentrations [24].

In aquatic systems, ENPs are likely to interact with natural colloids, suspended solids and other contaminants including other ENPs. Therefore, it is important to study not only the ENPs in their pure form, but also to study their fate and toxicity in the receiving environment where background chemicals may adsorb to the ENPs [25, 26]. Depending on the mechanisms of the interactions with other contaminants, especially carbon-based ENPs may reduce the freely dissolved concentration or bioavailability

of conventional organic toxicants and consequently affect their exposure and effects to biota. However, risks of ENPs may also relate to that of the associated toxicant, a phenomenon referred to as the ‘Trojan horse’ effect. ENPs may release associated toxicants when ingested by organisms, an exposure pathway which is shared with that in drug delivery applications [27]. Furthermore, inorganic ENPs may release ions, but also other chemical or biological transformations are possible that may influence exposure and toxicity [26, 27]. Although some studies on the binding of PAH to fullerenes and CNTs are available (e.g. [28, 29]), data for association of persistent organic pollutants (POPs) with ENPs and comparative data for different types of carbon-based ENPs including micro- and nanoplastics and the effects of sediment organic matter and salinity on the association are not yet available.

As outlined above, the transport process parameters governing aggregation, sedimentation and dissolution gained from experimental studies and model predictions could be used to determine the transport and retention of ENPs in aquatic systems. Furthermore, once the association with other contaminants is known, the contribution of ENPs in the retention of these traditional contaminants like for instance POPs can be assessed too. To date however, such an assessment of retention of ENPs in lakes and the implications of ENP retention on the retention of conventional pollutant categories like POPs has not been made.

Effects of ENPs in the aquatic environment

For conventional toxicants, effect assessment has evolved from laboratory scale single species standard toxicity tests to chronic and *in situ* effect studies with endpoints on the level of populations and communities [30]. For ENPs however, the standard toxicity tests used for traditional organic contaminants are not always suitable and the development of more appropriate tests for single species is still ongoing. Single species ecotoxicity tests may use different dose-response metrics, for example the median effect or median lethal concentration (EC_{50} , LC_{50}), or the no or lowest observed effect concentration (NOEC, LOEC), and may use different exposure times in order to distinguish between acute and chronic toxicity [31, 32]. In practice however, most ENP toxicity studies used 48, 72 or 96 hours of exposure, which all can be considered as short term tests. Furthermore, there is a wide variety of species used in ENP aquatic ecotoxicity tests, ranging from bacteria (e.g. *Fibrio fischeri*, *Escherchia coli*), to algae (e.g. *Pseudokirchneriella subcapitata*), to invertebrates (e.g. *Daphnia magna*) and vertebrates (e.g. *Pimephales promelas*, *Danio rerio*) [6, 30]. When the exposure pathways are known, it can be specified which organisms may potentially be at risk [6]. However, the exposure concentration in standard toxicity tests is hard to define because ENPs are in general insoluble and tend to aggregate and settle in a relatively short time [6, 33]. In this respect the question whether observed effects relate to the nano-scale, relate to ENP toxicity and/or partly relate to ions released from the particles also is very important [6, 17, 24, 26]. Most ENP single species laboratory tests include

high, environmentally unrealistic doses [6, 7, 14, 27, 33, 34]. Such tests however still are essential to assess the hazards of ENPs, the dose-response relationships required for risk assessment and to identify toxicity mechanisms on the species level [33].

Whereas single species toxicity tests will remain important for screening level or lower tier effect assessments, more ecological realism and relevance is required to assess the actual effects that may occur in the longer term or in the field. For conventional chemicals, long term community or model ecosystem (mesocosm) test protocols have been developed which are routinely used in the higher tiers of the effect assessment (e.g. [30]). For ENPs however, chronic effect studies, community studies, model ecosystem studies or field studies are hardly available. In the field, many natural processes occur that may influence the effect of ENPs on biota and that are not or less well accounted for in shorter term single species laboratory tests. It is important to know the effects of ENPs entering turbulent waters with natural organic matter, in the presence of other contaminants over longer periods, while accounting for community and food web interactions. Depending on the receiving environmental compartment and its physico-chemical characteristics, the bioavailability and toxicity of the aged, aggregated, biologically or chemically transformed ENPs can be very different from that of the original pristine ENPs [6].

In summary, there is an urgent need for the further development of standardized ecotoxicity test protocols for ENPs in order to quantify effect threshold concentrations to be used in risk assessments, which ideally cover all different levels of biological organisation.

Risks of ENPs in the aquatic environment

Risk assessment is a process of examining scenarios to evaluate the likelihood that an adverse event occurs. This is performed by estimation of the magnitude of exposure and relating effects that occur from such exposures to one or more hazards [35]. Hazards are the inherent properties of a biological, chemical or physical stressor that can have an adverse effect on a receptor [35]. When a hazard is identified, the exposure, which is the magnitude of contact that a receptor has with a hazard [35], needs to be determined. Especially for new chemicals like ENPs, this concentration, the predicted environmental concentration (PEC), is based on best educated predictions. Besides the exposure, also the effect, which is the biological response of an organism, population, or ecological system to a stressor, needs to be determined [35]. This relation between the dose of exposure and the occurrence and degree of the effect is based on ecotoxicity tests and provides predicted no effect concentrations (PNEC). Subsequently, the environmental risk, can be expressed as PEC/PNEC ratios [32]. This general paradigm of risk assessment has been identified as equally applicable to ENPs as to conventional categories of environmental contaminants [24].

To assess whether there is a risk of ENPs, their mobility, bioavailability and impact on aquatic and benthic communities needs to be understood in order to identify if there is a potential for exposure *and* a hazard. Risk assessment for ENPs

includes much higher uncertainty levels compared to traditional chemicals, because of the limited data available on exposure and effect assessment [24]. For conventional contaminants it has been assumed that the exposure concentration is dependent on the bioavailable part, the fraction that is available for uptake through the aqueous phase or by food ingestion. For ENPs however, the differences in speciation between dissolved, colloidal and particulate phases due to aggregation and dissolution can influence the bioavailable concentration and need to be included in the exposure assessment. Therefore, not only the pristine ENPs, but also the products in which ENPs are used and also the aged ENPs and their interaction with other toxicants need to be examined [24]. For traditional contaminants, environmental concentrations are mass based, but for ENPs it has been suggested to use particle number based concentrations because of the high surface area to volume ratios [14, 21].

Aim and outline of the thesis

With the increasing production and use of ENPs and the extended emissions to environmental bodies, a better understanding of their impact on the receiving environment is required. Aim of this thesis is to define the implications of ENPs in the aquatic environment, including the sediment, as it is expected that ENPs mainly will end up in aquatic sediments [4, 6, 7]. This includes filling some knowledge gaps with respect to ENP aggregation and sedimentation behaviour in natural waters, addressing the interaction between ENPs and conventional toxicants, evaluating standard toxicity test setups for use with ENPs, evaluating a new community approach in ENP effect assessment and integrating all these aspects using lake retention and ENP risks as measures of impact.

A broad range of ENP types is used in the experiments performed for this thesis (Table 1.1). In order to obtain sedimentation rates and heteroaggregation rates, ENP fate processes were studied by quantification of the ENP interactions with NC in different natural water types under quiescent settling conditions by measuring removal from the water phase (**Chapter 2**). Besides interactions with NC, also interactions with SS in more turbulent mixing conditions were studied by measurement of the removal of ENPs from the water phase in presence of NC and SS, leading to the quantification of sedimentation and heteroaggregation rates under turbulent conditions (**Chapter 3**). For some important classes of conventional and emerging chemicals, the association with carbon based ENPs was characterised. Interactions of ENPs to perfluorooctane sulfonate (PFOS) and 17 polychlorinated biphenyls (PCBs) were quantified by measuring the sorption behaviour of these compounds (**Chapter 4 and 5**). For the interaction studies with NC, SS and PCBs, also the influence of salinity was determined by performing the experiments in fresh and marine waters. The sorption of PCBs to two types of carbon ENPs: multiwalled carbon nanotubes (MWCNTs) and fullerene (C_{60}) was also compared to two types of plastic: nano-polystyrene (PS) and micro-polyethylene (PE) (**Chapter 5**). The latter plastic particles receive a lot of interest because of their possible role as vectors of plastic associated

chemicals to marine organisms. For a series of ENP types, several short term standard single species aquatic toxicity tests were evaluated for their suitability in the effect assessment of ENPs. This included extensive characterisation of the ENPs to be able to interpret the observed effects in terms of ENP behaviour, exposure and bioavailability in the tests (**Chapter 6**). In order to explore the potential of more ecologically realistic community effect assessments, long term (3 and 15 months) studies on the effects of MWCNTs on a benthic community were performed (**Chapter 7 and 8**). This study also interpreted community effects of a similar simultaneous experiment performed with a non-nanosized carbon material, activated carbon (**Chapter 8**). The new data obtained from the fate studies (**Chapters 2 and 3**), the sorption studies (**Chapters 4 and 5**) and the effect studies (**Chapters 6, 7, 8**) were integrated with recent literature data in a final synthesis (**Chapter 9**). In this integrating discussion chapter, the new sedimentation data were used to roughly estimate the retention of ENPs in lakes. In combination with the new data for sorption of POPs to ENPs, the relevance of ENP retention on the retention of POPs in lakes was estimated. An overview of effect thresholds from short term single species tests for the aquatic environment is provided that includes the new single species test results. These effect thresholds as well as the effect thresholds observed in the long term community tests are discussed in relation to model-based PEC values for present time and for the next century. Finally, this last chapter summarizes how the new information from the fate and effect experiments may lead to a better understanding of the risks of ENPs.

References

- [1] Feynman R. 1960. There's plenty of room at the bottom. *Engineering and Science magazine* 23:22-36.
- [2] Dexter EK. 1986. *Engines of Creation. The Coming Era of Nanotechnology*. Anchor Books, New York
- [3] European Commission. 2011. Commission recommendation of 18 October 2011 on the definition of nanomaterials (2011/696/EU). *Official Journal of the European Union* 54:38-40.
- [4] Koelmans AA, Nowack B, Wiesner MR. 2009. Comparison of manufactured and black carbon nanoparticle concentrations in aquatic sediments. *Environmental Pollution* 157:1110-1116.
- [5] Koelmans AA, Jonker MTO, Cornelissen G, Bucheli TD, Van Noort PCM, Gustafsson O. 2006. Black carbon: The reverse of its dark side. *Chemosphere* 63:365-377.
- [6] Klaine SJ, Alvarez PJJ, Batley GE, Fernandes TF, Handy RD, Lyon DY, Mahendra S, McLaughlin MJ, Lead JR. 2008. Nanomaterials in the environment: Behavior, fate, bioavailability, and effects. *Environmental Toxicology and Chemistry* 27:1825-1851.
- [7] Nowack B, Bucheli TD. 2007. Occurrence, behavior and effects of nanoparticles in the environment. *Environmental Pollution* 150:5-22.
- [8] Science Policy Council. 2007. U.S. Environmental Protection Agency Nanotechnology White Paper. EPA 100/B-07/001. U.S. Environmental Protection Agency, Washington, DC.
- [9] Gottschalk F, Nowack B. 2011. The release of engineered nanomaterials to the environment. *Journal of Environmental Monitoring* 13:1145-1155.
- [10] Wiesner MR, Lowry GV, Alvarez P, Dionysiou D, Biswas P. 2006. Assessing the risks of manufactured nanomaterials. *Environmental Science & Technology* 40:4336-4345.
- [11] Gottschalk F, Sun T, Nowack B. 2013. Environmental concentrations of engineered nanomaterials: Review of modeling and analytical studies. *Environmental Pollution* 181:287-300.
- [12] Gottschalk F, Sonderer T, Scholz RW, Nowack B. 2009. Modeled Environmental Concentrations of Engineered Nanomaterials (TiO₂, ZnO, Ag, CNT, Fullerenes) for Different Regions. *Environmental Science & Technology* 43:9216-9222.
- [13] Mueller NC, Nowack B. 2008. Exposure modeling of engineered nanoparticles in the environment. *Environmental Science & Technology* 42:4447-4453.
- [14] Handy RD, von der Kammer F, Lead JR, Hasselov M, Owen R, Crane M. 2008. The ecotoxicology and chemistry of manufactured nanoparticles. *Ecotoxicology* 17:287-314.
- [15] The Royal Society & The Royal Academy of Engineering. 2004. Nanoscience and nanotechnologies: opportunities and uncertainties. The Royal Society & The Royal Academy of Engineering, London.
- [16] Hoet P, Bruske-Hohlfeld I, Salata O. 2004. Nanoparticles - known and unknown health risks. *Journal of Nanobiotechnology* 2:12.

- [17] Westerhoff P, Nowack B. 2013. Searching for Global Descriptors of Engineered Nanomaterial Fate and Transport in the Environment. *Accounts of Chemical Research* 46:844-853.
- [18] Christian P, Von der Kammer F, Baalousha M, Hofmann T. 2008. Nanoparticles: structure, properties, preparation and behaviour in environmental media. *Ecotoxicology* 17:326-343.
- [19] Petosa AR, Jaisi DP, Quevedo IR, Elimelech M, Tufenkji N. 2010. Aggregation and Deposition of Engineered Nanomaterials in Aquatic Environments: Role of Physicochemical Interactions. *Environmental Science & Technology* 44:6532-6549.
- [20] Praetorius A, Scheringer M, Hungerbuhler K. 2012. Development of Environmental Fate Models for Engineered Nanoparticles-A Case Study of TiO₂ Nanoparticles in the Rhine River. *Environmental Science & Technology* 46:6705-6713.
- [21] Arvidsson R, Molander S, Sanden BA, Hasselov M. 2011. Challenges in Exposure Modeling of Nanoparticles in Aquatic Environments. *Human and Ecological Risk Assessment* 17:245-262.
- [22] Quik JTK, Vonk JA, Hansen SF, Baun A, Van De Meent D. 2011. How to assess exposure of aquatic organisms to manufactured nanoparticles? *Environment International* 37:1068-1077.
- [23] Quik JTK, Stuart MC, Wouterse M, Peijnenburg W, Hendriks AJ, van de Meent D. 2012. Natural colloids are the dominant factor in the sedimentation of nanoparticles. *Environmental Toxicology and Chemistry* 31:1019-1022.
- [24] Klaine SJ, Koelmans AA, Horne N, Carley S, Handy RD, Kapustka L, Nowack B, von der Kammer F. 2012. Paradigms to assess the environmental impact of manufactured nanomaterials. *Environmental Toxicology and Chemistry* 31:3-14.
- [25] Nowack B, Ranville JF, Diamond S, Gallego-Urrea JA, Metcalfe C, Rose J, Horne N, Koelmans AA, Klaine SJ. 2012. Potential scenarios for nanomaterial release and subsequent alteration in the environment. *Environmental Toxicology and Chemistry* 31:50-59.
- [26] Wiesner MR, Lowry GV, Jones KL, Hochella MF, Di Giulio RT, Casman E, Bernhardt ES. 2009. Decreasing Uncertainties in Assessing Environmental Exposure, Risk, and Ecological Implications of Nanomaterials. *Environmental Science & Technology* 43:6458-6462.
- [27] Farre M, Gajda-Schrantz K, Kantiani L, Barcelo D. 2009. Ecotoxicity and analysis of nanomaterials in the aquatic environment. *Analytical and Bioanalytical Chemistry* 393:81-95.
- [28] Kah M, Zhang X, Jonker MTO, Hofmann T. 2011. Measuring and Modeling Adsorption of PAHs to Carbon Nanotubes Over a Six Order of Magnitude Wide Concentration Range. *Environmental Science & Technology* 45:6011-6017.
- [29] Zhang X, Kah M, Jonker MTO, Hofmann T. 2012. Dispersion State and Humic Acids Concentration-Dependent Sorption of Pyrene to Carbon Nanotubes. *Environmental Science & Technology* 46:7166-7173.
- [30] Diepens NJ, Arts GHP, Brock TCM, Smidt H, Van Den Brink PJ, Van Den Heuvel-Greve MJ, Koelmans AA. 2013. Sediment Toxicity Testing of Organic Chemicals in the Context of Prospective Risk Assessment: A Review. *Critical Reviews in Environmental Science and Technology* 44:255-302.

- [31] Boersema J.J. CP, J.W., de Groot W.T. (ed). 1994. *Basisboek milieukunde*, 5th ed. Uitgeverij Boom, Den Haag, The Netherlands.
- [32] van Leeuwen CJ, Vermeire, T.G. (ed). 2007. *Risk assessment of chemicals*, 2nd ed. Springer, Dordrecht, The Netherlands.
- [33] Handy RD, Cornelis G, Fernandes T, Tsyusko O, Decho A, Sabo-Attwood T, Metcalfe C, Steevens JA, Klaine SJ, Koelmans AA, Horne N. 2012. Ecotoxicity test methods for engineered nanomaterials: Practical experiences and recommendations from the bench. *Environmental Toxicology and Chemistry* 31:15-31.
- [34] Velzeboer I, Hendriks AJ, Ragas AMJ, Van de Meent D. 2008. Aquatic ecotoxicity tests of some nanomaterials. *Environmental Toxicology and Chemistry* 27:1942-1947.
- [35] Kapustka L, Chan-Remillard, S., Goudey, S. 2009. *Developing an ecological risk framework to assess environmental safety of nanoscale products*. Springer, Dordrecht, The Netherlands.

Chapter 2



Heteroaggregation and sedimentation rates for nanomaterials in natural waters



TiO₂ MWCNTs ZrO₂ TiO₂ CeO₂ MWCNTs CeO₂ SWCNTs SiO₂-Ag
SWCNTs PMMA Al₂O₃ PFOS PVP-Ag CeO₂ MWCNTs PVP-Ag SWCNTs
nano-PS C₆₀ micro-PE C₆₀ SiO₂-Ag TiO₂ C₆₀
Al₂O₃ SiO₂-Ag MWCNTs PVP-Ag CeO₂ PVP-Ag C₆₀ MWCNTs PFOS micro-PE
SiO₂-Ag PMMA PVP-Ag nano-PS C₆₀ MWCNTs PFOS micro-PE
PCBs SiO₂-Ag PVP-Ag C₆₀ PVP-Ag nano-PS Al₂O₃ CeO₂ Al₂O₃
MWCNTs C₆₀ nano-PS MWCNTs CeO₂ micro-PE CeO₂ Al₂O₃
micro-PE PCBs MWCNTs CeO₂ CeO₂ ZrO₂ PVP-Ag TiO₂ PFOS
nano-PS Al₂O₃ CeO₂ PCBs CeO₂ SWCNTs nano-PS MWCNTs
SiO₂-Ag ZrO₂ C₆₀ MWCNTs ZrO₂ micro-PE SiO₂-Ag PMMA
C₆₀ PCBs SiO₂-Ag PFOS SiO₂-Ag PMMA Al₂O₃ MWCNTs ZrO₂
ZrO₂ TiO₂ PCBs SiO₂-Ag PVP-Ag PMMA Al₂O₃ MWCNTs TiO₂ C₆₀
MWCNTs SWCNTs ZrO₂ SWCNTs micro-PE SiO₂-Ag PMMA
CeO₂ SiO₂-Ag SWCNTs PFOS CeO₂ C₆₀ PFOS PMMA PVP-Ag
micro-PE nano-PS Al₂O₃ C₆₀ PFOS PMMA PVP-Ag
TiO₂ MWCNTs Al₂O₃ PFOS PVP-Ag SWCNTs PMMA TiO₂ CeO₂
PCBs micro-PE ZrO₂ C₆₀ SWCNTs PMMA nano-PS

Published as: Quik JTK, Velzeboer I, Wouterse M, Koelmans AA, van de Meent D. 2014. Heteroaggregation and sedimentation rates for nanomaterials in natural waters. *Water Research* 48:269-279.

Abstract

Exposure modeling of engineered nanoparticles requires input parameters such as sedimentation rates and heteroaggregation rates. Here, we estimate these rates using quiescent settling experiments under environmentally relevant conditions. We investigated 4 different nanoparticles (C_{60} , CeO_2 , SiO_2 -Ag and PVP-Ag) in 6 different water types ranging from a small stream to seawater. In the presence of natural colloids, sedimentation rates ranged from 0.0001 m d^{-1} for SiO_2 -Ag to 0.14 m d^{-1} for C_{60} . The apparent rates of heteroaggregation between nanoparticles and natural colloids were estimated using a novel method that separates heteroaggregation from homoaggregation using a simplified Smoluchowski-based aggregation-settling equation applied to data from unfiltered and filtered waters. The heteroaggregation rates ranged between 0.007 and $0.6 \text{ L mg}^{-1} \text{ d}^{-1}$, with the highest values observed in seawater. We argue that such system specific parameters are key to the development of dedicated water quality models for ENPs.

2.1 Introduction

The production and use of engineered nanoparticles (ENPs) are growing, which increases their emission to environmental compartments [1]. Consequently, understanding the safety, environmental and human health implications of nanotechnology-based products is of worldwide importance [2, 3]. Although the benefits of ENPs have shown to be manifold, the implication of large quantities of ENPs entering the environment has yet to be understood [4, 5]. There is a growing need for risk assessment of different nanoparticles in order to support their safe production and use [6]. The environmental risk assessment is based on the determination of adverse effects on organisms and on evaluation of the environmental concentrations to which biota are exposed [7, 8]. Recently, modeling approaches for estimating the environmental exposure concentration of nanoparticles have been suggested [8-11]. These studies acknowledge the lack of input parameters valid for environmentally relevant conditions, such as sedimentation rates in natural waters [8, 12] and heteroaggregation rates for collisions between natural colloids (NC) and ENPs [9, 11]. Since there is no validated framework for calculation of these parameters for ENPs, they need to be estimated experimentally [13-16].

The aggregation rate constants for heteroaggregation (k_{het}) can be split up in the product of collision frequency (K) and the attachment efficiency (α), i.e. $k_{het} = K \times \alpha$ [17, 18]. For homoaggregation, several studies use this approach to derive the attachment efficiency α_{homo} as an important parameter driving homoaggregation kinetics for a certain ENP under a range of test conditions, such as ionic strength or DOC concentration [19, 20]. Consequently, such attachment efficiencies are conditional and represent the average behaviour of particles present. The uncertain and conditional nature of K and α may be even bigger for heteroaggregation because

natural colloids can be assumed to be much more heterogeneous and fundamentally indeterminate. Current methods to estimate attachment efficiencies α from observed aggregation rates rely on the collision frequency K being constant or known among a range of test conditions. However, due to the range of water and NC characteristics present in natural systems, the collision frequency K will not be constant. Furthermore, current theory of colloid behaviour is not likely to be sufficient to estimate the collision frequency for natural systems. After all, this theory is based on ideal systems with spherical particles. In practice, fate models or water quality models for nanoparticles do not require separate attachment efficiencies α , nor separate collision frequencies K . They require the aforementioned product $k_{het} = K \times \alpha$ [9, 11]. The heteroaggregation rate constant k_{het} is the primary parameter used in current exposure modeling approaches which take heteroaggregation into account [11]. We argue that conditional values of k_{het} are highly needed for the further development of fate models for ENPs.

In the present study we provide estimates of sedimentation rates and heteroaggregation rate constants, based on sedimentation data for 4 different ENPs in the presence and absence of NC in 6 different natural water types. Heteroaggregation rates are usually measured by directly measuring the increase in particle size in time [21, 22]. For natural waters, direct measurement of aggregation rates is problematic due to the limitations of measurement techniques for such complex systems. We therefore propose a novel method to estimate these heteroaggregation rates from sedimentation data. We used fullerene (C_{60}) as a carbon based ENP, cerium dioxide (CeO_2) ENP as a metal oxide and silver (Ag) ENP with two different coatings, polyvinylpyrrolidone (PVP) and silicon dioxide (SiO_2). Quiescent settling was measured in water from six different water bodies ranging from a small pond and stream to lake and seawater. These water samples cover a range in water quality characteristics such as salinity, acidity and organic matter content. Earlier work showed that NC governed the sedimentation of ENPs in river water (Rhine and Meuse) [23]. Here, this mechanism is studied for a much wider range of water types, including brackish tidal water and marine water. Sedimentation rates and heteroaggregation rates for ENPs and NC are reported. To our knowledge, this is the first study that reports these parameters on the interaction of ENPs with NC in surface waters.

2.2 Materials and methods

Engineered nanoparticles

Polyvinylpyrrolidone coated silver (PVP-Ag) nanoparticles (hydrodynamic diameter (d_h): 90.5 nm) and SiO_2 coated silver (SiO_2 -Ag) nanoparticles (d_h : 124 nm) were purchased from nanoComposix (San Diego, CA). Ceriumdioxide (CeO_2) nanoparticles (d_h : 175 nm) were kindly supplied by Umicore Ltd. (Brussels), as part of the EU NanoInteract project. CeO_2 nanoparticles from the same batch have previously been used in several fate and effect studies [23-25]. Fullerene (C_{60} , d_h : 217

nm), 99 wt% purity was obtained as powder from Cheaptubes (Brattleboro, VT). A C_{60} nanoparticles stock suspension was prepared by dispersing $1 \text{ g L}^{-1} C_{60}$ in deionized water by shaking (150 rpm) for 4 weeks in a glass bottle screened from sunlight. Other properties and electron microscopy images of the ENPs are provided as Supporting Information (Table S2.1, Figure S2.1, Figure S2.2).

Particle size distribution and particle number concentration were measured using nanoparticle tracking analysis (NTA). This was done using the NanoSight LM 20 (NanoSight Ltd., Salisbury, UK) using a previously described method [26] and NTA software version 2.2. It should be noted that the NTA method is not very sensitive to particles $<50 \text{ nm}$ with a low refractive index and particles $>1500 \text{ nm}$. This implies that the NTA based characteristics are operationally defined. Electrophoretic mobility was measured with a Zeta-Sizer instrument (nano series, Malvern Instruments Ltd., Worcestershire, UK). Throughout this paper, the term ‘concentration’ refers to mass concentration unless indicated otherwise.

Water sampling

Six different natural waters were sampled using polyethylene containers. Samples were taken from the North Sea (NZ, coastal sea), Rhine (RL, river), Brabantse Aa (AA, small stream), IJsselmeer (IJ, freshwater lake), Nieuwe Waterweg (MS, tidal water), and Karregat (KG, small acid pond), all located in the Netherlands. Details on sampling and exact locations are provided as Supporting Information (Table S2.2). Sedimentation experiments were started on the same day of sampling. To remove NC, part of the water was filtered with 0.2 mm membrane filters (Nuclepore filters, PALL), following earlier studies [23, 27]. This filtration technique reduces NC concentrations to negligible levels (Figure S2.4). After measuring pH, EC and O_2 content, samples were stored at -20°C before further elemental analysis. Dissolved organic carbon (DOC) was measured by adding HNO_3 and purging with O_2 using HiperTOC (Thermo, Delft, NL). The six water types mainly differed in ionic strength, pH and DOC content (Table 2.1). Electric conductivity as an indicator of ionic strength ranged between $47,000 \mu\text{S cm}^{-1}$ for seawater (NZ), followed by brackish water (MS) and the different fresh water types (IJ, RL, AA, KG) of which the lowest value was $67.1 \mu\text{S cm}^{-1}$ (Table 2.1). DOC concentration was highest at AA (26 mg C L^{-1}) and lowest at NZ (0.17 mg C L^{-1}). The pH was lowest at KG (pH = 4.6) whereas the pH of the five other water types ranged from 6.7 to 8.3. MS and RL water had the highest concentration of natural particulate matter ($>10 \text{ mg L}^{-1}$), whereas NZ, KG and IJ water had the lowest concentration of natural particulate matter ($<3 \text{ mg L}^{-1}$). An overview of all chemical characteristics of the water samples is provided in Table 2.1.

Table 2.1 Characteristics of the natural waters: Karregat (KG), Brabantse Aa (AA), Rhine (RL), IJsselmeer (IJ), Maassluis (MS) and North Sea (NZ).

	KG	AA	RL	IJ	MS	NZ
pH (-)	4.61	6.69	7.95	8.33	7.89	7.78
EC ($\mu\text{S cm}^{-1}$)	67.1	434	584.3	763	7200	47,000
O ₂ (mg L ⁻¹)	8.94	7.55	9.27	10.83	7.92	8.38
Cl (mg L ⁻¹)	9.9	57.5	126	146	3970	28,600
NO ₃ + NO ₂ (mg N L ⁻¹)	0.2	6.25	2.75	1.88	2.44	0.26
PO ₄ ($\mu\text{g P L}^{-1}$)	48.2	102.4	36.1	28.4	103.4	n.a.
NH ₃ (mg N L ⁻¹)	0.18	0.59	0.03	0.1	0.07	0.02
total P (mg P L ⁻¹)	0.01	0.16	0.04	0.02	0.12	0.12
total N (mg N L ⁻¹)	0.34	5.14	1.68	1.45	1.72	0.06
Ca (mg L ⁻¹)	3.7	36	55.7	55.4	104	401
K (mg L ⁻¹)	1.2	13.7	4.4	7.4	50	371
Mg (mg L ⁻¹)	1.94	7.7	10.6	12.3	160	1233
Na (mg L ⁻¹)	13.9	22.7	46.2	59.1	1370	10,630
DIC (mg C L ⁻¹)	0.69	23.02	24.62	30.23	31.22	40.91
DOC (mg C L ⁻¹)	5.45	25.98	2.45	5.62	2.85	0.17
NC ^a (mg L ⁻¹)	1.9	7.1	10.3	2.9	11.9	2.6
NC ^b (10 ⁸ L ⁻¹)	0.65	3.39	0.72	0.51	0.54	0.10
radius NC ^b (nm)	351 ± 46	286 ± 31	291 ± 47	225 ± 30	319 ± 49	348 ± 163

n.a.: no data available

^a Measured using dry weight after filtration

^b Measured using nanoparticle tracking analysis

Sedimentation experiments

Sedimentation of CeO₂, PVP-Ag, SiO₂-Ag and C₆₀ nanoparticles was studied during 15 days with a method adapted from earlier work [23, 26]. Our experiments used a considerably longer sedimentation time than many other studies, in order to increase realism and accuracy in medium to long timescales. Three different doses of ENPs were added to each of the six water types in order to obtain dispersions of 0.5, 2.5 and, 10 mg L⁻¹ for the metal ENPs, and 5, 25 and, 100 mg L⁻¹ for the C₆₀ nanoparticles. For C₆₀ nanoparticles a higher dose was used because of the higher detection limit of the UV-vis method. After 0, 1, 2, 6, 10 and 15 days, samples were taken for characterization and analysis of ENP concentrations. Samples of 5 mL were carefully taken by pipette at 3 cm below the water surface. Concentrations of Ce and Ag were taken as a proxy for ENP mass, and were measured by high-resolution inductively coupled plasma mass spectroscopy (Element 2 HR-ICP-MS, Thermo, Bremen, Germany). Before analysis, 4 mL of the supernatant sample was weighed into 50-mL tubes for digestion with 7 mL 14.4 M nitric acid and 1 mL 9.8 M hydrogen peroxide at 103°C for 2 h (Ce measurements). For Ag measurement, 7 mL 37% w/w HCl was added. Concentration

of C_{60} were measured by extraction using 0.01 M $\text{Mg}(\text{ClO}_4)_2$ from water to 2.5 mL toluene after shaking for 30 min. Subsequently, the absorbance in 1 mL toluene C_{60} extracts was measured at 335 nm in triplicate.

Dissolution

At the start and after 15 days the dissolved fraction of metals in the water phase was measured by centrifugal filtering for 15 min at 14,000 rpm. Particulate and dissolved fractions were separated by means of 3 kDa filters (PALL). To prevent reported effects of Ag^+ loss from adsorption to the filter, filters were pre-treated with Cu solution [28]. 1 mL samples were collected from two filters and Ag and Ce concentration was measured using HR-ICP-MS (see above). The chemical speciation program CHEAQS [29] was used to calculate chemical species present at the measured water composition.

Estimation of sedimentation rates

Sedimentation data were interpreted using a semi-empirical model adapted from Newman et al. [30] and Quik et al. [23], which describes the concentrations of ENPs in the supernatant (C_t [g L^{-1}]) as a function of time:

$$C_t = (C_0 - C_{ns}) e^{-\left(\frac{v_s}{h} + k_{dis}\right)t} + C_{ns} \quad (2.1)$$

Table 2.2 Sedimentation rates (V_s), non-settling concentration (C_{ns}) and apparent heteroaggregation rate ($k_{het.crit}$) for C_{60} , CeO_2 , PVP-Ag and SiO_2 -Ag ENPs in natural waters in presence of natural colloids.

		KG	AA	RL	IJ	MS	NZ
C_{60}	V_s (m d^{-1})	0.102	0.109	0.136	$8.81 \cdot 10^{-2}$	0.139	$4.11 \cdot 10^{-2}$
	C_{ns} (mg L^{-1})	$4.06 \cdot 10^{-2}$	$7.17 \cdot 10^{-2}$	$6.09 \cdot 10^{-2}$	$1.78 \cdot 10^{-2}$	$1.81 \cdot 10^{-2}$	$2.29 \cdot 10^{-2}$
	$k_{het.crit}$ ($\text{L mg}^{-1} \text{d}^{-1}$) ^a	n.a. ^b	$6.82 \cdot 10^{-3}$	n.a. ^b	n.a. ^b	$1.49 \cdot 10^{-1}$	$6.00 \cdot 10^{-1}$
CeO_2	V_s (m d^{-1})	$6.10 \cdot 10^{-4}$	$1.39 \cdot 10^{-3}$	$3.09 \cdot 10^{-3}$	$5.44 \cdot 10^{-3}$	$7.83 \cdot 10^{-3}$	$6.94 \cdot 10^{-3}$
	C_{ns} (mg L^{-1})	0.270	0.309	$2.46 \cdot 10^{-2}$	$9.60 \cdot 10^{-2}$	$1.68 \cdot 10^{-2}$	$9.37 \cdot 10^{-3}$
	$k_{het.crit}$ ($\text{L mg}^{-1} \text{d}^{-1}$) ^a	$2.63 \cdot 10^{-2}$	n.a. ^b	$1.45 \cdot 10^{-1}$	$5.12 \cdot 10^{-2}$	$1.04 \cdot 10^{-1}$	$1.14 \cdot 10^{-1}$
PVP-Ag	V_s (m d^{-1})	$4.12 \cdot 10^{-3}$	$3.06 \cdot 10^{-3}$	$9.98 \cdot 10^{-3}$	$8.22 \cdot 10^{-4}$	n.a.	$1.61 \cdot 10^{-3}$
	C_{ns} (mg L^{-1})	0.141	0.316	$4.57 \cdot 10^{-2}$	0.116	$4.06 \cdot 10^{-2}$	0.218
	$k_{het.crit}$ ($\text{L mg}^{-1} \text{d}^{-1}$) ^a	$6.96 \cdot 10^{-2}$	n.a. ^b	$2.54 \cdot 10^{-2}$	$2.47 \cdot 10^{-2}$	$5.01 \cdot 10^{-2}$	$6.98 \cdot 10^{-2}$
SiO_2 -Ag	V_s (m d^{-1})	$1.01 \cdot 10^{-4}$	$1.34 \cdot 10^{-3}$	$5.97 \cdot 10^{-3}$	$2.42 \cdot 10^{-3}$	$1.00 \cdot 10^{-2}$	$5.33 \cdot 10^{-3}$
	C_{ns} (mg L^{-1})	0.285	0.179	$5.16 \cdot 10^{-2}$	0.152	$7.94 \cdot 10^{-2}$	0.164
	$k_{het.crit}$ ($\text{L mg}^{-1} \text{d}^{-1}$) ^a	n.a. ^b	$8.74 \cdot 10^{-3}$	$1.34 \cdot 10^{-2}$	$2.16 \cdot 10^{-2}$	$1.54 \cdot 10^{-2}$	$2.40 \cdot 10^{-2}$

n.a.: no data available

^a Start and single, final time point used in Eq. 2.5 to estimate $k_{hetero.crit}$

^b Not determined because of insufficient sedimentation due to heteroaggregation.

The non-settling concentration (C_{ns} [g L⁻¹]) represents the ENP concentration after infinite time based on data measured at 15 days. V_s [m d⁻¹] is the apparent sedimentation rate, h [m] is the sedimentation length, k_{dis} [d⁻¹] is the dissolution rate constant and t is time [d]. This model was fitted to the data using the nonlinear least squares method in package stats in R [31]. Due to the design of the sedimentation experiment, dissolution (k_{dis} in Eq. 2.1) could not be inferred from the elemental concentration measurement in the supernatants of the settling experiments. After all, Ce, Ag or C₆₀ in the supernatant were measured as total concentration, thus any decrease in concentration in time has to relate to sedimentation (V_s) and not to dissolution (k_{dis}). Instead, dissolution was studied by analysing the Ag and Ce ion concentrations in ultra-filtered water.

In order to compare the obtained sedimentation rates (Table 2.2, V_s) to literature data, we converted previously reported sedimentation rate constants [d⁻¹] [20, 32, 33] to true sedimentation rates [m d⁻¹] using a sedimentation length measured from the water surface to the measurement depth (calculations provided as Supporting Information).

Estimation of heteroaggregation rates

The basis for the calculation of the heteroaggregation rate is the combined Von Smoluchowski-Stokes equation [17]:

$$\frac{dN_j}{dt} = \frac{1}{2} \sum_{i=1}^{j-1} \alpha_{i,j-i} K_{i,j-i} N_i N_{j-i} - N_j \sum_{i=1}^{j-1} \alpha_{i,j} K_{i,j} N_i - \alpha_{NC,j} K_{NC,j} N_{NC} N_j - \frac{V_{s,j}}{h} N_j \quad (2.2)$$

in which α_{ij} is the attachment efficiency between ENP aggregates i and j , $\alpha_{NC,j}$ the attachment efficiency between ENP and NC, j the number of primary ENPs in ENP aggregate j , K_{ij} the collision frequency between ENP aggregates i and j [m³ s⁻¹], $K_{NC,j}$ the collision frequency between ENP particle aggregates j and NC [m³ s⁻¹], N_j is the number concentration of the ENP aggregate j [m⁻³], N_{NC} is concentration of NC [m⁻³], $v_{s,j}$ is the sedimentation rate of ENP aggregate j [m s⁻¹] and d_s is the sedimentation length [m]. In Eq. 2.2, the first two terms account for growth to and loss from ENP size class j due to homoaggregation, the third term accounts for heteroaggregation, and the last term for sedimentation of ENP aggregates. The concentration of natural colloids C_{NC} is assumed to decrease due to Stokes settling [34, 35]:

$$\frac{dN_{NC}}{dt} = -\frac{V_{s,NC}}{d_s} N_{NC} \quad (2.3)$$

Eq. 2.2 is simplified based on a few informed assumptions, which subsequently are validated against extensive simulations obtained using the full deterministic Eq. 2.2 (simulation results provided as Supporting Information). Following Farley and Morel [36], it is assumed that aggregation is the rate limiting process for the observed removal of ENPs from the water phase. This follows the logic that aggregates first need to be large enough for sedimentation to occur. This means that the aggregation terms in Eq. 2.2 are considered to be rate determining and that the last term in Eq. 2.2 can

be omitted. Second, it is assumed that the summations in Eq. 2.2 can be replaced by single terms accounting for the apparent critical collision behaviour for sedimentation. This is motivated as follows. The summation in Eq. 2.2 accounts for numerous collisions that will not (yet) lead to homo- or heteroaggregates large enough to settle. However, a certain fraction of all possible collisions will at some point reach a critical limit after which rapid settling occurs. The measured removal in the sedimentation experiments relate to this apparent removal of settleable ENPs only (ENP_{crit}). Because size distributions of these settling ENP aggregates may not be monodisperse, the single terms are governed by apparent parameters reflecting average properties of the particles at the onset of settling. Third, it is assumed that the ENP concentration change in the overlying water is determined by aggregation to settling particles only i.e. is not affected by progressive aggregation to larger particles. Progressive aggregation cannot affect ENP_{crit} concentrations beyond the critical size for sedimentation because they would have settled out already. This implies that the first two terms for aggregation in Eq. 2.2 can be combined. Consequently, Eq. 2.2 can be simplified to describe removal from the water column:

$$\frac{dC_{ENP,crit}}{dt} = -k_{hom,crit} C_{ENP,crit}^q - k_{het,crit} C_{NC} C_{ENP,crit} \quad (2.4)$$

in which $C_{ENP,crit}$ is the concentration of settleable ENPs [$g L^{-1}$], $k_{hom,crit}$ is the apparent aggregation rate for the formation of settleable ENP homoaggregates [$(L g^{-1})^{1-q} s^{-1}$], and $k_{het,crit}$ is the apparent aggregation rate for the formation of settleable ENP heteroaggregates [$L g^{-1} s^{-1}$]. The exponent q defines the kinetics for homoaggregation and was obtained by fitting the analytical solution of Eq. 2.4 against simulations based on the full Von Smoluchowski-Stokes equation (Eq. 2.2), yielding a value of $q \approx 1$ (details provided as Supporting Information). In summary, Eq. 2.4 describes how the concentration of the (operationally defined) settling ENP fraction changes over time, as a function of the processes that drive the production of aggregates. Aggregates that do not settle substantially in the time interval over which settling is monitored (15 days in the present experiments) are also formed. Primary particles may also be stabilized and not settle at all. The latter two categories of processes lead to an operationally defined non-settling fraction (C_{ns} in Eq. 2.1). Eq. 2.4 can be solved with $q = 1$ and with Eq. 2.3 for the time dependence of C_{NC} to yield the analytical solution:

$$C_{ENP,crit}(t) = C_{0,ENP,crit} e^{-A t + B (e^{-D t} - 1)} \quad (2.5)$$

where $A = k_{hom,crit}$, $B = k_{het,crit} C_{0,NC} d_s / v_{s,NC}$ and $D = v_{s,NC} / d_s$. The rate for heteroaggregation to settleable particles, $k_{het,crit}$ can be estimated by fitting Eq. 2.5 to the sedimentation data from the unfiltered systems using values for $k_{hom,crit}$ obtained from fitting Eq. 2.5 to sedimentation data for the filtered systems, with $C_{0,NC} = 0$. The fitting procedures may use all measured sedimentation data or may use C_0 and a single time point $C(t)$,

for instance after 15 d only. The latter approach is better if the differences between sedimentation in filtered vs. unfiltered water are too small for the early time points.

2.3 Results and discussion

Natural colloids and water types

In general, NC increased overall sedimentation of ENPs (mg L^{-1}). The obtained ENP sedimentation rates (m d^{-1}) were not significantly affected by the presence of NC in the surface waters, nor by the different water types (paired t-test, $p > 0.05$, Figure 2.1). For the non-settling fraction after 15 days (C_{15}/C_0), a significant decrease was observed in the presence of NC increased in presence of NC. In combination, identical sedimentation rates but higher settling fractions upon presence of NC, explain that NC increased overall sedimentation. Significant differences between the C_{15}/C_0 were also observed between most water types, except in the subsets RL, MS, NZ, and AA, KG, IJ (Figure 2.2). This suggests a communality in the characteristics of the water types in these sets. The KG, AA and to lesser extend IJ water show significantly higher non-settling fractions in the water phase after 15 days compared to RL, MS and NZ. The first mentioned group also possesses the more favourable conditions for stability against aggregation, such as higher DOC, lower EC, more extreme pH and lower NC mass [13, 20, 37]. In addition to ENP sedimentation being affected by the presence of NC, the sedimentation of NC may also be affected due to heteroaggregation with ENPs. However, using Al as a proxy for NC, we observed no significant effect of presence of ENPs on NC settling (Figure S2.3).

To better isolate the effect that NC may have on the sedimentation of ENPs from the water phase, we subtracted the C_{15}/C_0 in unfiltered water from that in filtered river water. This shows that NC generally increase sedimentation of ENPs (Figure 2.3) for the most environmentally relevant initial particle concentration (0.5 or 5 mg L^{-1} ENP). The fraction removed due to presence of NC varies per water type and particle type. In AA water the difference is negative for both CeO_2 and PVP-Ag ENPs suggesting a decrease in sedimentation in presence of NC. This is not in line with the total amount of NC present in AA water, which has the highest available surface area for interaction with ENPs compared to the other water types (Figure 2.4, Figure S2.4). This suggests that the NC present in AA water do not directly affect the sedimentation within 15 days. This could be due to the size of the NC in AA water, which were measured to be smaller than NC in the other water types. In the other waters, the larger NC settle much faster (Figure S2.3). The low fraction removed for AA water may also relate to the high DOC content of the water. DOC may indicate the presence of lower density NC, which might not settle within 15 days. Furthermore, DOC (as a proxy for natural organic matter) is known to reduce the attachment efficiency of ENPs resulting in a decrease in aggregation and sedimentation [26, 38].

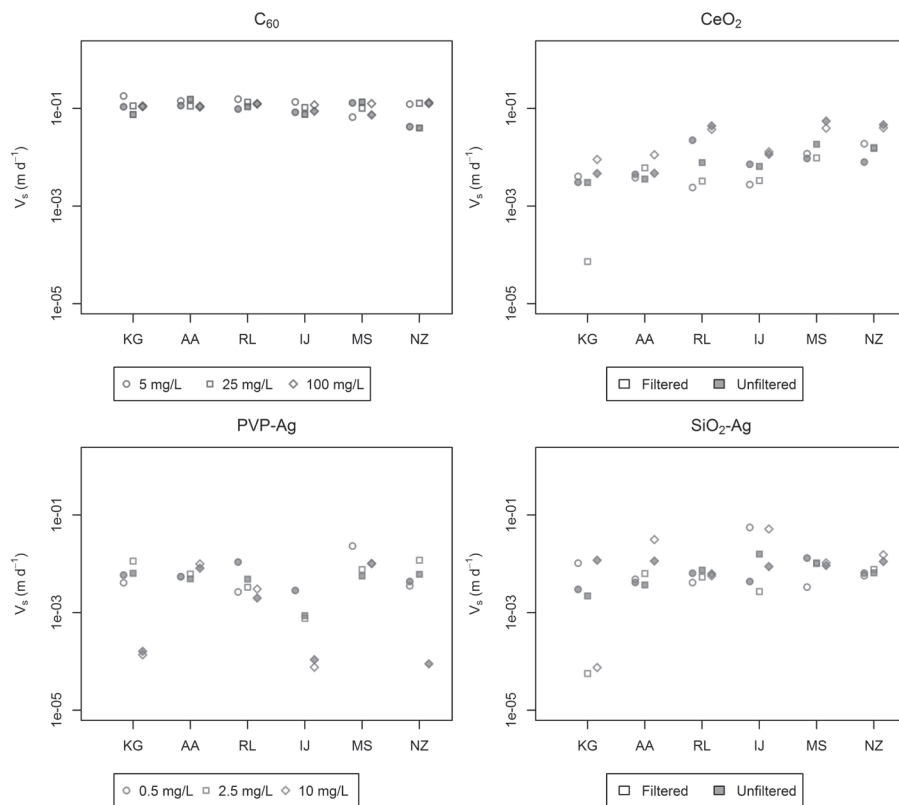


Figure 2.1 Sedimentation rates (V_s) for C_{60} , CeO_2 , PVP-Ag and SiO_2 -Ag nanoparticles in six different water types with (unfiltered) and without (filtered) natural colloids present, for three different initial ENP concentrations (0.5, 2.5 and 10 $mg L^{-1}$ for metal ENPs and 5, 25, 100 $mg L^{-1}$ for C_{60}). Water types: Karregat (KG), Brabantse Aa (AA), Rhine (RL), IJsselmeer (IJ), Maassluis (MS) and North Sea (NZ).

Sedimentation and stability of ENPs

The different ENPs showed significant differences in apparent sedimentation rate and C_{15}/C_0 (paired t-test, $p < 0.01$; Figure 2.1). The sedimentation rates ranged from 0.0048 $m d^{-1}$ for PVP-Ag to 0.12 $m d^{-1}$ for C_{60} . The apparent non-settling fractions (given as $C_{15}/C_0 \times 100\%$) after 15 d varied from 0.01% to 92% for the metal based ENPs. Only for C_{60} particles consistently low values of C_{15}/C_0 were observed in all waters; from 1 to 7%. A full overview of all the sedimentation rates and C_{15}/C_0 can be found in the Supporting Information (Table S2.5). In addition to differences in chemical composition, these ENPs differed in particle coating, size and initial particle number concentrations. The observed number concentrations (Figure 2.4) are discussed here because it is important for relative contributions of homo and heteroaggregation, discussed in the next section. The differences in particle size cause differences in

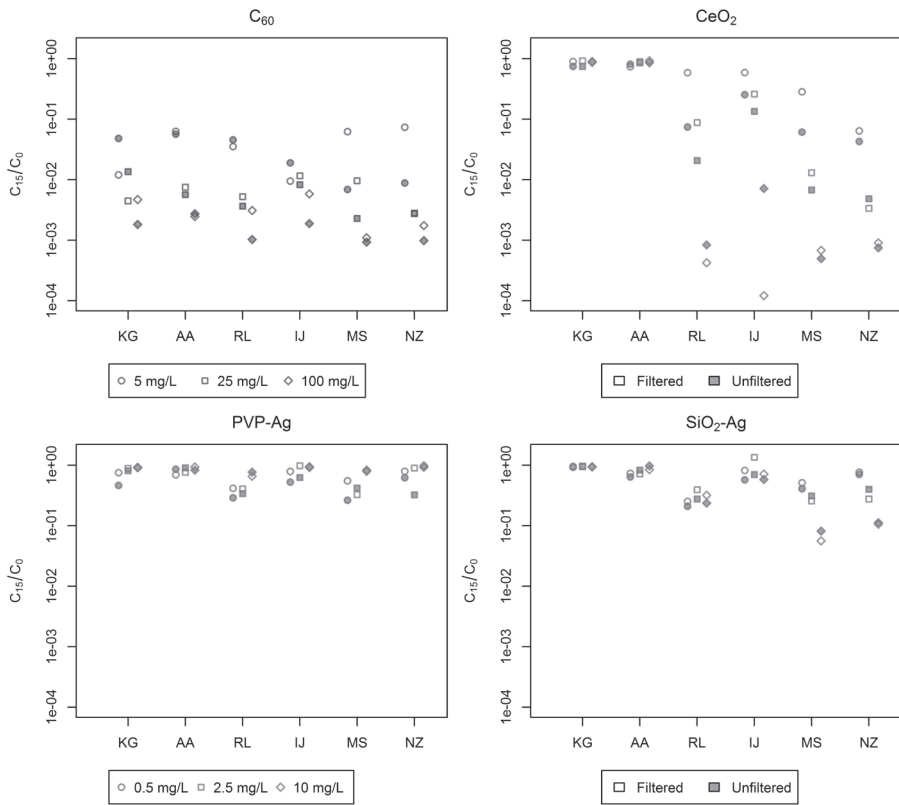


Figure 2.2 Non-settling fractions (C_{15}/C_0) for C_{60} , CeO_2 , PVP-Ag and SiO_2-Ag ENPs in six different water types with (unfiltered) and without (filtered) natural colloids (NC) present for three different initial ENP concentrations. Water types: Karregat (KG), Brabantse Aa (AA), Rhine (RL), IJsselmeer (IJ), Maassluis (MS) and North Sea (NZ).

particle number concentration for the same 0.5 mg L^{-1} mass concentration (Figure 2.4). The 0.5 mg L^{-1} PVP-Ag and SiO_2-Ag have similar particle number concentrations. CeO_2 however, shows significantly lower particle number concentrations. The 5 mg L^{-1} C_{60} particle number concentration (not shown) is even lower, but this is probably not representative due to limitations of the NTA measurement method with regard to large C_{60} aggregates ($>1 \text{ mm}$). Because (a) the initial ENP concentration appears to affect the sedimentation rate and C_{15}/C_0 of the ENPs (Figure 2.2 and 2.3), and (b) the lower concentrations have a higher environmental relevance, the discussion below will focus on the data obtained at the lowest initial ENP concentrations (Table 2.2).

Generally, sedimentation rates from other studies span a higher range compared to the range observed in our experiments with 6 different water types in the presence of NC (Figure 2.5). Only the sedimentation rates reported by Keller et al. [20] span down to similarly low values. There are too many differences in the set-up of

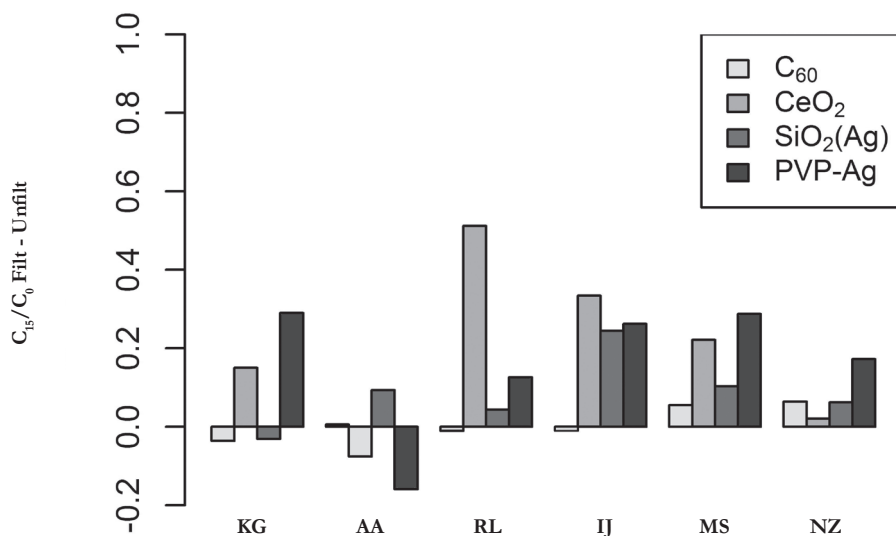


Figure 2.3 Fraction of ENP removed from the water phase due to the presence of NC. Calculated by subtraction of C_{15}/C_0 for unfiltered water from C_{15}/C_0 of filtered water, for 0.5 mg L^{-1} (metal ENP) and 5 mg L^{-1} (C_{60}) initial ENP concentration. Water types: Karregat (KG), Brabantse Aa (AA), Rhine (RL), IJsselmeer (IJ), Maassluis (MS) and North Sea (NZ).

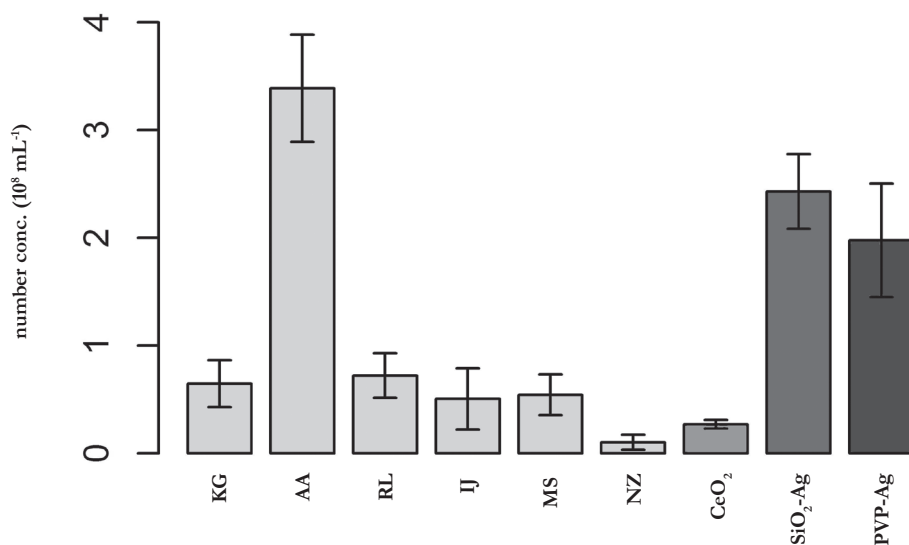


Figure 2.4 Number concentration of NC in original water and of 0.5 mg L^{-1} (metal ENP) and 5 mg L^{-1} (C_{60}) ENPs in deionized water as measured by nanoparticle tracking analysis. Water types: Karregat (KG), Brabantse Aa (AA), Rhine (RL), IJsselmeer (IJ), Maassluis (MS) and North Sea (NZ).

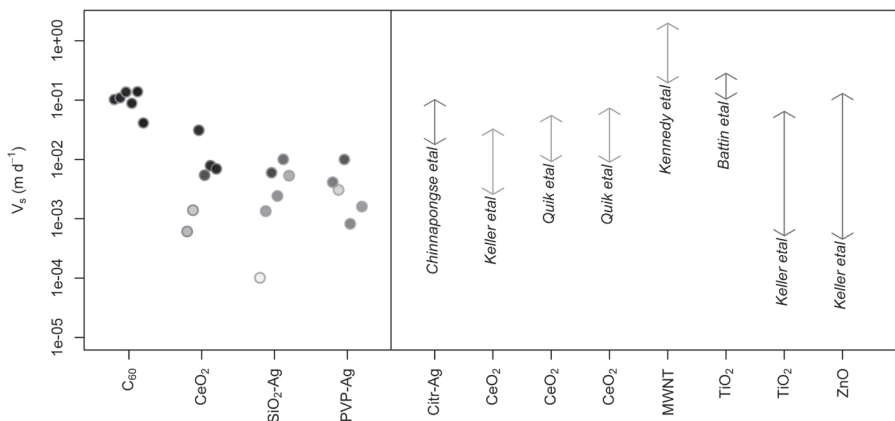


Figure 2.5 Comparison of sedimentation rates (points, this study) to ranges recalculated from literature data (arrows with citation Battin et al. [39], Chinnapongse et al. [32], Keller et al. [20], Quik et al. [26], Quik et al. [23])

these studies to unambiguously explain all differences in observed sedimentation rates. However, generally these earlier studies used higher initial ENP concentrations, which may explain the higher sedimentation rates for these ENPs. Remarkably, the highest sedimentation rates are observed for multi walled carbon nanotubes [33], regardless of the presence of DOC in the water. This agrees to the much higher sedimentation rates observed for C_{60} in the present study. Furthermore the study of Battin et al. [39] showed relatively high sedimentation rates: between 0.10 and 0.28 m d^{-1} using stream microcosms, with and without a biofilm present, as opposed to quiescent settling in the current study. The adsorption of the ENPs to the biofilm may have caused these higher sedimentation or removal rates. In our previous studies sedimentation of the same CeO_2 ENP as in the present study were tested in algae medium with and without DOC [26] and in two natural water samples from the Rhine and Meuse rivers [23]. The sedimentation rates for 1 mg L^{-1} CeO_2 suspensions in natural water were similar to the rates observed in the present study.

Given the importance of the particle number concentration on aggregation, the contribution of heteroaggregation can only be significant when there are more NC than ENP present in suspension. This idea has been postulated [8, 11] as a basis for exposure modeling where heteroaggregation is assumed to be the dominant process due to the abundance of NC being much higher than that of ENPs, given their current and anticipated levels of ENP emission [10]. For exposure modeling this simplifies Eq. 2.2 to only the heteroaggregation term. However, we observed the particle number concentration of both of our Ag nanoparticle types to be higher than the NC number concentrations present in the different water types (Figure 2.4). Only for CeO_2 similar or higher NC number concentrations than ENP number concentrations are observed. Nevertheless, for both Ag and CeO_2 ENPs a higher sedimentation is observed in most

water types when NC are present (Figure 2.3). This shows that even at these rather high ENP concentrations, NC affected sedimentation. However, homoaggregation cannot be excluded as shown by the removal of ENPs in filtered water. Note that, unlike Eq. 2.2 and 2.5, the empirical model used to estimate apparent sedimentation rates (Eq. 2.1) does not explicitly account for all the processes affecting sedimentation, such as homo- and heteroaggregation.

Dissolution

It has been reported that Ag dissolution is affected by Ag nanoparticle coating as well as by pH, oxygen content and ionic composition of the water [40-42]. CeO_2 is not expected to show any significant dissolution [8]. In general, dissolution was very limited, with values <1.5% for AA, RL, IJ and MS and similar for both PVP and SiO_2 coated Ag nanoparticles. Higher dissolution was measured in the acid pond water (KG), i.e. between 0.7 and 4% with a slightly higher dissolution of SiO_2 -Ag than PVP-Ag in these acidic conditions (Figure 2.6 and S2.5). Additionally, KG water is the only water type with a detectable fraction dissolved Ce: <0.4%. The highest percentage of dissolved Ag (7 – 12%), is measured in seawater (NZ).

The measured dissolved fraction of Ag and Ce after 15 days (Figure S2.5) was in most cases lower than at the start of the experiment (Figure 2.6). This suggests that the stable species of Ag is not a dissolved ion complex, but that precipitation occurs, most likely of $\text{AgCl}(s)$. Equilibrium speciation calculations suggest that in all water types except seawater, AgCl makes up more than 95% of the silver species present. For seawater, CHEAQS showed that 98.6% of Ag present should be in the form of AgCl_4^{3-} , which explains the higher dissolution in seawater consistent with literature, which indicated only minor effects of sulfide in seawater [41]. The diameter of the PVP-Ag particles was significantly lower after 10 days compared to day 1 (Figure S2.6). This supports the idea that there is continued dissolution causing the shrinking of the Ag ENPs in time. It is likely that the increase in the fraction dissolved Ag is not seen in the filtrate due to the formation of other Ag-containing solids after aging, which do not pass the 3 kDa filter. These observations illustrate the importance of addressing aging and alteration of ENPs under environmental conditions [43]

These results imply that for CeO_2 we can neglect k_{dis} in Eq. 2.1 compared to the sedimentation term (V_s/h), i.e. we may consider coagulation-sedimentation as the dominating removal process in fresh and brackish water types. This is not always the case for Ag ENPs but the dissolution data do not allow the estimation of k_{dis} . Dissolved Ag ENPs may however have contributed to the apparent non-settling fractions. Consequently, it can be speculated that for Ag ENPs the C_{ns} in Eq. 2.1 can be up to 12% lower in seawater. Further measurements aimed at measuring the dissolution kinetics are needed to estimate the dissolution rates under a range of different environmentally relevant conditions. Note that the fact that k_{dis} for Ag is indeterminate, does not imply that sedimentation rate estimates are inaccurate, as was explained in the materials and methods section.

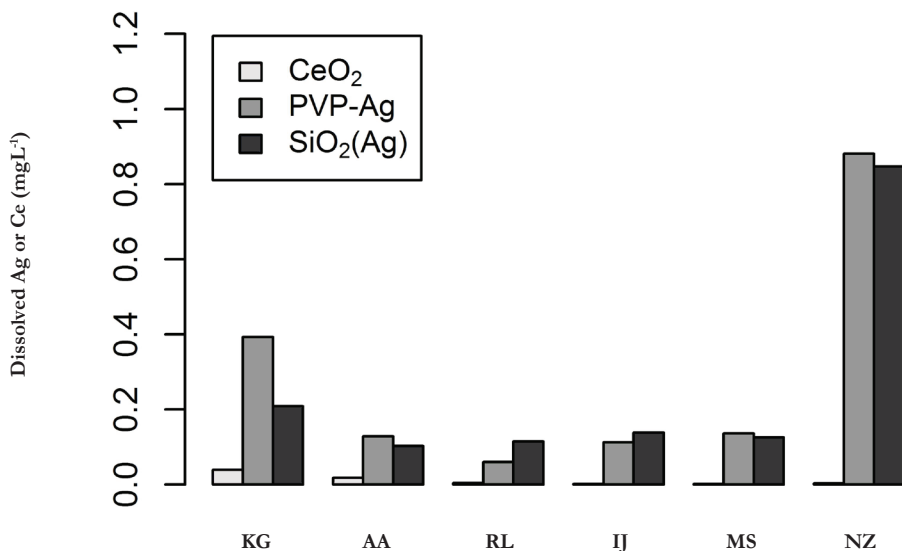


Figure 2.6 Dissolved metal ions, Ce and Ag, in 10 mg L⁻¹ ENP suspensions of CeO₂, SiO₂-Ag and PVP-Ag in six different water types. Water types: Karregat (KG), Brabantse Aa (AA), Rhine (RL), IJsselmeer (IJ), Maassluis (MS) and North Sea (NZ).

Heteroaggregation rates

The largest range of $k_{het,crit}$ values is observed for C₆₀ ENPs, followed by CeO₂, PVP-Ag and SiO₂-Ag ENPs. For all ENPs, the NC in seawater (NZ) have the highest $k_{het,crit}$ values, which is explained from the high ionic strength of seawater (Table 2.2). This agrees to a study by Keller et al. [20] who reported homoaggregation rates for CeO₂, TiO₂ and ZnO ENPs being the highest in seawater. Also in brackish water (MS) relatively high $k_{het,crit}$ values were observed. Only for CeO₂ in Rhine water (RL) a slightly higher $k_{het,crit}$ was measured compared to NZ water showing the dominant effect of the NC in Rhine water on CeO₂ ENPs, as previously reported [23]. The lowest $k_{het,crit}$ values are observed in AA and IJ water, indicating a stabilizing effect of the higher DOC concentrations in these waters (Table 2.2). This is in line with a study by Huynh et al. [22] that showed the total inhibition of heteroaggregation between multi walled carbon nanotubes and hematite nanoparticles upon addition of 0.5 mg L⁻¹ humic acid. Heteroaggregation data for CeO₂ and PVP-Ag ENPs could not be obtained for water with high DOC concentrations (AA water, Table 2.2). This is likely due to the fact that filtration also removed some of the natural organic matter leading to increased aggregation compared to the unfiltered sample. Also KG shows relatively low $k_{het,crit}$ values. This is explained from the stabilization of ENPs due to low ionic strength and low pH, which therefore showed low sedimentation of ENPs in either filtered or unfiltered systems (Figure 2.2). In general these results show that water types that generally stabilized ENPs also resulted in lower $k_{het,crit}$.

One disclaimer should be mentioned with respect to the use of the data from this study. The reported values are conditional and therefore useful only if applied to waters with similar characteristics. However, note that the use of conditional constants is common in reaction - and equilibrium kinetics, for instance in metal speciation modeling [44]. The parameters in Table 2.2 thus are primarily relevant for fate model implementations for the studied waters. Parameters for other systems, however, may be derived following the methodology proposed in the present work.

2.4 Conclusions

This study provided sedimentation rates, non-settling fractions and heteroaggregation rates for several representative ENPs and a wide range of natural water types. Heteroaggregation with NC has been shown to play a key role in the sedimentation of ENPs. Furthermore, dissolution has been shown to be relevant for specific combinations of ENP and water types. We conclude that these data as well as the approach to derive them will advance the development of fate and exposure models for ENPs. This study addressed quiescent settling conditions. Further research is needed to address the effect that turbulent conditions may have on heteroaggregation and sedimentation of ENPs.

Acknowledgments

We thank Ruud Jeths, Gerrie Pieper, Leo van Hal, Erik Steenbergen and Mieke Verheij for their assistance and cooperation regarding sampling of the different water types. This work was funded by the European Union Sixth Framework Program NanoInteract NMP4-CT-2006-033231, the RIVM strategic research program SOR-S340030, and by NanoNextNL, a micro and nanotechnology consortium of the Government of the Netherlands and 130 partners.

References

- [1] Nowack B, Bucheli TD. 2007. Occurrence, behavior and effects of nanoparticles in the environment. *Environmental Pollution* 150:5-22.
- [2] Klaine SJ, Koelmans AA, Horne N, Carley S, Handy RD, Kapustka L, Nowack B, von der Kammer F. 2012. Paradigms to assess the environmental impact of manufactured nanomaterials. *Environmental Toxicology and Chemistry* 31:3-14.
- [3] Wiesner MR, Lowry GV, Alvarez P, Dionysiou D, Biswas P. 2006. Assessing the risks of manufactured nanomaterials. *Environmental Science & Technology* 40:4336-4345.
- [4] Batley GE, Kirby JK, McLaughlin MJ. 2013. Fate and Risks of Nanomaterials in Aquatic and Terrestrial Environments. *Accounts of Chemical Research* 46:854-862.
- [5] Hendren CO, Mesnard X, Droge J, Wiesner MR. 2011. Estimating Production Data for Five Engineered Nanomaterials As a Basis for Exposure Assessment. *Environmental Science & Technology* 45:2562-2569.
- [6] Morris J, Willis J, De Martinis D, Hansen B, Laursen H, Sintes JR, Kearns P, Gonzalez M. 2011. Science policy considerations for responsible nanotechnology decisions. *Nature Nanotechnology* 6:73-77.
- [7] EU. 2008. European Union System for the Evaluation of Substances (EUSES). Version 2.1. Institute for Health and Consumer Protection, E.C.B.
- [8] Quik JTK, Vonk JA, Hansen SF, Baun A, Van De Meent D. 2011. How to assess exposure of aquatic organisms to manufactured nanoparticles? *Environment International* 37:1068-1077.
- [9] Arvidsson R, Molander S, Sanden BA, Hasselov M. 2011. Challenges in Exposure Modeling of Nanoparticles in Aquatic Environments. *Human and Ecological Risk Assessment* 17:245-262.
- [10] Gottschalk F, Ort C, Scholz RW, Nowack B. 2011. Engineered nanomaterials in rivers – Exposure scenarios for Switzerland at high spatial and temporal resolution. *Environmental Pollution* 159:3439-3445.
- [11] Praetorius A, Scheringer M, Hungerbühler K. 2012. Development of Environmental Fate Models for Engineered Nanoparticles-A Case Study of TiO₂ Nanoparticles in the Rhine River. *Environmental Science & Technology* 46:6705-6713.
- [12] Gottschalk F, Sonderer T, Scholz RW, Nowack B. 2010. Possibilities and limitations of modeling environmental exposure to engineered nanomaterials by probabilistic material flow analysis. *Environmental Toxicology and Chemistry* 29:1036-1048.
- [13] Hotze EM, Phenrat T, Lowry GV. 2010. Nanoparticle Aggregation: Challenges to Understanding Transport and Reactivity in the Environment. *Journal of Environmental Quality* 39:1909-1924.
- [14] Lin DH, Tian XL, Wu FC, Xing BS. 2010. Fate and Transport of Engineered Nanomaterials in the Environment. *Journal of Environmental Quality* 39:1896-1908.

- [15] Petersen EJ, Zhang L, Mattison NT, O'Carroll DM, Whelton AJ, Uddin N, Nguyen T, Huang Q, Henry TB, Holbrook RD, Chen KL. 2011. Potential Release Pathways, Environmental Fate, And Ecological Risks of Carbon Nanotubes. *Environmental Science & Technology* 45:9837-9856.
- [16] Westerhoff P, Nowack B. 2013. Searching for Global Descriptors of Engineered Nanomaterial Fate and Transport in the Environment. *Accounts of Chemical Research* 46:844-853.
- [17] Friedlander SK. 2000. *Smoke, Dust, and Haze: Fundamentals of Aerosol Behavior*. Oxford University Press, New York.
- [18] Petosa AR, Jaisi DP, Quevedo IR, Elimelech M, Tufenkji N. 2010. Aggregation and Deposition of Engineered Nanomaterials in Aquatic Environments: Role of Physicochemical Interactions. *Environmental Science & Technology* 44:6532-6549.
- [19] Chen KL, Elimelech M. 2008. Interaction of Fullerene (C-60) Nanoparticles with Humic Acid and Alginate Coated Silica Surfaces: Measurements, Mechanisms, and Environmental Implications. *Environmental Science & Technology* 42:7607-7614.
- [20] Keller AA, Wang HT, Zhou DX, Lenihan HS, Cherr G, Cardinale BJ, Miller R, Ji ZX. 2010. Stability and Aggregation of Metal Oxide Nanoparticles in Natural Aqueous Matrices. *Environmental Science & Technology* 44:1962-1967.
- [21] Afroz A, Khan IA, Hussain SM, Saleh NB. 2013. Mechanistic Heteroaggregation of Gold Nanoparticles in a Wide Range of Solution Chemistry. *Environmental Science & Technology* 47:1853-1860.
- [22] Huynh KA, McCaffery JM, Chen KL. 2012. Heteroaggregation of Multiwalled Carbon Nanotubes and Hematite Nanoparticles: Rates and Mechanisms. *Environmental Science & Technology* 46:5912-5920.
- [23] Quik JTK, Stuart MC, Wouterse M, Peijnenburg W, Hendriks AJ, van de Meent D. 2012. Natural colloids are the dominant factor in the sedimentation of nanoparticles. *Environmental Toxicology and Chemistry* 31:1019-1022.
- [24] Van Hoecke K, De Schampelaere KAC, Van der Meeren P, Smagghe G, Janssen CR. 2011. Aggregation and ecotoxicity of CeO₂ nanoparticles in synthetic and natural waters with variable pH, organic matter concentration and ionic strength. *Environmental Pollution* 159:970-976.
- [25] Van Hoecke K, Quik JTK, Mankiewicz-Boczek J, De Schampelaere KAC, Elsaesser A, Van der Meeren P, Barnes C, McKerr G, Howard CV, Van De Meent D, Rydzynski K, Dawson KA, Salvati A, Lesniak A, Lynch I, Silversmit G, De Samber B, Vincze L, Janssen CR. 2009. Fate and Effects of CeO₂ Nanoparticles in Aquatic Ecotoxicity Tests. *Environmental Science & Technology* 43:4537-4546.
- [26] Quik JTK, Lynch I, Van Hoecke K, Miermans CJH, De Schampelaere KAC, Janssen CR, Dawson KA, Stuart MAC, Van de Meent D. 2010. Effect of natural organic matter on cerium dioxide nanoparticles settling in model fresh water. *Chemosphere* 81:711-715.
- [27] Hyung H, Fortner JD, Hughes JB, Kim JH. 2007. Natural organic matter stabilizes carbon nanotubes in the aqueous phase. *Environmental Science & Technology* 41:179-184.
- [28] Cornelis G, Kirby JK, Beak D, Chittleborough D, McLaughlin MJ. 2010. A method for determination of retention of silver and cerium oxide manufactured nanoparticles in soils. *Environmental Chemistry* 7:298-308.

- [29] Verweij W. 2011. CHEAQS, Computer Program for Calculating CHemical Equilibria in AQuatic Systems.
- [30] Newman KA, Morel FMM, Stolzenbach KD. 1990. Settling and coagulation characteristics of fluorescent particles determined by flow-cytometry and fluorometry *Environmental Science & Technology* 24:506-513.
- [31] R Development Core Team. 2012. R: a Language and Environment for Statistical Computing. URL <http://www.R-project.org/>, Vienna, Austria.
- [32] Chinnapongse SL, MacCusprie RI, Hackley VA. 2011. Persistence of singly dispersed silver nanoparticles in natural freshwaters, synthetic seawater, and simulated estuarine waters. *Science of the Total Environment* 409:2443-2450.
- [33] Kennedy AJ, Hull MS, Steevens JA, Dontsova KM, Chappell MA, Gunter JC, Weiss Jr. CA. 2008. Factors influencing the partitioning and toxicity of nanotubes in the aquatic environment. *Environmental Toxicology and Chemistry*:1932-1941
- [34] Boyd CE. 1995. *Bottom Soils, Sediment, and Pond Aquaculture*. Chapman & Hall, New York.
- [35] Filella M. 2007. In: Wilkinson, K.J., Lead, J.R. (Eds), *Environmental Colloids and Particles: Behaviour, Separation, and Characterisation*. Wiley.
- [36] Farley KJ, Morel FMM. 1986. Role of coagulation in the kinetics of sedimentation. *Environmental Science & Technology* 20:187-195.
- [37] Ottofuelling S, Von der Kammer F, Hofmann T. 2011. Commercial Titanium Dioxide Nanoparticles in Both Natural and Synthetic Water: Comprehensive Multidimensional Testing and Prediction of Aggregation Behavior. *Environmental Science & Technology* 45:10045-10052.
- [38] Li KG, Chen YS. 2012. Effect of natural organic matter on the aggregation kinetics of CeO₂ nanoparticles in KCl and CaCl₂ solutions: Measurements and modeling. *Journal of Hazardous Materials* 209:264-270.
- [39] Battin TJ, Kammer FVD, Weilhartner A, Ottofuelling S, Hofmann T. 2009. Nanostructured TiO₂: Transport Behavior and Effects on Aquatic Microbial Communities under Environmental Conditions. *Environmental Science & Technology* 43:8098-8104.
- [40] Ho CM, Yau SKW, Lok CN, So MH, Che CM. 2010. Oxidative Dissolution of Silver Nanoparticles by Biologically Relevant Oxidants: A Kinetic and Mechanistic Study. *Chemistry-an Asian Journal* 5:285-293.
- [41] Levard C, Hotze EM, Lowry GV, Brown GE. 2012. Environmental Transformations of Silver Nanoparticles: Impact on Stability and Toxicity. *Environmental Science & Technology* 46:6900-6914.
- [42] Li X, Lenhart JJ, Walker HW. 2012. Aggregation Kinetics and Dissolution of Coated Silver Nanoparticles. *Langmuir* 28:1095-1104.
- [43] Nowack B, Ranville JF, Diamond S, Gallego-Urrea JA, Metcalfe C, Rose J, Horne N, Koelmans AA, Klaine SJ. 2012. Potential scenarios for nanomaterial release and subsequent alteration in the environment. *Environmental Toxicology and Chemistry* 31:50-59.
- [44] Radovanovic H, Koelmans AA. 1998. Prediction of in situ trace metal distribution coefficients for suspended solids in natural waters. *Environmental Science & Technology* 32:753-759.

Supporting Information

Table S2.1 Characteristics of the stock nanoparticle suspensions.

Particle	Diameter ^a (nm)	Hydrodynamic diameter ^b (nm)	Density ^c (kg m ⁻³)	ZP (mV)	pH ^d (-)	Mass conc. (g L ⁻¹)
PVP-Ag	51 ± 22.1	90.5	8478	-12.4	6.5	10.23
SiO ₂ -Ag	Core: 40.5 ± 20.5 Shell: 24.6	124	2664	25.4	6.2	4.66
CeO ₂	20	175	3070	38.7	4	100
C ₆₀	n.a.	217	1046	-13.7	5.6	1

^a Diameter measured by TEM/SEM

^b Diameter measured with Nanoparticle Tracking Analysis

^c Calculated from the radius of aggregate and primary particles and a fractal dimension of 2.5, assuming spheres

^d pH of stock suspensions

n.a.: no data available

Table S2.2 Water sampling locations and methods.

Water body	Sampling	Longitude	Latitude
Brabantse Aa (AA)	Bucket	51.391350°	5.741789°
Rhine (RL)	Pump	51.853845°	6.091116°
Nieuwe waterweg (MS)	Bucket	51.914349°	4.249928°
Karregat (KG)	Beaker on a pole	51.730449°	5.418963°
IJsselmeer (IJ)	Bucket	52.575146°	5.530710°
North Sea (NZ)	Ship	n.a.	n.a.

n.a.: no data available

CHEAQs speciation calculations

Table S2.3 Output from CHEAQs pro version P2012.1 of Ag speciation in RL, MS and NZ water covering a range in ionic strength and chloride content.

	Concentration (M)	% of dissolved concentration	% of total concentration	Activity (M)	Intrinsic equilibrium constant	Conditional equilibrium constant
Rhine (RL)						
Free Ag ⁺	1.066E-05	11.49	11.49	9.787E-06		
AgCl (aq)	6.308E-05	68.04	68.04	6.308E-05	3.310	3.236
AgCl ₂ ⁻	1.880E-05	20.37	20.37	1.734E-05	5.250	5.176
AgCl ₃ ²⁻	6.858E-08	0.07	0.07	4.879E-08	5.200	5.200
AgCl ₄ ³⁻	1.922E-08	0.02	0.02	8.936E-09	6.964	7.111
Total Ag	9.271E-05		100.00			
Nieuwe Waterweg (MS)						
Free Ag ⁺	1.835E-08	0.02	0.02	1.434E-08		
AgCl (aq)	2.482E-06	2.68	2.68	2.482E-06	3.310	3.095
AgCl ₂ ⁻	2.347E-05	25.32	25.32	1.833E-05	5.250	5.035
AgCl ₃ ²⁻	3.723E-06	4.02	4.02	1.386E-06	5.200	5.200
AgCl ₄ ³⁻	6.301E-05	67.97	67.97	6.817E-06	6.964	7.393
Total Ag	9.271E-05		100.00			
North Sea (NZ)						
Free Ag ⁺	1.246E-11	0.00	0.00	9.265E-12		
AgCl (aq)	6.884E-09	0.01	0.01	9.884E-09	3.310	3.053
AgCl ₂ ⁻	6.049E-07	0.65	0.65	4.498E-07	5.250	4.993
AgCl ₃ ²⁻	6.852E-07	0.74	0.74	2.095E-07	5.200	5.200
AgCl ₄ ³⁻	9.140E-05	98.60	98.60	6.350E-06	6.964	7.478
Total Ag	9.271E-05		100.00			

Table S2.4. Sedimentation rates and C_{15}/C_0

		V_s (m d ⁻¹)	Std.Error V_s (m d ⁻¹)	C_0 (mg L ⁻¹)	Std.Error C_0 (mg L ⁻¹)	C_{15}/C_0	
Filtered	Ag	0.5	5.42E-03 ±	7.13E-04	3.43E-01 ±	5.54E-03	6.95E-01
		2.5	6.19E-03 ±	1.32E-03	1.79E+00 ±	3.34E-02	7.64E-01
		10	9.94E-03 ±	5.49E-03	7.77E+00 ±	1.03E-01	9.38E-01
	C_{60}	5	1.42E-01 ±	1.13E-01	1.01E+00 ±	3.17E-02	6.27E-02
		25	1.12E-01 ±	6.92E-03	8.39E+00 ±	4.58E-02	7.52E-03
		100	1.07E-01 ±	7.74E-03	2.83E+01 ±	2.08E-01	2.47E-03
	CaO_2	0.5	3.82E-03 ±	7.81E-04	3.96E-01 ±	8.34E-03	7.34E-01
		2.5	6.07E-03 ±	3.37E-03	2.09E+00 ±	5.81E-02	8.92E-01
		10	1.12E-02 ±	6.45E-03	8.30E+00 ±	1.39E-01	9.22E-01
	SiO_2 -Ag	0.5	4.81E-03 ±	3.28E-03	2.58E-01 ±	1.41E-02	7.32E-01
		2.5	6.33E-03 ±	3.47E-03	1.41E+00 ±	7.01E-02	7.21E-01
		10	3.14E-02 ±	5.99E-03	5.98E+00 ±	7.49E-02	8.43E-01
Unfiltered	Ag	0.5	5.44E-03 ±	1.44E-03	3.70E-01 ±	5.42E-03	8.53E-01
		2.5	4.90E-03 ±	6.42E-04	1.93E+00 ±	9.98E-03	9.03E-01
		10	8.14E-03 ±	2.31E-03	8.20E+00 ±	1.52E-01	8.29E-01
	C_{60}	5	1.14E-01 ±	1.23E-02	1.27E+00 ±	1.11E-02	5.63E-02
		25	1.54E-01 ±	1.08E-02	1.38E+01 ±	2.96E-02	5.67E-03
		100	1.11E-01 ±	7.46E-03	3.59E+01 ±	2.17E-01	2.73E-03
	CaO_2	0.5	4.46E-03 ±	1.26E-03	3.94E-01 ±	9.14E-03	8.10E-01
		2.5	3.59E-03 ±	1.21E-03	2.03E+00 ±	4.55E-02	8.56E-01
		10	4.70E-03 ±	1.05E-03	8.29E+00 ±	1.15E-01	8.56E-01
	SiO_2 -Ag	0.5	4.13E-03 ±	6.01E-04	2.86E-01 ±	5.92E-03	6.38E-01
		2.5	3.69E-03 ±	9.20E-04	1.54E+00 ±	2.50E-02	8.27E-01
		10	1.14E-02 ±	1.38E-02	5.56E+00 ±	1.09E-01	9.72E-01
IJ Filtered	Ag	0.5	-2.16E-03	1.27E-02	1.85E-01	1.77E-02	
		2.5	7.60E-04	2.43E-03	1.31E+00	7.61E-02	
		10	7.60E-05 ^a ±	1.34E-04	7.01E+00 ±	2.40E-01	9.44E-01
	C_{60}	5	1.35E-01 ±	1.83E-02	2.61E+00 ±	1.73E-02	9.47E-03
		25	1.05E-01 ±	8.79E-03	5.58E+00 ±	4.97E-02	1.16E-02
		100	1.18E-01 ±	7.91E-03	3.92E+01 ±	1.99E-01	5.83E-03
	CaO_2	0.5	2.75E-03 ±	1.52E-03	2.41E-01 ±	1.83E-02	5.88E-01
		2.5	3.33E-03 ±	8.54E-04	1.81E+00 ±	1.27E-01	2.60E-01
		10	1.29E-02 ±	2.58E-03	8.63E+00 ±	6.85E-01	1.21E-04
	SiO_2 -Ag	0.5	5.54E-02 ±	2.00E-02	2.31E-01 ±	4.61E-03	8.17E-01
		2.5	2.71E-03	2.74E-03	9.25E-01	7.22E-02	
		10	5.15E-02 ±	1.35E-02	6.13E+00 ±	1.49E-01	7.12E-01

Table S2.4 (continued)

		V_s (m d ⁻¹)	Std.Error V_s (m d ⁻¹)	C_0 (mg L ⁻¹)	Std.Error C_0 (mg L ⁻¹)	C_{15}/C_0		
IJ	Unfiltered	0.5	2.84E-03 ±	2.98E-03	1.89E-01 ±	2.74E-02	5.24E-01	
		2.5	8.66E-04 ^a	1.41E-04	1.30E+00	4.34E-02	6.26E-01	
		10	1.08E-04 ±	8.77E-05	7.23E+00 ±	1.77E-01	9.14E-01	
	C ₆₀	5	8.34E-02 ±	5.87E-03	9.38E-01 ±	1.12E-02	1.90E-02	
		25	7.56E-02 ±	7.76E-03	2.94E+00 ±	6.13E-02	8.28E-03	
		100	8.75E-02 ±	4.38E-03	3.05E+01 ±	2.41E-01	1.88E-03	
	CeO ₂	0.5	7.18E-03 ±	2.06E-03	4.17E-01 ±	3.50E-02	2.54E-01	
		2.5	6.49E-03 ±	1.31E-03	1.83E+00 ±	1.23E-01	1.35E-01	
		10	1.15E-02 ±	2.07E-03	8.72E+00 ±	6.08E-01	7.14E-03	
	SiO ₂ -Ag	0.5	4.32E-03 ±	6.97E-04	2.63E-01 ±	6.85E-03	5.73E-01	
		2.5	1.58E-02 ±	4.59E-03	1.37E+00 ±	5.14E-02	7.00E-01	
		10	8.78E-03 ±	1.59E-03	6.13E+00 ±	1.70E-01	5.81E-01	
	KG	Filtered	0.5	4.08E-03 ±	9.71E-04	3.10E-01 ±	7.18E-03	7.52E-01
			2.5	1.13E-02 ±	5.37E-03	1.83E+00 ±	4.00E-02	8.88E-01
			10	1.37E-04 ^a ±	6.99E-05	7.72E+00 ±	1.41E-01	9.22E-01
C ₆₀		5	1.80E-01 ±	3.37E-02	3.20E+00 ±	8.87E-03	1.20E-02	
		25	1.13E-01 ±	8.62E-03	1.01E+01 ±	6.75E-02	4.46E-03	
		100	1.13E-01 ±	7.78E-03	3.34E+01 ±	2.01E-01	4.70E-03	
CeO ₂		0.5	4.04E-03 ±	2.45E-03	3.67E-01 ±	7.87E-03	8.95E-01	
		2.5	7.30E-05 ^a ±	1.00E-04	1.85E+00 ±	4.75E-02	9.22E-01	
		10	9.04E-03 ±	5.44E-03	7.85E+00 ±	1.82E-01	9.00E-01	
SiO ₂ -Ag		0.5	1.03E-02 ±	9.31E-03	3.09E-01 ±	7.64E-03	9.22E-01	
		2.5	5.66E-05 ^a ±	7.86E-05	1.52E+00 ±	3.08E-02	9.65E-01	
		10	7.52E-05 ^a ±	9.42E-05	5.85E+00 ±	1.41E-01	9.37E-01	
Unfiltered		Ag	0.5	5.87E-03 ±	1.86E-03	3.37E-01 ±	2.37E-02	4.62E-01
			2.5	6.38E-03 ±	2.60E-03	1.67E+00 ±	5.65E-02	8.09E-01
			10	1.61E-04 ^a ±	9.12E-05	7.45E+00 ±	1.77E-01	9.10E-01
	C ₆₀	5	1.08E-01 ±	9.42E-03	8.47E-01 ±	7.00E-03	4.79E-02	
		25	7.49E-02 ±	4.12E-03	3.47E+00 ±	3.90E-02	1.36E-02	
		100	1.08E-01 ±	8.65E-03	3.66E+01 ±	2.84E-01	1.82E-03	
	CeO ₂	0.5	3.06E-03 ±	1.12E-03	3.79E-01 ±	1.45E-02	7.44E-01	
		2.5	3.05E-03 ±	9.11E-04	1.99E+00 ±	5.79E-02	7.44E-01	
		10	4.66E-03 ±	9.86E-04	7.81E+00 ±	8.95E-02	8.69E-01	
	SiO ₂ -Ag	0.5	2.98E-03 ±	1.44E-03	3.01E-01 ±	2.86E-03	9.52E-01	
		2.5	2.20E-03 ±	1.69E-03	1.54E+00 ±	2.38E-02	9.45E-01	
		10	1.18E-02 ±	4.76E-03	6.12E+00 ±	5.78E-02	9.41E-01	

Table S2.4 (continued)

		V_s (m d ⁻¹)	Std.Error V_s (m d ⁻¹)	C_0 (mg L ⁻¹)	Std.Error C_0 (mg L ⁻¹)	C_{15}/C_0	
Filtered	Ag	0.5	2.31E-02 ±	2.83E-02	9.74E-02 ±	2.37E-02	5.50E-01
		2.5	7.63E-03 ±	3.60E-03	1.11E+00 ±	1.37E-01	3.27E-01
		10	1.01E-02 ±	8.06E-03	6.59E+00 ±	4.08E-01	7.92E-01
	C_{60}	5	6.61E-02 ±	8.34E-03	3.62E-01 ±	1.06E-02	6.22E-02
		25	1.01E-01 ±	9.05E-03	4.38E+00 ±	4.52E-02	9.61E-03
		100	1.26E-01 ±	7.74E-03	4.38E+01 ±	1.72E-01	1.10E-03
	CeO_2	0.5	1.18E-02 ±	7.07E-03	3.41E-01 ±	6.00E-02	2.83E-01
		2.5	9.72E-03 ±	2.99E-03	1.89E+00 ±	2.19E-01	1.30E-02
		10	3.94E-02 ±	8.28E-05	7.94E+00 ±	6.43E-03	6.80E-04
	SiO_2 -Ag	0.5	3.33E-03 ±	1.64E-03	1.26E-01 ±	2.30E-02	5.11E-01
		2.5	1.01E-02 ±	3.01E-03	6.87E-01 ±	5.99E-02	2.57E-01
		10	1.04E-02 ±	2.85E-03	4.58E+00 ±	4.56E-01	5.62E-02
MS Unfiltered	Ag	0.5	n.a.	n.a.	n.a.	n.a.	2.63E-01
		2.5	5.63E-03 ±	3.64E-03	1.05E+00 ±	1.52E-01	4.20E-01
		10	1.01E-02 ±	7.97E-03	6.55E+00 ±	2.89E-01	8.29E-01
	C_{60}	5	1.30E-01 ±	9.19E-03	2.63E+00 ±	1.07E-02	6.88E-03
		25	1.36E-01 ±	4.38E-03	1.28E+01 ±	2.02E-02	2.29E-03
		100	7.39E-02 ±	5.39E-04	4.08E+01 ±	6.30E-02	9.31E-04
	CeO_2	0.5	9.43E-03 ±	4.11E-03	2.72E-01 ±	4.24E-02	6.09E-02
		2.5	1.85E-02 ±	1.83E-03	1.87E+00 ±	7.77E-02	6.75E-03
		10	5.52E-02 ±	2.71E-03	7.98E+00 ±	1.19E-01	4.97E-04
	SiO_2 -Ag	0.5	1.31E-02 ±	6.82E-03	2.02E-01 ±	2.54E-02	4.07E-01
		2.5	1.04E-02 ±	4.37E-03	8.53E-01 ±	9.84E-02	3.11E-01
		10	9.22E-03 ±	1.69E-03	3.56E+00 ±	2.29E-01	8.14E-02
NZ Filtered	Ag	0.5	3.53E-03 ±	1.39E-03	3.64E-01 ±	9.98E-03	7.90E-01
		2.5	1.19E-02 ±	1.49E-02	1.79E+00 ±	1.03E-01	8.97E-01
		10	-1.71E-03	4.51E-03	5.52E+00	5.62E-01	
	C_{60}	5	1.22E-01 ±	9.45E-03	5.84E-01 ±	2.90E-03	7.33E-02
		25	1.28E-01 ±	2.06E-03	2.25E+01 ±	2.17E-02	2.75E-03
		100	1.33E-01 ±	4.59E-03	6.08E+01 ±	1.12E-01	1.75E-03
	CeO_2	0.5	1.88E-02 ±	1.50E-03	2.90E-01 ±	9.22E-03	6.38E-02
		2.5	1.58E-02 ±	1.50E-03	1.93E+00 ±	7.53E-02	3.36E-03
		10	4.01E-02 ±	1.50E-04	8.70E+00 ±	1.25E-02	9.04E-04
	SiO_2 -Ag	0.5	5.70E-03 ±	8.37E-04	2.97E-01 ±	3.88E-03	7.65E-01
		2.5	7.70E-03 ±	1.83E-03	1.50E+00 ±	9.78E-02	2.75E-01
		10	1.53E-02 ±	5.01E-03	6.18E+00 ±	7.46E-01	1.06E-01

Table S2.4 (continued)

		V_s (m d^{-1})	Std.Error V_s (m d^{-1})	C_0 (mg L^{-1})	Std.Error C_0 (mg L^{-1})	C_{15}/C_0	
NZ	Unfiltered	0.5	4.32E-03 ±	6.67E-04	3.57E-01 ±	8.24E-03	6.17E-01
		2.5	6.08E-03 ±	1.24E-03	1.52E+00 ±	7.75E-02	3.24E-01
		10	8.93E-05 ±	2.13E-03	6.56E+00 ±	3.51E-01	9.26E-01
	C_{60}	5	4.20E-02 ±	3.21E-03	2.61E+00 ±	7.38E-02	8.78E-03
		25	3.98E-02 ±	3.66E-03	1.05E+01 ±	3.69E-01	2.80E-03
		100	1.26E-01 ±	4.17E-03	6.16E+01 ±	1.30E-01	9.85E-04
	CeO_2	0.5	7.92E-03 ±	1.45E-03	2.21E-01 ±	1.47E-02	4.27E-02
		2.5	1.51E-02 ±	2.27E-03	1.57E+00 ±	9.60E-02	4.83E-03
		10	4.63E-02 ±	8.32E-03	8.03E+00 ±	5.06E-01	7.48E-04
	SiO_2 -Ag	0.5	6.44E-03 ±	5.94E-04	2.33E-01 ±	2.44E-03	7.02E-01
		2.5	6.52E-03 ±	1.11E-03	1.37E+00 ±	5.35E-02	3.98E-01
		10	1.11E-02 ±	1.86E-03	5.69E+00 ±	3.29E-01	1.12E-01
Filtered	Ag	0.5	2.64E-03 ±	1.60E-03	1.27E-01 ±	1.88E-02	4.14E-01
		2.5	3.31E-03 ±	9.51E-04	1.03E+00 ±	6.79E-02	4.06E-01
		10	3.04E-03 ±	1.44E-03	7.10E+00 ±	3.66E-01	6.57E-01
	C_{60}	5	1.54E-01 ±	4.91E-02	8.66E-01 ±	7.94E-03	3.52E-02
		25	1.35E-01 ±	1.13E-02	8.41E+00 ±	3.51E-02	5.24E-03
		100	1.23E-01 ±	7.00E-03	3.18E+01 ±	1.23E-01	3.10E-03
	CeO_2	0.5	2.40E-03 ±	1.21E-03	2.71E-01 ±	2.25E-02	5.86E-01
		2.5	3.25E-03 ±	1.75E-03	1.28E+00 ±	2.39E-01	8.78E-02
		10	3.72E-02 ±	9.76E-04	7.23E+00 ±	7.51E-02	4.24E-04
	SiO_2 -Ag	0.5	4.12E-03 ±	7.30E-04	1.96E-01 ±	9.85E-03	2.53E-01
		2.5	5.35E-03 ±	5.37E-04	1.25E+00 ±	2.96E-02	3.93E-01
		10	5.66E-03 ±	4.45E-04	5.92E+00 ±	1.22E-01	3.19E-01
RL	Ag	0.5	1.08E-02 ±	1.85E-03	1.64E-01 ±	7.81E-03	2.88E-01
		2.5	4.85E-03 ±	5.62E-04	1.20E+00 ±	3.52E-02	3.39E-01
		10	1.99E-03 ±	1.68E-03	6.79E+00 ±	3.35E-01	7.68E-01
	C_{60}	5	9.69E-02 ^a ±	2.21E-02	1.34E+00 ±	3.92E-02	4.54E-02
		25	1.09E-01 ±	8.06E-03	5.51E+00 ±	3.93E-02	3.66E-03
		100	1.26E-01 ±	7.76E-03	3.94E+01 ±	1.54E-01	1.03E-03
	CeO_2	0.5	2.23E-02 ±	7.48E-03	3.32E-01 ±	4.46E-02	7.41E-02
		2.5	7.79E-03 ±	8.83E-04	1.74E+00 ±	7.34E-02	2.07E-02
		10	4.39E-02 ±	1.63E-03	6.11E+00 ±	8.21E-02	8.35E-04
	SiO_2 -Ag	0.5	6.39E-03 ±	4.23E-04	2.45E-01 ±	4.87E-03	2.09E-01
		2.5	7.41E-03 ±	7.35E-04	1.34E+00 ±	3.62E-02	2.75E-01
		10	6.25E-03 ±	4.24E-04	6.01E+00 ±	1.19E-01	2.36E-01

n.a.: no data available

^a C_{ns} assumed 0 in order to estimate V_s .

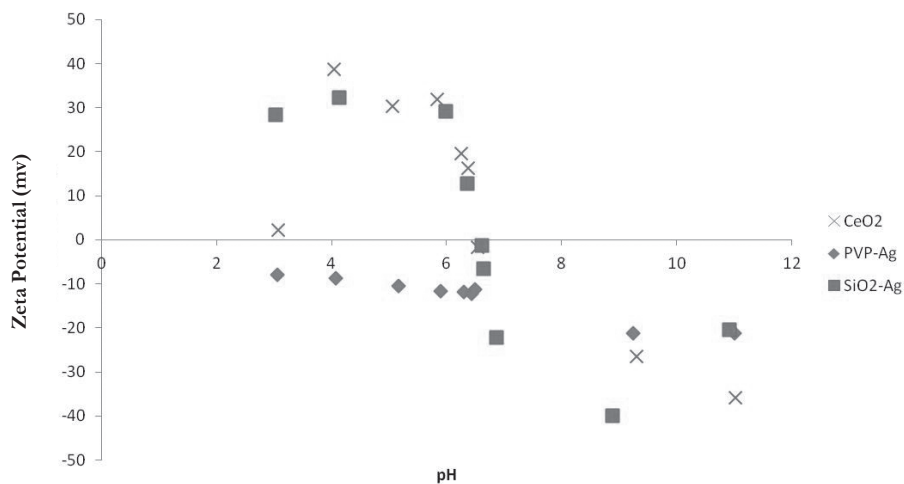


Figure S2.1 Zeta potential of 10 mg L⁻¹ dilution of nanoparticle stocks in deionized water as a function of pH.

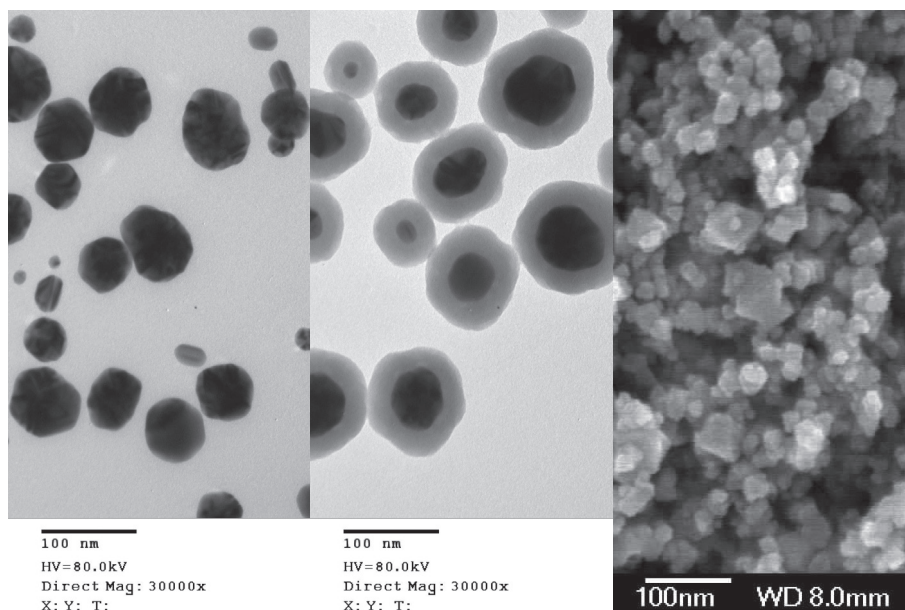


Figure S2.2 Transmission Electron Microscopy (JEOL 1010 Transmission Electron Microscope) images of PVP-Ag (left) and SiO₂-Ag nanoparticles (middle) kindly provided by NanoComposix and scanning electron microscopy image (20.0 kV) of CeO₂ nanoparticles (right).

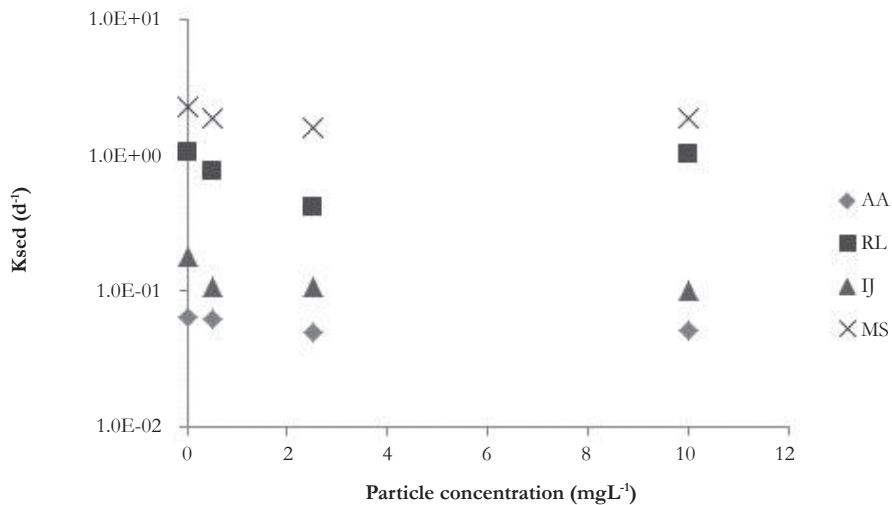


Figure S2.3 Sedimentation rate constants for NC, calculated for water types where Al could be used as proxy for the natural colloid fraction.

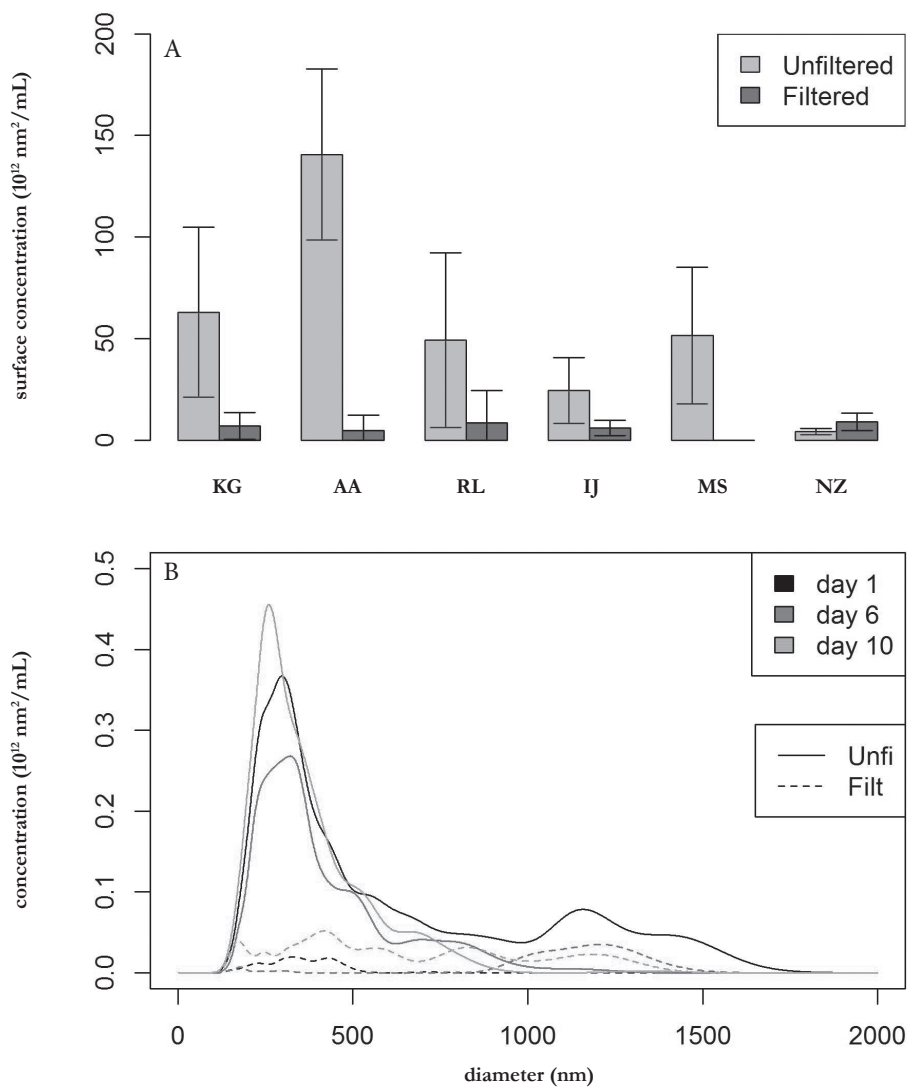


Figure S2.4 A: Total surface area concentration present in filtered and unfiltered natural waters.
B: Surface area distribution of filtered and unfiltered AA water.

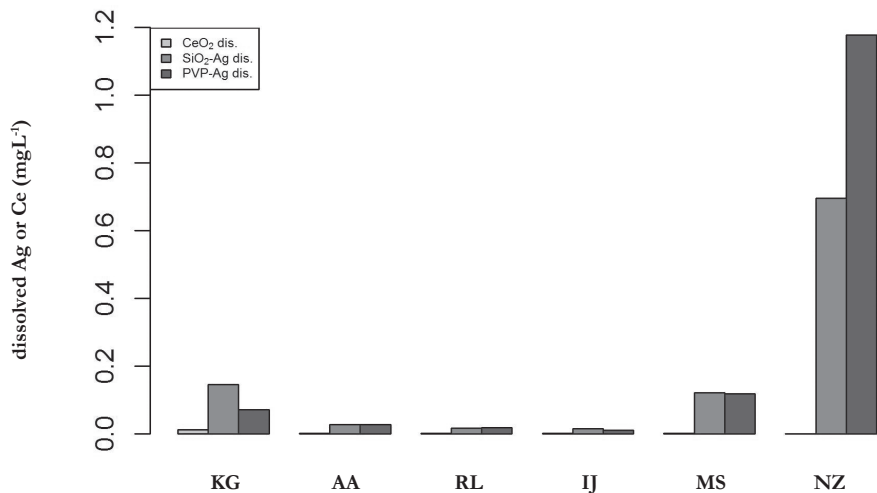


Figure S2.5 Concentration of dissolved metal (Me) Ag and Ce in MilliQ water after 15 days at pH ranging from 3 to 11. Initial particle suspensions contained 10 mg L⁻¹ CeO₂, SiO₂-Ag or PVP-Ag nanoparticles.

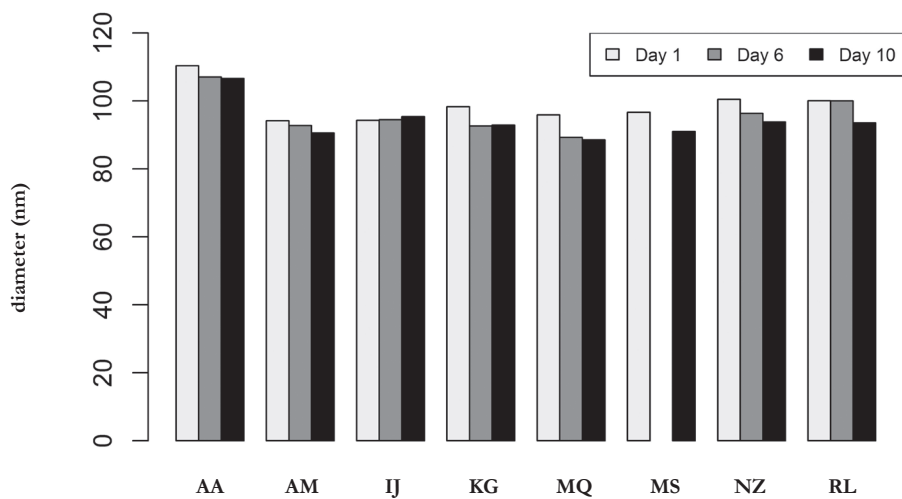


Figure S2.6 Average PVP-Ag particle diameter after 1, 6 and 10 days in different water types.

Estimating the heteroaggregation rate between nanoparticles and natural colloids from sedimentation experiments

This SI section describes the method to estimate the heteroaggregation rate from sedimentation experiments. First, an introductory outline of the approach is given. Then, the different steps in the calculation of k_{het} are described in terms of fundamental as well as simplified equations for aggregation-sedimentation. Finally, it is shown how the model equations fit to simulated aggregation-sedimentation data.

Principle

ENP sedimentation experiments were performed for filtered (no NC) and unfiltered natural water samples. In the unfiltered experimental systems, removal of the engineered nanoparticles (ENPs) from the water column can be assumed to be driven by (ENP-ENP) homoaggregation, (ENP-NC) heteroaggregation and/or settling of ENP aggregates [1-5]. To determine the heteroaggregation rate, the process parameters for heteroaggregation need to be isolated from those for homoaggregation and sedimentation. This is done as follows. First, it is assumed that aggregation is the rate limiting process for the observed removal of ENPs from the water phase. This is based on the logic that aggregates first need to be large enough for sedimentation to occur [6]. If aggregation is the rate determining process, the observed removal rates will depend on the parameters describing homo- and hetero-aggregation rather than on parameters describing sedimentation. Second, the process parameters for homoaggregation are estimated by fitting a homoaggregation-only process equation to the data for the sedimentation experiments with filtered water samples. This assumes that heteroaggregation does not occur in water samples where NC are removed by filtration. Finally, a process equation accounting for homo- and heteroaggregation is fitted to the data for the sedimentation experiments in unfiltered water samples, using the parameters for homoaggregation from the previous step. This leaves the process parameters for heteroaggregation as the only unknowns. The process equations and assumptions required in the different steps are discussed in the next section.

Model equations

The basics for the calculation of the contributions of homoaggregation and heteroaggregation to the removal of ENPs from the water phase are condensed in the combined Von Smoluchowski–Stokes equation [7]:

$$\frac{dNC_j}{dt} = \frac{1}{2} \sum_{i=1}^{j-1} \alpha_{i,j-i} K_{i,j-i} N_i N_{j-i} - N_j \sum_{i=1}^{i=\infty} \alpha_{i,j} K_{i,j} N_i - \alpha_{NC,j} K_{NC,j} N_{NC} N_j - \frac{v_{s,j}}{d_s} N_j \quad (S2.1)$$

With:

- α_{ij} : attachment efficiency between ENP aggregates i and j
- $\alpha_{NC,j}$: attachment efficiency between ENP and NC
- j : number of primary NPs in ENP aggregate
- K_{ij} : collision frequency between ENP aggregates i and j [$\text{m}^3 \text{s}^{-1}$]
- $K_{NC,j}$: collision frequency between ENP particle aggregates j and NC [$\text{m}^3 \text{s}^{-1}$]
- N_j : Number concentration of the ENP aggregate j [m^{-3}]
- N_{NC} : Number concentration of NC [m^{-3}]
- $v_{s,j}$: Sedimentation rate of ENP aggregate j [m s^{-1}]
- d_s : Sedimentation length [m]

and where the first two terms accounts for homoaggregation, the third term for heteroaggregation, and the last term for sedimentation of ENP aggregates.

The concentration of natural colloids N_{NC} is assumed to decrease due to Stokes settling [3, 8]:

$$\frac{dN_{NC}}{dt} = -\frac{v_{s,NC}}{d_s} N_{NC} \quad (\text{S2.2})$$

Below, Eq. S2.1 is simplified based on a series of informed assumptions, which subsequently are validated against simulations using the full deterministic Eq. S2.1. First it is assumed that aggregation is the rate limiting process for the observed removal of ENPs from the water phase. This is based on the logic that aggregates first need to be large enough for sedimentation to occur as outlined by [6]. This means that the aggregation terms in Eq. S2.1 are considered to be rate determining and that the last term in Eq. S2.1 can be omitted. Second, it is assumed that the summations in Eq. S2.1 can be replaced by single terms accounting for the apparent critical collision behaviour for sedimentation. This is motivated as follows. The summation in Eq. S2.1 accounts for numerous collisions that will not (yet) lead to homo- or heteroaggregates large enough to settle. However, a certain fraction of all possible collisions will at some point reach a critical limit after which rapid settling occurs. The measured removal in the sedimentation experiments relates to this apparent removal of settleable ENPs only (ENP_{crit}). Because size distributions of these settling ENP aggregates may not be monodisperse, the single terms are governed by apparent parameters reflecting average properties of the particles at the onset of settling. Third, it is assumed that the ENP concentration change in the overlying water is determined by aggregation to settling particles only i.e. is not affected by progressive aggregation to larger particles. Progressive aggregation cannot affect ENP_{crit} concentrations beyond the critical size for sedimentation because they would have settled already. This implies that the first two terms for aggregation in Eq. S2.1 can be combined. Consequently, Eq. S2.1 can be simplified to:

$$\frac{dC_{ENP,crit}}{dt} = -\alpha_{hom,crit} K_{hom,crit} C_{ENP,crit}^q - \alpha_{het,crit} K_{het,crit} C_{NC} C_{ENP,crit} \quad (\text{S2.3})$$

Where

$C_{ENP,crit}$ is the concentration of settleable ENPs

$K_{hom,crit}$ is the apparent collision rate constant for the formation of settleable ENP homoaggregates

$\alpha_{hom,crit}$ is the apparent attachment efficiency for settleable ENP homoaggregates

$\alpha_{het,crit}$ is the apparent attachment efficiency for settleable ENP-NC heteroaggregates

$K_{het,crit}$ is the apparent collision rate constant for the formation of settleable ENP heteroaggregates

The exponent q defines the kinetics for homoaggregation and may take a value between 1 and 2. For instance, the formation of doublets would follow second order kinetics ($q = 2$), whereas the kinetics of collisions between large aggregates and primary particles would approach pseudo first order kinetics ($q = 1$).

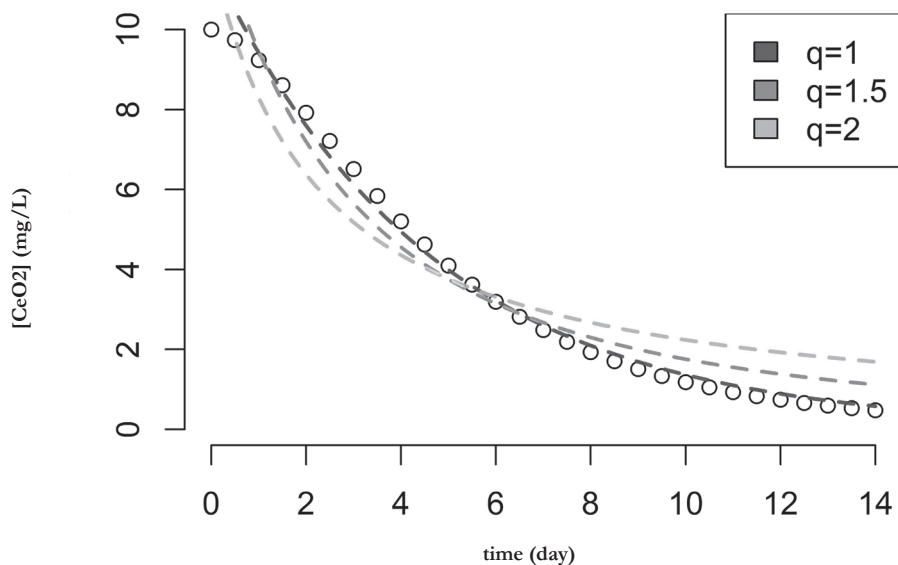


Figure S2.7 Fit of the homoaggregation term in Eq. S2.3 for q is 1, 1.5 and 2, to model simulation data calculated from a mechanistic numerical model based on the Von Smoluchowski–Stokes equation (Eq. S2.1 and Eq. S2.2). Mechanistic model for 10 mg L^{-1} 15 nm CeO_2 ENPs.

The best value for q was obtained by fitting the analytical solution to Eq. S2.3 for q is 1, 1.5 and 2 respectively, against simulations based on Eq. S2.1. The simulations used a numerical model, which takes into account all size classes up to 350 nm CeO_2 ENP aggregates and all processes as condensed in Eq. S2.1. The largest aggregate consists of 2629 primary particles with a fractal dimension of 2.5. The fit for removal due to homoaggregation only is given in Figure S2.7. The simulation shows a time lag

of about 1 day needed for the formation of aggregates large enough for settling. From day 2 onwards the removal of ENPs from the water phase is best described by apparent first order removal kinetics, i.e. $q = 1$. Simulations with $q = 1.5$ and $q = 2$ showed a worse overall quality of fit (see Figure S2.7). With $q = 1$ and combination of Eq. S2.2, Eq. S2.3 can be further simplified to:

$$\frac{dC_{ENP}}{dt} = -\alpha_{hom,crit}K_{hom,crit}C_{ENP} - \alpha_{het,crit}K_{het,crit}C_{0,NC}e^{-\frac{v_{s,NC}t}{d}}C_{ENP} \quad (S2.4)$$

In summary, Eq. S2.4 describes how the concentration of the (operationally defined) settling ENP fraction changes over time, as a function of the processes that drive the production of aggregates. Aggregates that do not settle substantially in the time interval over which settling is monitored (15 days in the present experiments) are also formed. Furthermore, primary particles may be stabilised and not settle at all. The latter two categories of processes lead to a residual fraction, which is also operationally defined (Table 2.2, main paper).

Calculating the heteroaggregation rate

Eq. S2.4 can be fitted to ENP sedimentation data in order to estimate the product $\alpha_{hom,crit} \times K_{hom,crit}$ in Eq. S2.4, which is equal to the apparent critical homoaggregation rate constant $k_{hom,crit}$ ($\alpha_{hom,crit} \times K_{hom,crit} = k_{hom,crit}$). Therefore the contribution of homoaggregation to the removal of ENPs from the water phase is separately assessed by fitting the solution of the first term in Eq. S2.4 to the ENP concentration in time for filtered water (Eq. S2.5).

$$C(t) = C_0 e^{-k_{hom,crit}t} \quad (S2.5)$$

This assumes that heteroaggregation in filtered water is negligible due to the absence of natural colloids. The estimated values for $k_{hom,crit}$ then are substituted in the solution of Eq. S2.4, in which $\alpha_{het,crit} \times K_{het,crit} = k_{het,crit}$, is the only unknown. $V_{s,NC}$ is calculated according to Stokes from the density and radius of the NC (Table 2.1, main paper). The analytical solution to Eq. S2.4 is:

$$C(t) = \frac{C_0 e^{-k_{hom,crit}t} e^{-\frac{v_{s,NC}t}{d}}}{e^{\frac{k_{het,crit}C_{0,NC}d_s}{v_{s,NC}}}} \quad (S2.6)$$

which then can be fitted to the sedimentation data in unfiltered water to obtain the heteroaggregation rate constant $k_{het,crit}$.

To show the validity of the simplified aggregation-sedimentation model Eq. S2.5 and S2.6 were fitted to simulation results calculated with the full Smoluchowski–Stokes model (i.e. Eq. S2.1 and S2.2), thus taking all homo- and heteroaggregation interactions into account (Figure S2.8). The simulations used a numerical model which

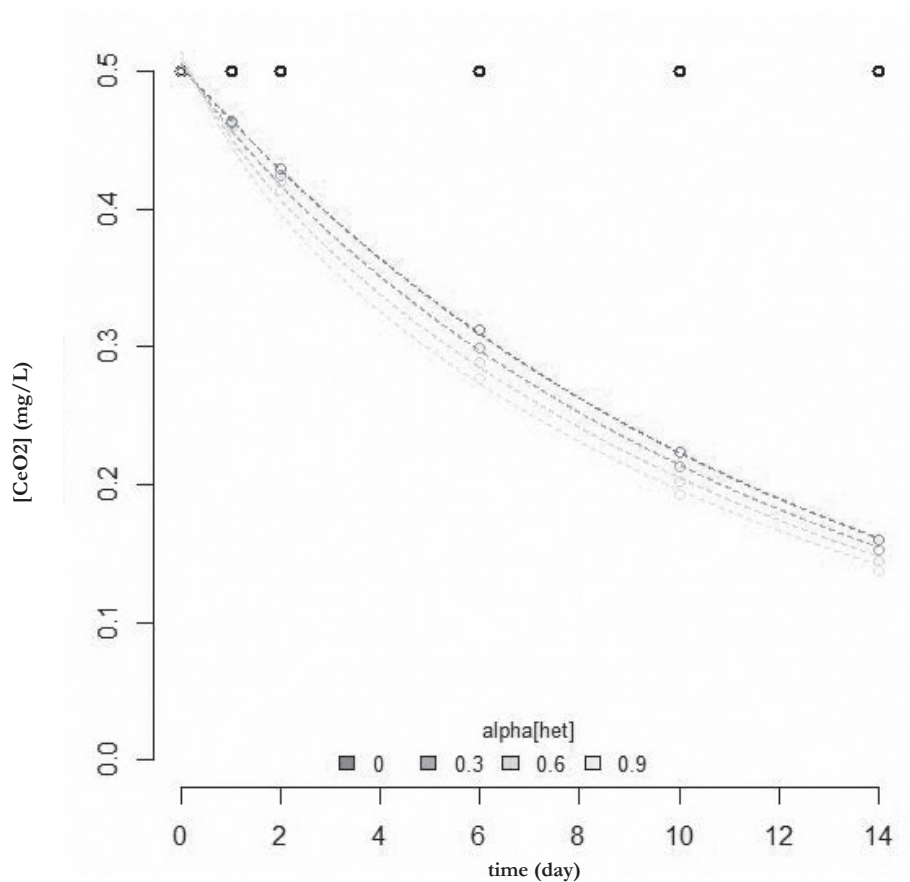


Figure S2.8 Plot of fit of Eq. S2.6 to simulated data. With simulated data of sedimentation of CeO₂ ENPs by homo- and heteroaggregation with α_{het} ranging between 0 and 0.9. Black open circles denote the total concentration of ENP homoaggregates and ENP-NC heteroaggregates in suspension and in the sediment.

takes into account all size classes up to 1 μm CeO₂ ENP aggregates and processes as given by Eq. S2.1. The primary CeO₂ particle size was 20 nm and an initial particle size distribution with an average size of 175 nm. The NC had an average radius of 0.5 μm , density of 1250 kg m⁻³, and 100 mg L⁻¹ initial concentration. A 0.5 mg L⁻¹ CeO₂ suspension with α_{het} set to 0, 0.3, 0.6, 0.9 were simulated. The case where α_{het} is 0 was used to estimate $k_{hom,crit}$ by fitting Eq. S2.5 to the simulated data using the non-linear least squares method in R. Subsequently Eq. S2.6 was fit to the simulated data. It appears from Figure S2.8 that the simplified model adequately captures the relationship between [CeO₂] and time as calculated by the full Smoluchowski–Stokes model.

Relationships between homo- and heteroaggregation rates, collision frequency and attachment efficiency

As the heteroaggregation rate $k_{het,crit}$ equates to the product of α_i and $K_{ENP,NC,i}$ (Eq. S2.1) in theory α values can be directly calculated, if $K_{ENP,NC}$ values are known. From basic colloid theory it is known that $K_{ENP,NC}$ can be estimated theoretically using the known description of the three main processes affecting the collision frequency: Brownian motion, shear rate and differential settling [6, 7]. The sum of the quantitative description of these three processes result in the collision frequency given by Eq. S2.7.

$$K_{ENP,NC} = \frac{\frac{2k_b T (a_{NC} + a_{ENP})^2}{3\mu a_{NC} a_{ENP}} + \frac{4}{3} G (a_{NC} + a_{ENP})^3 + \pi (a_{NC} + a_{ENP})^2 |v_{s,NC} - v_{s,ENP}|}{\rho_{NC} V_{NC}} \quad (S2.7)$$

Where

- k_b : Boltzman constant [$\text{m}^2 \text{kg s}^{-2} \text{K}^{-1}$]
- T : Temperature [K]
- μ : Viscosity [Pa s]
- a_{NC} : NC radius [m]
- a_{ENP} : ENP j radius [m]
- G : Shear rate [s^{-1}]
- v_s : Sedimentation rate [m s^{-1}]

with v_s given by:

$$v_s = \frac{2a^2 (\rho_p - \rho_w)g}{9\mu} \quad (S2.8)$$

in which

- ρ_p : Density of the ENP or NC [kg m^{-3}]
- ρ_w : Density of suspending medium [kg m^{-3}]
- g : Gravitational acceleration [m s^{-2}]

The density of the NC is calculated based on the dry weight (DW) and ash free dry weight (AFDW), by assuming that AFDW consists of an organic NC fraction with low density (1250 kg m^{-3}) and a mineral fraction with relatively high density (2700 kg m^{-3}) [9]. Because of the uncertainties in the applicability of Eq. S2.7 to the natural and heterogeneous conditions in our water samples, calculations of α and K were omitted.

Table S2.5. Homo and heteroaggregation rates (k_{crit}) obtained using Eq. S2.5 and S2.9 in 6 natural water with 4 ENP types at the lowest initial particle concentration.

		KG	AA	RL	IJ	MS	NZ
C_{60}	$k_{hom.crit}$	1.22E+00	1.11E+00	1.14E+00	1.23E+00	1.11E+00	1.10E+00
	$k_{het.crit}$	-1.98E+02	6.82E+00	-1.78E+01	-4.23E+01	1.49E+02	6.00E+02
CeO_2	$k_{hom.crit}$	9.28E-01	9.42E-01	9.57E-01	9.56E-01	1.01E+00	1.10E+00
	$k_{het.crit}$	2.63E+01	-6.28E+00	1.45E+02	5.12E+01	1.04E+02	1.14E+02
SiO_2 -Ag	$k_{hom.crit}$	9.26E-01	9.42E-01	1.01E+00	9.35E-01	9.66E-01	9.39E-01
	$k_{het.crit}$	-4.61E+00	8.74E+00	1.34E+01	2.16E+01	1.54E+01	2.40E+01
PVP-Ag	$k_{hom.crit}$	9.40E-01	9.45E-01	9.80E-01	9.37E-01	9.61E-01	9.37E-01
	$k_{het.crit}$	6.96E+01	-1.31E+01	2.54E+01	2.47E+01	5.01E+01	6.98E+01

$k_{hom.crit}$ in [d^{-1}], $k_{het.crit}$ in [$m^3 kg^{-1} d^{-1}$]

Sources of sedimentation rates obtained from the literature

Chinnapongse et al. [10]:

The sedimentation rates were obtained from the figures in their paper. The sedimentation rate was calculated by multiplying the observed rates with the sedimentation length (10.6 mm). The water surface reached 23 mm above the base of the cuvette. And the measurement height was between 9.2 mm and 15.6 mm above the base of the cuvette, this gives an average sedimentation length of 10.6 mm. It should also be noted that the k_{obs} was the rate of disappearance of absorbance from singly dispersed metallic silver nanoparticles. Potential mechanisms for their disappearance could range from agglomeration and sedimentation, to surface reactions that would quench the surface plasmon resonance absorbance of the silver metal nanoparticles, to dissolution of the particles.

Kennedy et al. [11]:

The raw sedimentation data was obtained from the author and Eq. 2.1 was fitted. The calculated sedimentation rates were obtained using a 16.75 mm sedimentation length. The water surface was 28-29 mm above the bottom of the cuvette. The exact measurement point was not clear, but most photo spectrometers measure between 8.5 and 15 mm above the bottom of the cuvette. In this case an average height of 11.75 mm is used resulting in a 16.75 mm sedimentation length.

Keller et al. [12]:

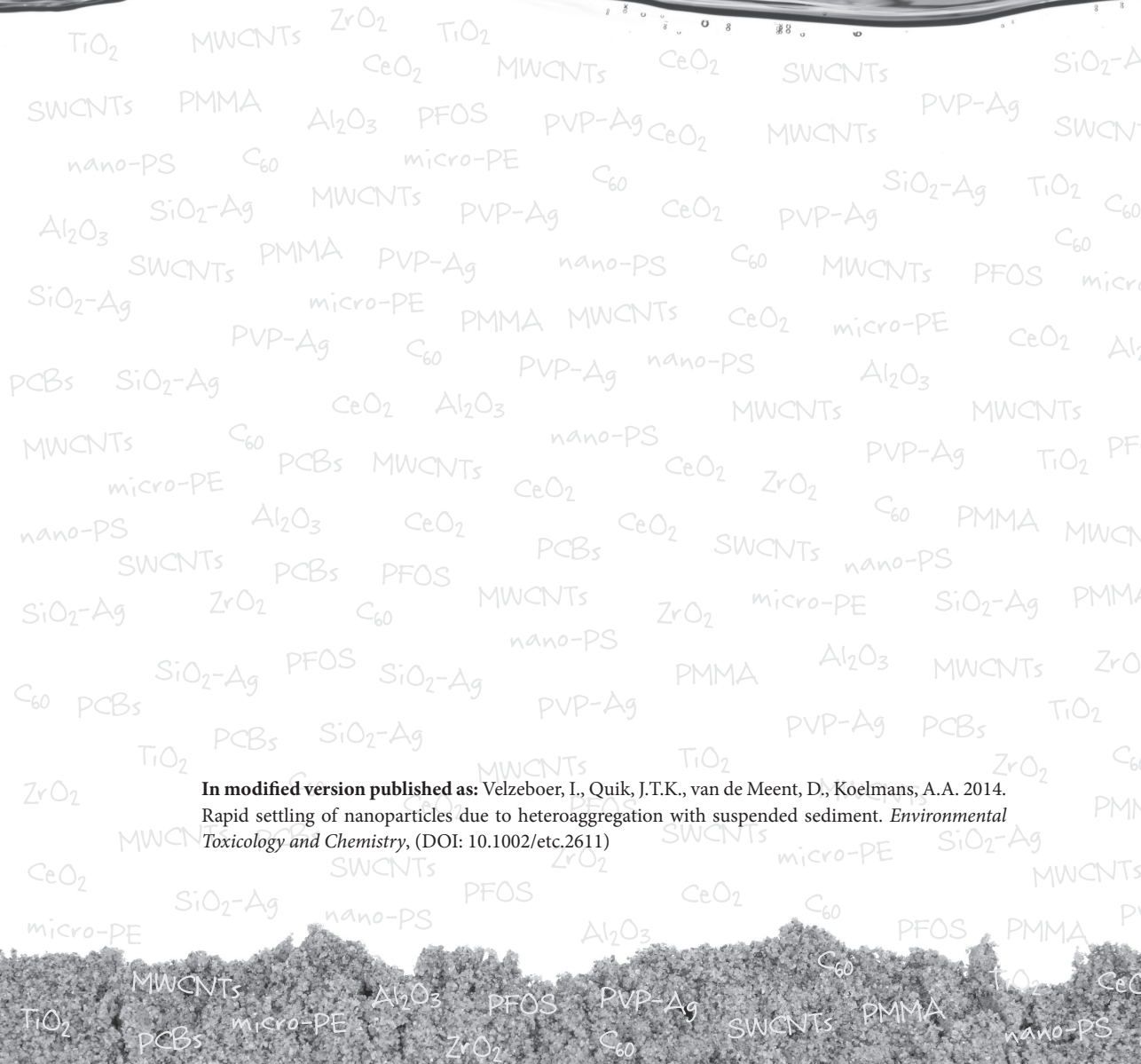
Sedimentation rates were obtained from the figures in their paper. The sedimentation length was 1 cm.

Chapter 3



TiO₂ C₆₀ ZrO₂ CeO₂ SWCNTs C₆₀ Al₂O₃
CNTs PMMA Al₂O₃ PFOS PVP-Ag MWCNTs PVP-Ag SWCNTs
nano-PS C₆₀ micro-PE PVP-Ag CeO₂ MWCNTs
SiO₂-Ag MWCNTs PVP-Ag C₆₀ CeO₂ PVP-Ag SiO₂-Ag TiO₂ SiO₂-Ag
ZrO₂ SWCNTs PMMA PVP-Ag nano-PS C₆₀ MWCNTs PFOS micro-PE
SiO₂-Ag micro-PE PMMA MWCNTs CeO₂ micro-PE CeO₂ Al₂O₃
SiO₂-Ag PVP-Ag C₆₀ PVP-Ag nano-PS Al₂O₃
CNTs C₆₀ nano-PS MWCNTs MWCNTs TiO₂
micro-PE PCBs MWCNTs CeO₂ CeO₂ ZrO₂ PVP-Ag TiO₂ PFOS
nano-PS Al₂O₃ CeO₂ PCBs CeO₂ SWCNTs C₆₀ PMMA MWCNTs
SWCNTs PCBs PFOS MWCNTs nano-PS ZrO₂ MWCNTs SiO₂-Ag PMMA
SiO₂-Ag PFOS SiO₂-Ag nano-PS PMMA Al₂O₃ MWCNTs ZrO₂
PCBs TiO₂ PCBs SiO₂-Ag PVP-Ag PVP-Ag PCBs TiO₂
TiO₂ PCBs SiO₂-Ag MWCNTs TiO₂ MWCNTs ZrO₂ C₆₀
micro-PE CeO₂ PFOS MWCNTs
MWCNTs PCBs SWCNTs micro-PE SiO₂-Ag PMMA
SiO₂-Ag SWCNTs PFOS ZrO₂ CeO₂ MWCNTs
nano-PS PMMA C₆₀ PFOS PVP-Ag C₆₀ PFOS PVP-Ag
MWCNTs Al₂O₃ PFOS TiO₂ CeO₂
PCBs micro-PE ZrO₂ C₆₀ SWCNTs PMMA nano-PS

Rapid settling of nanoparticles due to heteroaggregation with suspended sediment



In modified version published as: Velzeboer, I., Quik, J.T.K., van de Meent, D., Koelmans, A.A. 2014. Rapid settling of nanoparticles due to heteroaggregation with suspended sediment. *Environmental Toxicology and Chemistry*, (DOI: 10.1002/etc.2611)

Abstract

Sedimentation of engineered nanoparticles (ENPs) has been studied mainly in artificial media and stagnant systems mimicking natural waters. This neglects the role of turbulence and heteroaggregation with sediment. We studied the apparent sedimentation rates of selected ENPs (CeO_2 , PVP-Ag and SiO_2 -Ag) in agitated sediment-water systems resembling fresh, estuarine and marine waters. Experiments were designed to mimic low energy and periodically resuspended sediment water systems (14 days), followed by a long term aging, resuspension and settling phase (6 months), as would occur in receiving shallow lakes. ENPs in systems with periodical resuspension of sediment were removed with sedimentation rates between 0.14 and 0.50 m d^{-1} . The sedimentation rates did not vary much among ENP type, salinity and aging time, which is attributed to the capture of ENPs in sediment flocks. The sedimentation rates were one to two orders of magnitude higher than those reported for aggregation-sedimentation in stagnant systems without suspended sediment. Heteroaggregation rates were estimated and ranged between 0.151 and 0.547 $\text{L mg}^{-1} \text{d}^{-1}$, which is up to 29 times higher than those reported for natural colloids under quiescent settling conditions. We conclude that rapid scavenging and sedimentation drives removal of ENPs from the water column.

3.1 Introduction

Now that the use of engineered nanoparticles (ENPs) is increasing, the urge for refined exposure and risk assessment approaches for these materials is growing [1, 2]. For risk assessment, environmental concentrations of ENPs need to be known, in order to compare them with effect thresholds [3, 4]. Measurement of ENPs, however, is challenging, due to a lack of suitable methods for measuring low concentrations of ENPs in complex environmental matrices like natural waters, sediments or soils [5]. Consequently, exposure assessment needs to be assisted by modelling [6]. Modelling the fate of ENPs in surface waters, however, is also in its infancy and faces difficulties such as lack of data on ENP specific aggregation and sedimentation parameters. ENP fate models should quantify aggregation and sedimentation [7-10], which are crucial processes in natural waters. However, key factors that govern these processes like ENP aggregation rates, particle geometries and size distributions, as well as the influence of natural organic matter (NOM) and natural colloids (NC) typically are unknown [11-14]. Furthermore, it is not clear to what extent parameters driving the environmental fate of ENPs change with aging and alteration of the pristine primary ENPs [13].

Only recently studies start to focus on apparent conditional aggregation-sedimentation behaviour in laboratory tests mimicking natural water environments in order to find characteristic ranges of sedimentation behaviour as a function of particle type and main water characteristics [5, 8, 9, 15-17].

Several aquatic fate studies considered sedimentation of ENPs in stagnant systems focussing on the effects of water characteristics, including NOM [8, 9, 17-19]. In quiescent i.e. non-agitated conditions, ENPs settle very slowly. In waters with a depth ranging from a meter to several hundreds of meters they would remain in the water column for weeks to years if there are no other deposition mechanisms than the Stokes law of gravity settling and Brownian motion [20]. It has been shown that when attached to NOM, nanoparticles can form stable colloidal suspensions in the aqueous phase [21].

However, in more turbulent waters interaction will occur with much larger particles that enter the water column upon wind-induced resuspension or bioturbation. Turbulence may increase shear and hence the collision frequency, leading to faster and more extensive aggregation. Presence of NC and resuspended sediment particles (suspended solids, SS) may further increase the heteroaggregation and scavenging of ENPs that subsequently settle at much higher rates. Consequently, when sediment is present like in natural systems, nanoparticles are likely to end up in the sediment [7]. Stolzenbach et al. [22] argued that fine particles are preferentially removed from suspension by heteroaggregation in a hydrodynamically active “fluff” layer (porous and mobile layer) at the sediment-water interface driven by the near-bottom water motion or by activities of benthic organisms. Therefore, realistic conditions include turbulence and (periodic) resuspension of sediments in the water column. Especially in rivers and shallow lakes, SS loads have been reported to range from 5 to 200,000 mg L⁻¹ in some rivers [23]. This will obviously affect the cycling of NPs in water systems, and may overwhelm the settling rates observed in stagnant, low SS systems [24, 25]. As mentioned before, NOM can stabilize ENPs in the water phase, but SS can also increase the settling rates of ENPs or bring settled nanoparticles back into suspension. To date, the question whether resuspension leads to net mobilisation or removal of nanoparticles compared to stagnant systems has not been addressed. If resuspension of sediment plays an important role in scavenging ENPs from the water phase, it may be argued that water-only exposure is less relevant for the risk assessment of ENPs [5, 26].

Primary aim of the present study was to quantify the removal rates of selected ENPs in dynamic sediment-water systems for three water types; fresh, estuarine and marine, under realistic hydrodynamic conditions. Here, removal may include homo- and heteroaggregation, sedimentation and dissolution. Second aim was to infer ENP sedimentation rates and ENP-SS heteroaggregation rates from the removal rate data using a method outlined recently by Quik et al. [17]. Experimental systems and conditions were designed to mimic riverine low energy agitation and periodical resuspension of sediment water systems for a 14 day period. This was followed by a long term ENP aging phase of 6 months, in which the systems were periodically resuspended and allowed to settle, as would occur in a receiving stagnant reservoir, e.g. a shallow lake. After the 6 months aging period the systems were resuspended once again, but not agitated anymore, to mimic settling in such a truly stagnant

reservoir. This enabled us to quantify the removal rate for aged ENPs from the water column, including sediment interaction. Natural waters and sediment were used to mimic environmentally realistic systems. By using three types of water we could test the possible importance of aquatic geochemical variables. The observed sedimentation rates and heteroaggregation rates were evaluated against literature data recently reported for the same ENPs and waters in quiescent conditions [17].

3.2 Materials and methods

Chemicals

Ceriumdioxide (CeO_2) nanoparticles (20 nm) were supplied by Umicore Ltd. (Brussels), the suspension of 100 g L^{-1} in HNO_3 at pH 4 was made by University Collage Dublin. The CeO_2 ENP contained 81.4% (w/w) Ce, based on the defined ratio and molecular weight. Silica coated silver (SiO_2 -Ag) nanoparticles, with a stock suspension in water of 4.66 g L^{-1} and polyvinylpyrrolidone capped silver (PVP-Ag) nanoparticles, with a stock suspension of 10.23 g L^{-1} were purchased from nanoComposix (San Diego, CA). These nanoparticles represent important ENP classes and included two different functionalization types for one of the ENPs (Ag). The SiO_2 -Ag NPs consisted of a $40.5 \pm 20.5 \text{ nm}$ silver core and a 24.6 nm silica shell. Based on these dimensions, 86.9% (w/w) of SiO_2 -Ag NP is calculated to be silver. The capped PVP layer of the PVP-Ag NP ($51 \pm 22.1 \text{ nm}$) is thin and the mass contribution to the whole NP is negligible compared to the silver core. Parameters used for determination of the particle number concentration are listed in Table S3.1.

Water and sediment sampling

Water types were selected to cover a wide range of salinities. Marine water (MW) was collected during surveys on the North Sea. Estuarine water (EW) was sampled with a bucket from Nieuwe Waterweg at Maassluis ($51^\circ 54' 51.7'' \text{N}$, $4^\circ 14' 59.7'' \text{E}$). Fresh water (FW) was sampled via a pump from river Rhine at Lobith, The Netherlands ($51^\circ 51' 13.8'' \text{N}$, $6^\circ 5' 28'' \text{E}$). All samples were stored in polyethylene containers. Experiments were started immediately after arrival in the laboratory. Chloride, major anions and cations, dissolved inorganic and organic carbon (DIC, DOC), dry weight (DW) and ash free dry weight (AFDW) were determined.

Sediment was sampled with a van Veen grabber at lake Ketelmeer ($52^\circ 36' 40.8'' \text{N}$, $5^\circ 39' 35.8'' \text{E}$). This lake represents shallow buffered lakes as well as fresh tidal waters with fluctuations in water run-off and sedimentation area [27]. The wet sediment was sieved using a $500 \mu\text{m}$ mesh stainless-steel sieve to remove pebbles, shells and large organic debris. Particle size distribution (PSD) was measured with a Beckman Coulter LS 230 laser diffraction particle size analyser with Polarization Intensity Differential of Scattered Light (PIDS). Details are provided as Supporting Information. Four distinctive fractions were identified: $<1 \mu\text{m}$, 4.9%; 1 to $20 \mu\text{m}$,

54.6%; 20 to 100 μm , 31.2% and 100 to 400 μm , 9.3%. There were no particles detected in the 400 to 2000 μm fraction. Calcium carbonate (CaCO_3) was determined volumetrically according to Scheibler (NEN-ISO 10693) and was $8.66 \pm 0.05\%$ ($n = 4$). Sediment Organic carbon (OC) and black carbon (BC) content were measured using chemothermal oxidation (CTO-375 method) [28, 29] using a CHN analyser (EA 1110 CHN Elemental Analyzer, CE Instruments, Milan, Italy). OC was $2.24 \pm 0.61\%$ ($n = 5$) with one outlying data point rejected based on Dixons Q test, ($p < 0.05$) and BC was $0.22 \pm 0.06\%$ ($n = 6$).

ENP sedimentation experiments with sediment resuspension and aging

To create the systems, 7 g sediment (wet weight), 1 L water and one of the nanoparticle types CeO_2 , PVP-Ag or SiO_2 -Ag were added to 1 L glass jars (see schematic representation in Figure S1). Per water type, ENPs were added in three doses (0.5, 2.5 and 10 mg L^{-1}). In order to reach the lowest dose, for CeO_2 and PVP-Ag intermediate stock suspensions were made by diluting with Milli-Q water. These ENP concentrations are higher than anticipated in the environment but were required for accurate ENP quantification and still provide estimates of parameters that apply to lower concentrations. A blank system (sediment and water, no NPs) was included. For the sediment added, a particle number concentration was calculated as follows. The average sediment particle diameter based on PIDS was 15.7 μm (Figure S3.2). Based on Avnimelech et al. [30] a sediment density of 2.58 g cm^{-3} was calculated. When adding 7 g sediment, which translates to 3.5 g on a dry weight basis, this yields a particle number concentration of 10^{13} L^{-1} (Table S3.2 and Figure S3.2).

At time zero the systems were homogenized by shaking thoroughly for a minute, after which they were placed on a table shaker (100 rpm). On the table shaker the systems developed three phases: a bed sediment ($\sim 0.5 \text{ cm}$ layer), a transitional zone of settled but still slowly moving sediment particles ($\sim 3 \text{ cm}$ 'fluff' layer) and an overlying water phase ($\sim 10 \text{ cm}$), which remained slightly turbid throughout the experiment, but did not contain large sediment particles. This mimicked the conditions of a natural sediment bed under continuous flow. During the 14 day experiments, each working day, i.e. five times a week, resuspension events were simulated by shaking the system 5 times upside down by hand to mimic resuspension of the sediment top layer. Just before the resuspension events on days 0, 1, 7 and 14, overlying water samples (15 mL) were taken 7 cm under the water surface using a 25 mL pipet. These water column sample events were always 24 h after the previous resuspension, after which phase separation was caused by gravitational settling under semi-quiet conditions. Sampling caused a marginal column length reduction of 3.6%. This however did not affect the results because the subsamples were always taken 7 cm under the water surface in order to keep an identical sedimentation length. For the subsequent 6 months (180 days), resuspension was continued 5 times a week however without agitation in between resuspension events, in order to mimic settling and aging in a stagnant reservoir. After these 6 months, water column samples of the 0.5, 2.5

and 10 mg L⁻¹ ENP systems were taken as described above. Consequently, these latter samples relate to phase separation due to gravitational settling of aged ENPs under quiescent conditions. All overlying water samples were used for measurement of ENP electrophoretic mobility (zeta potential), ENP concentrations, particle- and aggregate size and general water characteristics (pH, EC). Elemental analysis of water column samples included Si and Al as a proxy for clay minerals [31] to be able to compare their sedimentation behaviour to that of the ENPs. In order to remove particles adhered to the container walls of the subsamples, they were sonicated for 15 minutes, shaken on a shaker table for 10 minutes and sonicated again for 10 minutes prior to analysis.

Characterization of ENPs

Particle size distributions (PSD) were measured by Nanoparticle Tracking Analysis (NTA) on a NanoSight LM20 (NanoSight Ltd., Salisbury, UK) with NTA software version 2.1 using a previously described method [18] (Table S3.4). The zeta potential (ZP) was determined by electrophoretic mobility measurements using phase analysis light scattering, based on Smoluchowski theory, with a ZetaSizer (nano series, Malvern Instruments Ltd., Worcestershire, UK). Ce, Ag, Al and Si elemental concentrations of were measured by high-resolution inductive coupled plasma mass spectroscopy (HR-ICP-MS, Element 2, Thermo, Bremen, Germany). For the CeO₂ NPs, 4 mL of sample was weighed in 50 mL tubes and destructed with 7 mL 14.4M HNO₃ and 3 mL 9.8 m H₂O₂ at 103°C for 2 hours. For Ag NPs, samples were destructed with 2 mL 14.4M HNO₃ and 7 mL 37% (w/w) HCl at 103°C for 1 hour. Subsamples were also measured with single particle ICP-MS, using a Thermo Scientific X series 2 spectrometer equipped with a Babington type nebulizer and a quartz impact bead spray chamber, to check on initial size and amount of nanoparticles. The recoveries for the measurement of CeO₂ ENPs in the water samples were >90% when compared to nominal CeO₂ concentrations. For PVP-Ag and SiO₂-Ag recoveries were a bit lower, i.e. between ~80 and 90%. In marine water recoveries were relatively low (>30%) due to the higher salt content which needed extra dilutions. The lower recovery did not affect the calculation of sedimentation rates because the recovery can be assumed similar for each individual ENP-water type combination. The single particle ICP-MS analysis revealed that CeO₂ nanoparticles had an average diameter of 19 nm, which agrees to the manufacturer specifications. PVP-Ag ENPs had an average diameter of 64 nm, which agrees with the 51.0 ± 22.1 nm size as specified by the manufacturer, based on TEM measurement.

Data analysis

First, ENP removal data were interpreted using a previously published semi-empirical first order settling rate model, describing ENP sedimentation in time [8, 24, 32]:

$$C_t = C_{res} + (C_0 - C_{res}) \cdot e^{-\left(\frac{V_s}{h} + k_{diss}\right)t} \quad (3.1)$$

in which C_t [mg L⁻¹] is the ENP concentration at time t , C_{res} [mg L⁻¹] is the residual

or non-settling concentration of ENPs at infinite time, C_0 [mg L⁻¹] is the initial concentration, V_s [m d⁻¹] is the sedimentation rate, h [m] is the sedimentation length; i.e. the distance from the water surface till the height where the samples were taken, k_{diss} is a dissolution rate constant [d⁻¹] and t [d] is sedimentation time. Dissolution is best described by shrinking particle models, which however can be approximated by first order kinetics [33-35]. The average concentrations measured 24 hours after resuspension, were only 2.4% of the initial concentration (to be discussed below), which implies that C_{res} can be considered negligible. The low residual concentrations also imply that dissolution probably was negligible compared to sedimentation, because dissolution would not result in lower concentrations in the water column as measured by total element analysis. Consequently, the removal data can be interpreted as sedimentation, and equation 3.1 can be reduced to:

$$C_t = C_0 e^{-\left(\frac{V_s}{h}\right) \cdot t} \quad (3.2)$$

Using equation 3.2, ENP sedimentation rates after 1, 7, 14 and 180 days of incubation were calculated. In all cases C_0 was the concentration ENPs as measured at start of the experiment assuming conservation of elemental mass. Measurements below the detection limit (LOD) were replaced by 50% of the LOD, which is normal procedure for non-detects [36].

Heteroaggregation rates between ENPs and SS (k_{het} ENP-SS) were estimated following a method recently described by Quik et al. [17]. A detailed description of the method and calculations used for estimating the heteroaggregation rates is provided as Supporting Information. In summary, this method calculates the heteroaggregation rate with equation 3.3, which is based on the Smoluchowski – Stokes equation and a series of informed assumptions, which were validated by simulations with the full Von Smoluchowski – Stokes equation (see the Supporting Information and [17] for details):

$$k_{het,crit} = \frac{V_{s,SS} \left(\ln \frac{C_t}{C_0} + k_{hom,crit} t \right)}{C_{SS} h \left(e^{\left(-\frac{V_{s,SS}}{h} t \right)} - 1 \right)} \quad (3.3)$$

where $k_{het,crit}$ [m³ kg⁻¹ d⁻¹] is the apparent aggregation rate for the formation of settleable ENP hetero-aggregates, $V_{s,SS}$ [m d⁻¹] is the average sedimentation rate of SS (calculated with Eq. S3.9), C_0 [kg m⁻³] and C_t [kg m⁻³] are the measured ENP concentrations at start and at time t , C_{SS} [kg m⁻³] is the concentration SS in the system (Table S2.2), and $k_{hom,crit}$ [m³ kg⁻¹ d⁻¹] is the apparent aggregation rate for the formation of settleable ENP homoaggregates. Homoaggregation (i.e. $k_{hom,crit}$) was neglected, because the high concentration of sediment causes heteroaggregation to dominate removal from the water phase [8, 11, 37]. For instance, Quik et al. [8] showed that 1 mg L⁻¹ of the same CeO₂ nanoparticles as used in the present study did hardly settle due to

homoaggregation. Furthermore, high concentrations of DOC like those originating from the present sediment have been shown to cause low attachment efficiencies for homoaggregation [9, 18].

3.3 Results and discussion

Water and sediment characteristics

Electric conductivity (EC) of the three water types FW, EW and MW ranged from 584 $\mu\text{S cm}^{-1}$ (FW) to 47000 $\mu\text{S cm}^{-1}$ (MW) illustrating the wide range of ionic strengths covered (Table S3.3). The pH of the waters was comparable at 7.8 to 7.9. Particulate matter was $>10 \text{ mg L}^{-1}$ for FW and EW, whereas MW had a much lower concentration ($<3 \text{ mg L}^{-1}$). More detail on the specific composition of the particulate matter is provided as Supporting Information (Table S3.3). After addition of sediment to the systems, the systems reached a stable pH of 7.2 to 7.3, buffered by calcium carbonate in the sediment. EC increased with 9 to 15% only, and was stable for each of the water types during the 14 day experiment, with an average of 642 $\mu\text{S cm}^{-1}$ for FW, 8009 $\mu\text{S cm}^{-1}$ for EW and 51730 $\mu\text{S cm}^{-1}$ for MW. Added ENPs had no influence on system pH or EC.

Non-settling fractions

Non-settling residual ENP concentrations after 14 and 180 d were low, i.e. 2.4% of the initial concentration on average (Table S3.5), which implies that removal was governed by sedimentation and that dissolution generally was negligible. Only for CeO_2 ENPs at 0.5 mgL^{-1} North Sea water, the residual concentration was 12% (Table S3.5). This residual percentage most probably relates to stabilised ENPs and not to dissolved cerium, because in parallel work using the same ENPs and waters, dissolution was shown to be negligible ($< 1 \mu\text{g L}^{-1}$) for CeO_2 ENPs in marine water [17]. Some dissolution of the Ag ENPs may have occurred [17]. However, Ag^+ (aq) ions formed probably precipitated to AgCl or AgS and thus settled with the resuspended SS, because the residual concentrations of Ag in the water column were low. We explain the present low residual ENP concentration after 14 and 180 days from fast aggregation and sedimentation with SS in the systems. This is in line with the increase in sedimentation rates in the presence of NC compared to filtered water as observed by Quik et al. [8, 17]. The present residual concentrations however are considerably lower than those caused by NC, which can be explained from SS having a higher mass and number concentrations than the NC in Quik et al. [17] (Table S3.2), which led to an increased collision frequency causing the higher removal of ENPs.

Sedimentation rates

The sedimentation rates (V_s) ranged between 0.14 and 0.50 m d^{-1} for the different water and ENP types and incubation times (Table S3.6). No clear differences were

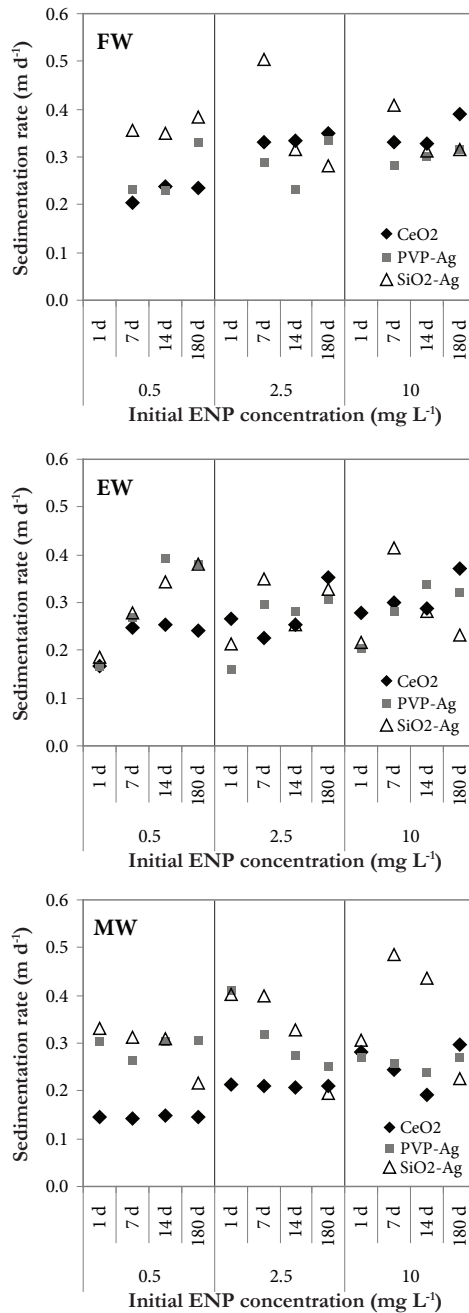


Figure 3.1 Sedimentation rates for CeO₂, PVP-Ag and SiO₂-Ag ENPs in fresh (FW), estuarine (EW) and marine water (MW), at 0.5, 2.5 and 10 mg L⁻¹ initial ENP concentration in the presence of suspended sediment after 1, 7, 14 and 180 days of incubation.

seen when comparing sedimentation rates for the different water and ENP types, except for the 0.5 mg L⁻¹ CeO₂ ENP suspension in marine water, which showed the lowest sedimentation rates (Figure 3.1). This was also observed at higher CeO₂ ENP concentration, but was less pronounced (Figure 3.1). That the sedimentation rate did not increase in marine water was unexpected. It was expected that the high salinity of marine water would provide favourable aggregation conditions, i.e. decreased colloid stability and a higher attachment efficiency and thus higher sedimentation rates [16]. These favourable aggregation conditions seem to be confirmed by the measured zeta-potentials. ZP were determined in the supernatant and therefore relate to the mix of non-settled NC from sediment and non-settled ENPs. These apparent ZP values decreased from -18 mV to -8 mV with increasing salinity (Table S3.7), which reflects lower stabilities at higher salinities [15]. Note that the ZP values do not directly relate to the ENPs that already were removed from the water column.

Table 3.1 Sedimentation rates (V_s) and heteroaggregation rates (k_{het}) for CeO₂, PVP-Ag and SiO₂-Ag ENPs at 0.5 mg L⁻¹ initial ENP concentration in fresh (FW), estuarine (EW) and marine (MW) water in the presence of suspended sediment (SS) and natural colloids (NC).

		FW	EW	MW
CeO ₂	V_s (water + SS) (m d ⁻¹) ^a	0.238	0.254	0.148
	V_s (water + NC) (m d ⁻¹) ^b	0.031	0.008	0.007
	k_{het} (ENP-SS) (L mg ⁻¹ d ⁻¹) ^a	0.259	0.291	0.157
	k_{het} (ENP-NC) (L mg ⁻¹ d ⁻¹) ^b	0.145	0.104	0.144
PVP -Ag	V_s (water + SS) (m d ⁻¹) ^a	0.229	0.394	0.304
	V_s (water + NC) (m d ⁻¹) ^b	0.010	n.m. ^c	0.002
	k_{het} (ENP-SS) (L mg ⁻¹ d ⁻¹) ^a	0.255	0.456	0.334
	k_{het} (ENP-NC) (L mg ⁻¹ d ⁻¹) ^b	0.025	0.050	0.070
SiO ₂ -Ag	V_s (water + SS) (m d ⁻¹) ^a	0.349	0.342	0.308
	V_s (water + NC) (m d ⁻¹) ^b	0.006	0.010	0.005
	k_{het} (ENP-SS) (L mg ⁻¹ d ⁻¹) ^a	0.383	0.388	0.328
	k_{het} (ENP-NC) (L mg ⁻¹ d ⁻¹) ^b	0.013	0.015	0.024

^a measured after 14 days incubation

^b literature data from a parallel study that used the same ENPs and water types under quiescent settling conditions, but with NC instead of SS [17]. This allows for direct comparison of the data.

^c not measured

Interestingly, there seemed to be only limited variation in sedimentation rate with aging time of the ENPs (Figure 3.1, Table 3.1 and Table S3.6). Only in estuarine water (EW) a statistically significant increase in V_s with aging time was observed, although these differences were not large.

For CeO₂ ENPs in estuarine water the sedimentation rates after 180 day incubation were a factor 1.4 higher compared to V_s after 1 day incubation ($p = 3 \times 10^{-3}$, paired t -test). For PVP-Ag ENPs the sedimentation rates after 7, 14 and 180 day

incubation in estuarine water were a factor of 1.6 to 1.9 higher than the after 1 day of incubation ($p = 2.6 \times 10^{-2}$ to 4.2×10^{-2} , paired t -test). For SiO_2 -Ag ENPs in estuarine water the sedimentation rates after 7 days incubation were a factor 1.7 higher compared to V_s after 1 day incubation ($p = 4.5 \times 10^{-2}$, paired t -test). After 180 day of incubation, larger aggregates were visually observed in all systems compared to the turbulent first 14 days of incubation (0-14 days), which may partly explain the aforementioned increase in V_s in EW. The low residual concentrations still observed after 180 days imply that long-term aging in the sediment did not lead to disaggregation but that the ENP stayed attached to the sediment. This is a useful finding for ENP fate modelling in aquatic systems.

There were no clear differences in sedimentation rates observed between the 0.5, 2.5 and 10 mg L^{-1} ENP concentrations (Table S3.6). As observed for stagnant fresh water systems [8, 17], it was expected that sedimentation rates (V_s) might increase with increasing ENP concentration in the turbulent systems. This follows from aggregation-sedimentation theory because aggregation is proportional to the increased collision frequency. However, this collision dependent effect was not clear in this study (Table S3.6). This is probably due to the fact that the particle number concentration of SS was 1 to 3 orders of magnitude higher than that of the ENPs (Table S3.1 and S3.2). An excess of SS causes the formation of heteroaggregates to be less sensitive to differences in NP concentration (Figure S3.3).

The present sedimentation rates in turbulent systems (Table 3.1) can directly be compared to those provided by Quik et al. [17], which are based on a parallel experiment with the same water types and ENPs with the same initial ENP concentrations as in the present study, but in quiescent conditions and without added sediment. The present sedimentation rates observed in the presence of sediment under more turbulent settling conditions are significantly higher ($p < 2 \times 10^{-5}$, $n = 8$, paired t -test) than in the non-agitated systems studied by Quik et al. [17], where only a low level of NC was present in unfiltered water samples. The higher sedimentation rates can be explained by the association of ENPs with sediment particles, which are larger than NC and thus have higher sedimentation rates. The aggregation rates will also be much faster because of the much higher particle concentration in the presence of SS (10^{13} L^{-1} , Table S3.2) compared to the NC ($10^7 - 10^8 \text{ L}^{-1}$) [17]. The sedimentation rates reported here are 7 to 187 times higher, indicating the large impact that resuspended sediment can have on the removal of ENPs from the water phase.

Consequently, we suggest that as soon as there is a resuspension event in natural waters, heteroaggregation with SS occurs and the subsequent sedimentation of ENP will coincide with that of SS. This implies that NP sedimentation rates can be equated to SS sedimentation rates, which is a helpful assumption for NP fate models (e.g. [7]).

Other sedimentation rates for citrate capped Ag, CeO_2 , TiO_2 and ZnO in the literature range between 10^{-3} to 10^{-1} m d^{-1} [8, 9, 18, 32], except for multiwalled carbon nanotubes (MWCNTs) [38] and TiO_2 in a turbulent system [39] which were much

higher and ranged from 10^{-1} to 1 m d^{-1} as recently reviewed by Quik et al. [17, 40]. The latter sedimentation rates for TiO_2 in stream microcosms with benthic biofilms of 0.10 to 0.28 m d^{-1} [39] were in the same range as those measured in the present study. Carbon nanoparticles also show rather high sedimentation rates even without turbulence, which can be explained by their hydrophobic character and large surface area, which enhances aggregation [17, 38].

The idea of co-sedimentation of ENP with SS is further supported by comparing the sedimentation rates of ENP with those of clay minerals. To this end Al and Si elemental concentrations were used as a proxy for concentrations of clay minerals. Note that calculation of V_s from Equation 3.2 requires concentrations relative to initial concentration only, that is, exact clay mineral concentrations are not required. V_s values for Al were similar to ENP sedimentation rates, implying similar sedimentation behaviour, whereas for Si the similarity was within a factor of two (Table 3.2; Table S3.6). This suggests that removal of the clay minerals and ENP associated elements related to the same particles or agglomerates, i.e. ENPs associate with the sedimentary clay minerals and are rapidly removed from the water.

Table 3.2 Sedimentation rates (V_s) determined for CeO_2 , PVP-Ag and SiO_2 -Ag ENPs, Al and Si of initial 0.5 mg L^{-1} ENP concentrations in fresh (FW), estuarine (EW) and marine (MW) water in the presence of suspended sediment after 14 days.

ENP	water	ENP	Al	Si
		$V_s \text{ (m d}^{-1}\text{)}$	$V_s \text{ (m d}^{-1}\text{)}$	$V_s \text{ (m d}^{-1}\text{)}$
CeO_2	FW	0.238	0.290	0.139
	EW	0.254	0.265	0.154
	MW	0.148	0.259	0.170
PVP-Ag	FW	0.229	0.200	0.117
	EW	0.394	0.293	0.174
	MW	0.304	0.291	0.184
SiO_2 -Ag	FW	0.349	0.261	0.154
	EW	0.342	0.285	0.165
	MW	0.308	0.255	0.173

Heteroaggregation rates between ENPs and suspended solids (SS)

Heteroaggregation rates of ENPs and SS (k_{het}) showed rather limited variation, with interquartile (IQR) ranges of 0.227 to $0.311 \text{ L mg}^{-1} \text{ d}^{-1}$ for CeO_2 , 0.281 to $0.347 \text{ L mg}^{-1} \text{ d}^{-1}$ for PVP-Ag and 0.306 to $0.421 \text{ L mg}^{-1} \text{ d}^{-1}$ for SiO_2 -Ag (Table S3.8). The variation among the water types and ENPs is comparable too and there is no clear consistent trend in k_{het} with water type, ENP type or with time. Furthermore, k_{het} does not seem to vary much with increasing initial ENP concentrations, e.g., k_{het} varies less than a factor 2 with C_0 varying up to a factor of 20 (See Table S3.8). This also supports the previous assumption that homoaggregation can be neglected. However, if in a worst case

scenario removal of ENPs due to homoaggregation is taken similar to what has been observed in our parallel study without added sediment in quiescent conditions [17], heteroaggregation rates would become between 13.7 and 54.2% lower. The resulting values however, still would be 1.3 to 23.5 times higher than for heteroaggregation with NC [17]. We argue that this level of uncertainty is acceptable in this type of estimations. Despite the rather limited variation we suggest that the values obtained at the lowest dose best represent the low concentrations that are anticipated to occur in the environment, which therefore are summarized in Table 3.1.

The heteroaggregation rates between ENPs and suspended solids were 1.1 to 29.5 times higher than the rates previously reported for heteroaggregation with natural colloids [17] (Table 3.1). The generally higher rates can be explained either by a higher attachment efficiency or a higher collision frequency compared to heteroaggregation with NC, or both. Attachment efficiencies cannot be directly deduced from the present data. Collision frequencies, however, are determined by contributions from Brownian motion, differential settling and shear stress (Eq. S3.7). Turbulent interactions with SS will cause much higher contributions from the latter two processes, compared to interactions of the same ENPs with NC in quiescent waters. Turbulence caused by shaking can be assumed to increase the contribution of shear stress, whereas the large size difference between SS particles and ENPs also increases the contribution of differential settling.

3.4 Summarizing discussion and implications

This study demonstrated that heteroaggregation of ENPs with SS in turbulent aquatic systems governs the sedimentation of ENPs irrespective of salinity and ENP type studied, leading to fairly similar sedimentation behaviour. Heteroaggregation of ENPs with SS followed by sedimentation explains the much shorter process time compared to those reported in the literature for stagnant systems without SS or with low SS concentrations. Further aging in the sediment bed with incidental resuspension over 6 months did not result in substantial differences in sedimentation rates or in apparent heteroaggregation rates, nor in ENPs being released again in the water column. These data suggest that ENP fate in turbulent river systems and shallow lakes may be described as sedimentation-resuspension of SS with lumped sedimentation rates between $0.14 - 0.50 \text{ m d}^{-1}$ leading to a much higher retention than in stagnant systems or deep lakes and oceans where sedimentation rates are much lower.

Furthermore, we argue that many ENPs entering water systems, most probably already are aggregated to particles and flocks and that water quality models may not need very ENP specific values for sedimentation or heteroaggregation. Furthermore homoaggregation is likely only relevant in certain specific scenarios, e.g. if (a) ENPs are entering water systems as nano-sized particles like soot i.e. through atmospheric deposition, and (b) suspended solids are absent or have a low concentration as in

stagnant deep lakes. Homoaggregation thus may be relevant for the fate of airborne ENPs in deep lakes and oceans.

Acknowledgements

We would like to thank Marja Wouterse (RIVM) for her assistance during the experiments, Cornelis Miermans (RIVM) for the ICP-MS measurements, Frits Gillissen, Wendy Beekman-Lucassen and Magdalena Rakowska (Wageningen University) for their contributions to measuring water and sediment characteristics, Ruud Peters (RIKILT) for the sp-ICP-MS measurements, NVI for the use of the Malvern ZetaSizer and RIVM for the use of the NanoSight LM20. A.A.K. and J.Q. acknowledge financial support from NanoNextNL, a micro and nanotechnology consortium of the Government of the Netherlands and 130 partners.

References

- [1] Nowack B, Bucheli TD. 2007. Occurrence, behavior and effects of nanoparticles in the environment. *Environ Pollut* 150:5-22.
- [2] Klaine SJ, Koelmans AA, Horne N, Carley S, Handy RD, Kapustka L, Nowack B, von der Kammer F. 2012. Paradigms to assess the environmental impact of manufactured nanomaterials. *Environ Toxicol Chem* 31:3-14.
- [3] Mueller NC, Nowack B. 2008. Exposure modeling of engineered nanoparticles in the environment. *Environ Sci Technol* 42:4447-4453.
- [4] Gottschalk F, Kost E, Nowack B. 2013. Engineered nanomaterials in water and soils: A risk quantification based on probabilistic exposure and effect modeling. *Environ Toxicol Chem* 32:1278-1287.
- [5] von der Kammer F, Ferguson PL, Holden PA, Masion A, Rogers KR, Klaine SJ, Koelmans AA, Horne N, Unrine JM. 2012. Analysis of engineered nanomaterials in complex matrices (environment and biota): General considerations and conceptual case studies. *Environ Toxicol Chem* 31:32-49.
- [6] Gottschalk F, Sun T, Nowack B. 2013. Environmental concentrations of engineered nanomaterials: Review of modeling and analytical studies. *Environ Pollut* 181:287-300.
- [7] Koelmans AA, Nowack B, Wiesner MR. 2009. Comparison of manufactured and black carbon nanoparticle concentrations in aquatic sediments. *Environ Pollut* 157:1110-1116.
- [8] Quik JTK, Stuart MC, Wouterse M, Peijnenburg W, Hendriks AJ, van de Meent D. 2012. Natural colloids are the dominant factor in the sedimentation of nanoparticles. *Environ Toxicol Chem* 31:1019-1022.
- [9] Keller AA, Wang HT, Zhou DX, Lenihan HS, Cherr G, Cardinale BJ, Miller R, Ji ZX. 2010. Stability and Aggregation of Metal Oxide Nanoparticles in Natural Aqueous Matrices. *Environ Sci Technol* 44:1962-1967.
- [10] Arvidsson R, Molander S, Sanden BA, Hasselov M. 2011. Challenges in Exposure Modeling of Nanoparticles in Aquatic Environments. *Hum Ecol Risk Assess* 17:245-262.
- [11] Praetorius A, Scheringer M, Hungerbuhler K. 2012. Development of Environmental Fate Models for Engineered Nanoparticles-A Case Study of TiO₂ Nanoparticles in the Rhine River. *Environ Sci Technol* 46:6705-6713.
- [12] Lowry GV, Gregory KB, Apte SC, Lead JR. 2012. Transformations of Nanomaterials in the Environment. *Environ Sci Technol* 46:6893-6899.
- [13] Nowack B, Ranville JF, Diamond S, Gallego-Urrea JA, Metcalfe C, Rose J, Horne N, Koelmans AA, Klaine SJ. 2012. Potential scenarios for nanomaterial release and subsequent alteration in the environment. *Environ Toxicol Chem* 31:50-59.
- [14] Velzeboer I, Hendriks AJ, Ragas AMJ, Van de Meent D. 2008. Aquatic ecotoxicity tests of some nanomaterials. *Environ Toxicol Chem* 27:1942-1947.
- [15] Thio BJR, Montes MO, Mahmoud MA, Lee DW, Zhou DX, Keller AA. 2012. Mobility of Capped Silver Nanoparticles under Environmentally Relevant Conditions. *Environ Sci Technol* 46:6985-6991.

- [16] Zhang W, Crittenden J, Li KG, Chen YS. 2012. Attachment Efficiency of Nanoparticle Aggregation in Aqueous Dispersions: Modeling and Experimental Validation. *Environ Sci Technol* 46:7054-7062.
- [17] Quik JTK, Velzeboer I, Wouterse M, Koelmans AA, van de Meent D. 2014. Heteroaggregation and sedimentation rates for nanomaterials in natural waters. *Water Res* 48:269-279.
- [18] Quik JTK, Lynch I, Van Hoecke K, Miermans CJH, De Schamphelaere KAC, Janssen CR, Dawson KA, Stuart MAC, Van de Meent D. 2010. Effect of natural organic matter on cerium dioxide nanoparticles settling in model fresh water. *Chemosphere* 81:711-715.
- [19] Petosa AR, Jaisi DP, Quevedo IR, Elimelech M, Tufenkji N. 2010. Aggregation and Deposition of Engineered Nanomaterials in Aquatic Environments: Role of Physicochemical Interactions. *Environ Sci Technol* 44:6532-6549.
- [20] McCave IN. 1984. Size spectra and aggregation of suspended particles in the deep ocean. *Deep-Sea Res* 31:329-352.
- [21] Hyung H, Fortner JD, Hughes JB, Kim JH. 2007. Natural organic matter stabilizes carbon nanotubes in the aqueous phase. *Environ Sci Technol* 41:179-184.
- [22] Stolzenbach KD, Newman KA, Wong CS. 1992. Aggregation of fine particles at the sediment-water interface. *J Geophys Res-Oceans* 97:17889-17898.
- [23] Bilotta GS, Brazier RE. 2008. Understanding the influence of suspended solids on water quality and aquatic biota. *Water Res* 42:2849-2861.
- [24] Newman KA, Morel FMM, Stolzenbach KD. 1990. Settling and coagulation characteristics of fluorescent particles determined by flow-cytometry and fluorometry *Environ Sci Technol* 24:506-513.
- [25] Farley KJ, Morel FMM. 1986. Role of coagulation in the kinetics of sedimentation. *Environ Sci Technol* 20:187-195.
- [26] Handy RD, Cornelis G, Fernandes T, Tsyusko O, Decho A, Sabo-Attwood T, Metcalfe C, Steevens JA, Klaine SJ, Koelmans AA, Horne N. 2012. Ecotoxicity test methods for engineered nanomaterials: Practical experiences and recommendations from the bench. *Environ Toxicol Chem* 31:15-31.
- [27] Peeters ETHM, de Lange, H.J., de la Haye, M.A.A. and Reeze A.J.G. 2010. KRW-maatlat macrofauna voor zoet getijdenwater (R8). report. Hoofdrapport. Grontmij. Rapportnummer:228629-1.
- [28] Gustafsson O, Haghseta F, Chan C, MacFarlane J, Gschwend PM. 1997. Quantification of the dilute sedimentary soot phase: Implications for PAH speciation and bioavailability. *Environ Sci Technol* 31:203-209.
- [29] Jonker MTO, Koelmans AA. 2002. Sorption of polycyclic aromatic hydrocarbons and polychlorinated biphenyls to soot and soot-like materials in the aqueous environment mechanistic considerations. *Environ Sci Technol* 36:3725-3734.
- [30] Avnimelech Y, Ritvo G, Meijer LE, Kochba M. 2001. Water content, organic carbon and dry bulk density in flooded sediments. *Aquacult Eng* 25:25-33.
- [31] Velde B. 1977. *Clays and clay minerals in natural and synthetic systems*. Elsevier Scientific Publishing Company, Amsterdam, the Netherlands.

- [32] Chinnapongse SL, MacCuspie RI, Hackley VA. 2011. Persistence of singly dispersed silver nanoparticles in natural freshwaters, synthetic seawater, and simulated estuarine waters. *Sci Total Environ* 409:2443-2450.
- [33] Zook JM, Long SE, Cleveland D, Geronimo CLA, MacCuspie RI. 2011. Measuring silver nanoparticle dissolution in complex biological and environmental matrices using UV-visible absorbance. *Anal Bioanal Chem* 401:1993-2002.
- [34] Ho CM, Yau SKW, Lok CN, So MH, Che CM. 2010. Oxidative Dissolution of Silver Nanoparticles by Biologically Relevant Oxidants: A Kinetic and Mechanistic Study. *Chem-Asian J* 5:285-293.
- [35] Poot A, Meerman E, Gillissen F, Koelmans AA. 2009. A kinetic approach to evaluate the association of acid volatile sulfide and simultaneously extracted metals in aquatic sediments. *Environ Toxicol Chem* 28:711-717.
- [36] D. L. Massart, B. G. M. Vandeginste, S. N. Deming, Y. Michotte, L. Kaufman. 1988. *Chemometrics: A textbook*. Elsevier, Amsterdam.
- [37] Hotze EM, Phenrat T, Lowry GV. 2010. Nanoparticle Aggregation: Challenges to Understanding Transport and Reactivity in the Environment. *J Environ Qual* 39:1909-1924.
- [38] Kennedy AJ, Hull MS, Steevens JA, Dontsova KM, Chappell MA, Gunter JC, Weiss Jr. CA. 2008. Factors influencing the partitioning and toxicity of nanotubes in the aquatic environment. *Environ Toxicol Chem*:1932-1941
- [39] Battin TJ, Kammer FVD, Weilhartner A, Ottofuelling S, Hofmann T. 2009. Nanostructured TiO₂: Transport Behavior and Effects on Aquatic Microbial Communities under Environmental Conditions. *Environ Sci Technol* 43:8098-8104.
- [40] Quik JTK, Vonk JA, Hansen SF, Baun A, Van De Meent D. 2011. How to assess exposure of aquatic organisms to manufactured nanoparticles? *Environ Int* 37:1068-1077.

Supporting Information

Table S3.1 Characteristics of the CeO₂, PVP-Ag and SiO₂-Ag stock suspensions and the estimated particle number concentration of ENPs in the systems with the 0.5, 2.5 and 10 mg L⁻¹ initial ENP concentrations.

Characteristic	CeO ₂	PVP-Ag	SiO ₂ -Ag
hydrodynamic diameter ^a (nm)	175	90.5	124
density ^b (g cm ⁻³)	3.07	8.48	2.66
ZP ^c (mV)	38.7	-12.4	25.4
pH ^c (-)	4	6.5	6.2
mass concentration ^c (g L ⁻¹)	100	10.23	4.66
mass particle (g)	8.63×10 ⁻¹⁵	3.29×10 ⁻¹⁵	2.66×10 ⁻¹⁵
Particle number concentration 0.5 mg L ^{-1 d} (L ⁻¹)	5.80×10 ¹⁰	1.52×10 ¹¹	1.88×10 ¹¹
Particle number concentration 2.5 mg L ^{-1 d} (L ⁻¹)	2.90×10 ¹¹	7.60×10 ¹¹	9.40×10 ¹¹
Particle number concentration 10 mg L ^{-1 d} (L ⁻¹)	1.16×10 ¹²	3.04×10 ¹²	3.76×10 ¹²

^a diameter measured by Nanoparticle Tracking Analysis (n = 3)

^b calculated from the radius of aggregate and primary particles and a fractal dimension of 2.5, assuming spheres

^c from stock suspension

^d calculated amount of ENPs by dividing the initial concentration of 0.5, 2.5 and 10 mg L⁻¹ by particle mass

Table S3.2 Average sediment particle number concentration (L⁻¹) added in fresh (FW), estuarine (EW) and marine water (MW).

	FW	EW	MW
mass added ^{a,b} (g)	3.410	3.318	3.451
concentration ^c (L ⁻¹)	1.18×10 ¹³	1.14×10 ¹³	1.19×10 ¹³

^a density of sediment was 2577 kg m⁻³ with 5.2% OM [1]

^b mass of the relative unit of sediment determined with PIDS was 2.90×10⁻¹³ g

^c particle number concentration

Table S3.3 Characteristics of the natural waters used in this study. Water types: fresh (FW), estuarine (EW) and marine (MW).

	FW	EW	MW
pH (-)	7.9	7.9	7.8
EC ($\mu\text{S cm}^{-1}$)	584	7200	47000
particulate matter (mg L^{-1})	10.3	11.9	2.7
O ₂ (mg L^{-1})	9.3	7.9	8.4
T (Celsius)	16.9	16.4	17.3
Salinity (‰)	n.m. ^a	4.4	34
Cl (mg L^{-1}) ^b	126	3970	28600
NO ₃ +NO ₂ (mg N L^{-1}) ^c	2.75	2.44	0.19
PO ₄ ($\mu\text{g P L}^{-1}$) ^c	36	103	344
NH ₃ (mg N L^{-1}) ^c	0.03	0.07	0.11
Total P (mg P L^{-1}) ^c	0.04	0.12	0.12
Total N (mg N L^{-1}) ^c	1.68	1.72	0.06
Ca (mg L^{-1}) ^d	56	104	401
K (mg L^{-1}) ^d	4.4	50	371
Mg (mg L^{-1}) ^d	10.6	160	1233
Na (mg L^{-1}) ^d	46	1370	10630
DIC (mg C L^{-1}) ^e	24.6	31.2	40.9
DOC (mg C L^{-1}) ^e	2.45	2.85	0.17
DW (mg L^{-1}) ^f	10.3	11.9	2.7
AFDW (mg L^{-1}) ^g	2.4	3.6	1.3

^a not measured

^b determined with ion selective electrode (Orion 94-17, Thermo Electron Corporation)

^c determined with continuous flow analyser (CFA, Skalar Analytical BV)

^d determined with radial ICP-AES (Vista PRO, Varian Inc)

^e determined with total organic carbon (TOC) analyser (Model 700, O.I.C. International BV)

^f determined using a 0.3 μm quartz filter (Sartorius Quartz-Microfibre Discs T293) and dried in a stove (Heraeus, type T6060) at 105°C for 2 h

^g DW filters determined in a muffle furnace (Heraeus electronic, type MR 170E) at 520°C for 3 h

Table S3.4 Average particle diameter measured in overlying water of the 0.5 mg L^{-1} CeO₂, PVP-Ag and SiO₂-Ag ENPs systems in the presence of suspended sediment with Nanoparticle Tracking Analysis (NTA), $n = 3$. Water types: fresh (FW), estuarine (EW) and marine (MW).

ENP	Average particle diameter (nm)								
	FW			EW			MW		
blank	405	±	31	429	±	42	423	±	94
CeO ₂	458	±	111	493	±	216	519	±	100
PVP-Ag	414	±	98	422	±	10	534	±	112
SiO ₂ -Ag	411	±	56	450	±	82	495	±	49
average	418			446			521		

Table S3.5 Elemental concentrations (Ce and Ag) of the CeO₂, PVP-Ag and SiO₂-Ag ENPs systems at 0.5, 2.5 and 10 mg L⁻¹ initial ENP concentration in 3 water types in the presence of suspended sediment at time 0, after 14 and 180 days, and the residual percentage after 14 and 180 days. Water types: fresh (FW), estuarine (EW) and marine (MW).

ENP	water	ENP content (mg L ⁻¹) ^a	C ₀ (mg L ⁻¹) ^b	Turbulent		Aged	
				C ₁₄ (mg L ⁻¹) ^c	Residual % ^d	C ₁₈₀ (mg L ⁻¹) ^c	Residual % ^d
CeO ₂	FW	0.5	0.40	0.01	3.32	0.01	3.48
		2.5	2.04	0.02	0.86	0.01	0.67
		10	8.60	0.08	0.92	0.03	0.38
	EW	0.5	0.46	0.01	2.67	0.01	3.16
		2.5	2.05	0.05	2.63	0.01	0.66
		10	7.21	0.12	1.64	0.04	0.51
	MW	0.5	0.37	0.04	12.08	0.05	12.69
		2.5	0.88	0.05	5.25	0.04	4.89
		10	2.71	0.18	6.57	0.04	1.44
PVP-Ag	FW	0.5	0.41	0.02	3.77	0.00	0.87
		2.5	2.20	0.08	3.63	0.02	0.84
		10	8.29	0.11	1.39	0.09	1.10
	EW	0.5	0.38	0.00	0.36	0.00	0.45
		2.5	2.06	0.04	1.78	0.03	1.27
		10	8.49	0.07	0.80	0.09	1.01
	MW	0.5	0.35	0.00	1.31	0.00	1.29
		2.5	1.79	0.03	1.93	0.05	2.77
		10	7.87	0.26	3.30	0.17	2.13
SiO ₂ -Ag	FW	0.5	0.32	0.00	0.69	0.00	0.42
		2.5	1.74	0.02	1.12	0.03	1.79
		10	6.57	0.08	1.15	0.07	1.08
	EW	0.5	0.33	0.00	0.75	0.00	0.43
		2.5	1.62	0.04	2.64	0.02	0.93
		10	6.30	0.12	1.83	0.23	3.63
	MW	0.5	0.40	0.00	1.22	0.02	4.51
		2.5	1.40	0.01	0.93	0.09	6.23
		10	4.50	0.01	0.20	0.18	3.98

^a ENP content is the initial (nominal) ENP mass concentration

^b C₀ is the measured elemental concentration

^c C₁₄ and C₁₈₀ are the measured elemental concentrations after 14 and 180 days incubation

^d Residual % is C_i/C₀ × 100%

Table S3.6 Sedimentation rates (V_s ; $m d^{-1}$) for CeO_2 , PVP-Ag and SiO_2 -Ag ENPs and Al and Si at 0.5, 2.5 and 10 $mg L^{-1}$ initial ENP concentration in 3 water types in the presence of suspended sediment determined after 1, 7, 14 and 180 days of incubation. Water types: fresh (FW), estuarine (EW) and marine (MW).

ENP	water ($mg L^{-1}$)	ENP content				Al				Si				
		V_{s1}	V_{s7}	V_{s14}	V_{s180}	V_{s1}	V_{s7}	V_{s14}	V_{s180}	V_{s1}	V_{s7}	V_{s14}	V_{s180}	
CeO_2	FW	0.5	n.m. ^a	0.204	0.238	0.235	n.m.	0.287	0.290	0.399	n.m.	0.145	0.139	0.137
		2.5	n.m.	0.332	0.333	0.351	n.m.	0.237	0.246	0.297	n.m.	0.145	0.133	0.125
		10	n.m.	0.330	0.329	0.391	n.m.	0.260	0.262	0.328	n.m.	0.159	0.152	0.140
	EW	0.5	0.167	0.246	0.254	0.242	0.279	0.253	0.265	0.357	0.173	0.151	0.154	0.155
		2.5	0.265	0.225	0.255	0.352	0.272	0.246	0.250	0.393	0.169	0.153	0.153	0.155
		10	0.279	0.299	0.288	0.370	0.280	0.300	0.286	0.333	0.173	0.179	0.166	0.152
	MW	0.5	0.146	0.143	0.148	0.144	0.206	0.219	0.259	0.362	0.213	0.164	0.170	0.154
		2.5	0.214	0.211	0.206	0.211	0.229	0.232	0.223	0.357	0.202	0.171	0.148	0.145
		10	0.283	0.243	0.191	0.297	0.221	0.233	0.203	0.329	0.188	0.157	0.134	0.131
PVP-Ag	FW	0.5	n.m.	0.232	0.229	0.332	n.m.	0.246	0.200	0.256	n.m.	0.138	0.117	0.109
		2.5	n.m.	0.289	0.232	0.334	n.m.	0.257	0.215	0.285	n.m.	0.153	0.129	0.122
		10	n.m.	0.283	0.299	0.316	n.m.	0.293	0.262	0.267	n.m.	0.153	0.134	0.117
	EW	0.5	0.167	0.269	0.394	0.379	0.291	0.264	0.293	0.305	0.186	0.170	0.174	0.150
		2.5	0.162	0.297	0.282	0.306	0.282	0.293	0.288	0.300	0.185	0.182	0.176	0.153
		10	0.206	0.282	0.338	0.322	0.285	0.295	0.323	0.316	0.180	0.174	0.184	0.154
	MW	0.5	0.302	0.262	0.304	0.305	0.335	0.255	0.291	0.355	0.210	0.177	0.184	0.157
		2.5	0.412	0.320	0.276	0.251	0.345	0.324	0.292	0.360	0.211	0.196	0.176	0.159
		10	0.268	0.256	0.239	0.269	0.333	0.342	0.261	0.351	0.196	0.204	0.151	0.146
SiO_2 -Ag	FW	0.5	n.m.	0.357	0.349	0.383	n.m.	0.302	0.261	0.294	n.m.	0.170	0.154	0.143
		2.5	n.m.	0.503	0.315	0.282	n.m.	0.355	0.252	0.239	n.m.	0.164	0.137	0.117
		10	n.m.	0.410	0.313	0.317	n.m.	0.327	0.226	0.260	n.m.	0.148	0.121	0.116
	EW	0.5	0.187	0.278	0.342	0.381	0.303	0.258	0.285	0.317	0.187	0.156	0.165	0.144
		2.5	0.215	0.350	0.254	0.327	0.345	0.326	0.248	0.303	0.186	0.180	0.152	0.143
		10	0.216	0.414	0.280	0.232	0.406	0.362	0.274	0.266	0.186	0.172	0.149	0.131
	MW	0.5	0.332	0.312	0.308	0.217	0.376	0.295	0.255	0.334	0.241	0.183	0.173	0.155
		2.5	0.401	0.399	0.328	0.194	0.316	0.313	0.301	0.308	0.188	0.176	0.162	0.132
		10	0.305	0.485	0.435	0.226	0.281	0.289	0.301	0.293	0.163	0.137	0.127	0.100

^a not measured

Table S3.7 Zeta Potential (ZP) measured in overlying water of the CeO₂, PVP-Ag and SiO₂-Ag ENPs systems at 0.5, 2.5 and 10 mg L⁻¹ initial ENP concentration in 3 water types in the presence of suspended sediment measured after 1, 7 and 14 days of incubation. Water types: fresh (FW), estuarine (EW) and marine (MW).

NP	water	ENP content (mg L ⁻¹)	ZP (mV)		
			day 1	day 7	day 14
CeO ₂	FW	0.5	n.m. ^a	-18.8	-16.7
		2.5	n.m.	-18.8	-17.2
		10	n.m.	-19.6	-17.0
	EW	0.5	n.m.	-11.0	-13.9
		2.5	n.m.	-11.7	-13.5
		10	n.m.	-13.2	-14.1
	MW	0.5	-10.6	-8.3	-7.7
		2.5	-5.9	-7.1	-8.7
		10	-10.3	-8.0	-9.0
PVP-Ag	FW	0.5	n.m.	-20.0	-17.3
		2.5	n.m.	-18.7	-16.5
		10	n.m.	-18.7	-17.7
	EW	0.5	n.m.	-11.9	-13.9
		2.5	n.m.	-11.9	-12.7
		10	n.m.	-12.0	-14.1
	MW	0.5	-8.7	-7.8	-8.1
		2.5	-5.1	-7.9	-8.6
		10	-8.2	-5.6	-7.7
SiO ₂ -Ag	FW	0.5	n.m.	-19.5	-16.2
		2.5	n.m.	-18.5	-17.5
		10	n.m.	-18.2	-17.4
	EW	0.5	n.m.	-12.8	-13.9
		2.5	n.m.	-12.0	-13.2
		10	n.m.	-12.5	-13.9
	MW	0.5	-9.3	-6.2	-9.7
		2.5	-6.6	-10.7	-8.4
		10	-8.8	-15.0	-7.4

^a not measured

Table S3.8 Heteroaggregation rates (k_{het} ; $L\ mg^{-1}\ d^{-1}$) of ENPs and SS of the CeO_2 , PVP-Ag and SiO_2 -Ag ENPs systems at 0.5, 2.5 and 10 $mg\ L^{-1}$ initial ENP concentration in 3 water types in the presence of suspended sediment determined after 1, 7, 14 and 180 days of incubation. Water types: fresh (FW), estuarine (EW) and marine (MW).

NP	water	ENP content ($mg\ L^{-1}$)	ENP			
			k_{het1} ($L\ mg^{-1}\ d^{-1}$)	k_{het7} ($L\ mg^{-1}\ d^{-1}$)	k_{het14} ($L\ mg^{-1}\ d^{-1}$)	k_{het180} ($L\ mg^{-1}\ d^{-1}$)
CeO_2	FW	0.5	n.m. ^a	0.222	0.259	0.255
		2.5	n.m.	0.363	0.364	0.384
		10	n.m.	0.361	0.360	0.428
	EW	0.5	0.192	0.283	0.291	0.278
		2.5	0.293	0.250	0.282	0.389
		10	0.287	0.307	0.295	0.380
	MW	0.5	0.155	0.151	0.157	0.153
		2.5	0.230	0.227	0.221	0.227
		10	0.296	0.254	0.199	0.311
PVP-Ag	FW	0.5	n.m.	0.258	0.255	0.369
		2.5	n.m.	0.313	0.252	0.362
		10	n.m.	0.310	0.329	0.347
	EW	0.5	0.193	0.311	0.456	0.438
		2.5	0.181	0.332	0.316	0.342
		10	0.229	0.314	0.376	0.358
	MW	0.5	0.332	0.288	0.334	0.335
		2.5	0.460	0.357	0.309	0.281
		10	0.281	0.269	0.251	0.283
SiO_2 -Ag	FW	0.5	n.m.	0.392	0.383	0.421
		2.5	n.m.	0.547	0.342	0.306
		10	n.m.	0.454	0.346	0.351
	EW	0.5	0.212	0.316	0.388	0.433
		2.5	0.251	0.409	0.297	0.382
		10	0.253	0.486	0.329	0.272
	MW	0.5	0.353	0.332	0.328	0.230
		2.5	0.450	0.447	0.368	0.218
		10	0.340	0.541	0.485	0.251

^a not measured

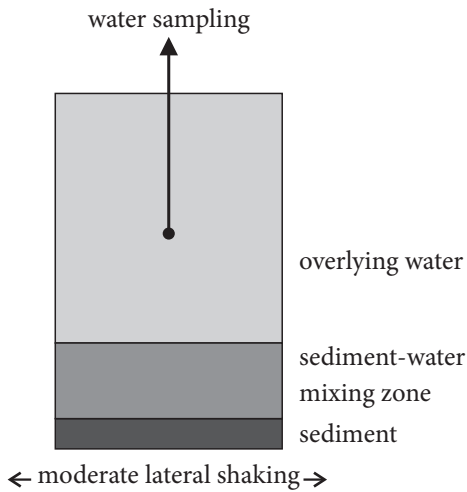


Figure S3.1. Schematic representation of the experimental set-up.

Particle size distribution

Sediment

Wet sediment from lake Ketelmeer was characterized for particle size distribution (PSD) (Figure S3.2) with Beckman Coulter LS 230 laser diffraction particle size analyser with Polarization Intensity Differential of Scattered Light (PIDS). The Fraunhofer theory of light scattering was used to determine the PSD. Sediment samples were brought into suspension in demineralized water and well homogenized prior to particle size analysis. The injected suspension volume was controlled to obtain a total obscuration level of $10 \pm 3\%$ and a PIDS obscuration of $50 \pm 10\%$.

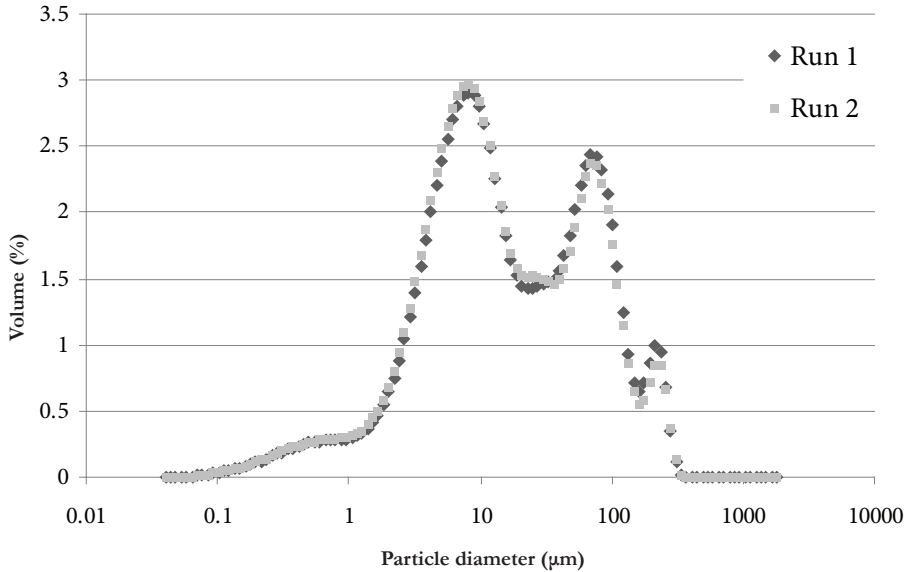


Figure S3.2 Particle size distribution of Ketelmeer sediment, measured by laser diffraction.

Water

Particle size distributions and average particle sizes, measured with Nanoparticle Tracking Analysis (NTA) in all water column samples, show that non-settling particles were still in suspension. As mentioned earlier, hardly any ENPs were present already after one day, so the average particle size relates mainly to suspended non-settling colloids originating from sediment and water. The average particle sizes were 418 nm, 446 nm and 521 nm in FW, EW and MW, respectively (Table S3.4). Because the particle sizes are based on suspended colloids mostly coming from the sediment, the average sedimentation rate can be calculated with Stokes law, using the density of organic matter (1.25 g cm^{-3} ; [2]) as a proxy for the present particles. With this assumption, V_s is 2.1×10^{-3} , 2.3×10^{-3} and $3.1 \times 10^{-3} \text{ m d}^{-1}$ for FW, EW and MW, respectively for particles still suspended in the water phase. V_s estimated for the ENPs was higher, which makes the sedimentation of the ENPs feasible. Heteroaggregation with bigger SS (corresponding to the higher V_s) coming from the sediment is thus indicated rather than with the 418 to 521 nm colloids, otherwise the ENPs would still be suspended in the water phase.

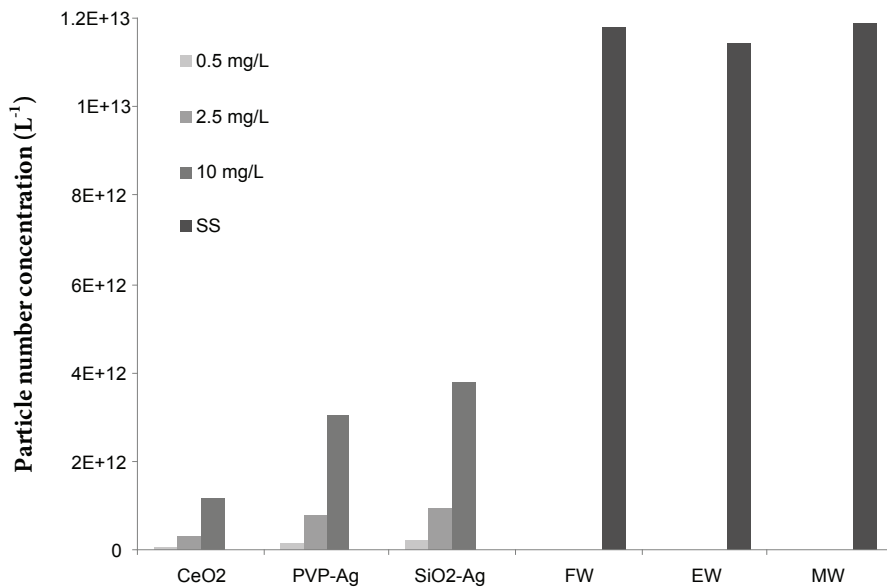


Figure S3.3 Particle number concentration (L^{-1}) of CeO₂, PVP-Ag and SiO₂-Ag ENPs in the systems of the 0.5, 2.5 and 10 mg L^{-1} initial ENP concentrations and the average sediment particle number concentration (L^{-1}) in 3 water types. Water types: fresh (FW), estuarine (EW) and marine (MW).

Estimating the heteroaggregation rate between nanoparticles and natural colloids or suspended sediments from sedimentation experiments. Modified from [3]

This SI section describes the method to estimate heteroaggregation rates (k_{het}) from sedimentation experiments between nanoparticles and natural particles, such as natural colloids (NC) [3] or suspended solids (SS). This method is applied to estimate k_{het} between nanoparticles and suspended sediment. First, an introductory outline of the approach is given. Then, the different steps in the calculation of k_{het} are described in terms of fundamental as well as simplified equations for aggregation-sedimentation. Finally, it is shown how the model equations can be used to fit values for k_{het} from the data. This final section also presents a validation of the simplified model approach by comparing its results against predictions of an aggregation-sedimentation model without simplifications. Finally it is shown how k_{het} can be interpreted in terms of attachment efficiencies and collision frequencies.

Principle

ENP sedimentation experiments were first performed for filtered (no NC or SS) and unfiltered natural water samples [3]. In the unfiltered experimental systems, removal of the engineered nanoparticles (ENPs) from the water column can be assumed to be driven by (ENP-ENP) homoaggregation, (ENP-NC) heteroaggregation and/or settling of ENP aggregates [4-6]. To determine heteroaggregation rates, the process parameters for heteroaggregation need to be isolated from those for homoaggregation and sedimentation. This is done as follows. First, it is assumed that aggregation is the rate limiting process for the observed removal of ENPs from the water phase. This is based on the logic that aggregates first need to be large enough for sedimentation to occur [7]. If aggregation is the rate determining process, the observed removal rates will depend on the parameters describing homo- and heteroaggregation rather than on parameters describing sedimentation. Second, the process parameters for homoaggregation are estimated by fitting a homoaggregation-only process equation to the data for the sedimentation experiments with filtered water samples. This assumes that heteroaggregation does not occur in water samples where NCs are removed by filtration. Finally, a process equation accounting for homo- and heteroaggregation is fitted to the data for the sedimentation experiments in unfiltered water samples, using the parameters for homoaggregation from the previous step. This leaves the process parameters for heteroaggregation as the only unknowns. The process equations and assumptions required in the different steps are discussed in the next section.

Model equations

The basics for the calculation of the contributions of homoaggregation and heteroaggregation to the removal of ENPs from the water phase are condensed in the combined Von Smoluchowski –Stokes equation [8]:

$$\frac{dC_{SS,j}}{dt} = \frac{1}{2} \sum_{i=1}^{j-1} \alpha_{i,j-i} K_{i,j-i} N_i N_{j-i} - N_j \sum_{i=1}^{j-1} \alpha_{i,j} K_{i,j} N_i - \alpha_{SS,j} K_{SS,j} N_{SS} N_j - \frac{V_{s,j}}{h} N_j \quad (S3.1)$$

With:

- $\alpha_{i,j}$: attachment efficiency between ENP aggregates i and j
- $\alpha_{SS,j}$: attachment efficiency between ENP and SS
- j : number of primary NPs in ENP aggregate
- $K_{i,j}$: Collision frequency between ENP aggregates i and j [$\text{m}^3 \text{s}^{-1}$]
- $K_{SS,j}$: Collision frequency between ENP particle aggregates j and SS [$\text{m}^3 \text{s}^{-1}$]
- N_j : Number of the ENP aggregate j [m^{-3}]
- N_{SS} : Number of SS [m^{-3}]
- $V_{s,j}$: Sedimentation rate of ENP aggregate j [m s^{-1}]
- h : Sedimentation length [m]

and where the first two terms accounts for homoaggregation, the third term for heteroaggregation, and the last term for sedimentation of ENP aggregates.

The concentration of suspended solids C_{SS} is assumed to decrease due to Stokes settling [5, 9];

$$\frac{dN_{SS}}{dt} = -\frac{V_{s,SS}}{h} N_{SS} \quad (S3.2)$$

Below, Eq. S3.1 is simplified based on a series of informed assumptions, which subsequently are validated against simulations using the full deterministic Eq. S3.1. First it is assumed that aggregation is the rate limiting process for the observed removal of ENPs from the water phase. This is based on the logic that aggregates first need to be large enough for sedimentation to occur [7]. This means that the aggregation terms in Eq. S3.1 are considered to be rate determining and that the last term in Eq. S3.1 can be omitted. Second, it is assumed that the summations in Eq. S3.1 can be replaced by single terms accounting for the *apparent critical* collision behaviour for sedimentation. This is motivated as follows. The summation in Eq. S3.1 accounts for numerous collisions that will not (yet) lead to homo- or hetero-aggregates large enough to settle. However, a certain fraction of all possible collisions will at some point reach a critical limit after which rapid settling occurs. The measured removal in the sedimentation experiments relates to this apparent removal of settleable ENPs only (ENP_{crit}). Because size distributions of these settling ENP aggregates may not be monodisperse, the single terms are governed by apparent parameters reflecting average properties of the particles at the onset of settling. Third, it is assumed that the ENP concentration change in the overlying water is determined by aggregation to settling particles only i.e. is not affected by progressive aggregation to larger particles. Progressive aggregation cannot affect ENP_{crit} concentrations beyond the critical size for sedimentation because they would have settled already. This implies that the first two terms for aggregation in Eq. S3.1 can be combined. Consequently, Eq. S3.1 can be simplified to:

$$\frac{dC_{ENP,crit}}{dt} = -\alpha_{hom,crit}K_{hom,crit}C_{ENP,crit}^q - \alpha_{het,crit}K_{het,crit}C_{SS}C_{ENP,crit} \quad (S3.3)$$

Where

$C_{ENP,crit}$ is the concentration of settleable ENPs

$K_{hom,crit}$ is the apparent collision rate constant for the formation of settleable ENP homo-aggregates

$\alpha_{hom,crit}$ is the apparent attachment efficiency for settleable ENP homoaggregates

$\alpha_{het,crit}$ is the apparent attachment efficiency for settleable ENP-SS heteroaggregates

$K_{het,crit}$ is the apparent collision rate constant for the formation of settleable ENP hetero-aggregates

The exponent q defines the kinetics for homoaggregation and may take a value between 1 and 2. For instance, the formation of doublets would follow second order kinetics ($q = 2$), whereas the kinetics of collisions between large aggregates and primary particles would approach pseudo first order kinetics ($q = 1$).

The best value for q was obtained by fitting the analytical solution to Eq. S3.3 for q is 1, 1.5 and 2 respectively, against simulations based on Eq. S3.1. The simulations used a numerical model, which takes into account all size classes up to 350 nm CeO₂ ENP aggregates and all processes as condensed in Eq. S3.1. The largest aggregate consists of 2629 primary particles with a fractal dimension of 2.5. The fit for removal due to homoaggregation only is given in Figure S3.4. The simulation shows a time lag of about 1 day needed for the formation of aggregates large enough for settling. From day 2 onwards the removal of ENPs from the water phase is best described by apparent first order removal kinetics, i.e. $q = 1$. Simulations with $q = 1.5$ and $q = 2$ showed a worse overall quality of fit (see Figure S3.4). With $q = 1$ and combination of Eq. S3.2, Eq. S3.3 can be further simplified to:

$$\frac{dC_{ENP}}{dt} = -\alpha_{hom,crit}K_{hom,crit}C_{ENP} - \alpha_{het,crit}K_{het,crit}C_{0,SS}e^{-\frac{V_{s,SS}}{h}t}C_{ENP} \quad (S3.4)$$

In summary, Eq. S3.4 describes how the concentration of the (operationally defined) settling ENP fraction changes over time, as a function of the processes that drive the production of aggregates. Aggregates that do not settle substantially in the time interval over which settling is monitored (1 days in the present experiments, 14 d in ref [3]) are also formed. Furthermore, primary particles may be stabilised and not settle at all. The latter two categories of processes lead to a residual fraction, which is also operationally defined (Table S3.5).

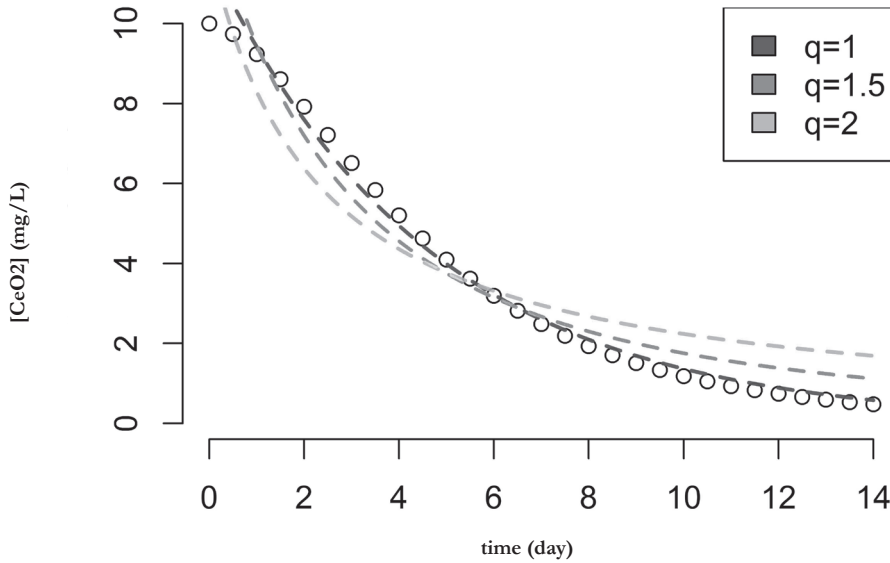


Figure S3.4 Fit of the homoaggregation term in equation S3.3 for q is 1, 1.5 and 2, to model simulation data calculated from a mechanistic numerical model based on the Von Smoluchowski-Stokes equation (Eq. S3.1 and S3.2). Mechanistic model for 10 mg L^{-1} 15 nm CeO_2 ENPs.

Calculating the heteroaggregation rate

Eq. S3.4 can be fitted to ENP sedimentation data in order to estimate the product $\alpha_{hom,crit} K_{hom,crit}$ in Eq. S3.4, which is equal to the apparent critical homoaggregation rate constant $k_{hom,crit}$ ($\alpha_{hom,crit} K_{hom,crit} = k_{hom,crit}$). Therefore the contribution of homoaggregation to the removal of ENPs from the water phase is separately assessed by fitting the solution of the first term in Eq. S3.4 to the ENP concentration in time for filtered water (Eq. S3.5).

$$C(t) = C_0 e^{-k_{hom,crit} t} \quad (\text{S3.5})$$

This assumes that heteroaggregation in filtered water is negligible due to the absence of natural colloids or suspended solids. The estimated values for $k_{hom,crit}$ then are substituted in the solution of Eq. S3.4, in which $\alpha_{het,crit} K_{het,crit} = k_{het,crit}$, as the only unknown. $V_{s,SS}$ is calculated according to Stokes from the density and radius of the SS. The analytical solution to Eq. S3.4 is:

$$C(t) = \frac{C_0 e^{\frac{-k_{hom,crit} t V_{s,SS} + k_{het,crit} h C_{0,SS} e^{-\frac{V_{s,SS} t}{h}}}{V_{s,SS}}}}{e^{\frac{k_{het,crit} C_{0,SS} h}{V_{s,SS}}}} \quad (\text{S3.6})$$

which then can be fitted to the sedimentation data in unfiltered water to obtain the heteroaggregation rate constant $k_{het,crit}$.

Alternatively, heteroaggregation rate constants $k_{het,crit}$ can be calculated directly by rearrangement of Eq. S3.6:

$$k_{het,crit} = \frac{v_{s,SS} \left(\ln \frac{C_t}{C_0} + k_{hom,crit} t \right)}{C_{SS} h \left(e^{\left(-\frac{v_{s,SS}}{h} t \right)} - 1 \right)} \quad (S3.7)$$

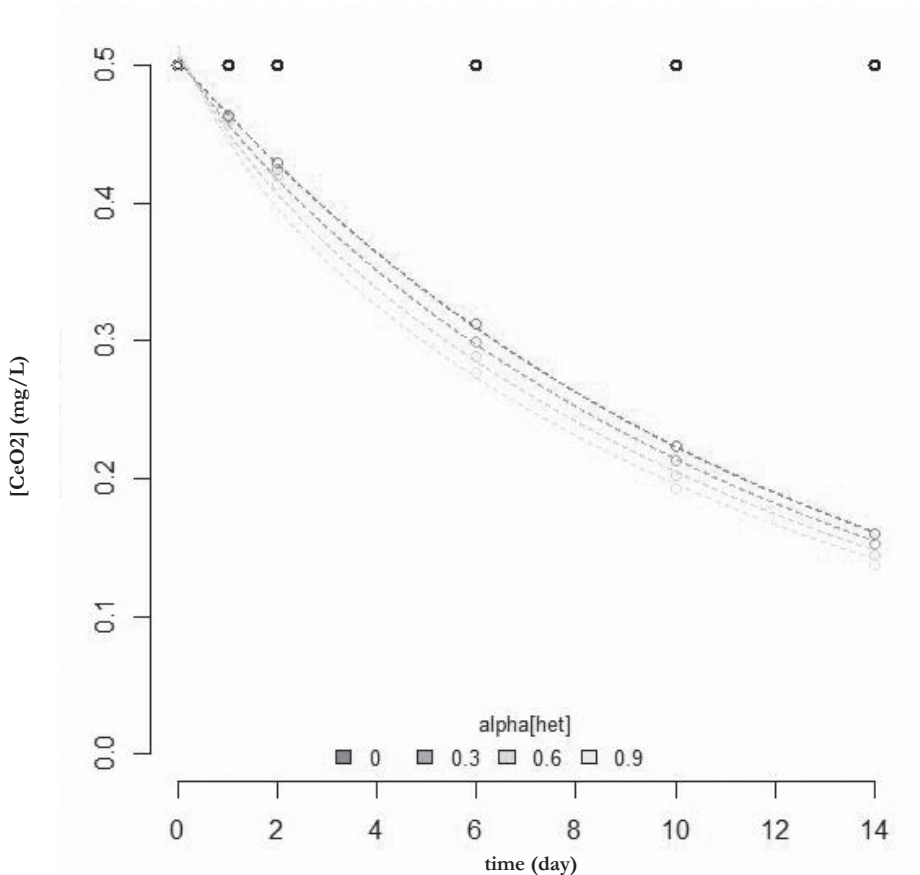


Figure S3.5 Plot of fit of Eq. S3.6 to simulated data. With simulated data of sedimentation of CeO_2 ENPs by homo- and heteroaggregation with α_{het} ranging between 0 and 0.9. Black open circles denote the total concentration of ENP homoaggregates and ENP-NC heteroaggregates in suspension and in the sediment.

To show the validity of the simplified aggregation-sedimentation model, Eq. S3.5 and S3.6 were fitted to simulation results calculated with the full Smoluchowski-Stokes model (i.e. Eq. S3.1 and S3.2), thus taking all homo- and heteroaggregation interactions into account (Figure S3.5). The simulation used a numerical model which takes into account all size classes up to 1 μm CeO_2 ENP aggregates and processes as given by Eq. S3.1. The primary CeO_2 particle size was 20 nm and an initial particle size distribution with an average size of 175 nm. The NC had an average radius of 0.5 μm , density of 1250 kg m^{-3} , and 100 mg L^{-1} initial concentration. A 0.5 mg L^{-1} CeO_2 suspension with α_{het} set to 0, 0.3, 0.6, 0.9 were simulated. The case where α_{het} is 0 was used to estimate $k_{hom,crit}$ by fitting Eq. S3.5 to the simulated data using the non-linear least squares method in R. Subsequently Eq. S3.6 was fit to the simulated data. It appears from Figure S3.5 that the simplified model adequately captures the relationship between $[\text{CeO}_2]$ and time as calculated by the full Smoluchowski-Stokes model.

Relationships between homo- and heteroaggregation rates, collision frequency and attachment efficiency

As the heteroaggregation rate $k_{het,crit}$ equates to the product of α_i and $K_{ENP,SS,p}$ (Eq. S3.1) in theory α values can be directly calculated, if $K_{ENP,SS}$ values are known. From basic colloid theory it is known that $K_{ENP,SS}$ can be estimated theoretically using the known description of the three main processes affecting the collision frequency: Brownian motion, shear rate and differential settling [7, 8]. The sum of the quantitative description of these three processes result in the collision frequency given by Eq. S3.8.

$$K_{ENP,SS} = \frac{\frac{2k_b T}{3\mu} \frac{(a_{SS} + a_{ENP})^2}{a_{SS} a_{ENP}} + \frac{4}{3} G (a_{SS} + a_{ENP})^3 + \pi (a_{SS} + a_{ENP})^2 |V_{s,SS} - V_{s,ENP}|}{\rho_{SS} V_{SS}} \quad (\text{S3.8})$$

Where

- k_b : Boltzman constant [$\text{m}^2 \text{kg}^{-1} \text{s}^{-2} \text{K}$]
- T : Temperature [K]
- μ : Viscosity [Pa·s]
- a_{SS} : NC radius [m]
- a_{ENP} : ENP radius [m]
- G : Shear rate [s^{-1}]
- V_s : Sedimentation rate [m s^{-1}]

with V_s given by:

$$V_s = \frac{2a^2 (\rho_p - \rho_w) g}{9\mu} \quad (\text{S3.9})$$

in which

ρ_p : Density of the ENP or SS [kg m^{-3}]

ρ_w : Density of suspending medium [kg m^{-3}]

g : Gravitational acceleration [m s^{-2}]

The density of the SS is calculated as weighed average sediment particle density [1] with an organic matter (OM) fraction with low density (1250 kg m^{-3}) and a mineral fraction with relatively high density (2650 kg m^{-3})[2]. OM is 5.20%, the density is 2577 kg m^{-3} .

Because of the uncertainties in the applicability of Eq. S3.8 to the natural and heterogeneous conditions in our water samples, calculations of α and K were omitted at this stage. However, in better characterised laboratory systems, the method presented in this paper can be used to estimate attachment efficiencies.

References Supporting Information

- [1] Avnimelech Y, Ritvo G, Meijer LE, Kochba M. 2001. Water content, organic carbon and dry bulk density in flooded sediments. *Aquacult Eng* 25:25-33.
- [2] Boyd CE. 1995. *Bottom Soils, Sediment, and Pond Aquaculture*. Chapman & Hall, New York.
- [3] Quik JTK, Velzeboer I, Wouterse M, Koelmans AA, van de Meent D. 2014. Heteroaggregation and sedimentation rates for nanomaterials in natural waters. *Water Res* 48:269-279.
- [4] Quik JTK, Vonk JA, Hansen SF, Baun A, Van De Meent D. 2011. How to assess exposure of aquatic organisms to manufactured nanoparticles? *Environ Int* 37:1068-1077.
- [5] Quik JTK, Stuart MC, Wouterse M, Peijnenburg W, Hendriks AJ, van de Meent D. 2012. Natural colloids are the dominant factor in the sedimentation of nanoparticles. *Environ Toxicol Chem* 31:1019-1022.
- [6] Hotze EM, Phenrat T, Lowry GV. 2010. Nanoparticle Aggregation: Challenges to Understanding Transport and Reactivity in the Environment. *J Environ Qual* 39:1909-1924.
- [7] Farley KJ, Morel FMM. 1986. Role of coagulation in the kinetics of sedimentation. *Environ Sci Technol* 20:187-195.
- [8] Friedlander SK. 2000. *Smoke, dust, and haze: fundamentals of aerosol behavior*, Second ed. Oxford University Press, New York.
- [9] Filella M. 2007. Chapter 2. Colloidal Properties of Submicron Particles in Natural Waters. In Wilkinson KJ, Lead JR, eds, *Environmental Colloids and Particles: behaviour, separation, and characterisation*. Wiley.

Chapter 4



TiO₂ C₆₀ ZrO₂ CeO₂ SWCNTs C₆₀ Al₂O₃
CNTs PMMA Al₂O₃ PFOS PVP-Ag MWCNTs PVP-Ag SWCNTs
nano-PS C₆₀ micro-PE PVP-Ag CeO₂ MWCNTs
SiO₂-Ag MWCNTs PVP-Ag C₆₀ CeO₂ PVP-Ag SiO₂-Ag TiO₂ SiO₂-Ag
ZrO₂ SWCNTs PMMA PVP-Ag nano-PS C₆₀ MWCNTs PFOS micro-PE
SiO₂-Ag micro-PE PMMA MWCNTs CeO₂ micro-PE CeO₂ Al₂O₃
PVP-Ag C₆₀ PVP-Ag nano-PS Al₂O₃
SiO₂-Ag CeO₂ Al₂O₃ MWCNTs MWCNTs TiO₂
CNTs C₆₀ nano-PS MWCNTs PVP-Ag TiO₂ PFOS
micro-PE PCBs MWCNTs CeO₂ CeO₂ ZrO₂ C₆₀ PMMA MWCNTs
nano-PS Al₂O₃ CeO₂ PCBs CeO₂ SWCNTs nano-PS PMMA MWCNTs
SWCNTs PCBs PFOS MWCNTs ZrO₂ MWCNTs SiO₂-Ag PMMA
ZrO₂ C₆₀ nano-PS SiO₂-Ag PFOS SiO₂-Ag PMMA Al₂O₃ MWCNTs ZrO₂
PCBs SiO₂-Ag PFOS SiO₂-Ag PVP-Ag PMMA MWCNTs TiO₂
TiO₂ PCBs SiO₂-Ag MWCNTs TiO₂ PVP-Ag PCBs TiO₂ C₆₀
ZrO₂ micro-PE CeO₂ PFOS MWCNTs MWCNTs ZrO₂ C₆₀
MWCNTs PCBs SWCNTs micro-PE SiO₂-Ag PMMA
SiO₂-Ag SWCNTs PFOS ZrO₂ CeO₂ MWCNTs
nano-PS PMMA C₆₀ PFOS PVP-Ag C₆₀ PFOS PVP-Ag
MWCNTs Al₂O₃ PFOS TiO₂ CeO₂
PCBs micro-PE ZrO₂ C₆₀ SWCNTs PMMA nano-PS

Sorption of perfluorooctane sulfonate to carbon nanotubes in aquatic sediments



TiO₂ MWCNTs ZrO₂ TiO₂ CeO₂ MWCNTs CeO₂ SWCNTs SiO₂-Ag
SWCNTs PMMA Al₂O₃ PFOS PVP-Ag CeO₂ MWCNTs PVP-Ag SWCNTs
nano-PS C₆₀ micro-PE C₆₀ SiO₂-Ag TiO₂ C₆₀
Al₂O₃ SiO₂-Ag MWCNTs PVP-Ag CeO₂ PVP-Ag C₆₀ MWCNTs PFOS micro-PE
SiO₂-Ag PMMA PVP-Ag nano-PS C₆₀ MWCNTs PFOS micro-PE
PCBs SiO₂-Ag CeO₂ Al₂O₃ PVP-Ag nano-PS Al₂O₃ CeO₂ Al₂O₃
MWCNTs C₆₀ nano-PS MWCNTs CeO₂ micro-PE CeO₂ Al₂O₃ MWCNTs TiO₂ PFOS
micro-PE PCBs MWCNTs CeO₂ CeO₂ ZrO₂ C₆₀ PMMA MWCNTs
nano-PS Al₂O₃ CeO₂ PCBs CeO₂ SWCNTs nano-PS MWCNTs
SiO₂-Ag ZrO₂ C₆₀ MWCNTs ZrO₂ micro-PE SiO₂-Ag PMMA
C₆₀ PCBs SiO₂-Ag PFOS SiO₂-Ag PMMA Al₂O₃ MWCNTs ZrO₂
ZrO₂ TiO₂ PCBs SiO₂-Ag PVP-Ag PMMA Al₂O₃ MWCNTs TiO₂
C₆₀ TiO₂ C₆₀ MWCNTs TiO₂ MWCNTs ZrO₂ C₆₀ PMMA
CeO₂ MWCNTs SWCNTs PFOS ZrO₂ micro-PE SiO₂-Ag MWCNTs
micro-PE SiO₂-Ag nano-PS PFOS CeO₂ C₆₀ PFOS PMMA PVP-Ag
TiO₂ MWCNTs Al₂O₃ PFOS PVP-Ag SWCNTs PMMA TiO₂ CeO₂
PCBs micro-PE Al₂O₃ PFOS PVP-Ag SWCNTs PMMA nano-PS
TiO₂ MWCNTs Al₂O₃ PFOS PVP-Ag SWCNTs PMMA nano-PS

Published as: Kwadijk CJAF, Velzeboer I, Koelmans AA. 2013. Sorption of perfluorooctane sulfonate to carbon nanotubes in aquatic sediments. *Chemosphere* 90:1631-1636.

Abstracts

To date, sorption of organic compounds to nanomaterials has mainly been studied for the nanomaterial in its pristine state. However, sorption may be different when nanomaterials are buried in sediments. Here, we studied sorption of perfluorooctane sulfonate (PFOS) to sediment and to sediment with 4% multiwalled carbon nanotubes (MWCNTs), as a function of factors affecting PFOS sorption; aqueous concentration, pH and Ca^{2+} concentration. Sorption to MWCNTs in the sediment–MWCNT mixtures was assessed by subtracting the contribution of PFOS sorption to sediment-only from PFOS sorption to the total sediment–MWCNT mixture. PFOS $\log K_d$ values ranged 0.52–1.62 L kg^{-1} for sediment and 1.91–2.90 L kg^{-1} for MWCNTs present in the sediment. The latter values are relatively low, which is attributed to fouling of MWCNTs by sediment organic matter. PFOS sorption was near-linear for sediment (Freundlich exponent of 0.92 ± 0.063) but non-linear for MWCNTs (Freundlich exponent of 0.66 ± 0.03). Consequently, the impact of MWCNTs on sorption in the mixture was larger at low PFOS aqueous concentration. Effects of pH and Ca^{2+} on PFOS sorption to MWCNTs were statistically significant. We conclude that MWCNTs fouling and PFOS concentration dependency are important factors affecting PFOS–MWCNT interactions in sediments.

4.1 Introduction

Perfluorinated Alkylated Substances (PFAS) are a group of surfactants that have been produced and subsequently emitted into the environment for over 50 years [1]. Perfluorooctane sulfonate (PFOS) is the PFAS that has raised the most concern as it has been detected in humans, fish and wildlife all over the globe, including the arctic [1]. Transport in the aquatic environment is considered an important process in the distribution and fate of chemicals such as PFOS [2, 3]. Earlier PFOS sorption studies identified organic carbon content to be the dominant parameter affecting sorption [3–5]. Consequently, understanding interactions of PFAS with components of the carbon cycle is crucial to understand the environmental fate, bioavailability and effects of this group of surfactants. Besides organic matter, pH and aqueous Ca^{2+} concentration are two other variables that have been mentioned as important factors affecting sorption equilibrium for PFOS [4, 6, 7], although the number of studies addressing such effects still is limited. Absorption or limited penetration of anionic PFAS into sediment organic matter seems to be the dominant mechanism of sorption [4]. pH-effects on PFOS sorption are expected to be caused by pH-dependent changes in sediment, such as organic matter charge, while Ca^{2+} effects on PFOS sorption are explained from a reduction in the charge on the organic matter [4].

Nanomaterials such as carbon nanotubes (CNTs) are another group of materials of emerging concern [8, 9]. Although CNTs may exert direct toxic effects

in soils, sediments and the aqueous phase, a growing body of evidence shows that effect thresholds are orders of magnitude higher than expected environmental concentrations [8, 10, 11]. However, CNTs are shown to be taken up in the gastrointestinal tract of several aquatic and terrestrial organisms and may act as a carrier for traditional toxic chemicals, a mechanism often referred to as the Trojan horse effect [12, 13]. Furthermore, nanomaterials such as CNTs are increasingly being used for pollution prevention, treatment, and cleanup (nanoremediation) [14]. This is why recent studies addressed the strong sorption of organic chemicals to CNTs, such as chlorobenzenes [15] and polycyclic aromatic hydrocarbons (PAHs) [16]. We are aware of only one study on sorption of PFOS to CNTs [17]. Because hard carbon materials like CNTs will increasingly be spread into the environment it is important to understand the effect they will have on the fate of PFOS. Previous studies on sorption of organic chemicals to CNTs typically used pristine CNTs in water-only systems [15-17]. The realism of such test conditions may be limited for two reasons. First, the presence of dissolved organic matter (DOM) will probably lower the adsorption efficiency of organic chemicals, a process commonly referred to as organic matter fouling [18, 19]. Second, it is not the pristine nanoparticles but their altered and aged form that will be found in the environment [20, 21]. Interactions with sediment organic matter and DOM are reported to affect the stability and toxicological effects of CNTs [22-24]. Consequently, it is most relevant to study the interactions of CNTs with PFOS in the presence of sediment organic material.

The aim of this study was (a) to characterize the effect of CNT amendments on sediment water partitioning of PFOS and (b) to assess the effect of pH and Ca^{2+} on sorption to sediment and sediment amended with CNTs under field relevant conditions. To this end, experiments were performed to study the differences in sorption when CNTs are added and pH and Ca are varied. Multiwalled carbon nanotubes (MWCNTs) were chosen for this experiment since they are expected to dominate over single walled nanotubes in the environment [25].

4.2 Materials and methods

Chemicals and reagents

Acetonitrile, acetone, n-hexane, hydrochloric acid, sodium hydroxide and methanol were obtained from LGC Standards (Wesel, Germany). Ammoniumformiate and calcium carbonate were obtained from Sigma-Aldrich (Zwijndrecht, Netherlands). Standard solution mixtures for the sulfonates in concentrations of $2 \mu\text{g mL}^{-1}$ in methanol as well as $^{13}\text{C}_4$ labeled PFOS were obtained from Wellington Laboratories (Guelph, Canada). Sodium sulfate was dried for 20 h at 450°C before use. Fifty nanograms of $^{13}\text{C}_4$ -PFOS in methanol:water(1:1) was used as internal standard solution. Dutch Standard Water (DSW) was prepared as deionized water with $200 \text{ mg L}^{-1} \text{CaCl}_2 \cdot 2\text{H}_2\text{O}$, $180 \text{ mg L}^{-1} \text{MgSO}_4 \cdot \text{H}_2\text{O}$, $100 \text{ mg L}^{-1} \text{NaHCO}_3$, and $20 \text{ mg L}^{-1} \text{KHCO}_3$;

pH \approx 8.2. Nanotubes (MWCNTs) were obtained from Cheaptubes (Brattleboro, VT, USA) and had an inner diameter of 5–10 nm, outer diameter of 20–30 nm, length of 10–30 μm , specific surface area of 110 $\text{m}^2 \text{g}^{-1}$ and a purity of 95 wt.% [11].

Sediment

Sediment was sampled from Lake Ketelmeer in the Netherlands in October 2009 using a van Veen grabber. The sediment was sieved and the fraction $<63 \mu\text{m}$ was homogenized in a barrel. Representative subsamples of 1 g of the homogenized sediment were transferred to 50 mL polypropylene tubes. Organic matter content (f_{om}) was determined gravimetrically as loss on ignition (550°C for 3 h), and was 5.2 wt.%. Calcium carbonate was gas volumetrically determined, according to Scheibler (NEN-ISO 10693), and was 8.69%.

Experimental setup

Modified DSW was prepared with a nominal Ca^{2+} concentration of 40 mg L^{-1} to mimic fresh water concentrations, 100 mg L^{-1} to mimic brackish water concentrations and 400 mg L^{-1} to mimic salt water concentrations. Other cations like for instance sodium were reported not to affect PFOS sorption [4] and therefore were not varied. A volume of 20 mL of each DSW type was then added to 1 g of sediment. Subsequently, PFOS concentrations were brought to 0.05, 0.5 and 5 mg L^{-1} . pH was set to nominal initial values of 4, 6, 8 and 10 using sodium hydroxide and hydrochloric acid. All batches were prepared in triplicate. Previous studies have shown that PFOS sorption equilibrium between water and sediment is established within 30 d [4, 15]. Therefore, samples were equilibrated for 30 d on a shaking machine. During equilibration, the nominal pH, dissolved calcium concentrations ($[\text{Ca}^{2+}]$) and PFOS concentrations change due to sediment–water interactions. Therefore, after equilibration pH was measured and PFOS concentrations were determined as specified below. Dissolved calcium concentrations $[\text{Ca}^{2+}]$ after equilibration were calculated from the known a priori water chemical composition, sediment calcium carbonate content and final pH, using the CHEAQS equilibrium speciation program [26].

To study the impact of the presence of CNTs on the sediment–water distribution, the experiments were repeated with 40 mg MWCNTs added per batch. This yielded a MWCNT percentage of 4% on a dry weight basis, a percentage much higher than environmentally expected concentrations of MWCNTs [10], but close to percentages of carbon used for sediment remediation with in situ sorbent amendments [27].

Sample extraction and analysis

Samples were extracted and analysed using previously published procedures [3]. In short, sediments were extracted using acetonitrile and cleaned up using hexane (LGC Standards, Wesel, Germany) and ENVIcarb (Sigma–Aldrich, Zwijndrecht, Netherlands).

Quality assurance

Blanks were performed for each series of samples and were below LOD (<0.5 ng) for all series. Internal reference material was analysed along with each set of samples. All calibration curves had an $R^2 \geq 0.99$. Samples were weighed before and after equilibration to monitor leakage. If leakage occurred batches were removed from the experiment. Recoveries ranged between 80% and 110%, which complies to GLP standards.

Instrumentation

A Thermo Finnigan (Waltham, United States) Surveyor Autosampler and HPLC coupled with a Thermo Finnigan LCQ advantage Ion-Trap MS with electrospray (ESI-MS/MS) was used for quantification and detection. Separation was performed on a 50×2.00 mm (3 μ m) Hypersil BDS C18 column using ammoniumformate and formic acid in acetonitrile as mobile phase A and ammonium formate and formic acid in demineralized water as mobile phase B. The following ions were monitored to determine the target compounds: 499 for PFOS and 503 for $^{13}\text{C}_4$ -PFOS. Calibration curves for each compound consisted of eight points between 0.1 ng mL^{-1} and 300 ng mL^{-1} .

Data analysis

Statistical treatment was performed using regression from the data analysis toolpack in Microsoft Excel 2010. Speciation calculations were performed using CHEAQS [26]. Known concentrations of Na, Mg, Ca, CO_3 , etc. and sample specific conditions such as pH were used to calculate final $[\text{Ca}^{2+}]$ for each sample.

4.3 Results and discussion

Sorption of PFOS to sediment

Here, we discuss the primary data on sorption of PFOS to Ketelmeer sediment using the nominal $[\text{Ca}^{2+}]$ and pH values. The $n = 3$ replicated treatments had a satisfactory median standard error in the measured sediment PFOS concentration of 16% (range 4.7–26%), except for the treatment with the lowest PFOS spike and a nominal pH of 4, which had an outlying relative standard deviation of 51% ($n = 3$). Note that the variance did not only originate from analytical error but also to variation in pH and $[\text{Ca}^{2+}]$ between individual batches. The quantity of PFOS adsorbed to sediment after equilibration varied from 7% to 80% of the added total at time zero, which implies most batches fulfilled the OECD106 guideline of >20% adsorption in a batch sorption test and at most a factor of 2–3 deviation from the guideline in the remaining batches [28].

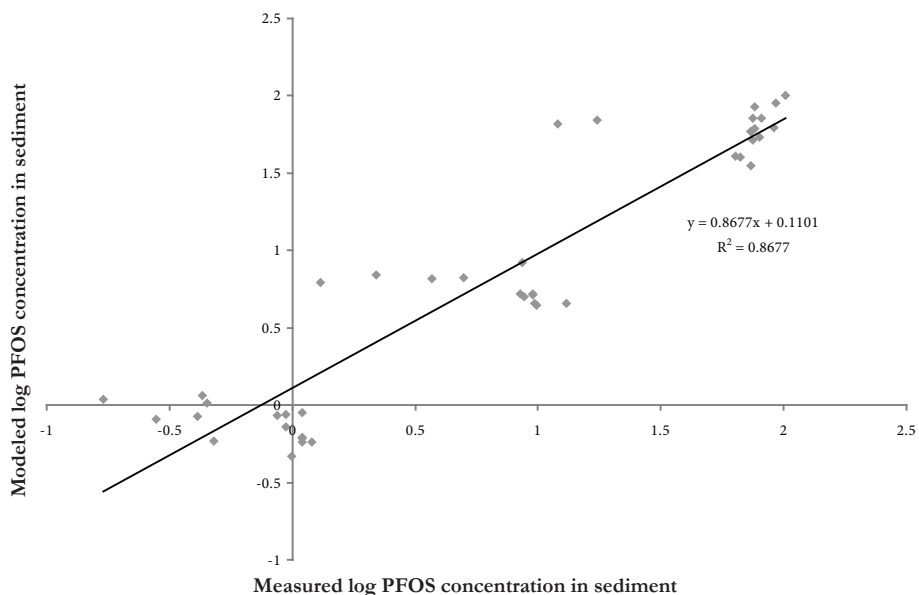


Figure 4.1 $\log K_d$ as a function of the fraction of organic carbon (f_{oc}) in sediment, using data from this study and from the literature. Regression calculated from data measured at near neutral pH.

Conditional distribution coefficients, K_d ($L\ kg^{-1}$), were calculated as the ratio of adsorbed and aqueous phase concentration. Here, ‘conditional’ relates to the fact that these K_d values may vary with water and sediment characteristics as well as with water concentration in case of a non-linear sorption isotherm (yet, isotherms for sediment were linear see below). The observed $\log K_d$ values varied between 0.38 and 1.77, that is, within 1.5 order of magnitude (Figure 4.1). The K_d values can be compared to literature values measured for sediments with varying organic matter content at similar pH and $[Ca^{2+}]$ concentration. It appears that our $\log K_d$ values at pH = 6 and $[Ca^{2+}] = 100\ mg\ L^{-1}$ with range 1.32–1.77, agree well with those reported by Higgins and Luthy [4] of 1.5 (Figure 4.1), and also comply to a general $\log K_d - f_{oc}$ relationship (Figure 4.1). Our current values, however, are lower than our previous field based values [3], which relate to sediments with a higher organic matter content and lower PFOS concentrations in the water phase (Figure 4.1). Our other current K_d values are much lower compared to previously reported values and trends, especially those at pH = 4. This is in agreement with earlier studies from You et al. [6], who found a decrease in sorption with a decrease in pH for their sediment and also used a sediment with low f_{oc} (0.16–1.5%) [6].

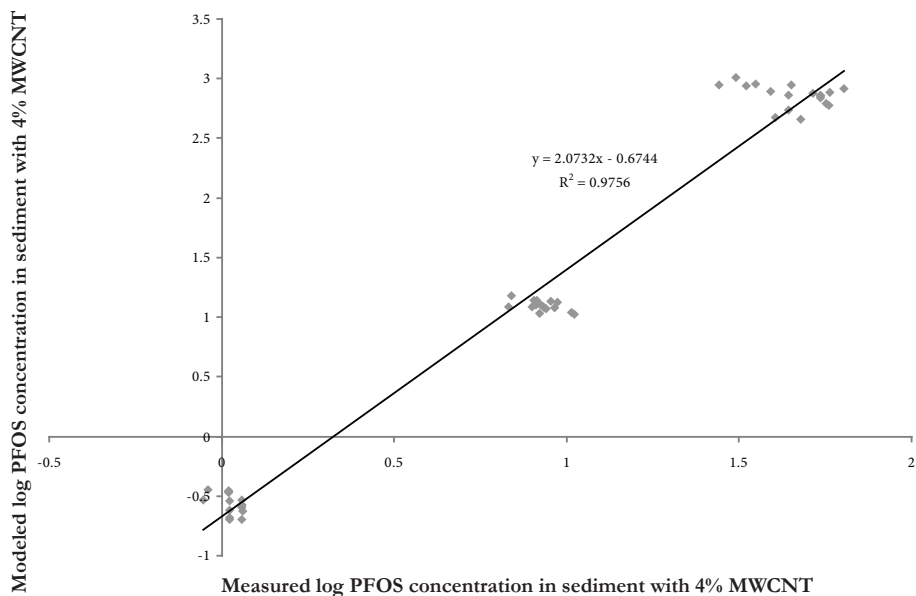


Figure 4.2 PFOS sorption to sediment-only, and to sediment amended with 4% MWCNT, as a function of pH, for three nominal PFOS concentrations (0.05, 0.5 and 5 mg L⁻¹)

Sorption of PFOS to MWCNT amended sediment

The sorption experiments were repeated with 4% (w:w) MWCNTs added to the sediment. After 30 d, sorption of PFOS to the sediment was higher for the samples amended with MWCNTs when exposed to 0.05 mg L⁻¹ nominal PFOS, slightly higher for those exposed to 0.5 mg L⁻¹ and lower for the 5 mg L⁻¹ group (Figure 4.2). So, for lower PFOS concentrations at pH 4 and 6 it seems that MWCNTs contributes significantly to sorption to sediment (significant at $p = 0.04$ and 1.9×10^{-5} respectively, t -test). At these low levels, 4% of MWCNTs added increases $\log K_d$ from 1.28 (0.52–1.62) to 1.58 (1.43–1.66) L kg⁻¹. Consequently, individual $\log K_d$'s for MWCNTs range from 1.91 to 2.90. These values are two to three orders of magnitude lower than the 6.0, 5.4 and 4.7 respectively, found for SWCNT, MWCNT10 and MWCNT50 calculated from isotherm data provided by Chen et al. [17]. Considering the surface area of the material our MWCNTs are best compared to the MWCNT50 from that study (110 m² g⁻¹ for our MWCNTs compared to 97.2 m² g⁻¹ for the MWCNT50) [17]. The difference in $\log K_d$ can be explained by the fact that the present study used a mixture of sediment and MWCNTs whereas Chen et al. [17] used pristine MWCNTs. We hypothesise that sediment organic matter attenuated sorption of PFOS to MWCNTs, by either sorption competition or limiting access of PFOS to adsorption sites.

At higher PFOS concentrations however, at pH 6 and 8, addition of MWCNTs results in lower total sorption to the mixture (significant at $p = 0.03$ and 0.006 respectively, t -test). This may be explained by saturation of the MWCNT surface by PFOS. Consequently, at 5 mg L^{-1} nominal PFOS concentration, MWCNTs constitute a less strong sorbent compared to the sediment organic matter, thus decreasing total PFOS sorption to the MWCNT–sediment mixture. The observed concentration dependent effect is in agreement with the effect found by Chen et al. [15] for PFOS sorption to black carbon (BC), which is also similar to non-linear sorption of many other hydrophobic organic chemicals to activated carbon or BC [29]. Similar to the sorption to organic matter in this study, Chen et al. [15] found PFOS sorption to black carbon to be stronger at lower concentration levels.

The previous discussion shows direct effects of the presence of MWCNTs on total PFOS sorption, implicitly assuming treatments can be compared based on their initial nominal concentrations, pH and $[\text{Ca}^{2+}]$. However, these conditions can be expected to hold only during the first stage of equilibration. Although differences are not that large, this comparison may be obscured by the fact that systems that are identical at start (based on their nominal pH, $[\text{Ca}^{2+}]$ and aqueous phase concentration), become different as pH and $[\text{Ca}^{2+}]$ values slowly change during equilibration. This is why we characterized the systems again at $t = 30 \text{ d}$ and interpret the adsorbed PFOS concentration data using a multiple regression model approach that accounts for $[\text{Ca}^{2+}]$, pH and aqueous phase PFOS concentration after 30 d.

Modeling sorption of PFOS to sediment

The possible influence of pH and $[\text{Ca}^{2+}]$ on sorption of PFOS to sediment has been shown in earlier reports [4, 7]. Such effects of calcium and pH on non-linear sorption to a soil or sediment can be described by a semi-empirical Three Species Freundlich model [30]:

$$C_{sed} = f_{om} K_f (H^+)^a [\text{Ca}^{2+}]^b C_w^c \quad (4.1)$$

which can be linearized into

$$\log C_{sed} = \log(K_f f_{om}) - a \text{pH} + b \log[\text{Ca}^{2+}] + c \log C_w \quad (4.2)$$

where K_f is the Freundlich constant ($\mu\text{g}^{(1-c)} \text{ L}^c \text{ kg}^{-1}$), f_{om} is the fraction organic matter in sediment (-), C_{sed} is the concentration in sediment ($\mu\text{g kg}^{-1}$), C_w is the concentration in water ($\mu\text{g L}^{-1}$) and $[\text{Ca}^{2+}]$ the dissolved calcium ion concentration in mol L^{-1} . Parameters in Eq. 4.2 were obtained by fitting the equation to the data for PFOS sorption to sediment, using the pH and $[\text{Ca}^{2+}]$ values after equilibration (Table 4.1). The model explains 87% of the variation in the data (Figure S4.1 in the Supporting Information). It appears that parameters ‘ a ’ and ‘ b ’ could not be estimated accurately.

The Freundlich exponent ‘ c ’ linked to the concentration of PFOS in the water, is found to be the only parameter to be statistically relevant ($p = 1.96 \times 10^{-17}$). The value of $c = 0.92 \pm 0.063$ implies that PFOS sorption to the sediment was near-linear in the studied PFOS concentration range.

Apart from trivial random error in the data, the lack of significance for pH-parameter ‘ a ’ may be explained by the limited and near-neutral range in our pH values (pH = 5.4–6.2), which in turn can be explained from carbonate buffering by the calcareous Ketelmeer sediment. Higgins and Luthy [4] did not detect a pH effect between pH 6 and 6.5 either, whereas earlier data for sorption of PFOS to sediments in the Netherlands also did not show an effect of pH on sorption of PFOS [3]. Similarly, the lack of significance for Ca-parameter ‘ b ’ may be explained from a relatively small range in $[Ca^{2+}]$ values after 30 d of equilibration. Earlier studies that did show a significant positive effect for pH and Ca^{2+} [4, 6, 15], covered wider and more extreme pH ranges, such as 2.03–5.05 for the study by Chen et al. [15], or pH 5.7–7.5 for Higgins and Luthy [4]. However, because pH and $[Ca^{2+}]$ effects have been convincingly shown in other studies, we conclude they are relevant for consistency and mechanistical reasons, and therefore kept in the model.

Table 4.1. PFOS Sorption parameters for sediment and MWCNTs^a

	<i>Coefficients</i>	<i>Standard Error</i>	<i>p-value</i>
<i>Multiple regression parameters Eq. 4.2 (n=43)</i>			
Intercept	6.2	2.1	0.006
a (pH)	-0.53	0.35	0.13
b ($\log C_a$)	1.1	0.83	0.18
c ($\log C_w$)	0.92	0.063	1.96×10^{-17}
<i>Multiple regression parameters Eq. 4.4 (n=33)</i>			
Intercept	-3.2	0.75	0.00023
x (pH)	0.29	0.080	0.0010
y ($\log C_a$)	-1.3	0.40	0.0036
z ($\log C_w$)	0.66	0.030	1.64×10^{-19}

^a Parameters obtained by multiple regression of $\log C_{sed}$ (Eq. 4.2) or $\log C_{MWCNT}$ (Eq. 4.4) against independent variables pH, Ca^{2+} and C_w .

Modeling sorption of PFOS on MWCNTs in sediment

PFOS sorption to MWCNTs in the presence of sediment was not measured directly but calculated as total sorption to the sediment–MWCNT mixture, minus sorption to the sediment. This assumed that PFOS sorption to the sediment in the mixture was not affected by the presence of 4% MWCNTs. PFOS sorption to MWCNTs is calculated using:

$$\log C_{MWCNT} = \log(C_{total} - C_{sed}) \quad (4.3)$$

where C_{total} is the concentration of PFOS measured in the sediment mixed with MWCNTs ($\mu\text{g kg}^{-1}$), C_{sed} is the concentration of PFOS in sediment only ($\mu\text{g kg}^{-1}$) and C_{MWCNT} is the adsorbed concentration of PFOS in MWCNT ($\mu\text{g kg}^{-1}$). Per individual batch, C_{sed} is calculated for the actual pH, $[\text{Ca}^{2+}]$ and C_w using Eq. 4.2 with the parameters in Table 4.1. This yields values for PFOS sorbed to MWCNTs in the MWCNT/sediment mixture (C_{MWCNT}) for each of the individual batches. Multiple regression is then applied using:

$$\log C_{MWCNT} = \log(K_{f,MWCNT} f_{MWCNT}) - x \text{pH} + y \log[\text{Ca}^{2+}] + z \log C_w \quad (4.4)$$

where $K_{f,MWCNT}$ is the Freundlich constant ($\mu\text{g}^{(1-z)} \text{L}^z \text{kg}^{-1}$) and f_{MWCNT} is the fraction of MWCNTs in the MWCNT amended sediment (-). Only those data points were included in the regression where sorption was significant, i.e. $C_{total} > C_{sed}$. When using the resulting parameters to plot results from the experiment versus the results calculated with Eq. 4.3 good linearity is achieved ($r^2 = 0.98$, $n = 49$) (see Figure S4.2 in the Supporting Information). Contrary to the earlier results for sediment without MWCNTs, pH and $[\text{Ca}^{2+}]$ are now found to have a significant impact on the sorption of PFOS ($p = 0.001$ and $p = 0.0036$ respectively, Table 4.1). Apparently, pH and $[\text{Ca}^{2+}]$ effects were more distinct when 4% d.w. of MWCNTs was added. We have two explanations for this difference. First, in the experiment with MWCNTs, the pH range was 0.6 log unit – i.e. a factor 4 in $[\text{H}^+]$ – larger than it was for the experiment with sediment only (5.4–6.8 versus 5.4–6.2 for the experiment with sediment), which may explain why a significant effect was observed with the MWCNTs but not with the earlier experiment. Log $[\text{Ca}^{2+}]$ range was slightly smaller in the experiment with the MWCNTs (-1.75 to -1.53 versus -1.76 to -1.48 for the experiment with sediment), but the difference is only 0.06 on the log scale. Second, MWCNTs can be assumed to represent a much more homogeneous surface for sorption, as compared to the natural sediment with its mineral, soft and hard carbon phases. Effects of pH and $[\text{Ca}^{2+}]$ will generally be more pronounced for a homogeneous surface.

The sign of the parameter for pH appears to be positive ($x = 0.29$, Table 4.1), which means that sorption decreased with increasing pH (see Eq. 4.4). The parameter for $[\text{Ca}^{2+}]$ is negative ($y = -1.3$, Table 4.1), which implies sorption is less at higher Ca^{2+} concentrations and may point to a mechanisms of calcium sorption competition. This contrasts to sorption of PFOS to sediment-only, for which positive effects of pH and $[\text{Ca}^{2+}]$ have been reported [6, 7, 31].

Whereas near-linear sorption was observed for the sediment ($c = 0.92$, Table 4.1), the fitted Freundlich exponent 'z' for MWCNTs was 0.66 ± 0.03 , meaning that PFOS sorption to MWCNTs in sediment was highly non-linear. This value of 0.66 is fairly close to a recently reported value for the Freundlich exponent for sorption of

PFOS to a similar, yet pristine MWCNTs, of 0.569 [17]. These values are consistent with the observation discussed above that sorption to MWCNTs was stronger at low PFOS concentration and weaker at high PFOS concentrations, due to saturation of the surface.

4.4 Implications

Our data showed that sorption of PFOS to MWCNTs in the presence of sediment, is one to two orders of magnitude lower than recent literature data for MWCNTs obtained without the presence of sediment, and is dependent on pH and Ca^{2+} concentration. This illustrates the importance of fouling and competition mechanisms for the interactions between organic contaminants and MWCNTs. Where MWCNTs act as a carrier for organic contaminants to benthic organisms, it is plausible that such mechanisms will reduce the uptake of these contaminants through particle ingestion.

A second potential implication of this study is that MWCNTs may dominate PFOS sorption in sediment at low PFOS concentration, due to a non-linear PFOS isotherm for MWCNTs and a near-linear isotherm for sediment organic matter. However, this was measured for 4% MWCNTs, a percentage that may represent conditions when MWCNTs are applied in a remediation scenario, but is not likely to occur in natural sediments.

Acknowledgment

We would like to thank Mr. Dennis Kuijper for his skilled lab work.

References

- [1] Houde M, De Silva AO, Muir DCG, Letcher RJ. 2011. Monitoring of Perfluorinated Compounds in Aquatic Biota: An Updated Review PFCs in Aquatic Biota. *Environmental Science & Technology* 45:7962-7973.
- [2] Chu SG, Letcher RJ. 2009. Linear and Branched Perfluorooctane Sulfonate Isomers in Technical Product and Environmental Samples by In-Port Derivatization-Gas Chromatography-Mass Spectrometry. *Analytical Chemistry* 81:4256-4262.
- [3] Kwadijk C, Korytar P, Koelmans AA. 2010. Distribution of Perfluorinated Compounds in Aquatic Systems in The Netherlands. *Environmental Science & Technology* 44:3746-3751.
- [4] Higgins CP, Luthy RG. 2006. Sorption of perfluorinated surfactants on sediments. *Environmental Science & Technology* 40:7251-7256.
- [5] Johnson RL, Anschutz AJ, Smolen JM, Simcik MF, Penn RL. 2007. The adsorption of perfluorooctane sulfonate onto sand, clay, and iron oxide surfaces. *Journal of Chemical and Engineering Data* 52:1165-1170.
- [6] You C, Jia CX, Pan G. 2010. Effect of salinity and sediment characteristics on the sorption and desorption of perfluorooctane sulfonate at sediment-water interface. *Environmental Pollution* 158:1343-1347.
- [7] Chen H, Zhang C, Yu YX, Han JB. 2012. Sorption of perfluorooctane sulfonate (PFOS) on marine sediments. *Marine Pollution Bulletin* 64:902-906.
- [8] Petersen EJ, Zhang L, Mattison NT, O'Carroll DM, Whelton AJ, Uddin N, Nguyen T, Huang Q, Henry TB, Holbrook RD, Chen KL. 2011. Potential Release Pathways, Environmental Fate, And Ecological Risks of Carbon Nanotubes. *Environmental Science & Technology* 45:9837-9856.
- [9] Klaine SJ, Koelmans AA, Horne N, Carley S, Handy RD, Kapustka L, Nowack B, von der Kammer F. 2012. Paradigms to assess the environmental impact of manufactured nanomaterials. *Environmental Toxicology and Chemistry* 31:3-14.
- [10] Koelmans AA, Nowack B, Wiesner MR. 2009. Comparison of manufactured and black carbon nanoparticle concentrations in aquatic sediments. *Environmental Pollution* 157:1110-1116.
- [11] Velzeboer I, Kupryianchyk D, Peeters ETHM, Koelmans AA. 2011. Community effects of carbon nanotubes in aquatic sediments. *Environment International* 37:1126-1130.
- [12] Hurt RH, Monthieux M, Kane A. 2006. Toxicology of carbon nanomaterials: Status, trends, and perspectives on the special issue. *Carbon* 44:1028-1033.
- [13] Cho HH, Smith BA, Wnuk JD, Fairbrother DH, Ball WP. 2008. Influence of surface oxides on the adsorption of naphthalene onto multiwalled carbon nanotubes. *Environmental Science & Technology* 42:2899-2905.
- [14] Karn B, Kuiken T, Otto M. 2009. Nanotechnology and in Situ Remediation: A Review of the Benefits and Potential Risks. *Environmental Health Perspectives* 117:1823-1831.
- [15] Chen H, Chen S, Quan X, Zhao YZ, Zhao HM. 2009. Sorption of perfluorooctane sulfonate (PFOS) on oil and oil-derived black carbon: Influence of solution pH and [Ca²⁺]. *Chemosphere* 77:1406-1411.

- [16] Yang K, Zhu L, Xing B. 2006. Adsorption of Polycyclic Aromatic Hydrocarbons by Carbon Nanomaterials. *Environmental Science & Technology* 40:1855-1861.
- [17] Chen X, Xia XH, Wang XL, Qiao JP, Chen HT. 2011. A comparative study on sorption of perfluorooctane sulfonate (PFOS) by chars, ash and carbon nanotubes. *Chemosphere* 83:1313-1319.
- [18] Pignatello JJ, Kwon S, Lu YF. 2006. Effect of natural organic substances on the surface and adsorptive properties of environmental black carbon (char): Attenuation of surface activity by humic and fulvic acids. *Environmental Science & Technology* 40:7757-7763.
- [19] Koelmans AA, Meulman B, Meijer T, Jonker MTO. 2009. Attenuation of Polychlorinated Biphenyl Sorption to Charcoal by Humic Acids. *Environmental Science & Technology* 43:736-742.
- [20] Wiesner MR, Lowry GV, Casman E, Bertsch PM, Matson CW, Di Giulio RT, Liu J, Hochella MF. 2011. Meditations on the Ubiquity and Mutability of Nano-Sized Materials in the Environment. *Acs Nano* 5:8466-8470.
- [21] Nowack B, Ranville JF, Diamond S, Gallego-Urrea JA, Metcalfe C, Rose J, Horne N, Koelmans AA, Klaine SJ. 2012. Potential scenarios for nanomaterial release and subsequent alteration in the environment. *Environmental Toxicology and Chemistry* 31:50-59.
- [22] Hyung H, Fortner JD, Hughes JB, Kim JH. 2007. Natural organic matter stabilizes carbon nanotubes in the aqueous phase. *Environmental Science & Technology* 41:179-184.
- [23] Hyung H, Kim JH. 2008. Natural organic matter (NOM) adsorption to multi-walled carbon nanotubes: Effect of NOM characteristics and water quality parameters. *Environmental Science & Technology* 42:4416-4421.
- [24] Edgington AJ, Roberts AP, Taylor LM, Alloy MM, Reppert J, Rao AM, Mao J, Klaine SJ. 2010. The influence of natural organic matter on the toxicity of multiwalled carbon nanotubes. *Environmental Toxicology and Chemistry* 29:2511-2518.
- [25] The Royal Society & The Royal Academy of Engineering. 2004. Nanoscience and nanotechnologies: opportunities and uncertainties. The Royal Society & The Royal Academy of Engineering, London.
- [26] Verweij W. 2011. CHEAQS, Computer Program for Calculating CHEmical Equilibria in AQUatic Systems.
- [27] Rakowska MI, Kupryianchuk D, Harmsen J, Grotenhuis T, Koelmans AA. 2012. In situ remediation of contaminated sediments using carbonaceous materials. *Environmental Toxicology and Chemistry* 31:693-704.
- [28] OECD/OCDE. 2000. OECD guideline for testing of chemicals: adsorption-desorption. Using a Batch Equilibrium Methods, OECD/OCDE 106.
- [29] Pikaar I, Koelmans AA, van Noort PCM. 2006. Sorption of organic compounds to activated carbons. Evaluation of isotherm models. *Chemosphere* 65:2343-2351.
- [30] Temminghoff EJM, VanderZee S, DeHaan FAM. 1995. Speciation and calcium competition effects on cadmium sorption by sandy soil at various pHs. *European Journal of Soil Science* 46:649-655.
- [31] Jeon J, Kannan K, Lim BJ, An KG, Kim SD. 2011. Effects of salinity and organic matter on the partitioning of perfluoroalkyl acid (PFAs) to clay particles. *Journal of Environmental Monitoring* 13:1803-1810.

Supporting Information

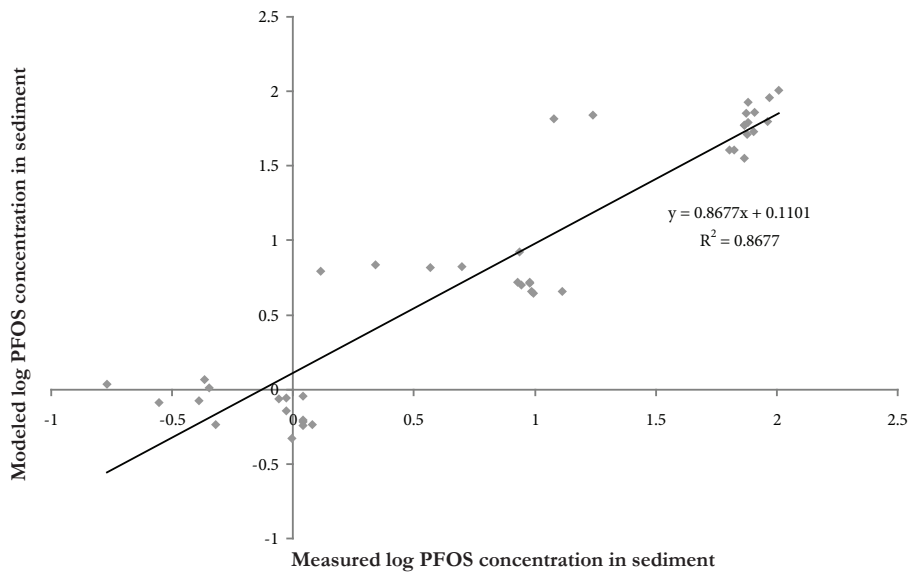


Figure S4.1 Modeled versus measured log PFOS concentrations in Ketelmeer sediment. Modeled values were calculated with multiple regression according to Equation 4.2.

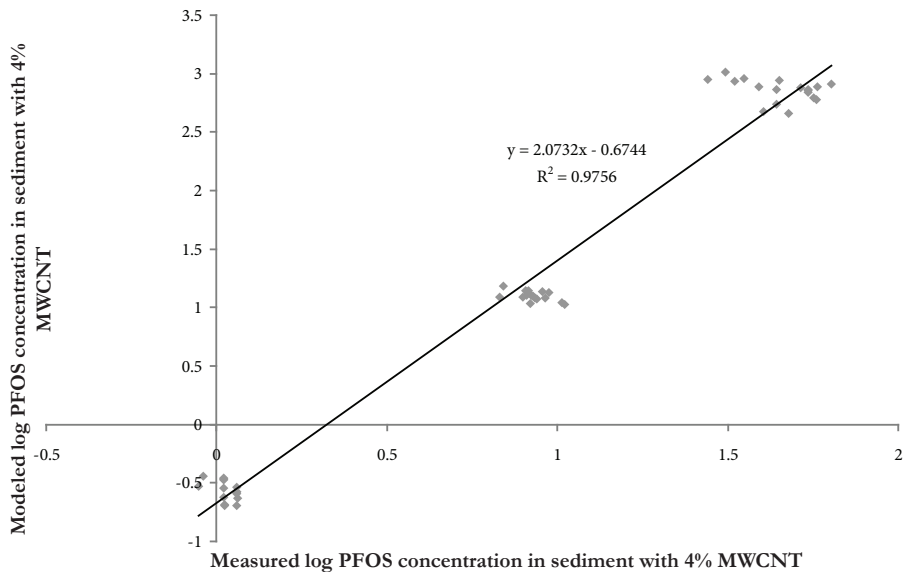
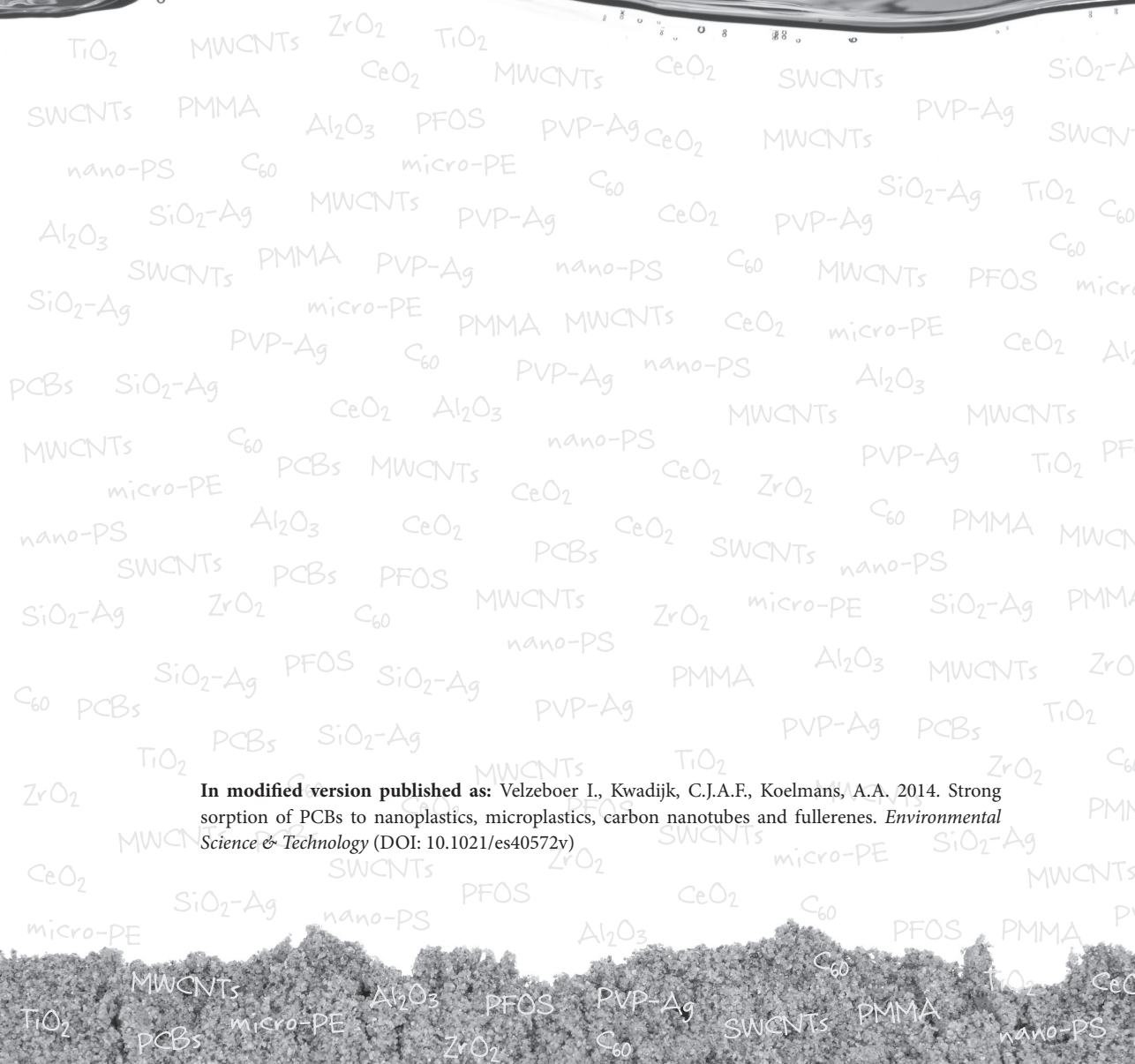


Figure S4.2 Modeled versus measured log PFOS concentrations in Ketelmeer sediment amended with 4% MWCNTs. Modeled values were calculated with multiple regression according to Equation 4.4.

Strong sorption of PCBs to nanoplastics, microplastics, carbon nanotubes and fullerenes



In modified version published as: Velzeboer I, Kwadijk, C.J.A.F., Koelmans, A.A. 2014. Strong sorption of PCBs to nanoplastics, microplastics, carbon nanotubes and fullerenes. *Environmental Science & Technology* (DOI: 10.1021/es40572v)

Abstract

The presence of microplastic and carbon-based nanoparticles in the environment may have implications for the fate and effects of traditional hydrophobic chemicals. Here we present parameters for the sorption of 17 CB congeners to 10-180 μm sized polyethylene (micro-PE), 70 nm polystyrene (nano-PS), multiwalled carbon nanotubes (MWCNTs), fullerene (C_{60}) and a natural sediment, in the environmentally relevant 10^{-5} to 10^{-1} $\mu\text{g L}^{-1}$ concentration range. Effects of salinity and sediment organic matter fouling were assessed by measuring the isotherms in fresh- and seawater, with and without sediment present. Sorption to the 'bulk' sorbents sediment organic matter (OM) and micro-PE occurred through linear hydrophobic partitioning with OM and micro-PE having similar sorption affinity. Sorption to MWCNTs and nano-PS was non-linear. PCB sorption to MWCNTs and C_{60} was 3 to 4 orders of magnitude stronger than to OM and micro-PE. Sorption to nano-PS was 1 to 2 orders of magnitude stronger than to micro-PE, which was attributed to the higher surface-volume ratio of nano-PS. Organic matter effects varied among sorbents, with the largest OM fouling effect observed for the high surface sorbents MWCNTs and nano-PS. Salinity decreased sorption for sediment and MWCNTs, but increased sorption for the polymers nano-PS and micro-PE. The exceptionally strong sorption of (planar) PCBs to C_{60} , MWCNTs and nano-PS may imply increased hazards upon membrane transfer of these particles.

5.1 Introduction

The past years, sorption of hydrophobic organic chemicals (HOCs) to nano- and micrometer sized carbon-based particles received growing interest. These particles, like fullerenes, carbon nanotubes (CNTs), nano- and microplastics may form a direct threat to aquatic organisms (eg., [1, 2]) but are also hypothesised to act as a carrier for HOCs [3, 4], thus potentially changing the exposure and risks to these chemicals. Furthermore, carbon-based nanomaterials may find applications as adsorbents in water purification or sediment remediation [2, 5, 6].

Sorption of HOCs to MWCNTs has been studied mainly for polycyclic aromatic hydrocarbons (PAH) at relatively high concentrations in the microgram per litre range [7-10]. The environmentally relevant pg to $\mu\text{g L}^{-1}$ range has been studied two times for PAHs [11, 12], but not yet for polychlorinated biphenyls (PCBs). PCBs make up an important class of pollutants, cover a wide range of hydrophobicities (i.e. $\log K_{ow}$) and enable studying the effects of hydrophobicity and molecular planarity on sorption to carbonaceous materials [13].

Nano- and micrometer sized plastic particles are known to be ingested by marine species such as fish, benthic worms and mussels [3, 14-16]. Some single solute sorption studies have been performed, which used mm-sized particles in the pure polymer state or used particles in a weathered state in seawater [17-20]. To our

knowledge there are no studies addressing sorption to nanoplastics. Nanoplastics have been found to penetrate cell walls and reach the circulatory system of for instance mussels [21]. It can be hypothesized that at the nanoscale, sorption may be different from that to the same polymer in bulk form because surface adsorption may dominate over partitioning into the bulk polymer. The combination of increased sorption and increased penetration may constitute an unforeseen risk.

For activated carbon, or natural carbon-based nanoparticles such as soot and black carbon, it has been shown that presence of organic matter may change the sorption properties *in situ*, either through fouling of surface sites or through a change in the state of the particles [22]. Carbon-based nanoparticles have been shown to aggregate rapidly [23, 24] and thus are likely to end up in the sediment [25] where sediment organic matter may affect their sorption properties. Similarly, salinity is known to affect the aggregation state of nanoparticles, which in turn may affect the sorption properties for HOCs [9].

The aim of the present study was to assess the sorption of 17 CB congeners to five types of particles: a natural sediment, fullerene (C_{60}), multiwalled carbon nanotubes (MWCNTs), micrometer sized polyethylene (micro-PE) and nano-polystyrene (nano-PS). Experiments were performed in fresh- and seawater to assess the effect of salinity, and for the nano- and microparticles with and without the presence of sediment to assess the effect of suppression of sorption by sediment organic matter. MWCNTs and nano-PS allow direct comparison of sorption to graphene layer based - versus polymer based carbon nanoparticles. Nanosized PE was not available but comparing nano-PS and micro-PE still may allow inferences on relative roles of surface sorption versus bulk partitioning. Because in the environment HOCs will be present in a mixture, the experiments were multi-solute experiments following established methodology previously developed in our lab (eg. [11-13, 22, 26-28]), to obtain sorption isotherms at realistic environmental concentrations of 10^{-5} to 10^{-1} $\mu\text{g L}^{-1}$, spanning a wide range of chemical hydrophobicity. Polyoxymethylene (POM) passive samplers were used to assess aquatic phase measurements without nanoparticle-water phase separation required. This polymer material was designed specifically for nano-sized carbon based particles in our previous work [13, 27] and used afterwards for various similar studies of PAH sorption to MWCNTs [11, 12].

5.2 Materials and methods

Materials

MWCNTs were obtained from Cheaptubes (Brattleboro VT, USA) as a powder with an inner diameter of 5 – 10 nm, outer diameter of 20 – 30 nm, length of 10 – 30 μm , and a purity of 95 wt.% [1, 29, 30]. Fullerene C_{60} was also obtained from Cheaptubes and had a declared purity of 99.0 wt%. Green fluorescent polyethylene (micro-PE) microspheres were obtained from Cospheric LLC (Santa Barbara CA, USA) with a

diameter of 10 – 180 μm . Polystyrene (nano-PS) nanospheres were kindly supplied by Joris Sprakel (AVT-PCC, Wageningen UR, the Netherlands). The 70 nm spheres were functionalised with carboxylic acid groups and were supplied as dispersion at 20% by weight. Particle sizes of micro-PE and nano-PS were characterized as described below and in the Supporting Information. Sediment was sampled from the Oesterput, a tidal flat in the Eastern Scheldt estuary (The Netherlands) in autumn 2012 and sieved with a 2 mm screen. Organic matter (OM) content was measured as loss on ignition (3 h at 550°C) and was $1.19 \pm 0.05\%$ ($n = 6$). Total organic carbon (TOC) was measured spectrophotometrically according to Kurmies and was $0.5 \pm 0.1 \%$ ($n = 2$). Calcium carbonate (CaCO_3) was determined volumetrically according to Scheibler (NEN-ISO 10693) and was $7.00 \pm 0.15\%$ ($n = 2$). Oesterput is a clean reference sediment site and used as such in many ecotoxicological studies in The Netherlands (eg. [3, 31, 32]).

POM sheets (76 μm thickness) were obtained from CS Hyde Company (Lake Villa IL, USA), cut into pieces of desired weight (5 – 500 mg, with 100 mg POM sheet having a size of 2.5×3.5 cm), washed ultrasonically with *n*-hexane (Promochem; picograde) and methanol (Promochem; optigrade), and air-dried before use.

Seventeen CB congeners (IUPAC no. 28, 31, 44, 52, 74, 77, 101, 105, 118, 126, 138, 149, 153, 156, 169, 170, and 180) were obtained from Dr. Ehrenstorfer GmbH, Augsburg, Germany and had a declared purity of > 97%. The selected PCBs included tri- to heptachloro congeners to span a range of $\log K_{ow}$ values of 5.7 to 7.4. Furthermore, this series includes tri- to non-ortho substituted PCBs to be able to assess effects of molecular planarity (Table S5.1). All stock solutions were prepared in acetone (Promochem; picograde). Dutch Standard fresh Water (DSW), was prepared as deionized water with calcium chloride ($\text{CaCl}_2 \cdot 2\text{H}_2\text{O}$; 0.2 g L^{-1} , VWR), magnesium sulphate ($\text{MgSO}_4 \cdot 7\text{H}_2\text{O}$; 0.18 g L^{-1} ; VWR), sodium hydrogen carbonate (NaHCO_3 ; 0.1 g L^{-1} , VWR) and potassium hydrogen carbonate (KHCO_3 ; 0.02 g L^{-1} , VWR). Seawater was sampled from the North Sea (SW), had a salinity of 34‰ and had a dissolved organic matter (DOC) concentration of 0.17 mg C L^{-1} . Sodium azide (NaN_3) was obtained from Aldrich (99%). Other chemical used were *n*-pentane (Promochem; picograde), 2,2,4-trimethylpentane (iso-octane; Promochem; picograde) and dichloromethane (Promochem; picograde).

Sorption experiments

All experiments were performed in 250 mL all-glass bottles and used 25 mg L^{-1} NaN_3 as biocide. To increase environmental relevance, particles were added such that an aggregation state would be reached more or less similar to what can be expected in the natural water system. Therefore sonication or forced predispersion in separate solutions was avoided. Sediment was added as wet sediment, micro-PE and C_{60} were slowly added as dry powder and nano-PS was added directly from the 20 wt% suspension. Only MWCNTs had to be predispersed as a 5 mg mL^{-1} suspension in vigorously agitated demineralised water and directly added to the bottles, because weighing the low amount of dry powder was not accurate enough. Particle and

aggregate sizes were assessed (see below). PCB sorption isotherms were measured for sediment, MWCNTs, nano-PS and micro-PE in fresh- and seawater. This was done by spiking PCBs to the bottles, which contained predesigned quantities of water, POM and adsorbent (see Table S5.2). The volume of acetone (spiking solvent) was less than 0.22% (v:v) for all samples to avoid solvent effects. Isotherms were also measured in parallel experiments where besides MWCNT, nano-PS and micro-PE, also suspended sediment was present, thus mimicking natural conditions (Table S5.2). Specific ‘intrinsic’ sorption to MWCNT, nano-PS and micro-PE in the latter experiments was calculated by subtracting the contribution of sorption to sediment from total sorption to the mixture, which is an established procedure described in the literature [22, 28, 30]. At the end of the experiments with sediment, DOC was enhanced to 0.27 ± 0.06 and $1.73 \pm 0.23 \text{ mg C L}^{-1}$ ($n = 3$) for fresh- and seawater respectively. For C_{60} only single point distribution coefficients were measured in freshwater.

The bottles were placed on an orbital shaker (100 rpm) at 20°C for equilibration [33]. After 6 weeks, the POM strips were removed from the bottles with tweezers, sprayed with demineralized water and wiped with a tissue [22, 27, 33]. Microscopic inspection confirmed that no particles remained at the surface. The strips were extracted with pentane-dichloromethane (85:15) by accelerated solvent extraction (Dionex ASE 350, Thermo Scientific), with ^{13}C -PCB28 and ^{13}C -PCB153 in iso-octane as internal standards. PCBs were analysed with GC-MS using a Shimadzu 2010 Plus GC coupled to a Shimadzu GC-MS-QP2010 Ultra quadrupole MS detector (’s Hertogenbosch, The Netherlands) equipped with a HT8 column with a 30 m x 0.25 mm i.d. and a film thickness of 0.25 μm as described in [34].

Characterisation of particles and aggregates

Most nanoparticle size characterisation methods are known to disturb the original aggregation state of the particles or to only provide a spherical equivalent measure of size [35]. Because of the sizes of the aggregates formed and in order to preserve the aggregates, we chose to characterise the sizes in solution as much as possible using light microscopy photographs (Olympus BX43F with Evolution MP colour camera). Additionally, for the MWCNT and PS nanoparticles, also transmission electron microscopy (TEM; JEOL JEM1011 with Veleta 2Kx2K camera (SIS)) image analysis was used. Size information is summarized in Table S5.3 and in Figures S5.1-S5.17.

Data analysis

Aqueous phase PCB concentrations were calculated from concentrations in POM using previously published POM-water equilibrium partition coefficients (K_{POM} ; $\text{L kg}^{-1} \text{ POM}$) [33]. K_{POM} values for seawater were not corrected for the salting out effect because differences between fresh- and seawater K_{POM} values have been shown to be small (i.e. < 0.1 log value) and not to be statistically different [27, 36, 37]. Adsorbed PCB concentrations were calculated from the spiked quantities and quantities detected in POM and water, using the mass balance [11-13, 22, 27, 28]. The ‘intrinsic’

sorption of PCBs to MWCNTs, nano-PS and micro-PE in the presence of sediment was determined by subtracting the contribution of PCB sorption to sediment from PCB sorption to the mixture of sediment and each of these particle types. Sorption to sediment was quantified by the K_p value for each individual PCB in either fresh- or seawater. This established procedure [12, 22, 28] assumes that partitioning of PCBs to the bulk dissolved or particulate sediment organic matter is not affected by the relatively low quantities of other particles present. An overview of equations used in the calculations is provided as Supporting Information (Table S5.4) [22]. Isotherms were constructed and interpreted with the Freundlich model $C_{ads} = K_f \times C_w^n$, with parameters $\log K_f$ and n obtained from linear regression analysis [38]. Differences in sorption parameters among treatments of fresh versus seawater and with/without sediment present were tested with generalized linear models (GLM) ($p < 0.05$) using SPSS (IBM SPSS Statistics 19.0, IBM, Armonk, NY, USA).

5.3 Results and discussion

Sorption to sediment

Sorption of PCBs to sediment is well-studied and is included here only for the sake of comparison and because the sediment K_p values are required to calculate intrinsic sorption to micro-PE, nano-PS and MWCNTs in the presence of sediment. PCB isotherms for sediment were linear (Figure 5.1 and Figure S5.21-37) with Freundlich exponent (n) values generally close to 1 (Table S5.5). Therefore, besides Freundlich coefficients, linear sorption partition coefficients K_p ($L\ kg^{-1}$) were calculated (Table S5.6). The partition coefficients for freshwater were up to 1.5 log unit higher than in seawater. It is unlikely that this difference is caused by the salting out effect, because this effect relates to the aqueous activity of the PCBs and thus would affect the POM-water and sediment-water partitioning equally and therefore would cancel out. Furthermore, POM-water coefficients were shown not to differ between fresh- and seawater [27, 36, 37]. Finally, a salting out effect would cause higher coefficients in seawater, which is the opposite of what we observed. The generally lower K_p values in seawater may be explained from a higher extent of aggregation of sediment borne colloids and humic acids [39].

To enable comparison with literature data, the partition coefficients were normalized to the sediment organic carbon content ($f_{oc} = 0.005$) and regressed against $\log K_{ow}$ yielding $\log K_{oc} = (1.02 \pm 0.11) \times \log K_{ow} + (0.65 \pm 0.73)$ ($R^2 = 0.85$) for freshwater and $\log K_{oc} = (1.39 \pm 0.19) \times \log K_{ow} - (2.24 \pm 1.24)$ ($R^2 = 0.79$) for seawater. Overall, the regression of the partition coefficients for freshwater against $\log K_{ow}$ was significantly higher than for seawater (GLM: $F = 4.959$, $p = 0.026$). The regression for freshwater can also be compared to the linear free-energy relationships (LFER) provided by Seth et al. [40]: $\log K_{oc} = \log K_{ow} - (0.48 \pm 0.42)$, which shows equal slope but an order of magnitude lower $\log K_{oc}$ values, perhaps due to differences in organic matter quality.

However, due to the 1 to 1.5 order of magnitude uncertainty in the intercepts in these regressions, the difference was not significant.

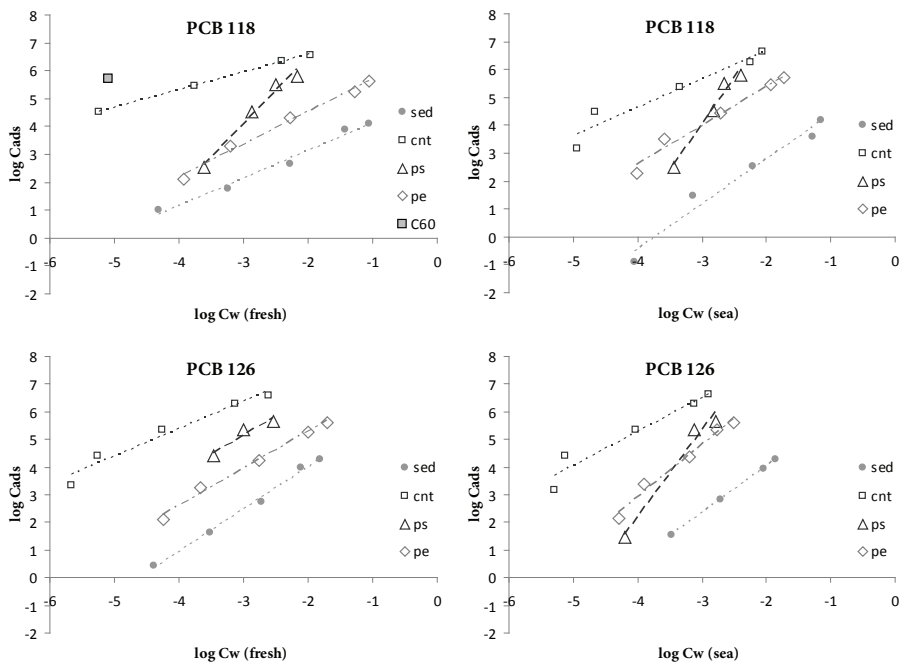


Figure 5.1 Isotherms of mono-ortho PCB 118 and non-ortho PCB 126 for sediment, MWCNTs, nano-PS and micro-PE (and C_{60} for PCB 118 in freshwater) in fresh- and seawater.

Sorption to micro-polyethylene (micro-PE)

In freshwater, sorption of PCBs to micro-PE was linear with Freundlich exponents (n) close to 1 (Figure 5.1, Figure S5.21-37 and Table S5.5). In seawater, isotherms were slightly concave, with Freundlich exponents up to 1.9 (Table S5.5). Because of the (near-) linearity and to enable comparison with literature data, linear partitioning coefficients were calculated (Table S5.6). In freshwater, regression of $\log K_p$ against $\log K_{ow}$ yielded the regression $\log K_p = (1.48 \pm 0.10) \times \log K_{ow} - (3.41 \pm 0.65)$ ($R^2 = 0.94$), which has a little higher slope but lower intercept compared to the regression reported for PE by Lohmann [41]; $\log K_p = (1.14 \pm 0.04) \times \log K_{ow} - (1.14 \pm 0.26)$ (Figure 5.2). Sorption for the average PCB however (i.e. at $\log K_{ow} = 6.68$) was comparable. The total surface area of micro-PE spheres in the experimental systems was 0.003 m^2 and seemed not to be reduced due to clustering or aggregation (Figure S5.12-15). Based on the measured adsorbed Σ PCB concentrations and the molecular surface areas of individual PCB congeners, the monolayer surface area coverage would be 38, 360, 3000, 30000 and 60000 % for the increasing system PCB loadings respectively (PCB

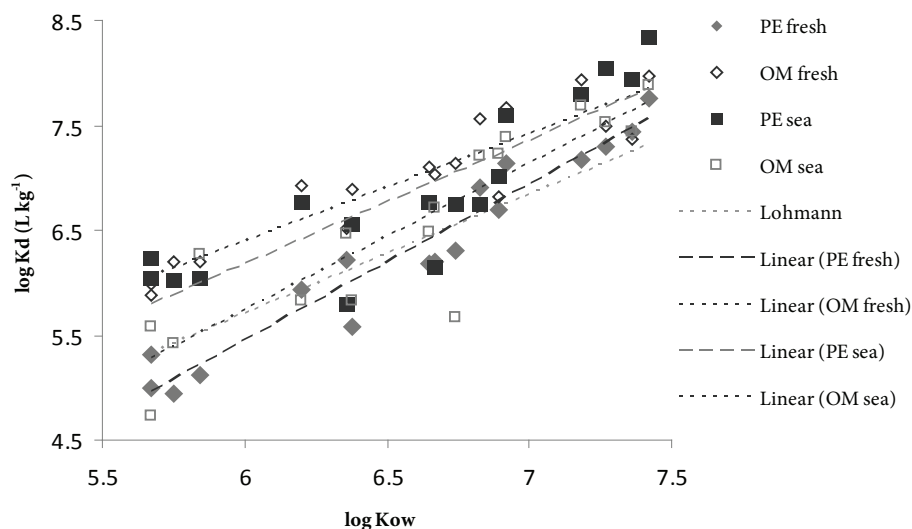


Figure 5.2 Partition coefficients $\log K_p$ for PCB sorption to μ -micro PE in fresh- and seawater as a function of $\log K_{ow}$ compared to (a) partition coefficients for sediment OM in fresh- and seawater, $\log K_{om}$ and (b) partition coefficients and $\log K_p$ for PE from the literature ($\log K_p = (1.14 \pm 0.041 \times \log K_{ow} - (1.14 \pm 0.26)$ [41]).

surface data in Table S5.1; coverage parameters in Table S5.7 and S5.8), which means that surface adsorption probably played a limited role compared to partitioning in the bulk polymer.

In seawater, sorption to micro-PE was higher than in freshwater (up to 1 log unit) for most PCBs. The overall regression of $\log K_p$ against $\log K_{ow}$ ($\log K_p = (1.18 \pm 0.18 \times \log K_{ow} - (0.88 \pm 1.17)$ ($R^2 = 0.75$) for seawater was in good agreement with the aforementioned regression provided by Lohmann [41].

To compare the sorption of PCBs to micro-PE with that to sediment organic matter, sediment-water distribution coefficients were normalized to the sediment organic matter content. In freshwater the regression was $\log K_{om} = (1.02 \pm 0.11) \times \log K_{ow} + (0.27 \pm 0.73)$ ($R^2 = 0.85$), which resembles stronger sorption than to μ -micro-PE (GLM: $F = 4.544$, $p = 0.033$). In seawater the regression was $\log K_{om} = (1.39 \pm 0.19) \times \log K_{ow} - (2.62 \pm 1.24)$ ($R^2 = 0.79$), which was not significantly different from that to micro-PE (GLM: $F = 0.224$, $p = 0.636$).

Previous work has shown that suspending and agitating sediment in water generates dissolved organic matter (DOM) [42] and that fouling by DOM may suppress surface sorption to carbonaceous materials (eg. [12, 22]). For micro-PE in the presence of sediment, intrinsic freshwater $\log K_p$ values were 0 to 0.7 log units lower than without sediment, leading to a decreased regression slope (Table S5.6, Figure S5.18), but overall this was not significant (GLM; $F = 1.146$, $p = 0.284$). With increasing $\log K_{ow}$, the suppression of sorption by sediment was higher. In seawater,

presence of sediment caused 0.7 log units higher intrinsic $\log K_p$ values at $\log K_{ow} < 6.7$, and up to 0.5 log units lower $\log K_p$ values at higher K_{ow} values. The overall difference however was again not significant (GLM: $F = 1.802$, $p = 0.180$). So, although some effects of the presence of sediment on intrinsic $\log K_p$ values for micro-PE were observed, a clear and statistically significant suppression effect by DOM was not detected. This is consistent with the earlier reasoning that sorption to micro-PE is dominated by partitioning into the bulk polymer. In summary, the observed linearity of the regressions, the agreements with sorption to sediment OM and an apparent lack of substantial effects of sediment organic matter fouling support the idea that sorption to micro-PE mainly is a linear partitioning process.

Sorption to nano-polystyrene (nano-PS)

Unlike sorption to sediment and to micro-PE, sorption to nano-PS was highly non-linear, with Freundlich exponents > 1 (Figure 5.1, Figure S5.21-37 and Table S5.5). Isotherms were concave or S-shaped, which implies that neither the Freundlich model nor a linear model fitted well to the data. Several other sorption models are available like Langmuir, Polanyi, Toth or dual domain models [9, 38], but the number of data points in our isotherms was too low to enable fitting and statistical evaluation of these alternative sorption models most of which use more than two parameters.

Because of the concentration dependence of sorption, nano-PS distribution coefficients per PCB congener varied over three orders of magnitude with C_w , from $10^4 - 10^5 \text{ L kg}^{-1}$ up to very high values of 10^9 L kg^{-1} for the more hydrophobic PCBs at the higher ends of the isotherms (Figure S5.19). We are not aware of earlier data on HOC distribution coefficients for nano-sized PS or other polymers. For bulk PS, PCB sorption coefficients are available from Pascall et al. [43], which however are in the range of $10^{2.5} - 10^{3.1} \text{ L kg}^{-1}$, i.e. a factor of $10^3 - 10^6$ lower than the present values. Previous research has shown that sorption of HOCs to carbon based nanoparticles is highly dependent on specific surface area [7, 8, 44]. Therefore, we assume that the present high values can be explained by the very high nano-PS surface area of 4 m^2 present in the experimental systems, which is about 1330 times higher than for the PE microspheres in the present study and also 400 times higher than the PS surface area in the experiments by Pascall et al. [43], which was calculated to be 0.01 m^2 . Based on the adsorbed ΣPCB concentrations and the molecular surface areas of PCB congeners (Table S5.1), the monolayer surface area coverage would be 0.03, 0.3, 2.3, 22 and 44% for the present sorption to nano-PS (Table S5.7 and S5.8), compared to 265% surface coverage for PS in the experiments by Pascall et al. [43]. This means that the contribution of surface adsorption is much higher than for bulk PS or bulk micro-PE, where sorption is dominated by hydrophobic partitioning into the polymer matrix.

The sorption isotherms have the same shape for fresh- and seawater. Depending on the PCB concentration, $\log K_d$ in freshwater ranged from 0.2 log units lower to 0.5 log units higher than the values in seawater. Aggregates in freshwater had a smaller diameter than in seawater (199 versus 361 nm, Table S5.3), which may

have resulted in a better accessibility of the surface of nano-PS and thus may have contributed to the stronger sorption in freshwater.

In presence of sediment, isotherms still had the same shape. In freshwater, $\log K_d$ was between 0.3 log units lower to 0.3 log units higher than in the systems without sediment, with some exceptions where $\log K_d$ was up to 0.75 log units lower for the lowest spike concentration. In seawater, sediment decreased $\log K_d$ up to 0.2 log units, with one outlier for the lowest spike concentration (PCB 118), which was 1.2 log units lower. The present S-shaped isotherms for nano-PS without clear effects of salinity or presence of sediment were not observed for micrometer-sized PS in the literature [45] nor for our present micro-PE, which suggests that the present nano-PS particles may have had a nano-specific influence on the sorption of PCBs. The absence of DOM fouling can be explained from the much higher surface area of nano-PS. If sorption attenuation by DOM primarily is a surface competition effect, then the excess sites may have limited the effect for nano-PS.

Remarkably, sorption increased with aqueous phase concentration. We have no conclusive explanation for this phenomenon but there may be several plausible explanations. First of all, according to the literature concave or S-type isotherms originate from a) strong adsorption of the solvent, b) strong intermolecular attraction within the adsorbed layers, c) penetration of the solute in the adsorbent and/or d) monofunctional nature of the adsorbate [46], conditions that all apply to the nano-PS systems. There is a strong interaction between water and our nano-PS due to the COOH functionalization of the nano-PS which keeps the particles in suspension. Water-PS hydrogen-bond forces may counteract sorption of PCBs to PS [44], whereas formation of hydrogen-bonds may also occur. Hence, sorption is not only controlled by general hydrophobic forces and the S-shape isotherms may be explained from the trade-off between these factors. Second, the fact that monolayer surface coverage was less than 100% implies that the shape of the isotherms probably relates to density and heterogeneity of the sorption sites at the surface of the nano-PS. The effects of site heterogeneity are well understood, but would yield a decrease in sorption at higher concentration because sorption to the higher energy sites would occur first. We therefore hypothesise that there was no a priori fixed distribution, but that progressive adsorption of PCBs changed the site density and heterogeneity by affecting the aggregation state of the nanoparticles. The 199 ± 176 nm nano-PS in freshwater was observed to form 361 ± 465 nm sized aggregates in seawater (Table S5.3). In particular divalent cations (i.e. Ca^{2+}) may have caused further aggregation by screening the negative charges on the nano-PS surface [47]. The extent of aggregation however, may also depend on the surface coverage of the nano-PS if the strong hydrophobic interactions between PCBs and nano-PS in fact shield part of the surface groups. Shielding of surface COOH groups would hinder and reduce the association with cations, i.e. Ca^{2+} yielding better dispersion and higher available surface.

Sorption to multiwalled carbon nanotubes (MWCNTs)

In fresh water, sorption to MWCNTs was non-linear (Figure 5.1, Figure S5.21-37), with convex isotherms and Freundlich exponents (n) between 0.5 and 0.7, except for the planar PCBs 77 and 126, for which $n = 1$ (Table S5.5). In general this agrees to earlier reports that showed non-linear sorption of HOCs to carbon based nanoparticles [7, 8, 12, 26]. The total surface area for MWCNTs was 0.55 m^2 , translating into a 0.2, 2, 17, 165 and 330% coverage if monolayer adsorption by PCBs would be assumed (Table S5.7 and S5.8). These percentages support that surface saturation may have occurred, which is consistent with the observed non-linearity. We are not aware of earlier data on PCB sorption to MWCNTs in the present low concentration range. However, we can compare the PCB data with those reported for the lower ends of the PAH isotherms by Kah et al. [11]. PCB distribution coefficients (L kg^{-1}) for an aqueous concentration of $C_w = 0.001 \mu\text{g L}^{-1}$ were calculated from the present Freundlich isotherm parameters and plotted against $\log K_{ow}$ (Figure 5.3). This yields a linear relationship with $\log K_d = (0.77 \pm 0.05) \times \log K_{ow} + (3.62 \pm 0.34)$ ($R^2 = 0.95$) showing an initially 0.3 log unit higher sorption than observed for PAH, increasing to a 1 log unit higher sorption at higher $\log K_{ow}$ values. Aggregate sizes were quite similar for our fresh- and seawater systems with and without sediment (range 20 – 28 μm , Table S5.3). The aggregate size in Kah et al. [11, 12] ranged between 40 and 500 μm (Kah, personal communication). Our aggregates thus were much smaller, which may partly explain the higher sorption of PCBs compared to PAH at equal $\log K_{ow}$.

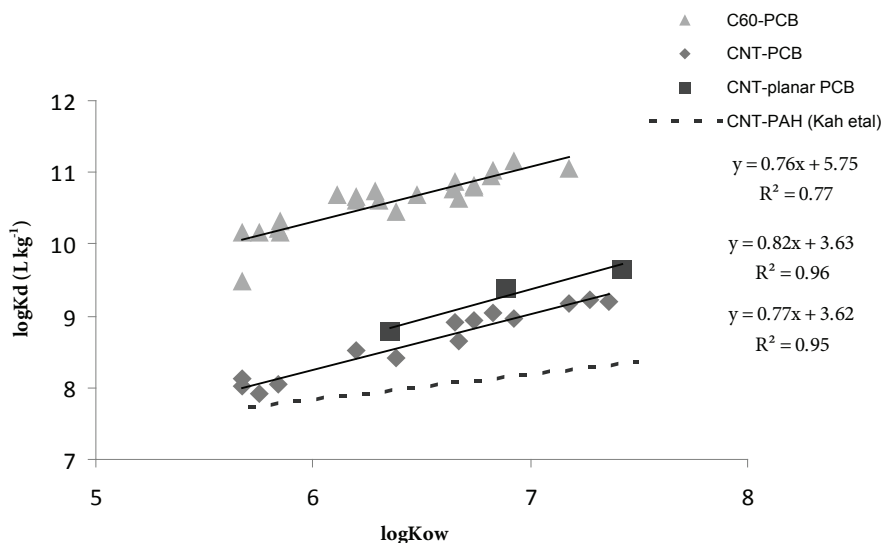


Figure 5.3 PCB distribution coefficients for C_{60} at an aqueous concentration of $C_w = 2 \times 10^{-6} - 6 \times 10^{-5} \mu\text{g L}^{-1}$, and for MWCNTs interpolated to an aqueous concentration of $C_w = 0.001 \mu\text{g L}^{-1}$ as function of $\log K_{ow}$, compared to PAH distribution coefficients reported by Kah et al. [11] (---). For MWCNTs, K_d values for planar and non-planar PCBs are plotted separately.

For seawater, the Freundlich exponent n was close to 1 and therefore linear sorption K_p values were derived (Table S5.6). The higher salinity of seawater caused K_p values to be up to 2.2 log units lower compared to K_p values for fresh water (GLM: $F = 12.973$, $p = 0.001$). Two mechanisms may explain the lower sorption affinity in seawater. First, the higher ionic strength will cause a higher extent of MWCNT aggregation, which will reduce available surface and thus sorption affinity. Observed aggregate sizes, however did not show clear differences (Table S5.3), rendering this mechanism less plausible. Second, a natural seawater was used, which had a higher DOC concentration than the artificial freshwater. DOM competes with HOCs for sorption sites on the MWCNT surface and thus may have suppressed sorption [7, 12]. DOM sorption also explains the linear sorption isotherms, because a DOM coated surface can be considered to contain more homogeneous sites for sorption of PCBs than the original heterogeneous MWCNT surface [48].

It is most plausible that the latter mechanism of 'DOM fouling' also explained the up to 0.8 log unit lower K_p values for MWCNTs in freshwater in presence of sediment. Similarly, in seawater K_p decreased up to 1.7 log units for the PCBs with $K_{ow} < 6.9$ and increased slightly up to 0.2 log units for PCBs with higher K_{ow} , upon addition of sediment, differences that resulted in a significantly different $\log K_p - \log K_{ow}$ relationship (GLM: $F = 9.107$, $p = 0.005$). A higher decrease for PCBs with lower $\log K_{ow}$ may be explained from the larger contribution of MWCNT pore sorption to overall sorption. Pore sorption would suffer from DOM pore blocking as well as competitive sorption, whereas pore blocking would be less relevant for more hydrophobic PCBs [7, 22].

Sorption to C_{60}

Sorption of PCBs to C_{60} was measured by single point distribution coefficients (K_d ; $L\ kg^{-1}$) in duplicate. The C_{60} surface area was assumed to be so high (see below) that single point coefficients were considered to represent the linear portion of the lower end of the isotherm, as was observed previously for nano-sized soot particles [13, 26]. Replicate K_d values typically deviated by 0.11 – 0.54% from the average, which illustrates the accuracy of the POM passive sampling method. The distribution coefficients related to aqueous concentrations between $C_w = 2 \cdot 10^{-6}$ and $6 \cdot 10^{-5} \mu g\ L^{-1}$ and increased linearly with $\log K_{ow}$ (Figure 5.3). $\log K_d$ ranged between 9.5 and 11.2, which is 1 to 2 orders of magnitude higher than the $\log K_d$ values for the MWCNTs. Total surface area of C_{60} in the systems was $53\ m^2$ which translates into a monolayer surface area coverage of 0.59%. This low percentage supports the validity of the aforementioned assumption regarding the linear portion of the isotherm and also implies that they may be compared with the K_d values for MWCNTs that were interpolated at low C_w . We assume that the generally higher surface coverage of the MWCNTs (up to 330%, see above) explain their lower K_d values compared to C_{60} .

Effect of PCB planarity

Planar PCBs are supposed to show stronger surface adsorption because of the ability of planar molecules to move closer to the sorption surface than the more bulky non-planar congeners. Here, planarity effects were assessed by comparing K_d values for the 3 planar, non-*ortho* substituted PCBs 77, 126 and 169 with non-planar mono- and di-*ortho* substituted PCBs 74, 101, 138, 153 and 180. Hydrophobicity effects were cancelled by only comparing planar/non-planar PCB couples of approximately equal $\log K_{ow}$. For sediment and micro-PE in freshwater, planarity effects were not consistently or significantly different (Figure S5.20). In seawater only planar PCBs 77 and 169 adsorbed more strongly, a pattern that was also seen for sediment, which suggests that salinity may have a different influence on planar and non-planar congeners. For MWCNTs the K_d values interpolated to $C_w = 0.001 \mu\text{g L}^{-1}$ were considered, which all appeared to be about an order of magnitude higher for the planar PCBs. This agrees to previous data for soot-like materials [13, 49], which can be understood from the similarities in these condensed carbon phases. For nano-PS, single point K_d values taken from the higher ends of the non-linear isotherms were used, which showed higher $\log K_d$ values for the planar PCBs, a difference that increased with increasing $\log K_{ow}$, i.e. with steeper regression slopes for the planar PCBs (Figure S5.20).

5.4 Implications

In summary, sorption to micro-PE and sediment OM was based on linear hydrophobic partitioning and had very similar magnitude. The nanoparticles nano-PS, MWCNT and C_{60} showed much stronger sorption, with $\log K_d$ values ranging up to 11.2 for C_{60} . Sorption to nano-PS and MWCNTS was non-linear. We suggest that changes in aggregate state may explain the increase in sorption to nano-PS with PCB concentration. However, further research should confirm this hypothesis.

Although future abundance of MWCNTs and C_{60} in the environment are not yet clear, the strong sorption of PCBs to these particles implies that they may affect transport and bioavailability in the environment. The preferential toxicity of planar PCBs also is relevant because they are known to be the most toxic congeners. They have a relatively high affinity for the Ah receptor and therefore show dioxin-like toxicity. For micro- and millimeter sized plastics, previous research has shown that extra exposure to aquatic organisms is not expected due to insufficient gradient between chemical fugacities in plastic and in biota lipids and rapid egestion of the particles [4]. For nanoplastics however, the present data show much higher distribution coefficients than for the bulk polymer, with values that are one to two orders of magnitude higher than K_{ow} for the higher substituted PCBs. Nanoplastics have been shown to pass through the chorion of fish eggs [50] and have been shown to move directly from the digestive tract of mussels into their circulatory system [21]. This implies that occurrence of

PCB contaminated nanoplastics in the environment may potentially enhance uptake, whereas a gradient for PCB transport from nanoplastic to biota lipids is likely.

Presence of sediment caused decreased sorption to the other particles studied, an effect that was most pronounced for MWCNTs, and that was explained from fouling with DOM. This implies that fate or effect assessment models should not use coefficients for pristine MWCNTs because DOM is ubiquitous in natural waters. Salinity decreased PCB sorption for sediment and MWCNTs, whereas for the polymers nano-PS and micro-PE salinity increased sorption. Similarly, fate or effect assessment models may need to account for these differences.

Acknowledgements

Jan van Lent and Marcel Giesbers (Wageningen EM Center, Wageningen UR, the Netherlands) are acknowledged for performing TEM analyses, Joris Sprakel (AVT-PCC, Wageningen UR, the Netherlands) for supplying the PS nanoparticles. A.A.K. acknowledges financial support from NanoNextNL, a micro and nanotechnology consortium of the Government of the Netherlands and 130 partners.

References

- [1] Velzeboer I, Peeters E, Koelmans AA. 2013. Multiwalled Carbon Nanotubes at Environmentally Relevant Concentrations Affect the Composition of Benthic Communities. *Environmental Science & Technology* 47:7475-7482.
- [2] Petersen EJ, Zhang L, Mattison NT, O'Carroll DM, Whelton AJ, Uddin N, Nguyen T, Huang Q, Henry TB, Holbrook RD, Chen KL. 2011. Potential Release Pathways, Environmental Fate, And Ecological Risks of Carbon Nanotubes. *Environmental Science & Technology* 45:9837-9856.
- [3] Besseling E, Wegner A, Foekema EM, van den Heuvel-Greve MJ, Koelmans AA. 2013. Effects of Microplastic on Fitness and PCB Bioaccumulation by the Lugworm *Arenicola marina* (L.). *Environmental Science & Technology* 47:593-600.
- [4] Koelmans AA, Besseling E, Wegner A, Foekema EM. 2013. Plastic as a Carrier of POPs to Aquatic Organisms: A Model Analysis. *Environmental Science & Technology* 47:7812-7820.
- [5] Karn B, Kuiken T, Otto M. 2009. Nanotechnology and in Situ Remediation: A Review of the Benefits and Potential Risks. *Environmental Health Perspectives* 117:1823-1831.
- [6] Theron J, Walker JA, Cloete TE. 2008. Nanotechnology and water treatment: Applications and emerging opportunities. *Critical Reviews in Microbiology* 34:43-69.
- [7] Wang XL, Tao S, Xing BS. 2009. Sorption and Competition of Aromatic Compounds and Humic Acid on Multiwalled Carbon Nanotubes. *Environmental Science & Technology* 43:6214-6219.
- [8] Yang K, Zhu L, Xing B. 2006. Adsorption of Polycyclic Aromatic Hydrocarbons by Carbon Nanomaterials. *Environmental Science & Technology* 40:1855-1861.
- [9] Yang K, Jing QF, Wu WH, Zhu LZ, Xing BS. 2010. Adsorption and Conformation of a Cationic Surfactant on Single-Walled Carbon Nanotubes and Their Influence on Naphthalene Sorption. *Environmental Science & Technology* 44:681-687.
- [10] Li S, Turaga U, Shrestha B, Anderson TA, Ramkumar SS, Green MJ, Das S, Cañas-Carrell JE. 2013. Mobility of polyaromatic hydrocarbons (PAHs) in soil in the presence of carbon nanotubes. *Ecotoxicology and Environmental Safety* 96:168-174.
- [11] Kah M, Zhang X, Jonker MTO, Hofmann T. 2011. Measuring and Modeling Adsorption of PAHs to Carbon Nanotubes Over a Six Order of Magnitude Wide Concentration Range. *Environmental Science & Technology* 45:6011-6017.
- [12] Zhang X, Kah M, Jonker MTO, Hofmann T. 2012. Dispersion State and Humic Acids Concentration-Dependent Sorption of Pyrene to Carbon Nanotubes. *Environmental Science & Technology* 46:7166-7173.
- [13] Jonker MTO, Koelmans AA. 2002. Sorption of polycyclic aromatic hydrocarbons and polychlorinated biphenyls to soot and soot-like materials in the aqueous environment mechanistic considerations. *Environmental Science & Technology* 36:3725-3734.
- [14] Wegner A, Besseling E, Foekema EM, Kamermans P, Koelmans AA. 2012. Effects of nanopolystyrene on the feeding behavior of the blue mussel (*Mytilus edulis* L.). *Environmental Toxicology and Chemistry* 31:2490-2497.

- [15] Foekema EM, De Gruijter C, Mergia MT, van Franeker JA, Murk AJ, Koelmans AA. 2013. Plastic in North Sea Fish. *Environmental Science & Technology* 47:8818-8824.
- [16] Hammer J, Kraak MHS, Parsons JR. 2012. Plastics in the Marine Environment: The Dark Side of a Modern Gift. In Whitacre DM, ed, *Reviews of Environmental Contamination and Toxicology*, Vol 220. Vol 220-Reviews of Environmental Contamination and Toxicology, pp 1-44.
- [17] Teuten EL, Saquing JM, Knappe DRU, Barlaz MA, Jonsson S, Bjorn A, Rowland SJ, Thompson RC, Galloway TS, Yamashita R, Ochi D, Watanuki Y, Moore C, Pham HV, Tana TS, Prudente M, Boonyatumanond R, Zakaria MP, Akkhangong K, Ogata Y, Hirai H, Iwasa S, Mizukawa K, Hagino Y, Imamura A, Saha M, Takada H. 2009. Transport and release of chemicals from plastics to the environment and to wildlife. *Philosophical Transactions of the Royal Society B-Biological Sciences* 364:2027-2045.
- [18] Rochman CM, Hoh E, Hentschel BT, Kaye S. 2013. Long-Term Field Measurement of Sorption of Organic Contaminants to Five Types of Plastic Pellets: Implications for Plastic Marine Debris. *Environmental Science & Technology* 47:1646-1654.
- [19] Endo S, Yuyama M, Takada H. 2013. Desorption kinetics of hydrophobic organic contaminants from marine plastic pellets. *Marine Pollution Bulletin* 74:125-131.
- [20] Karapanagioti HK, Klontza I. 2008. Testing phenanthrene distribution properties of virgin plastic pellets and plastic eroded pellets found on Lesvos island beaches (Greece). *Marine Environmental Research* 65:283-290.
- [21] Browne MA, Dissanayake A, Galloway TS, Lowe DM, Thompson RC. 2008. Ingested Microscopic Plastic Translocates to the Circulatory System of the Mussel, *Mytilus edulis* (L.). *Environmental Science & Technology* 42:5026-5031.
- [22] Koelmans AA, Meulman B, Meijer T, Jonker MTO. 2009. Attenuation of Polychlorinated Biphenyl Sorption to Charcoal by Humic Acids. *Environmental Science & Technology* 43:736-742.
- [23] Quik JTK, Velzeboer I, Wouterse M, Koelmans AA, van de Meent D. 2014. Heteroaggregation and Sedimentation Rates for Nanomaterials in Natural Waters. *Water Research*. 48:269-279
- [24] Brant J, Lecoanet H, Wiesner MR. 2005. Aggregation and deposition characteristics of fullerene nanoparticles in aqueous systems. *Journal of Nanoparticle Research* 7:545-553.
- [25] Koelmans AA, Nowack B, Wiesner MR. 2009. Comparison of manufactured and black carbon nanoparticle concentrations in aquatic sediments. *Environmental Pollution* 157:1110-1116.
- [26] Jantunen APK, Koelmans AA, Jonker MTO. 2010. Modeling polychlorinated biphenyl sorption isotherms for soot and coal. *Environmental Pollution* 158:2672-2678.
- [27] Jonker MTO, Koelmans AA. 2001. Polyoxymethylene solid phase extraction as a partitioning method for hydrophobic organic chemicals in sediment and soot. *Environmental Science & Technology* 35:3742-3748.
- [28] Rakowska MI, Kupryianchyk D, Grotenhuis T, Rijnaarts HHM, Koelmans AA. 2013. Extraction of sediment-associated polycyclic aromatic hydrocarbons with granular activated carbon. *Environmental Toxicology and Chemistry* 32:304-311.

- [29] Velzeboer I, Kupryianchyk D, Peeters ETHM, Koelmans AA. 2011. Community effects of carbon nanotubes in aquatic sediments. *Environment International* 37:1126-1130.
- [30] Kwadijk CJAF, Velzeboer I, Koelmans AA. 2013. Sorption of perfluorooctane sulfonate to carbon nanotubes in aquatic sediments. *Chemosphere* 90:1631-1636.
- [31] Jonker MTO, Brils JM, Sinke AJC, Murk AJ, Koelmans AA. 2006. Weathering and toxicity of marine sediments contaminated with oils and polycyclic aromatic hydrocarbons. *Environmental Toxicology and Chemistry* 25:1345-1353.
- [32] Smit MGD, Kater BJ, Jak RG, van den Heuvel-Greve MJ. 2006. Translating bioassay results to field population responses using a Leslie-matrix model for the marine amphipod *Corophium volutator*. *Ecological Modelling* 196:515-526.
- [33] Hawthorne SB, Miller DJ, Grabanski CB. 2009. Measuring Low Picogram Per Liter Concentrations of Freely Dissolved Polychlorinated Biphenyls in Sediment Pore Water Using Passive Sampling with Polyoxymethylene. *Analytical Chemistry* 81:9472-9480.
- [34] Kupryianchyk D, Rakowska MI, Roessink I, Reichman EP, Grotenhuis JTC, Koelmans AA. 2013. In situ Treatment with Activated Carbon Reduces Bioaccumulation in Aquatic Food Chains. *Environmental Science & Technology* 47:4563-4571.
- [35] von der Kammer F, Ferguson PL, Holden PA, Masion A, Rogers KR, Klaine SJ, Koelmans AA, Horne N, Unrine JM. 2012. Analysis of engineered nanomaterials in complex matrices (environment and biota): General considerations and conceptual case studies. *Environmental Toxicology and Chemistry* 31:32-49.
- [36] Jonker MTO, Sinke AJC, Brils JM, Koelmans AA. 2003. Sorption of polycyclic aromatic hydrocarbons to oil contaminated sediment: Unresolved complex? *Environmental Science & Technology* 37:5197-5203.
- [37] Jonker MTO, Muijs B. 2010. Using solid phase micro extraction to determine salting-out (Setschenow) constants for hydrophobic organic chemicals. *Chemosphere* 80:223-227.
- [38] Pikaar I, Koelmans AA, van Noort PCM. 2006. Sorption of organic compounds to activated carbons. Evaluation of isotherm models. *Chemosphere* 65:2343-2351.
- [39] Buffle J, Wilkinson KJ, Stoll S, Filella M, Zhang JW. 1998. A generalized description of aquatic colloidal interactions: The three-colloidal component approach. *Environmental Science & Technology* 32:2887-2899.
- [40] Seth R, Mackay D, Muncke J. 1999. Estimating the organic carbon partition coefficient and its variability for hydrophobic chemicals. *Environmental Science & Technology* 33:2390-2394.
- [41] Lohmann R. 2011. Critical Review of Low-Density Polyethylene's Partitioning and Diffusion Coefficients for Trace Organic Contaminants and Implications for Its Use As a Passive Sampler. *Environmental Science & Technology* 46:606-618.
- [42] Koelmans AA, Prevo L. 2003. Production of dissolved organic carbon in aquatic sediment suspensions. *Water Research* 37:2217-2222.
- [43] Pascall MA, Zabik ME, Zabik MJ, Hernandez RJ. 2005. Uptake of polychlorinated biphenyls (PCBs) from an aqueous medium by polyethylene, polyvinyl chloride, and polystyrene films. *Journal of Agricultural and Food Chemistry* 53:164-169.

- [44] Isaacson PJ, Frink CR. 1984. Nonreversible Sorption of Phenolic Compounds by Sediment Fractions: The Role of Sediment Organic Matter. *Environmental Science & Technology* 18:43-48.
- [45] Lee H, Shim WJ, Kwon J-H. Sorption capacity of plastic debris for hydrophobic organic chemicals. *Science of The Total Environment*.
- [46] Haque R, Coshov WR. 1971. Adsorption of Isocil and Bromacil from Aqueous Solution onto Some Mineral Surfaces. *Environmental Science & Technology* 5:139-&.
- [47] Schwyzer I, Kaegi R, Sigg L, Smajda R, Magrez A, Nowack B. 2012. Long-term colloidal stability of 10 carbon nanotube types in the absence/presence of humic acid and calcium. *Environmental Pollution* 169:64-73.
- [48] Yang K, Wang X, Zhu L, Xing B. 2006. Competitive Sorption of Pyrene, Phenanthrene, and Naphthalene on Multiwalled Carbon Nanotubes. *Environmental Science & Technology* 40:5804-5810.
- [49] Jonker MTO, Smedes F. 2000. Preferential sorption of planar contaminants in sediments from Lake Ketelmeer, The Netherlands. *Environmental Science & Technology* 34:1620-1626.
- [50] Kashiwada S. 2006. Distribution of nanoparticles in the see-through medaka (*Oryzias latipes*). *Environmental Health Perspectives* 114:1697-1702.

Supporting Information

Table S5.1 Polychlorinated biphenyl (PCB) properties.

Congener	Molecular formula	Molecular weight (g mol ⁻¹)	Molar volume ^a (cm ³ mol ⁻¹)	Total surface area ^b (Å ²)	log K _{ow} ^b	Planarity (no. of ortho substituents)
PCB 28	C ₁₂ H ₇ Cl ₃	257.5	247.3	230.8	5.67	non planar (1)
PCB 31	C ₁₂ H ₇ Cl ₃	257.5	247.3	230.7	5.67	non planar (1)
PCB 44	C ₁₂ H ₆ Cl ₄	292.0	268.2	233.2	5.75	non planar (2)
PCB 52	C ₁₂ H ₆ Cl ₄	292.0	268.2	235.8	5.84	non planar (2)
PCB 74	C ₁₂ H ₆ Cl ₄	292.0	268.2	246.4	6.20	non planar (1)
PCB 101	C ₁₂ H ₅ Cl ₅	326.4	289.1	251.6	6.38	non planar (2)
PCB 105	C ₁₂ H ₅ Cl ₅	326.4	289.1	259.4	6.65	non planar (1)
PCB 149	C ₁₂ H ₄ Cl ₆	360.9	310.0	260.0	6.67	non planar (3)
PCB 118	C ₁₂ H ₅ Cl ₅	326.4	289.1	262.0	6.74	non planar (1)
PCB 138	C ₁₂ H ₄ Cl ₆	360.9	310.0	264.8	6.83	non planar (2)
PCB 153	C ₁₂ H ₄ Cl ₆	360.9	310.0	267.4	6.92	non planar (2)
PCB 156	C ₁₂ H ₄ Cl ₆	360.9	310.0	275.0	7.18	non planar (1)
PCB 170	C ₁₂ H ₃ Cl ₇	395.3	330.9	277.7	7.27	non planar (2)
PCB 180	C ₁₂ H ₃ Cl ₇	395.3	330.9	280.4	7.36	non planar (2)
PCB 77	C ₁₂ H ₆ Cl ₄	292.0	268.2	251.0	6.36	planar (0)
PCB 126	C ₁₂ H ₅ Cl ₅	326.4	289.1	266.6	6.89	planar (0)
PCB 169	C ₁₂ H ₄ Cl ₆	360.9	310.0	282.2	7.42	planar (0)

^a from Mackay et al. [1]

^b from Hawker et al. [2]

Table S5.2 Experimental set-up of isotherm systems. The table defines volume of water and masses of POM, sediment and adsorbent used in experiment 1 through 14.

Experiment	Water type	V_w (L)	M_{POM} (mg)	M_{sed} (g dw)	Particle type	Mass (mg)	Q_T^{PCB} (7 conc.; μg)
1	DSW ^a	0.230	100	1	-	-	0 – 20
2	DSW	0.230	50	-	MWCNT	5	0 – 20
3	DSW	0.230	50	1	MWCNT	5	0 – 20
4	DSW	0.230	5	-	nano-PS	50	0 – 20
5	DSW	0.230	5	1	nano-PS	50	0 – 20
6	DSW	0.230	500	-	micro-PE	50	0 – 20
7	DSW	0.230	500	1	micro-PE	50	0 – 20
8	SW ^b	0.230	100	1	-	-	0 – 20
9	SW	0.230	50	-	MWCNT	5	0 – 20
10	SW	0.230	50	1	MWCNT	5	0 – 20
11	SW	0.230	5	-	nano-PS	50	0 – 20
12	SW	0.230	5	1	nano-PS	50	0 – 20
13	SW	0.230	500	-	micro-PE	50	0 – 20
14	SW	0.230	500	1	micro-PE	50	0 – 20

^a DSW = Dutch standard water (= freshwater)

^b SW = Seawater

Table S5.3 Summary of particle size information obtained, from electron- and light microscopy image analysis.

Particles or aggregates	System	Instrument	Particle or aggregate size
MWCNT particle	fresh / sea water	TEM	20 – 30 nm (outer diameter) ~1000 nm (length)
MWCNT aggregates	freshwater	LM	28 ± 21 μm
MWCNT aggregates	freshwater + sediment.	LM	23 ± 11 μm
MWCNT aggregates	seawater	LM	20 ± 12 μm
MWCNT aggregates	seawater + sediment	LM	24 ± 17 μm
nano-PS particle	all systems	TEM	60 ± 25 nm
nano-PS aggregates	fresh water	TEM	199.3 ± 176.3 nm
nano-PS aggregates	sea water	TEM	361.1 ± 465.1 nm
micro-PE particles	all systems	LM	99 ± 39 μm
C_{60} aggregates	freshwater	LM	179 ± 128 μm

Table S5.4 Equations to quantify sorption of PCBs to sediment and the carbon-based particles (CBPs; MWCNTs, nano-PS, micro-PE) using the polyoxymethylene-solid phase extraction (POM-SPE) [3].

	Equation
Mass balance for partitioning of total amount (T) of PCBs into water (w), POM, sediment (sed) and CBPs (CBP)	(1) $Q_T = C_w V_w + C_{POM} M_{POM} + C_{sed} M_{sed} + C_{CBP} M_{CBP}$
Equilibrium partition ratio between PCB concentration in POM and water	(2) $C_{POM} = K_{POM} C_w$
Equilibrium partition ratio between PCB concentration in sediment and water	(3) $C_{sed} = K_{sed} C_w$
PCB concentration in sediment calculated from system characteristics and $\frac{C_{POM}}$	(4) $C_{sed} = \frac{1}{M_{sed}} \left(Q_T - \frac{C_{POM}}{K_{POM}} V_w - C_{POM} M_{POM} \right)$
PCB distribution ratio for sediment calculated from system characteristics and $\frac{C_{POM}}$	(5) $K_{sed} = \frac{1}{M_{sed}} \left(\frac{K_{POM} Q_{POM}}{C_{POM}} - V_w - K_{POM} M_{POM} \right)$
PCB concentration in CBPs calculated from system characteristics and C_{POM} (intrinsic sorption)	(6) $C_{CBP} = \frac{1}{M_{CBP}} \left(Q_T - \frac{C_{POM}}{K_{POM}} V_w - C_{POM} M_{POM} - K_{sed} \left(\frac{C_{POM}}{K_{POM}} \right) M_{sed} \right)$

- Q_T = total amount of PCBs in the system (μg)
 C_w = concentration PCBs in water ($\mu\text{g kg}^{-1}$)
 V_w = volume water ($\mu\text{g L}^{-1}$)
 C_{POM} = concentration PCBs in POM ($\mu\text{g kg}^{-1}$)
 M_{POM} = mass of POM (kg)
 C_{sed} = concentration PCBs in sediment ($\mu\text{g kg}^{-1}$)
 M_{sed} = mass of sediment (kg)
 C_{CBP} = concentration PCBs in CBPs ($\mu\text{g kg}^{-1}$)
 M_{CBP} = mass of CBPs (kg)
 K_{POM} = POM-water distribution coefficient (L kg^{-1} POM)
 K_{sed} = sediment-water distribution coefficient (L kg^{-1} sediment)
 Q_{POM} = total amount of PCBs in POM (μg)

Table S5.5 Freundlich sorption parameters (K_f ; ($\mu\text{g kg}^{-1}/\mu\text{g L}^{-1}$)ⁿ, and n)
a) Freshwater

	sediment				micro-PE				micro-PE + sediment ^a							
	PCB	$\log K_f$	SE	n	SE	R ² (n ^b)	$\log K_f$	SE	n	SE	R ² (n ^b)	$\log K_f$	SE	n	SE	R ² (n ^b)
28	4.04	0.23	1.02	1.02	0.11	0.97(5)	5.26	0.13	0.97	0.10	0.98(4)	5.43	0.33	1.05	0.19	0.97(3)
31	3.91	0.24	1.02	1.02	0.12	0.96(5)	4.93	0.23	0.94	0.17	0.94(4)	5.06	0.20	0.96	0.13	0.98(3)
44	3.98	0.26	0.93	0.12	0.95(5)	4.98	0.23	1.02	1.02	0.17	0.94(4)	6.56	0.00	1.87	0.00	1.00(2)
52	4.21	0.21	1.00	1.00	0.10	0.97(5)	5.19	0.18	1.06	0.14	0.97(4)	5.16	0.00	1.09	0.00	1.00(2)
74	4.20	0.37	0.91	0.12	0.93(6)	6.01	0.09	1.04	0.05	1.00(4)	6.00	0.17	1.00	0.08	0.99(3)	
101	4.33	0.26	0.83	0.10	0.96(5)	6.06	0.15	1.15	0.07	0.99(5)	5.27	0.84	1.00	0.42	0.85(3)	
105	5.22	0.23	1.03	0.08	0.98(5)	7.01	0.26	1.22	0.09	0.98(5)	6.50	0.52	1.07	0.20	0.97(3)	
149	4.37	0.42	0.80	0.16	0.90(5)	6.24	0.11	1.02	0.04	0.99(5)	5.97	0.68	1.08	0.32	0.92(3)	
118	5.12	0.21	0.99	0.08	0.98(5)	6.87	0.18	1.17	0.07	0.99(5)	6.49	0.47	1.10	0.19	0.97(3)	
138	5.14	0.41	0.89	0.13	0.94(5)	6.92	0.10	1.01	0.03	1.00(5)	6.71	0.54	1.12	0.21	0.97(3)	
153	5.00	0.47	0.85	0.14	0.92(5)	6.80	0.15	0.92	0.05	0.99(5)	6.72	0.37	1.03	0.13	0.99(3)	
156	5.26	0.46	0.86	0.13	0.93(5)	7.11	0.07	0.98	0.02	1.00(4)	7.18	0.60	1.16	0.20	0.97(3)	
170	5.83	0.13	1.08	0.05	1.00(3)	6.84	0.09	0.85	0.03	1.00(3)	6.30	0.00	0.87	0.00	1.00(2)	
180	5.98	0.35	1.17	0.13	0.98(4)	6.85	0.06	0.82	0.02	1.00(4)	6.71	0.33	0.95	0.11	0.99(3)	
77	5.71	0.25	1.36	0.10	0.99(4)	6.62	0.08	1.15	0.03	1.00(4)	6.09	0.36	1.01	0.13	0.98(3)	
126	7.06	0.20	1.52	0.06	0.99(5)	7.96	0.25	1.34	0.08	0.99(5)	6.54	0.86	1.11	0.27	0.90(4)	
169	7.35	0.62	1.31	0.17	0.95(5)	7.99	0.18	1.07	0.06	0.99(4)	6.24	0.64	0.77	0.15	0.96(3)	

^a '4+ sediment' means that the data refer to the intrinsic sorption to the particle type mentioned, in the presence of sediment.

^b number of data points

Table S5.5. a) Continued

PCB	MWCNT					MWCNT + sediment ^a					nano-PS					nano-PS + sediment ^a				
	$\log K_f$	SE	n	SE	R ² (n ^b)	$\log K_f$	SE	n	SE	R ² (n ^b)	$\log K_f$	SE	n	SE	R ² (n ^b)	$\log K_f$	SE	n	SE	R ² (n ^b)
28	6.75	0.03	0.54	0.01	1.00(4)	6.67	0.15	0.59	0.04	0.98(5)	9.88	1.66	2.33	0.61	0.79(5)	10.30	2.12	2.47	0.85	0.74(5)
31	6.65	0.04	0.54	0.02	1.00(4)	6.36	0.20	0.55	0.06	0.96(5)	9.21	1.07	2.10	0.44	0.88(5)	10.73	1.63	2.77	0.67	0.85(5)
44	6.60	0.11	0.56	0.05	0.99(4)	5.57	0.54	0.39	0.17	0.63(5)	7.46	0.79	1.35	0.38	0.87(4)	7.15	0.52	1.07	0.27	0.94(3)
52	6.86	0.07	0.61	0.02	1.00(5)	6.41	0.18	0.57	0.06	0.97(5)	7.47	0.74	1.34	0.35	0.88(4)	9.61	1.58	2.51	0.68	0.82(5)
74	7.27	0.02	0.58	0.01	1.00(4)	7.09	0.18	0.63	0.05	0.98(5)	11.85	1.73	2.74	0.59	0.88(4)	10.40	1.49	2.13	0.53	0.89(4)
101	7.15	0.04	0.58	0.01	1.00(4)	6.59	0.10	0.52	0.03	0.99(4)	9.80	1.67	2.35	0.76	0.83(4)	11.76	3.07	3.23	1.38	0.73(4)
105	7.76	0.03	0.62	0.01	1.00(4)	7.50	0.05	0.64	0.02	1.00(4)	9.16	0.91	1.44	0.32	0.95(3)	9.45	1.63	1.51	0.56	0.88(3)
149	7.38	0.10	0.57	0.03	0.99(4)	7.08	0.07	0.62	0.03	1.00(4)	7.45	0.00	0.92	0.00	1.00(2)	9.59	1.46	1.85	0.61	0.90(3)
118	7.81	0.03	0.62	0.01	1.00(4)	7.67	0.06	0.69	0.02	1.00(4)	11.16	0.72	2.36	0.25	0.98(4)	13.37	4.43	3.31	1.69	0.66(4)
138	7.94	0.11	0.63	0.03	1.00(4)	7.82	0.05	0.73	0.01	1.00(4)	11.78	1.31	2.45	0.43	0.92(5)	7.90	0.00	0.87	0.00	1.00(2)
153	7.74	0.14	0.59	0.03	0.99(4)	7.76	0.04	0.71	0.01	1.00(4)	7.72	0.00	0.84	0.00	1.00(2)	11.95	3.42	2.29	1.11	0.81(3)
156	8.07	0.14	0.63	0.03	0.99(4)	8.44	0.16	0.83	0.04	1.00(4)	9.60	0.00	1.47	0.00	1.00(2)	19.40	9.26	4.75	2.93	0.72(3)
170	7.94	0.07	0.57	0.02	1.00(3)	8.42	0.05	0.84	0.01	1.00(3)	12.02	1.45	2.28	0.43	0.97(3)	17.46	5.72	4.12	1.83	0.83(3)
180	8.22	0.24	0.67	0.07	0.99(3)	8.36	0.18	0.81	0.05	0.99(4)	139.12	0.00	43.00	0.00	1.00(2)	9.30	0.00	1.28	0.00	1.00(2)
77	8.75	0.75	0.99	0.18	0.91(5)	8.10	0.17	0.83	0.05	0.99(4)	34.02	0.00	10.60	0.00	1.00(2)	16.21	8.68	4.16	3.02	0.66(3)
126	9.37	0.53	0.99	0.12	0.96(5)	9.36	0.36	1.06	0.09	0.98(5)	81.43	3.36	23.21	1.11	1.00(3)	11.40	1.91	2.13	0.57	0.93(3)
169	8.76	0.21	0.70	0.05	0.99(4)	9.50	0.24	0.97	0.06	0.99(4)	15.52	2.41	3.16	0.65	0.96(3)	7.10	0.00	0.47	0.00	1.00(2)

^a '+ sediment' means that the data refer to the intrinsic sorption to the particle type mentioned, in the presence of sediment.^b number of data points

Table S5.5. b) Seawater

PCB	sediment				micro-PE				micro-PE + sediment ^a						
	$\log K_f$	SE	n	SE	R^2 (n ^b)	$\log K_f$	SE	n	SE	R^2 (n ^b)	$\log K_f$	SE	n	SE	R^2 (n ^b)
28	3.36	0.22	0.91	0.09	0.98(4)	6.36	0.02	1.07	0.01	1.00(4)	6.56	0.01	1.06	0.00	1.00(3)
31	3.72	0.00	1.69	0.00	1.00(2)	6.12	0.02	1.04	0.01	1.00(4)	6.35	0.00	1.05	0.00	1.00(2)
44	nd	nd	nd	nd	nd(-)	6.22	0.02	1.11	0.01	1.00(4)	nd	nd	nd	nd	nd(-)
52	3.31	0.25	0.77	0.09	0.99(3)	6.26	0.01	1.12	0.01	1.00(4)	6.39	0.00	1.03	0.00	1.00(2)
74	3.23	0.00	0.26	0.00	1.00(2)	7.20	0.03	1.18	0.01	1.00(4)	7.04	0.00	0.99	0.00	1.00(2)
101	4.43	0.18	1.16	0.08	0.99(5)	7.09	0.20	1.30	0.08	0.99(5)	6.77	0.06	1.06	0.03	1.00(4)
105	5.46	0.15	1.22	0.05	1.00(5)	8.65	0.39	1.56	0.13	0.98(5)	7.65	0.03	1.15	0.01	1.00(4)
149	4.73	0.35	1.02	0.14	0.95(5)	7.15	0.12	1.12	0.04	1.00(5)	7.52	0.42	1.33	0.15	0.96(5)
118	5.96	0.45	1.60	0.17	0.97(5)	8.20	0.39	1.40	0.13	0.97(5)	8.21	0.65	1.45	0.22	0.93(5)
138	5.62	0.40	1.11	0.13	0.96(5)	9.17	0.54	1.64	0.17	0.97(5)	8.07	0.06	1.25	0.02	1.00(4)
153	5.46	0.53	1.03	0.16	0.93(5)	8.04	0.17	1.13	0.05	1.00(4)	7.83	0.09	1.10	0.03	1.00(5)
156	5.74	0.48	1.02	0.14	0.95(5)	8.19	0.20	1.11	0.06	0.99(4)	7.96	0.16	1.11	0.05	1.00(4)
170	6.47	0.31	1.28	0.12	0.99(3)	7.58	0.03	0.88	0.01	1.00(3)	7.68	0.03	1.02	0.01	1.00(3)
180	6.78	0.36	1.39	0.13	0.98(4)	8.30	0.11	1.12	0.04	1.00(3)	7.45	0.21	0.90	0.06	0.99(4)
77	5.72	0.10	1.38	0.04	1.00(4)	8.94	0.81	1.75	0.26	0.94(5)	7.74	0.03	1.26	0.01	1.00(4)
126	7.43	0.05	1.69	0.02	1.00(4)	10.39	0.52	1.87	0.15	0.98(5)	9.11	0.34	1.51	0.11	0.99(4)
169	7.61	0.51	1.39	0.14	0.97(5)	10.43	0.84	1.53	0.22	0.96(4)	10.28	0.76	1.59	0.21	0.97(4)

^a '+ sediment' means that the data refer to the intrinsic sorption to the particle type mentioned, in the presence of sediment.

^b number of data points

Table S5.5. b) Continued

PCB	MWCNT				MWCNT + sediment ^a				nano-PS				nano-PS + sediment ^a							
	$\log K_f$	SE	<i>n</i>	SE	R^2 (n ^b)	$\log K_f$	SE	<i>n</i>	SE	R^2 (n ^b)	$\log K_f$	SE	<i>n</i>	SE	R^2 (n ^b)	$\log K_f$	SE	<i>n</i>	SE	R^2 (n ^b)
28	7.04	0.62	0.86	0.19	0.87(5)	7.63	0.19	0.91	0.10	0.99(3)	10.66	1.20	2.45	0.46	0.91(5)	10.03	3.02	2.17	1.34	0.72(3)
31	7.10	0.92	1.05	0.29	0.81(5)	7.32	0.00	0.84	0.00	1.00(2)	10.98	1.41	2.80	0.58	0.89(5)	36.46	0.00	14.24	0.00	1.00(2)
44	6.52	0.39	0.67	0.15	0.95(3)	nd	nd	nd	nd	nd(-)	8.87	0.86	1.93	0.35	0.91(5)	nd	nd	nd	nd	nd(-)
52	7.36	0.98	1.16	0.36	0.78(5)	7.98	0.00	1.25	0.00	1.00(2)	9.78	1.08	2.41	0.42	0.92(5)	6.84	0.00	0.78	0.00	1.00(2)
74	7.64	0.57	0.88	0.16	0.91(5)	8.43	0.00	1.12	0.00	1.00(2)	9.45	1.37	1.63	0.52	0.91(3)	7.46	0.00	0.78	0.00	1.00(2)
101	7.58	0.39	0.89	0.12	0.95(5)	7.71	0.12	0.88	0.04	0.99(5)	17.30	4.29	5.77	1.86	0.83(4)	12.94	2.80	3.72	1.25	0.81(4)
105	8.95	0.55	1.09	0.13	0.95(6)	9.00	0.48	1.07	0.12	0.97(5)	12.46	0.95	2.50	0.29	0.97(4)	10.88	1.95	1.97	0.66	0.90(3)
149	7.82	0.22	0.83	0.06	0.98(5)	7.85	0.13	0.84	0.04	0.99(4)	15.60	2.22	4.34	0.86	0.96(3)	10.06	0.79	2.07	0.33	0.97(3)
118	8.67	0.61	1.01	0.17	0.92(5)	8.53	0.27	0.93	0.07	0.98(5)	13.91	1.06	3.31	0.37	0.98(4)	23.46	7.98	7.14	2.99	0.74(4)
138	8.70	0.28	0.94	0.07	0.98(5)	8.64	0.20	0.91	0.06	0.99(4)	9.11	0.00	1.26	0.00	1.00(2)	9.46	0.00	1.43	0.00	1.00(2)
153	8.71	0.29	0.92	0.07	0.98(5)	8.53	0.23	0.87	0.06	0.99(4)	15.91	2.87	3.50	0.92	0.94(3)	14.17	2.58	2.99	0.83	0.93(3)
156	9.06	0.37	0.93	0.08	0.98(5)	9.27	0.26	1.00	0.07	0.99(4)	15.23	7.21	3.18	2.23	0.67(3)	14.78	1.90	3.09	0.60	0.96(3)
170	9.05	0.32	0.92	0.08	0.99(3)	9.18	0.37	1.00	0.10	0.99(3)	nd	nd	nd	nd	nd(-)	19.56	0.00	4.83	0.00	1.00(2)
180	9.22	0.52	0.97	0.13	0.96(4)	8.94	0.39	0.91	0.10	0.98(4)	9.61	0.00	1.34	0.00	1.00(2)	19.96	8.24	4.75	2.52	0.64(4)
77	8.41	0.17	0.89	0.04	1.00(4)	8.70	0.22	0.95	0.06	0.99(4)	14.25	5.00	3.31	1.72	0.79(3)	15.18	5.27	3.63	1.81	0.80(3)
126	10.27	0.82	1.25	0.19	0.93(5)	9.84	0.19	1.09	0.05	1.00(4)	14.79	1.85	3.16	0.54	0.97(3)	8.00	0.00	0.85	0.00	1.00(2)
169	10.39	0.45	1.10	0.10	0.98(4)	11.11	0.38	1.27	0.09	0.99(4)	17.08	5.16	3.23	1.36	0.85(3)	8.08	0.00	0.73	0.00	1.00(2)

nd: no data

^a '+ sediment' means that the data refer to the intrinsic sorption to the particle type mentioned, in the presence of sediment.

^b number of data points

Table S5.6 Partition coefficients K_p ($L \text{ kg}^{-1}$).

PCB	Freshwater										Seawater								
	sediment					micro-PE + MWCNT					sediment			micro-PE + MWCNT			MWCNT + sediment		
	$\log K_{ow}^a$	$\log K_p$	$\log K_{oc}^b$	$\log K_p$	$\log K_p$	$\log K_p$	$\log K_p$	$\log K_p$	$\log K_p$	$\log K_p$	$\log K_p$	$\log K_p$	$\log K_p$	$\log K_p$	$\log K_p$	$\log K_p$	$\log K_p$	$\log K_p$	$\log K_p$
28	5.67	4.06	6.36	5.31	5.31	8.02	8.13	8.13	3.66	5.96	6.23	6.47	7.29	7.80					
31	5.67	3.96	6.26	5.00	5.11	7.87	7.90	7.90	2.81	5.11	6.05	6.27	6.00	7.66					
44	5.75	4.28	6.58	4.95	4.68	7.72	7.42	7.42	3.50	5.80	6.03	6.35	7.36	7.56					
52	5.84	4.28	6.58	5.11	4.98	8.30	7.83	7.83	4.35	6.65	6.04	6.37	6.07	7.63					
74	6.20	5.01	7.31	5.93	5.98	8.65	8.54	8.54	3.89	6.20	6.77	7.06	7.97	8.21					
101	6.38	5.11	7.26	5.58	5.18	8.49	7.93	7.93	3.90	6.20	6.55	7.21	7.91	8.12					
105	6.65	4.96	7.47	6.18	6.28	9.25	8.76	8.76	4.55	6.85	6.77	6.24	8.34	8.46					
149	6.67	5.17	7.41	6.21	5.73	8.85	8.20	8.20	4.78	7.08	6.15	6.64	8.45	8.33					
118	6.74	5.21	7.51	6.30	6.22	9.21	8.69	8.69	3.74	6.04	6.30	6.48	8.52	8.78					
138	6.83	5.64	7.94	6.91	6.35	9.39	8.77	8.77	5.29	7.59	6.74	7.31	8.97	8.97					
153	6.92	5.75	8.05	7.14	6.61	9.53	8.87	8.87	5.46	7.76	7.59	7.38	9.10	9.05					
156	7.18	6.00	8.30	7.18	6.63	9.75	9.10	9.10	5.76	8.06	7.80	7.58	9.40	9.26					
170	7.27	5.57	7.87	7.30	6.73	9.83	9.03	9.03	5.60	7.90	8.03	7.61	9.38	9.16					
180	7.36	5.44	7.74	7.43	6.87	9.39	9.12	9.12	5.51	7.81	7.94	7.80	9.34	9.31					
77	6.36	4.59	6.89	6.22	6.04	8.68	8.78	8.78	4.55	6.85	5.79	6.90	8.83	8.92					
126	6.89	4.90	7.20	6.69	6.00	9.33	9.07	9.07	5.30	7.61	7.02	7.46	9.03	9.46					
169	7.42	6.05	8.35	7.77	7.31	10.17	9.63	9.63	5.96	8.26	8.34	8.04	9.96	9.89					

^a from [2]^b $K_{oc} = K_p^{sed}$ normalized to sediment organic carbon content ($f_{oc} = 0.005$)^c '+ sediment' means that the data refer to the intrinsic sorption to the particle type mentioned, in the presence of sediment.

Table S5.7 Particle parameters of the tested sorbents for calculation of the total surface area of the sorbents in the systems.

	sediment OM	micro-PE	nano-PS	MWCNT	C ₆₀
average particle diameter ^a (m)	5E-5	1E-4	7E-8	1E-8	7E-10
sorbent density (kg m ⁻³)	2.6E3	1.0E3	1.1E3	2.1E3	1.7E3
single particle surface area ^b (m ²)	7.9E-09	3.1E-08	1.5E-14	1.5E-12	1.5E-18
single particle mass ^c (kg)	1.7E-10	5.2E-10	1.9E-19	1.3E-17	2.8E-25
total sorbent mass in system (kg)	1E-03	5E-05	5E-05	5E-06	1E-05
number of particles in system ^d (-)	5.8E+06	9.7E+04	2.7E+14	3.8E+11	3.6E+19
total surface area sorbent in system ^e (m ²)	4.6E-02	3.1E-03	4.1E+00	5.5E-01	5.3E+01

^a based on PSD for sediment OM, based on supplier information for the other sorbents

^b based on average particle diameter, for MWCNT surface area was calculated based on rod-shape with an average length of 2.3E-5 m

^c = density × volume of single particle

^d = total sorbent mass in system / single particle mass

^e = single particle surface area × number of particles in system

Table S5.8 Total surface area coverage of ΣPCB onto the sorbents at different PCB levels.

Hypothetical surface coverage (%) ^a						
Q _T ^b	total surface area ΣPCB (m ²)	sediment OM	micro-PE	nano-PS	MWCNT	C ₆₀
1 µg	3.13E-01 ^c					0.59
0.01 µg	1.16E-03	2.6	37.9	0.03	0.21	
0.1 µg	1.10E-02	24.3	361	0.27	2.0	
1 µg	9.39E-02	206	3068	2.3	17.1	
10 µg	9.05E-01	1988	29570	22.2	165	
20 µg	1.81E+00	3975	59140	44.3	329	

^a Hypothetical coverage assuming monolayer sorption of all sorbed CB congeners. A percentage >> 100% implies that surface adsorption cannot explain the observed sorption and that therefore bulk partitioning is indicated

^b Q_T = total amount per CB congener in the system

^c CB congeners in the C₆₀ experiment did not contain planar PCBs

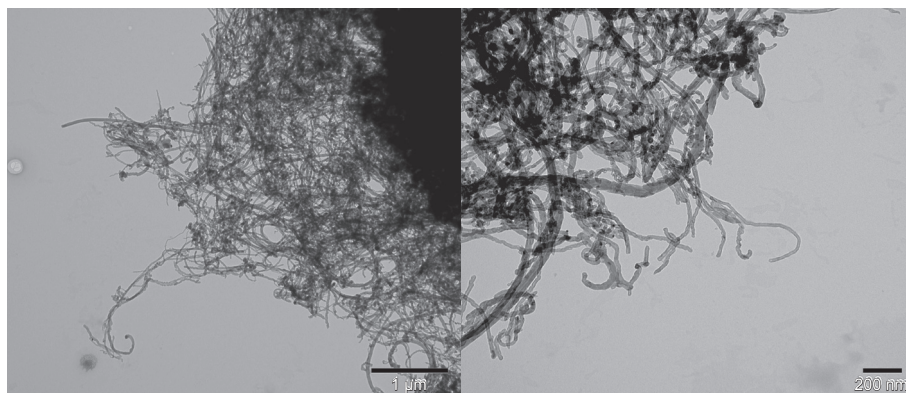


Figure S5.1 TEM images of MWCNT aggregates in freshwater. The images confirm the outer diameter of 20 – 30 nm as provided by the supplier.

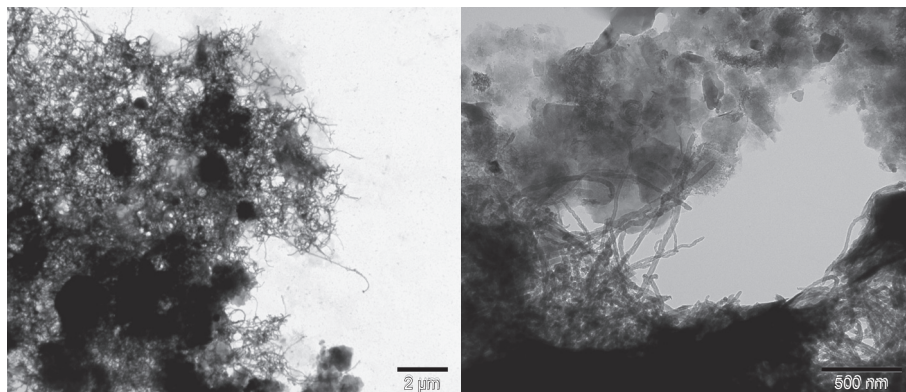


Figure S5.2 MWCNTs in freshwater in the presence of sediment. The typical wire like shape of the MWCNTs can be clearly distinguished from the bulk sediment particles.

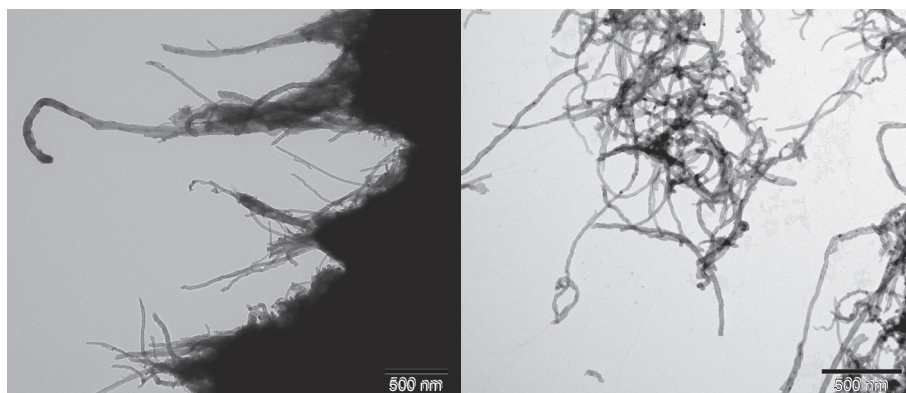


Figure S5.3 TEM pictures of MWCNT aggregates in seawater.

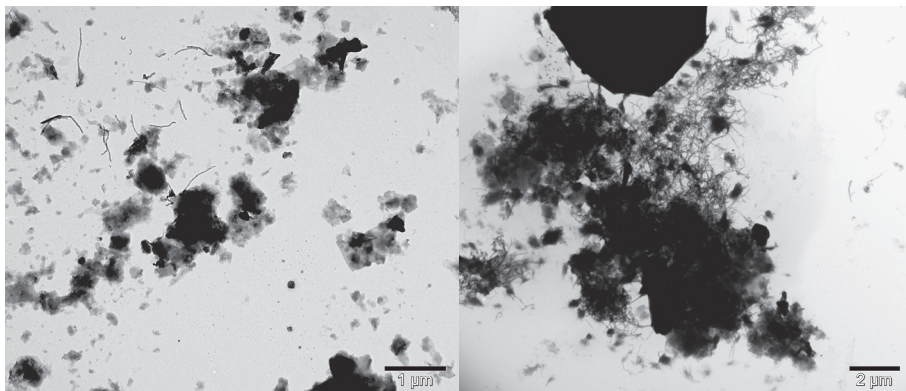


Figure S5.4 TEM pictures of MWCNT aggregates in seawater in the presence of sediment. Besides aggregates and sediment particles some individual 1 μm length MWCNT strains can be distinguished.

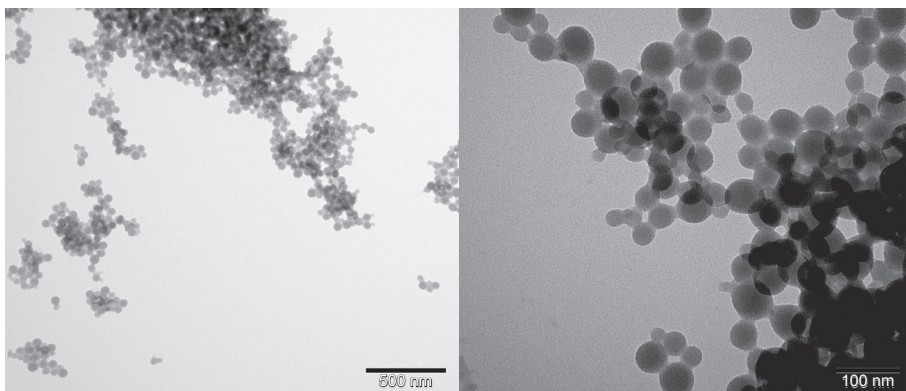


Figure S5.5 TEM images of nano-PS in freshwater (left) and seawater (right) confirming the size of the ~70 nm primary particles and the open aggregate structure.

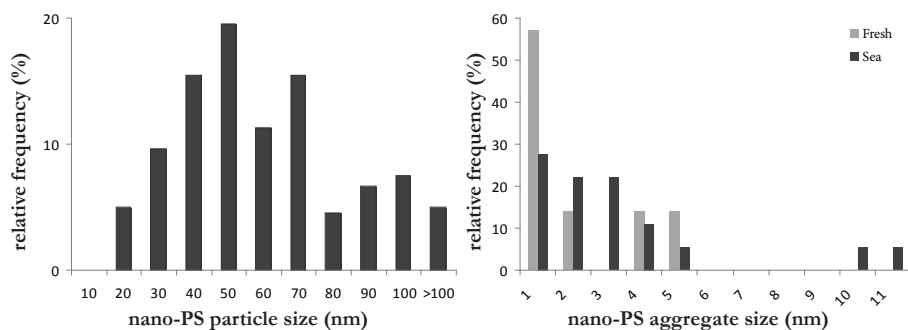


Figure S5.6 Primary particle size distribution (left) and aggregate size distribution (right) of nano-PS particles based on TEM image analysis. Average particle size is 60 ± 25 nm, which is within the range stated by the supplier (70 nm). Average aggregate size is 199 ± 176 nm (freshwater) and 361 ± 465 nm (seawater). Note that the TEM based data may reflect in situ conditions to a lesser extent than light microscopy data because of the TEM preparation procedure.

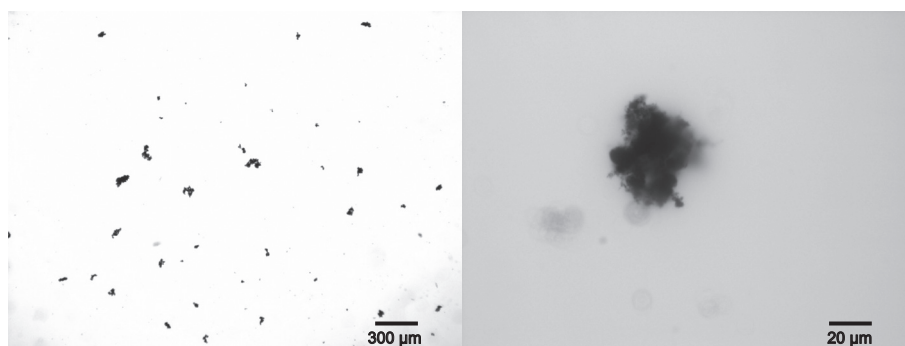


Figure S5.7 Light microscope images of MWCNT aggregates in freshwater. Average aggregate size is 28 ± 21 μm.

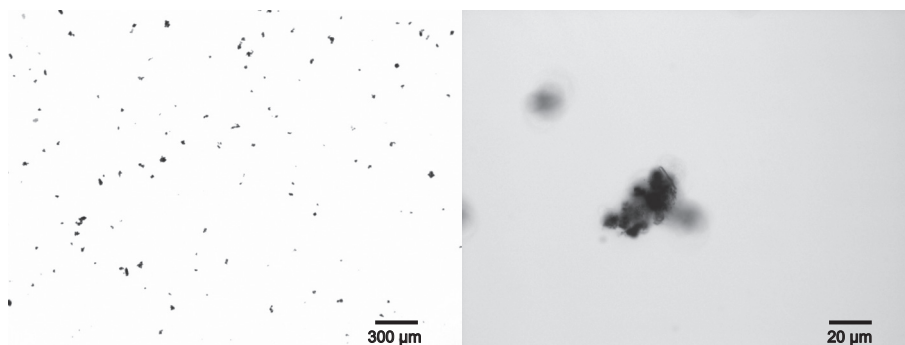


Figure S5.8 Light microscope images of MWCNT aggregates in freshwater in presence of sediment. Average aggregate size is 23 ± 11 μm.

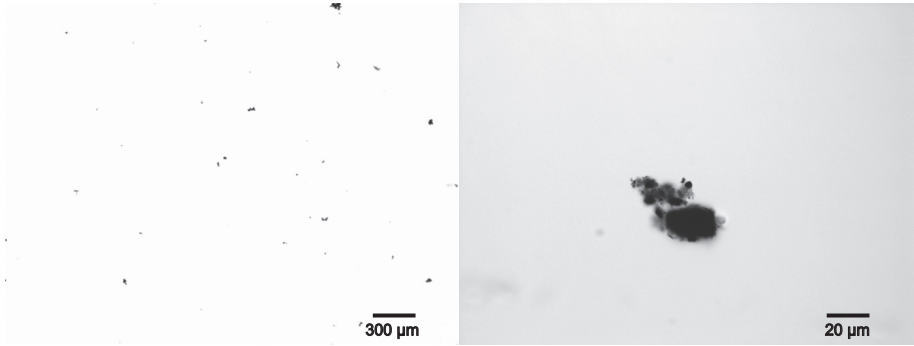


Figure S5.9 Light microscope images of MWCNT aggregates in seawater. Average aggregate size is $20 \pm 12 \mu\text{m}$.

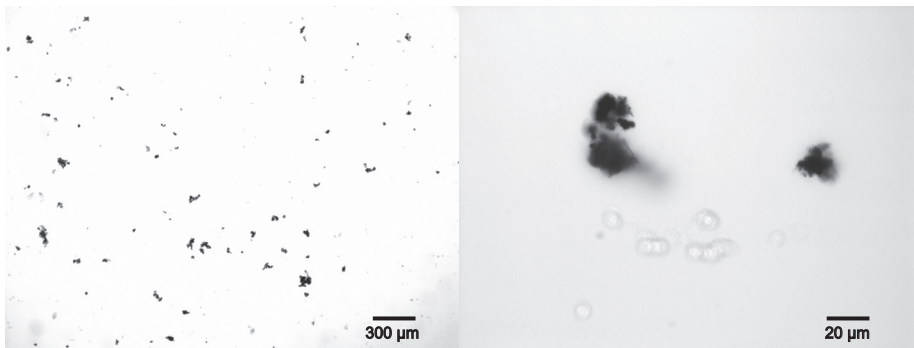


Figure S5.10 Light microscope images of MWCNT aggregates in seawater in presence of sediment. Average aggregate size is $24 \pm 17 \mu\text{m}$.

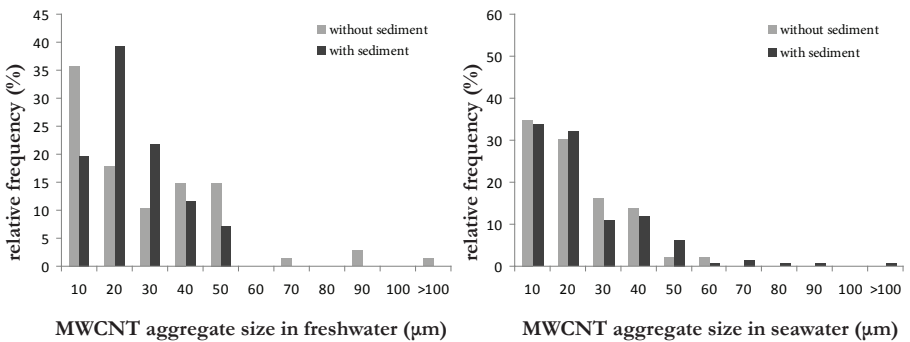


Figure S5.11 MWCNT aggregate size distribution obtained from light microscope image analysis.

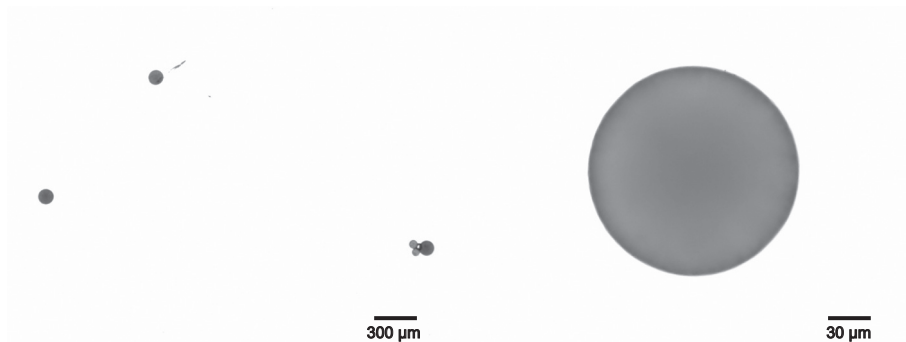


Figure S5.12 Light microscope images of micro-PE in freshwater

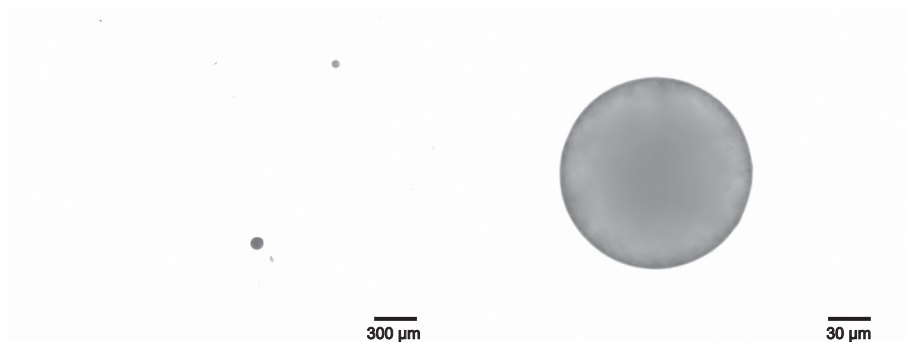


Figure S5.13. Light microscope images of micro-PE in freshwater in presence of sediment.

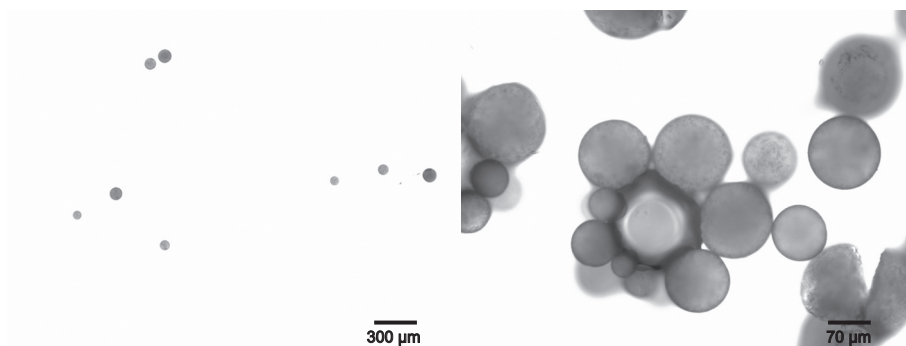


Figure S5.14 Light microscope images of micro-PE in seawater.

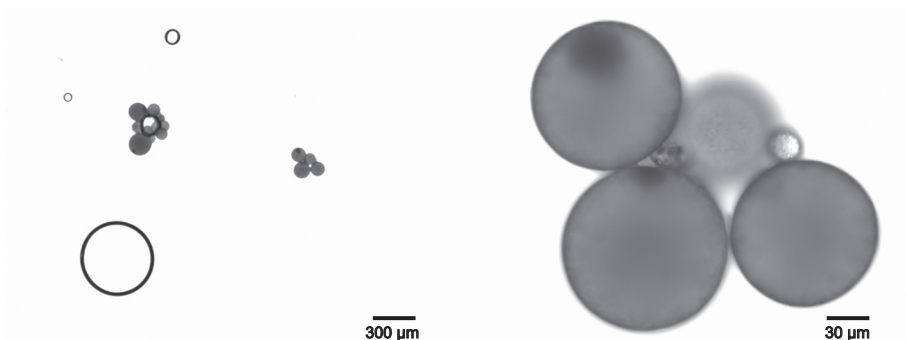


Figure S5.15 Light microscope images of micro-PE in seawater in the presence of sediment.

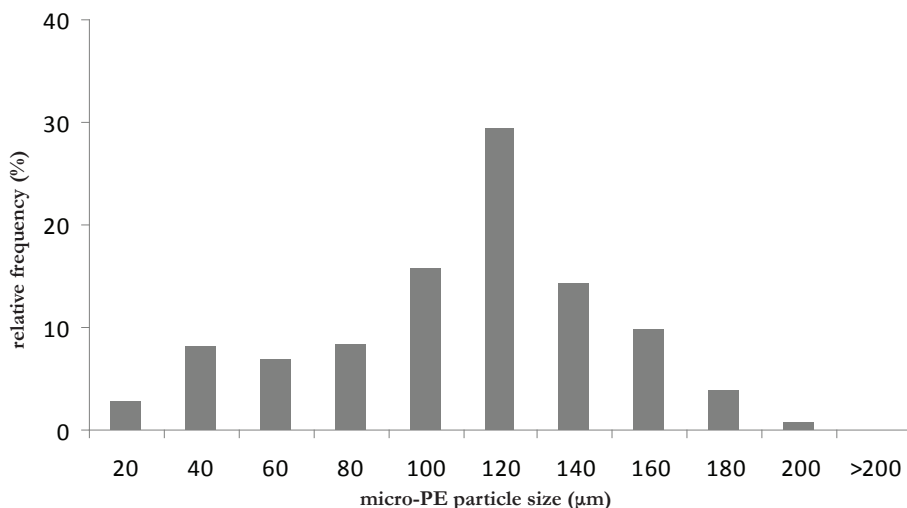


Figure S5.16 Micro-PE particle size distribution based on light microscope image analysis. The average particle size is 99 ± 39 .

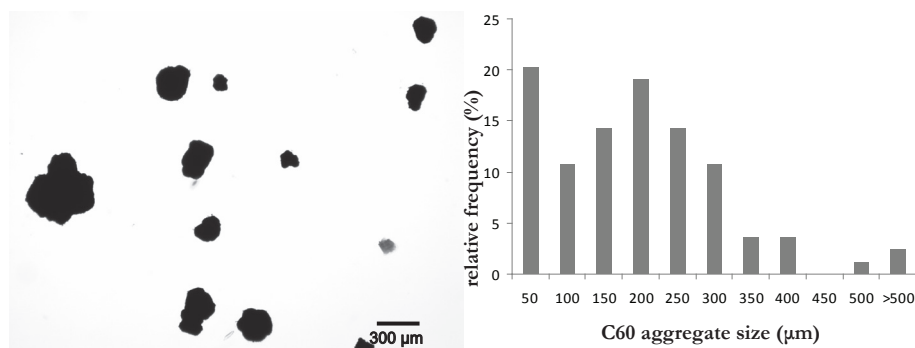


Figure S5.17 Left: Light microscope images of C_{60} aggregates in fresh water. Right: C_{60} aggregate size distribution based on light microscope image analysis. The average aggregate size is 179 ± 128 μm.

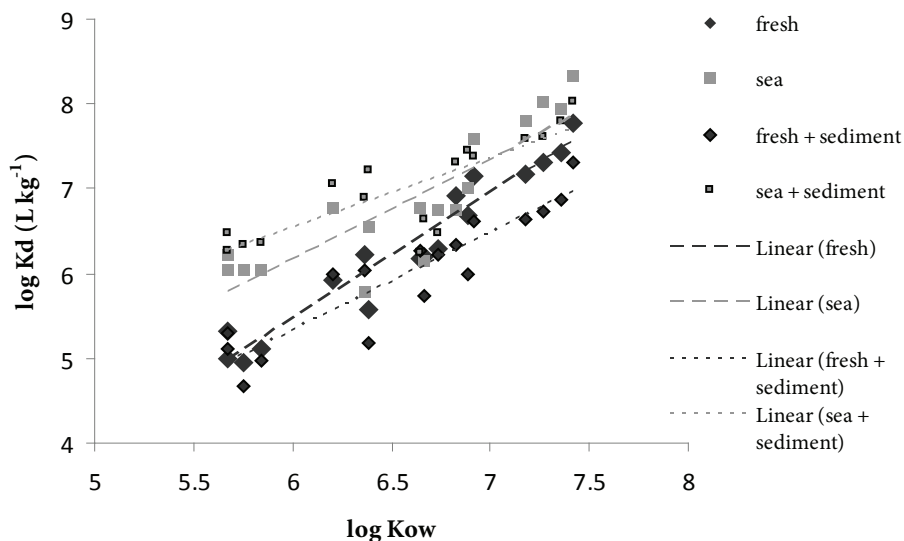


Figure S5.18 Partition coefficients $\log K_d$ for PCB sorption to micro-PE in fresh- and seawater with and without the presence of sediment, as function of $\log K_{ow}$.

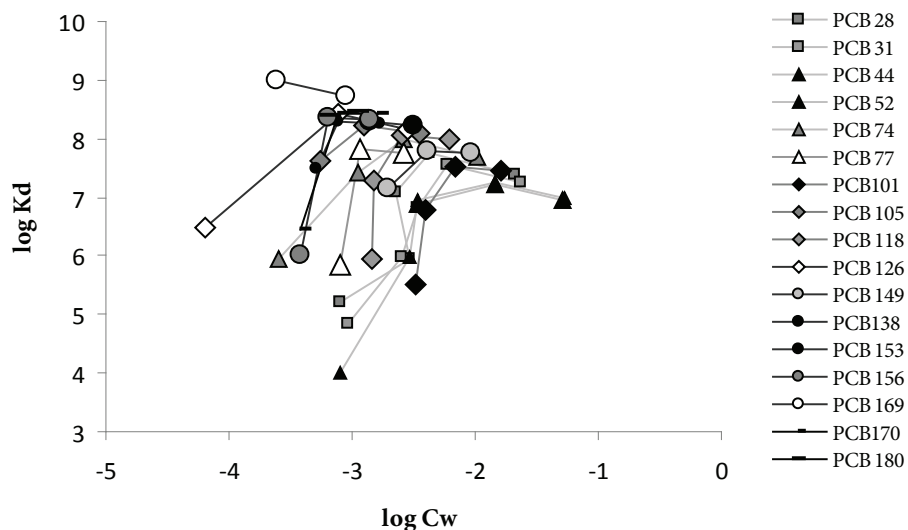


Figure S5.19 Distribution coefficients $\log K_d$ for PCB sorption to nano-PS in freshwater as function of the concentration $\log C_w$. White markers refer to non-ortho (planar), grey ones to mono-ortho (non-planar), black ones to di-ortho (non-planar) and blue ones to tri-ortho (non-planar) – substituted PCB congeners.

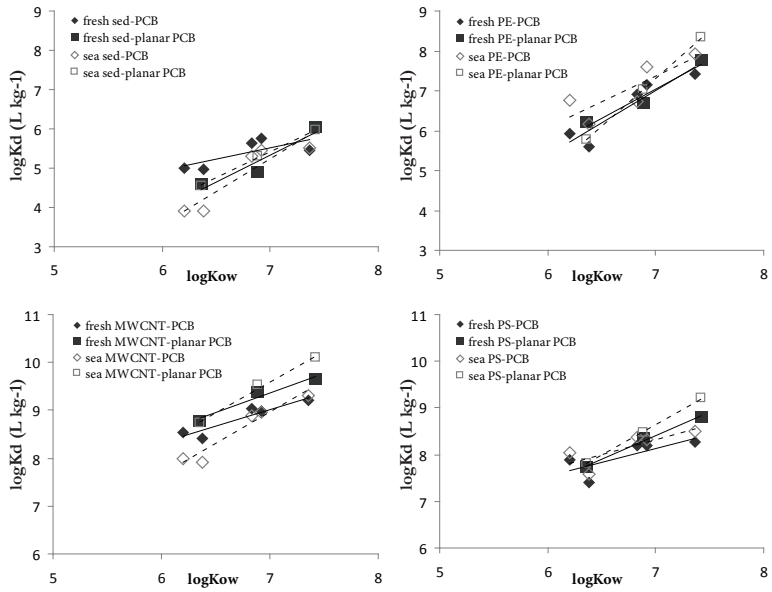


Figure S5.20 Distribution coefficients $\log K_d$ for planar (PCB 77, 126 and 169) and non-planar PCBs (PCB 74, 101, 138, 153 and 180) to sediment (upper left), micro-PE (upper right), MWCNTs (lower left) and nano-PS (lower right) in fresh- and seawater as function of $\log K_{ow}$.

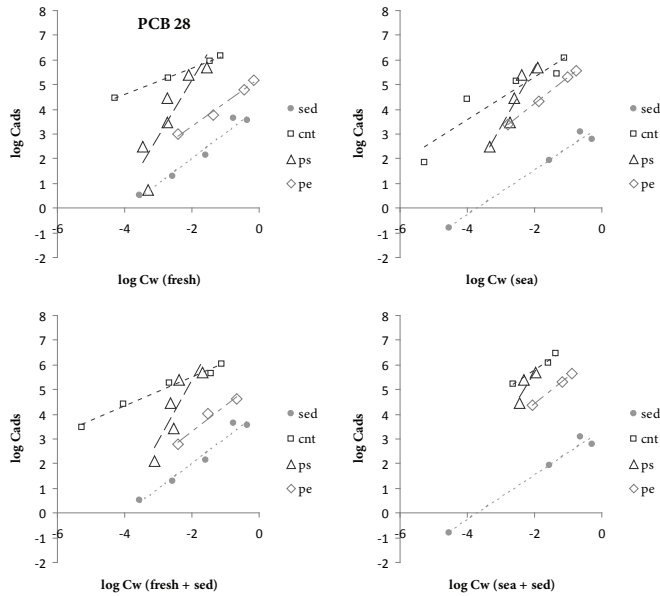


Figure S5.21 Isotherms of PCB 28 for sediment, MWCNTs, nano-PS and micro-PE in fresh- (upper left) and seawater (upper right) and in presence of sediment (for fresh: lower left, for sea: lower right).

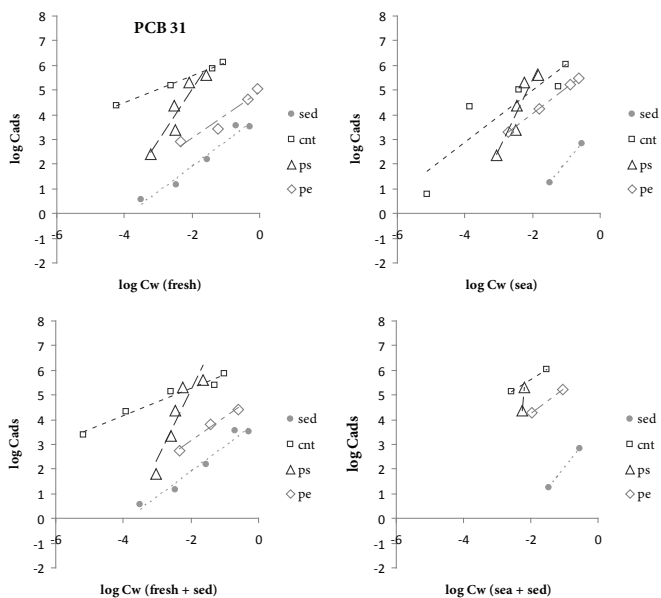


Figure S5.22 Isotherms of PCB 31 for sediment, MWCNTs, nano-PS and micro-PE in fresh- (upper left) and seawater (upper right) and in presence of sediment (for fresh: lower left, for sea: lower right).

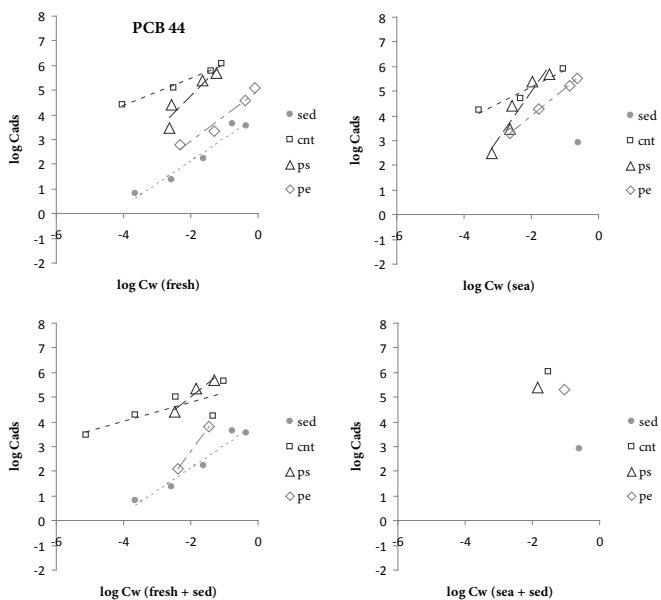


Figure S5.23 Isotherms of PCB 44 for sediment, MWCNTs, nano-PS and micro-PE in fresh- (upper left) and seawater (upper right) and in presence of sediment (for fresh: lower left, for sea: lower right).

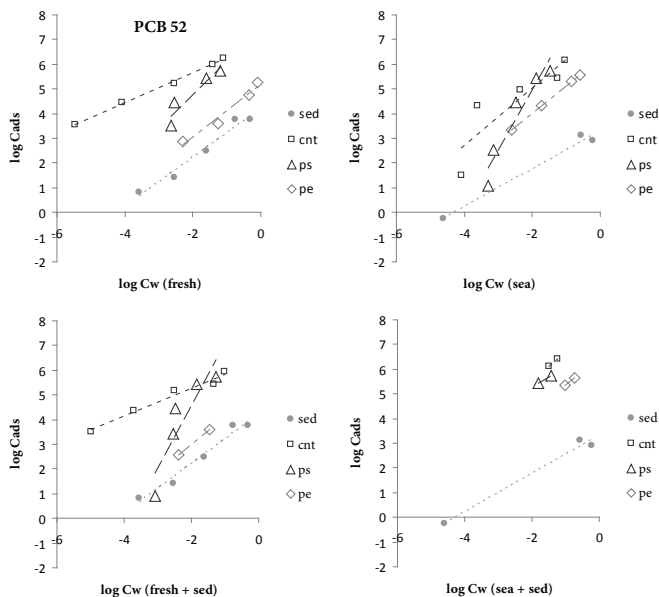


Figure S5.24 Isotherms of PCB 52 for sediment, MWCNTs, nano-PS and micro-PE in fresh- (upper left) and seawater (upper right) and in presence of sediment (for fresh: lower left, for sea: lower right).

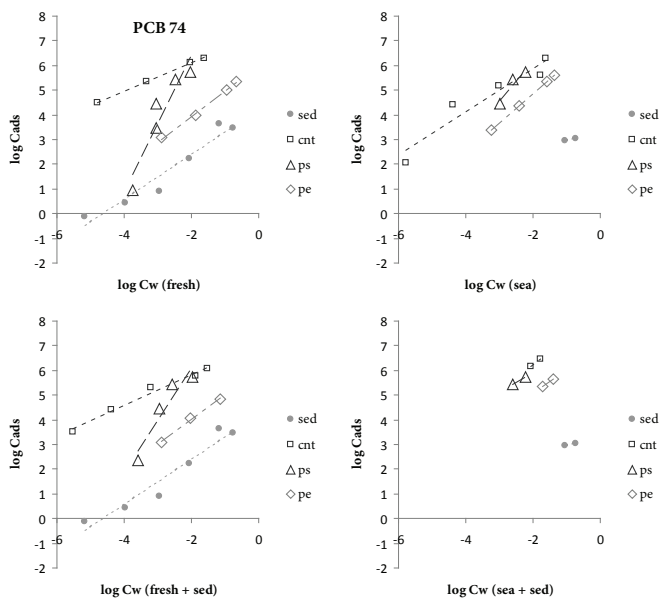


Figure S5.25 Isotherms of PCB 74 for sediment, MWCNTs, nano-PS and micro-PE in fresh- (upper left) and seawater (upper right) and in presence of sediment (for fresh: lower left, for sea: lower right).

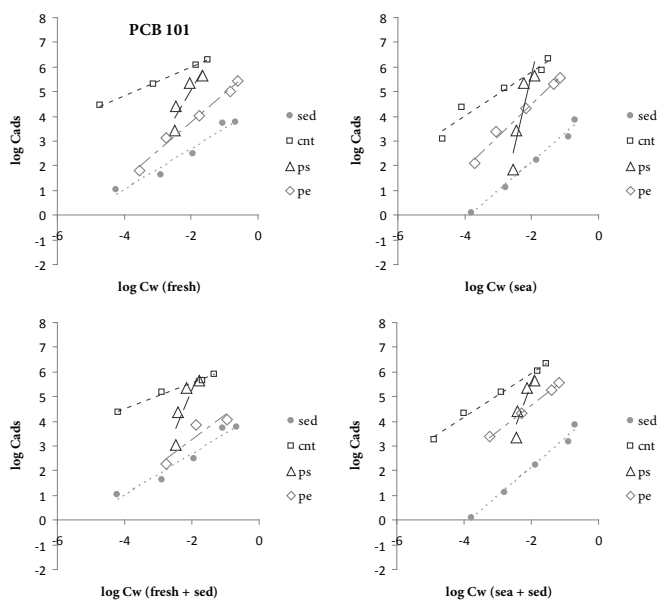


Figure S5.26 Isotherms of PCB 101 for sediment, MWCNTs, nano-PS and micro-PE in fresh- (upper left) and seawater (upper right) and in presence of sediment (for fresh: lower left, for sea: lower right).

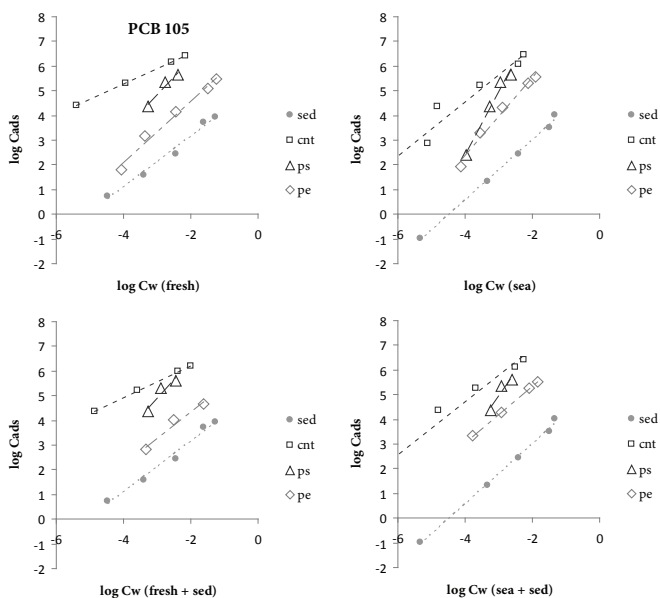


Figure S5.27 Isotherms of PCB 105 for sediment, MWCNTs, nano-PS and micro-PE in fresh- (upper left) and seawater (upper right) and in presence of sediment (for fresh: lower left, for sea: lower right).

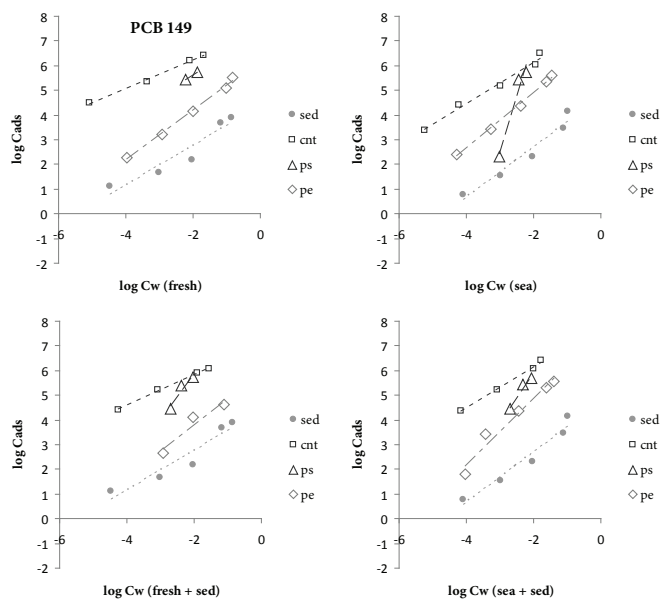


Figure S5.28 Isotherms of PCB 149 for sediment, MWCNTs, nano-PS and micro-PE in fresh- (upper left) and seawater (upper right) and in presence of sediment (for fresh: lower left, for sea: lower right).

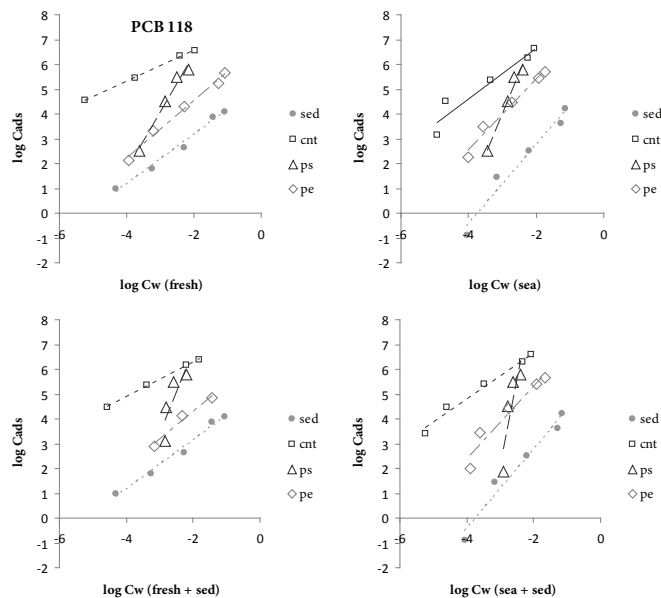


Figure S5.29 Isotherms of PCB 118 for sediment, MWCNTs, nano-PS and micro-PE in fresh- (upper left) and seawater (upper right) and in presence of sediment (for fresh: lower left, for sea: lower right).

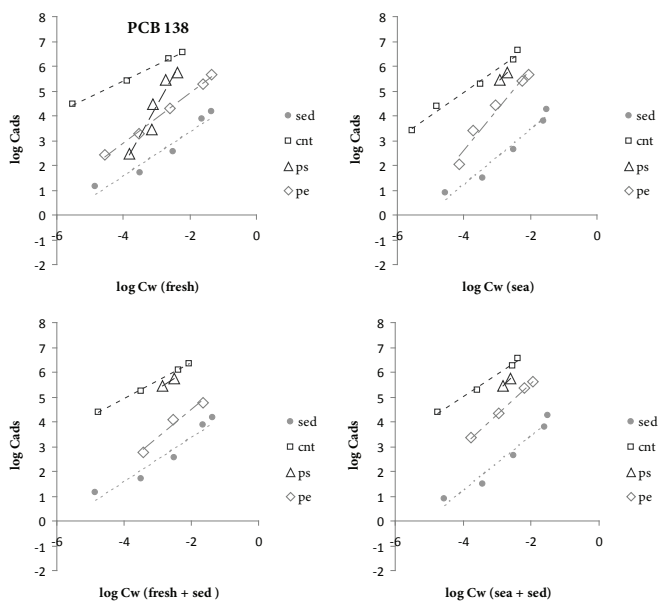


Figure S5.30 Isotherms of PCB 138 for sediment, MWCNTs, nano-PS and micro-PE in fresh- (upper left) and seawater (upper right) and in presence of sediment (for fresh: lower left, for sea: lower right).

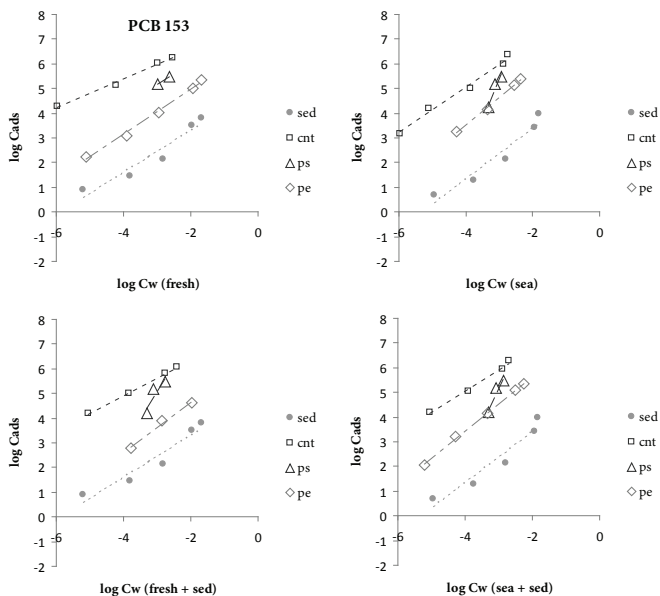


Figure S5.31 Isotherms of PCB 153 for sediment, MWCNTs, nano-PS and micro-PE in fresh- (upper left) and seawater (upper right) and in presence of sediment (for fresh: lower left, for sea: lower right).

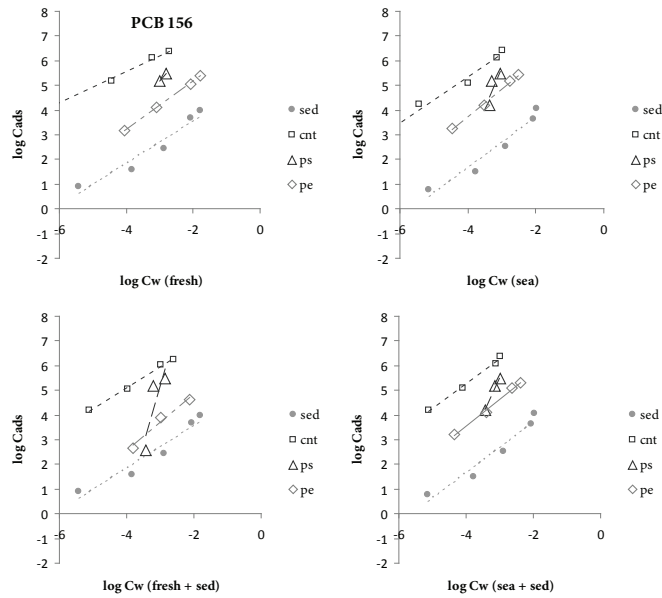


Figure S5.32 Isotherms of PCB 156 for sediment, MWCNTs, nano-PS and micro-PE in fresh- (upper left) and seawater (upper right) and in presence of sediment (for fresh: lower left, for sea: lower right).

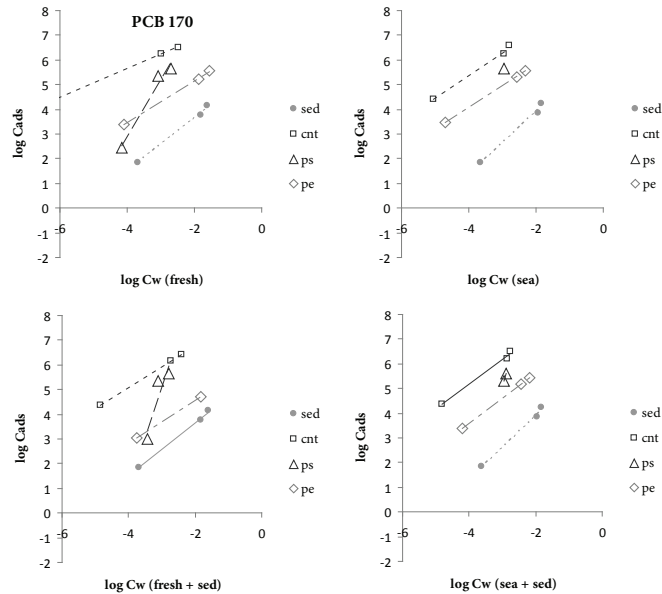


Figure S5.33 Isotherms of PCB 170 for sediment, MWCNTs, nano-PS and micro-PE in fresh- (upper left) and seawater (upper right) and in presence of sediment (for fresh: lower left, for sea: lower right).

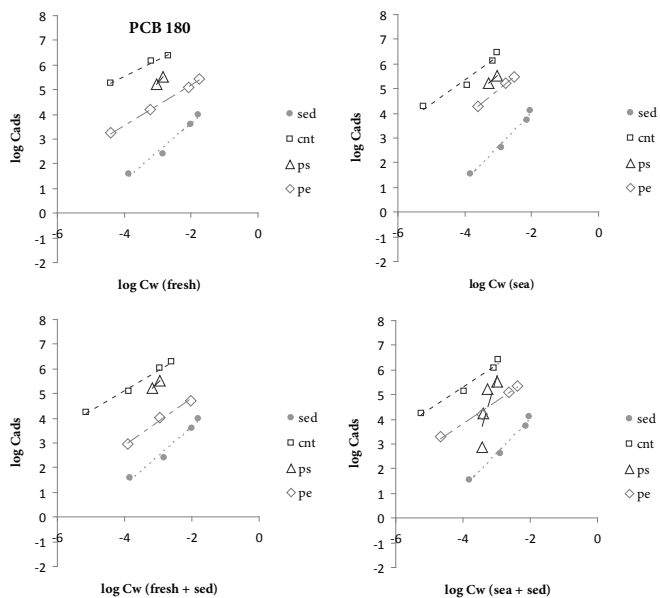


Figure S5.34 Isotherms of PCB 180 for sediment, MWCNTs, nano-PS and micro-PE in fresh- (upper left) and seawater (upper right) and in presence of sediment (for fresh: lower left, for sea: lower right).

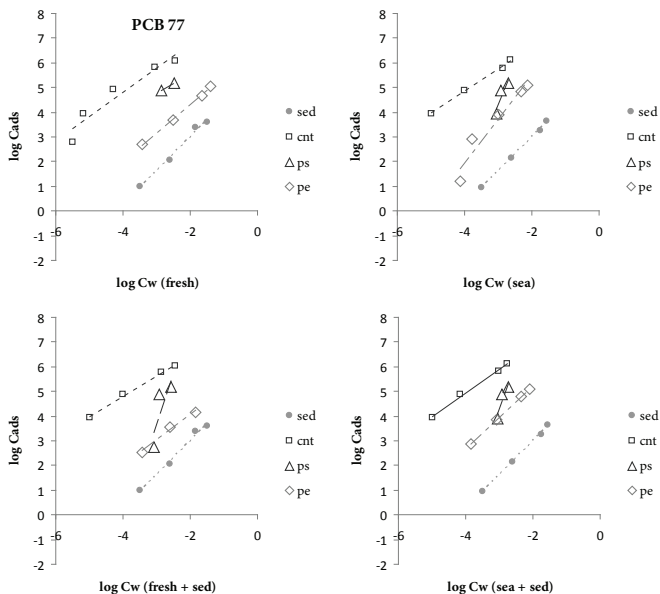


Figure S5.35 Isotherms of PCB 77 for sediment, MWCNTs, nano-PS and micro-PE in fresh- (upper left) and seawater (upper right) and in presence of sediment (for fresh: lower left, for sea: lower right).

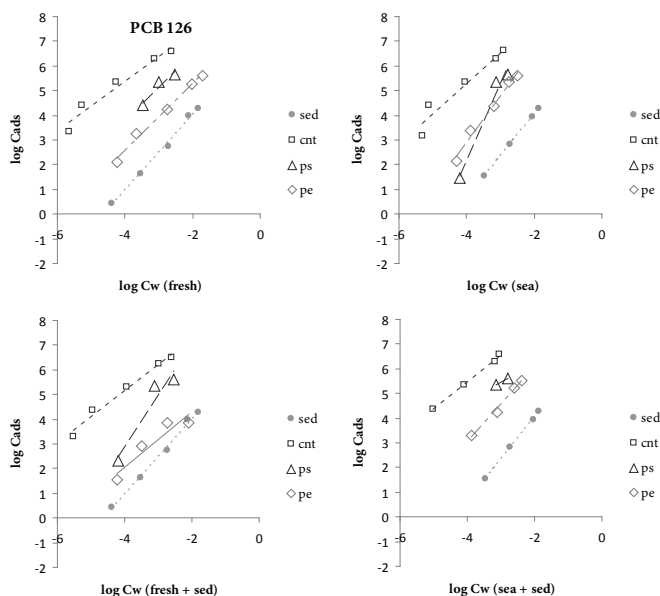


Figure S5.36 Isotherms of PCB 126 for sediment, MWCNTs, nano-PS and micro-PE in fresh- (upper left) and seawater (upper right) and in presence of sediment (for fresh: lower left, for sea: lower right).

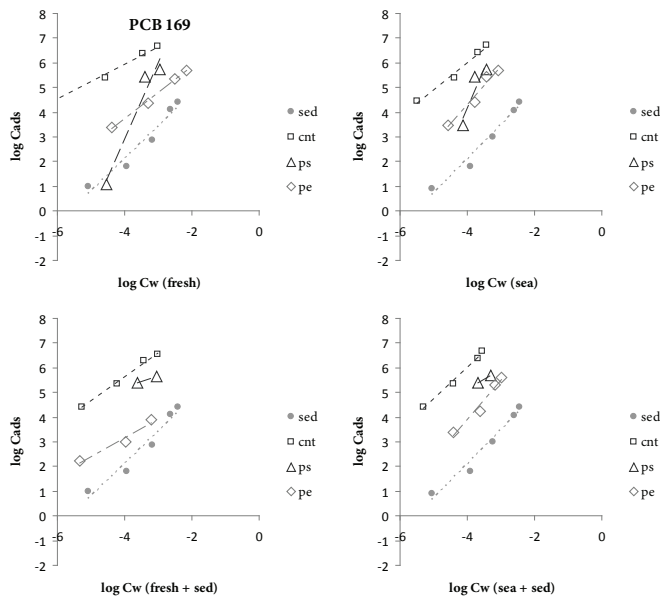


Figure S5.37 Isotherms of PCB 169 for sediment, MWCNTs, nano-PS and micro-PE in fresh- (upper left) and seawater (upper right) and in presence of sediment (for fresh: lower left, for sea: lower right).

References Supporting Information

- [1] Mackay D, Shiu WY, Ma KC, Lee SC. 2006. *Handbook of physical-chemical properties and environmental fate for organic chemicals. 2nd ed. Volume II: Halogenated hydrocarbons.* CRC/Taylor & Francis, Boca Raton, FL.
- [2] Hawker DW, Connell DW. 1988. Octanol Water Partition-Coefficients of Polychlorinated Biphenyl Congeners. *Environmental Science & Technology* 22:382-387.
- [3] Koelmans AA, Meulman B, Meijer T, Jonker MTO. 2009. Attenuation of Polychlorinated Biphenyl Sorption to Charcoal by Humic Acids. *Environmental Science & Technology* 43:736-742.

Aquatic ecotoxicity tests of some nanomaterials



TiO₂ MWCNTs ZrO₂ TiO₂ CeO₂ MWCNTs CeO₂ SWCNTs SiO₂-Ag
SWCNTs PMMA Al₂O₃ PFOS PVP-Ag CeO₂ MWCNTs PVP-Ag SWCNTs
nano-PS C₆₀ micro-PE C₆₀ SiO₂-Ag TiO₂ C₆₀
Al₂O₃ SiO₂-Ag MWCNTs PVP-Ag CeO₂ PVP-Ag C₆₀ MWCNTs PFOS micro-PE
SiO₂-Ag PMMA PVP-Ag nano-PS C₆₀ MWCNTs PFOS micro-PE
PVP-Ag C₆₀ PMMA MWCNTs CeO₂ micro-PE CeO₂ Al₂O₃
PCBs SiO₂-Ag CeO₂ Al₂O₃ MWCNTs MWCNTs CeO₂ Al₂O₃
MWCNTs C₆₀ nano-PS PVP-Ag nano-PS Al₂O₃ MWCNTs TiO₂ PFOS
micro-PE PCBs MWCNTs CeO₂ CeO₂ ZrO₂ C₆₀ PMMA MWCNTs
nano-PS Al₂O₃ CeO₂ PCBs CeO₂ SWCNTs nano-PS MWCNTs
SiO₂-Ag ZrO₂ C₆₀ MWCNTs ZrO₂ micro-PE SiO₂-Ag PMMA
C₆₀ PCBs SiO₂-Ag PFOS SiO₂-Ag PMMA Al₂O₃ MWCNTs ZrO₂
ZrO₂ TiO₂ C₆₀ nano-PS PVP-Ag PMMA Al₂O₃ MWCNTs ZrO₂ C₆₀
MWCNTs PFOS SiO₂-Ag PVP-Ag PCBs TiO₂ C₆₀ PMMA
CeO₂ SWCNTs ZrO₂ TiO₂ MWCNTs micro-PE SiO₂-Ag MWCNTs
micro-PE SiO₂-Ag nano-PS PFOS CeO₂ C₆₀ PFOS PMMA PVP-Ag
MWCNTs Al₂O₃ Al₂O₃ PFOS PVP-Ag SWCNTs PMMA TiO₂ CeO₂
TiO₂ PCBs micro-PE Al₂O₃ PFOS PVP-Ag SWCNTs PMMA nano-PS

Published as: Velzeboer I, Hendriks AJ, Ragas AMJ, Van de Meent D. 2008. Aquatic ecotoxicity tests of some nanomaterials. *Environmental Toxicology and Chemistry* 27:1942-1947.

Abstract

Nanoparticles of TiO_2 , ZrO_2 , Al_2O_3 , CeO_2 , fullerene (C_{60}), single-walled carbon nanotubes, and polymethylmethacrylate were tested for ecotoxic effects using one or more ecotoxicity endpoints: Microtox (bacteria), pulse-amplitude modulation (algae), Chydotox (crustaceans), and Biolog (soil enzymes). No appreciable effects were observed at nominal concentrations of up to 100 mg L^{-1} . Dilution of nanoparticle suspensions, either in ultrapure (Milli-Q) water or in natural (pond) water, led to formation of larger particles, which settled easily. (Nano)particles in water were characterized by means of atomic force microscopy, energy-dispersive x-ray analysis, inductively coupled plasma–mass spectrometry, flow cytometry, and spectrophotometry. It is concluded that the absence of ecotoxicity is the result of low concentrations of free nanoparticles in the tests, and it is suggested that colloid (in) stability is of primary importance in explaining ecotoxic effects of nanoparticles in the natural environment.

6.1 Introduction

Nanotechnology makes possible the manufacture of materials at atomic and molecular scales to obtain new materials and create new processes [1]. Currently, the use of nanomaterials is increasing rapidly. As a result, an increase of (unintended) emissions to air, water, and soil is expected [2]. Concerns about possible adverse consequences for human and environmental health have been raised [3, 4]. Literature reviews show that basic data regarding the physicochemical and ecotoxicological properties of nanoparticles are not plentiful [5-9]. Information concerning the fate of nanoparticles in air, water, and soil also is limited [10]. Much information about health effects of nanoparticles comes from medical studies because of interest in their medical applications [4, 11].

Generally, synthetic nanoparticles consist of solid matter, and they usually are designed to persist as particulate matter in aqueous media. Because of their size, they share some properties with dissolved molecules (e.g., ability to pass biological membranes) and some properties of particles (e.g., active surface). Also by design, physical and chemical properties of nanoparticles may differ distinctly from the properties of bulk materials of the same chemical composition [12]. Nanoparticles have a larger surface area than bigger particles of equal mass, and many nanomaterials have specific physical and chemical properties that are related to their small size, such as the size-dependent colour of quantum dots.

As a consequence, one should expect that nanoparticles differ in their environmental behaviour both from traditional chemicals that partly dissolve in water and from particulate matter of greater than nano size. Also, nanoparticles may show specific ecotoxic effects. Several studies indicate that nanoparticles are more toxic

than comparable particles of micro size [6, 13]. Nanoparticles in water form colloidal suspensions. The colloidal particles show Brownian motion and interaction with other particles and dissolved molecules. Nanoparticles may interact with each other and with other colloidal surfaces; aggregates and agglomerates are likely to precipitate. By this mechanism, nanoparticles may be transported easily from water to sediment. Therefore, understanding the stability of a colloidal suspension may be of great importance in describing and predicting the environmental fate of nanoparticles in water [14]. Significant concentrations of nano-sized material ought to be expected in natural water only if stabilizing factors are favourable [15]. Simple linear partitioning behaviour between water and solids, as commonly observed for truly dissolved chemical substances, is not to be expected for nanoparticles [16]. Because of this, current models for environmental exposure assessment, to which such predictive partitioning behaviour between environmental phases is prerequisite, may not be applicable to these new materials.

The aim of the present study was to explore the two main aspects of environmental risk of nanoparticles, toxicity and exposure. To investigate whether nanoparticles are ecotoxic, a suite of nanoparticles was tested for their effects on a series of different endpoints and species. A suite of simple toxicity tests was selected to get an impression of the potential biological impact of nanoparticles on water organisms. The toxicity of nanoparticles of TiO_2 , ZrO_2 , Al_2O_3 , CeO_2 , carbon (fullerene, C_{60} ; single-walled carbon nanotubes [SWCNTs]), and polymethylmethacrylate (PMMA) was tested using one or more ecotoxicity tests for bacteria (Microtox, Carlsbad, CA, USA), algae (pulse-amplitude modulation [PAM]), crustaceans (Chydotox), and metabolic processes in soil (Biolog, Hayward, CA, USA). To investigate whether exposure of organisms via water is likely under natural conditions, some exploratory characterization experiments were conducted.

In the present study, we adopted the exploratory test strategy, as commonly used during the early years of ecotoxicological testing of potentially harmful materials. Acknowledging that little is known about the behaviour of nanoparticles in water and that it is difficult (if even possible at all) to measure concentrations and properties of nanoparticles in test samples, we chose to test the nanomaterials as such, simulating under laboratory conditions what might occur on release of the material into the environment. The results of the present experiments were interpreted as the combined result of hazard and likelihood of exposure.

6.2 Materials and methods

Nanoparticles used

A number of readily available nanoparticles were used in the present study: TiO_2 , ZrO_2 , Al_2O_3 , CeO_2 , SWCNTs, fullerene, and three sizes of PMMA (0.06, 0.41, and 1.08 μm). The PMMA particles were from Bangs Laboratories (Fishers, IN, USA). The other

nanoparticles were obtained from Sigma-Aldrich (Zwijndrecht, The Netherlands). The metal oxides and PMMA were ordered as 10% (w/w) dispersions in water. Ecotoxicity test dispersions were prepared from these by dilution with test medium. Fullerene and SWCNTs were not available as dispersions in water and, therefore, were ordered as powders. The preparation of fullerene and SWCNTs in water was done according to the protocol described by Oberdörster [7], in which carbon particles are stirred in water without addition of solvents. This protocol was used for both fullerene and SWCNTs. Suspensions were stirred for four months before the concentration was measured with spectrophotometry.

Ecotoxicity tests

Four different ecotoxicity tests were performed: Microtox test, PAM test, Chydotox test, and Biolog test.

Microtox test. The Microtox method used bioluminescent bacteria -specifically, the strain *Vibrio fischeri* NRRL B-11177 [17]. The median effective concentration was determined by the difference in the light output between the sample and the control. The test started with a basic test of a phenol standard of 100 mg L⁻¹. For TiO₂, ZrO₂, Al₂O₃, and CeO₂, dilutions with concentrations of 100, 10, and 1 mg L⁻¹ were used. Single concentrations were tested for PMMA and fullerene (100 and 1 mg L⁻¹, respectively). The concentration of SWCNTs was unknown, because analytical techniques to determine the concentration were unavailable. The tests were performed by running the 81.9% basic test, which consisted of nine dilutions, and by following the instructions of the test tutorial, with measurements at 0, 5, 15, and 30 min.

PAM test. The PAM test used the green alga *Pseudokirchneriella subcapitata* [18]. The effects of the toxicant on the efficiency of photosynthesis were quantified (i.e., median effective concentration). The nanoparticles TiO₂, ZrO₂, Al₂O₃, CeO₂ and PMMA (0.06, 0.41, and 1.08 μm) with concentrations of 100 mg L⁻¹ were tested. To check the sensitivity of the test system, an atrazine standard (Riedel-de-Haën, Seelze, Germany) in 98% ethanol with a concentration of 0.1311 mM was used. The test consisted of seven dilutions of the toxicant with Dutch standard water (Milli-Q, Amsterdam, The Netherlands) and NaHCO₃, KHCO₃, CaCl₂·2H₂O, and MgSO₄·7H₂O. After adding the algae, the samples were incubated at a constant temperature of 20°C, continuous light exposure (100 μE m⁻²s⁻¹, 650 nm), and continuous shaking during 4.5 h. Afterward, the efficiency of photosynthesis was measured with a PAM fluorometer (Walz, Effeltich, Germany).

Chydotox test. The Chydotox test [19] was based on the survival of *Chydorus sphaericus*, a small, benthic cladoceran. This chydorid was exposed to a nanoparticle dilution for 48 h without food. The mortality of the chydorids was counted at $t = 0$ and 48 h with an inverted microscope. These data were converted to a median lethal concentration by nonlinear regression. The tested dilutions were dispersions of 100 mg L⁻¹ of TiO₂, Al₂O₃, CeO₂, and PMMA (0.06, 0.41, and 1.08 μm). The dilutions of the nanoparticles were made with tap water. To start the Chydotox test, approximately five

chydorids were put into the 1-ml vials. The exact amount of chydorids was counted at $t = 0$ h. The vials were put away for 48 h in a climate chamber at 20°C with a 17:7-h light:dark photoperiod. At $t = 48$ h, the chydorids were counted again. No positive-control experiments are run in this test protocol.

Biolog test. The Biolog test contains a mix of soil bacteria to determine toxicity via multivariate analysis [20]. Specific multiwell plates were used; these plates contained one organic substrate in each well together with a tetrazolium violet redox dye. Reductions in the colour development on toxicant amendment were used to derive dose-response relationships, and the median lethal concentration was determined for each substrate. The toxicant used for this experiment was TiO_2 (100 mg L⁻¹). For the Biolog test, no extra positive control was conducted. This control was included into the multiwell plates. For this experiment, soil bacteria sampled at Demmerik (The Netherlands; 52°12'0"N, 4°56'0"E; May 19, 2005) were added to 10 M sterile Bis-tris (2-(bis(2-hydroxyethyl)amino)-2-(hydroxymethyl) propane-1,3-diol; EMD Chemicals, Gibbstown, NJ, USA) at pH 7. After 24 h of incubation, the samples were transferred into the multiwell, gram-positive plates (Biolog). During one week, the colour development was measured every day (except for the weekend) with the plate reader.

Particle characterization

Experiments were done to determine if the particles remain nanoparticles, coagulate to each other, or aggregate to other particles in surface water and if the particles could be centrifuged out. Particles as supplied were inspected by atomic force microscopy (AFM) and energy-dispersive x-ray analysis. Dispersions were made in different types of water to nominal concentrations of 100 mg L⁻¹ (maximum concentration tested). Suspensions were determined before and after centrifugation. Milli-Q water, centrifuged pond water, and untreated pond water were used for the dilutions of the TiO_2 samples. Surface water was used to determine the effect of organic matter in water on nanoparticles. Surface water was sampled from a pond at the National Institute of Public Health and the Environment site in Bilthoven (The Netherlands).

Centrifugation. A Europe 24 centrifuge (Measuring and Scientific Equipment, Crawley, UK) was used for centrifuging surface water and samples. Pond water and TiO_2 samples were first centrifuged for 15 min at 10,000 g. With a pipette, the upper half of the sample was transferred to a new tube, which subsequently was centrifuged again for 15 min at 10,000 g. The fullerene samples were centrifuged two times for 20 min at 5,000 g each time to remove only the larger particulate material.

Microscopy. Atomic force microscopy was used for visualizing TiO_2 nanoparticles. The stock solution of 10% (w/w) TiO_2 and a dilution of TiO_2 in Milli-Q water (100 mg L⁻¹) were measured. The samples were dried in an oven to remove the water. Energy-dispersive x-ray analysis was used to determine which elements were in the TiO_2 sample.

Inductively coupled plasma–mass spectrometry. Inductively coupled plasma–mass spectrometry (ICP-MS; HP 4500; Agilent Technologies, Amstelveen, The Netherlands) [21] was used to measure the total titanium content of TiO₂ nanoparticles suspensions. Ordinarily, ICP-MS is used to measure dissolved TiO₂ in water after atomization in the plasma. When particle suspensions are measured, atomization may lead to clouds of titanium atoms entering the detector. This may explain the high relative standard deviation of the measurements.

Spectrophotometry. Ultraviolet-visible light spectrophotometry (Lambda 11/bio; PerkinElmer, Waltham, MA, USA) was used to measure concentrations of TiO₂ and fullerene nanoparticles by measuring light intensity as a function of the wavelength of light. The concentration of the sample was determined with a calibration curve. This method did not work for SWCNTs.

Flow cytometry. Flow cytometry can measure both numbers and sizes of larger particles (>0.5 μm). We used flow cytometry to detect the extent to which particles larger than 0.5 μm had formed under our experimental conditions. For the experiments with the TiO₂ nanoparticles, the MoFlow Cell Sorter (DAKO NL, Heverlee, Belgium; <http://www.dakobv.nl/>). The TiO₂ particles passed through a laser beam, which caused light to scatter. This scattering - a function of the size, shape, and structure of the particle - was recorded.

6.3 Results

Ecotoxicity tests

The energy-dispersive x-ray analysis results confirmed that the 10% (w/w) TiO₂ solution contained titanium and oxygen atoms but no others. The particles were not coated with other material and contained no additions to stabilize the solution. The AFM pictures showed that the particles size was between 50 and 150 nm.

Table 6.1 summarizes the results of the ecotoxicity tests. The Microtox experiments did not induce measurable effects for *V. fischeri* with a concentration of 100 mg L⁻¹, except for SWCNTs and fullerene. The PAM experiments show similar results for *P. subcapitata*. The SWCNTs and fullerene were not tested with PAM. The Chydotox experiments did not induce measurable effects for *C. sphaericus*. Zirconium oxide, SWCNTs, and fullerene were not tested. The Biolog experiment was only done with TiO₂. The quantity of TiO₂ added according to this procedure did not induce measurable effects for soil bacteria.

A few noticeable observations were made during the ecotoxicity test. First, the 100 mg L⁻¹ suspensions were not transparent and had a white turbidity, which can affect the Microtox and PAM measurements because of quenching (absorbing light). Second, the 100 mg L⁻¹ suspensions were unstable and tended to precipitate after some time. In the PAM test, particles visibly adhered to the glassware when using concentrations of 100 mg L⁻¹. In the Chydotox tests, diluting the suspensions with tap

water caused the nanoparticles to visibly aggregate and precipitate to a greater extent than in Milli-Q water.

Table 6.1 EC50/LC50 of the ecotoxicity tests

	Microtox EC ₅₀ 15 min, mg L ⁻¹	PAM EC ₅₀ 4.5h, mg L ⁻¹	Chydotox LC ₅₀ 48h, mg L ⁻¹	Biolog EC ₅₀ 7d, mg L ⁻¹
TiO ₂	> 100	> 100	> 100	> 100
ZrO ₂	> 100	> 100		
Al ₂ O ₃	> 100	> 100	> 100	
CeO ₂	> 100	> 100	> 100	
C _n (SWCNTs)	> ?			
C ₆₀	> 1			
PMMA (0.06)	> 100	> 100	> 100	
PMMA (0.41)	> 100	> 100	> 100	
PMMA (1.08)	> 100	> 100	> 100	

Particle characterization

Table 6.2 shows the effect of centrifugation on concentrations of particles in the supernatant. The ICP-MS analyses of the TiO₂ dilutions in pond water and in centrifuged pond water showed that almost all the titanium was removed from the water phase by centrifugation, whereas for the TiO₂ in Milli-Q, a higher portion of titanium remained in suspension. The spectrophotometer measurements showed that almost all TiO₂ from the 10% (w/w) suspension (as supplied) was removed by centrifugation. After four months of stirring, the fullerene concentration, as measured with spectrophotometry, was very low. Almost all fullerene was removed by centrifugation.

Table 6.2 Concentration of the particles before and after centrifugation measured with ICP-MS or spectrophotometry

	Method	Before centrifugation	After centrifugation
TiO ₂ + MilliQ	ICP-MS	100 µg L ⁻¹	10 µg L ⁻¹
TiO ₂ + centr. pond water	ICP-MS	14 µg L ⁻¹	1 µg L ⁻¹
TiO ₂ + pond water	ICP-MS	200 µg L ⁻¹ ^a	1 µg L ⁻¹
TiO ₂ (10wt%)	Spectrophotometer	1×10 ⁵ mg L ⁻¹	1 mg L ⁻¹
C ₆₀ + MilliQ	Spectrophotometer	>140 mg L ⁻¹	1 mg L ⁻¹

^a added, not measured

Figure 6.1 shows the results of the flow cytometry. In terms of particle numbers, the majority of the particles were in the small size range in each of the suspensions tested. In all cases, most of the mass was present in larger particles. The TiO₂ particles clearly aggregated to a larger extent in centrifuged pond water than in Milli-Q water. The flow cytometry results demonstrated that in all suspensions tested, larger particles (>0.5 μm) readily formed and could be easily removed by centrifugation.

6.4 Discussion

Ecotoxicity of nanoparticles

No ecotoxic effects have been observed for the selected nanoparticles at the doses applied. This contrasts with the findings of others, such as Lovern and Klaper [22], who reported the effects of TiO₂ and fullerene on *Daphnia magna*. Those authors prepared the solutions of the nanoparticles by filtration in tetrahydrofuran and by sonication. The filtered samples showed mortality; the sonicated samples did not. Lovern and Klaper [22] suggested that particle aggregation likely is the reason for the absence of effects. This could explain why no appreciable effects were observed with the Chydotox tests in the present study. In comparison with the results of Lovern and Klaper [22], no appreciable differences were determined in the present study. Our findings, however, are in line with those of Klaine et al. (S.J. Klaine, oral presentation at Nanotoxicology 2007, Venice, Italy, April 21, 2007), who mentioned that they were unable to reproduce the results of Lovern and Klaper [22]. We hypothesize that the absence of ecotoxic effects in the present experiments may be explained, at least in part, by low concentrations of small particles in suspension. The actual concentrations of nano-sized materials to which our test organisms were exposed probably were far lower than the nominally added 100 mg L⁻¹.

Exposure concentrations of nanoparticles

The particle characterization experiments clearly show that for TiO₂ and fullerene, most of the mass of the particulate matter was present in the form of relatively large particles. This became immediately evident during laboratory manipulations, when formation of flocks had been observed by the naked eye. As seen from Table 6.2, much of the material was easily removed by centrifugation. Presence of predominantly large (larger than nano size) particles was further confirmed quantitatively by flow cytometry (Figure 6.1).

Because the flow cytometric method applied in the present study cannot detect particles smaller than 0.5 μm, these measurements do not indicate whether nanoparticles of TiO₂ were still present in the diluted suspensions. Based on particle counts and diameters, known particle densities, and assumed spherical shape, however, it could be estimated that the bulk of the original TiO₂ mass was present as large particles (Figure 6.1, open bars).

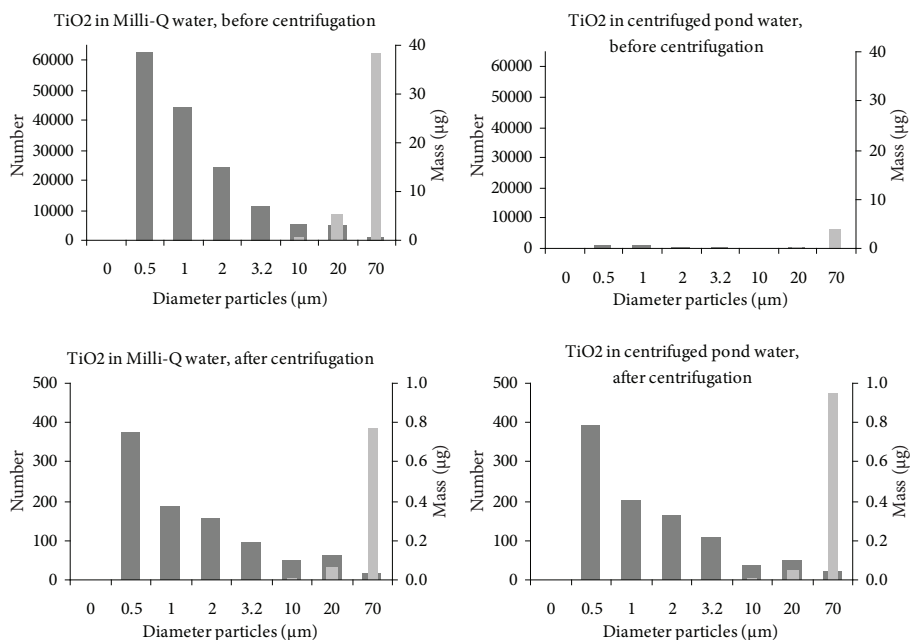


Figure 6.1 Numbers and masses of TiO_2 particles per size class in MilliQ water and centrifuged pond water before and after centrifugation

The TiO_2 particles were nearly quantitatively removed from suspension by centrifugation. Had the particles been nano size, removal should have occurred to a much lesser extent. As demonstrated in the Supporting Information, removal efficiencies of TiO_2 from aqueous suspension can be readily predicted for particles of known size (i.e., mass). Assuming the particles to be spherical, and assuming further a TiO_2 crystal density of $4,320 \text{ kg m}^{-3}$, Equation S6.4 in the Supporting Information was used to calculate the expected removal fractions from a 10-cm centrifuge tube. Results are plotted for various gravitational accelerations in Figure 6.2.

On the basis of these findings, TiO_2 particles smaller than approximately 20 nm are expected to remain in suspension even under strong centrifugation (10,000 g). Particles larger than approximately 10 μm , however, are expected to settle even without centrifugation (1 g).

According to the supplier, the original TiO_2 particles were smaller than 40 nm. Although AFM observations indicated somewhat larger particle diameters, the starting material clearly was nano size. Therefore, the large particles must have formed by aggregation after dilution. This should not come as a surprise. It is well known in colloid chemistry that stabilization measures need to be taken to prevent the inevitable collisions of small particles that lead to the formation of larger aggregates. The Derjaguin, Landau, Verwey, and Overbeek (DLVO) theory [23] explains that

colloidal systems may be stabilized as a result of electrostatic forces (repulsion of equally charged particles) or steric hindrance (prevents particles from getting close enough to each other for Van der Waals attraction to become dominant). As supplied, TiO_2 suspensions may owe their stability to the presence of a negative particle charge and an absence of other dissolved or particulate materials that could interact with the TiO_2 nanoparticles. This stability may have been lost on dilution as a result of loss of surface charge (dilution in Milli-Q water) or because of interactions with other materials (dilution in pond water). In either case, coagulation of nanoparticles may have led to the formation of larger particles, which subsequently settled under normal or enhanced gravitation. In the present study with natural pond water, the presence of other colloidal and dissolved materials may have resulted in very low exposure concentrations of free nanoparticles, but it also seems possible that the presence of natural organic matter in water has a stabilizing effect on nanoparticles. Hyung et al. [15] found that higher concentrations of free, multiwalled carbon nanotubes in water can exist in the presence of higher concentrations of natural organic matter. Their results can be explained as an example of steric stabilization of colloidal suspensions.

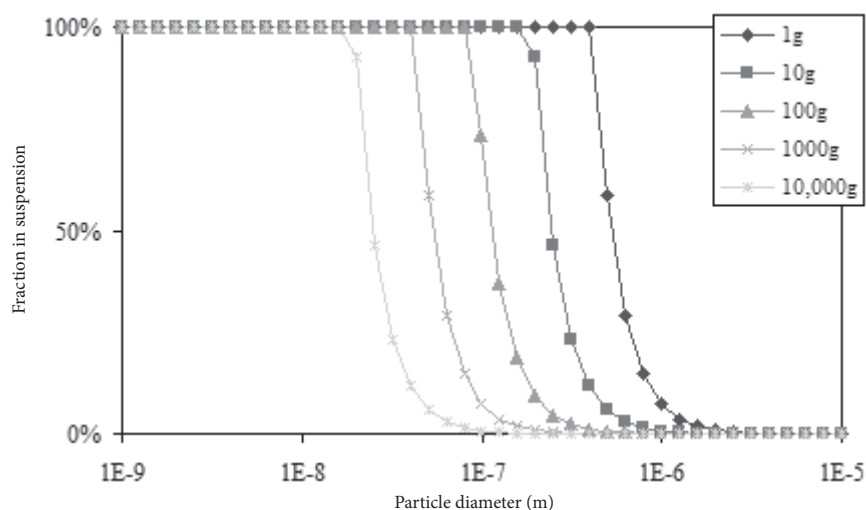


Figure 6.2 Removal of TiO_2 particles from aqueous suspensions under centrifugation, as calculated by equation S6.4 (Supporting Information). Particles smaller than approximately 20 nm are expected to remain in suspension, even under strong centrifugation (10,000 g), whereas particles larger than approximately 10mm are expected to settle even without centrifugation (1 g).

For fullerene, we were not able to prepare suspensions with concentrations of greater than 1 mg L^{-1} . After four months of stirring, the concentration of fullerene, as measured with spectrophotometry, was very low. A higher concentration was expected. Brant et al. [24] used the same method; with extended mixing with water, those authors obtained concentrations of 100 mg L^{-1} and mentioned a mean particle size of 180 nm after filtration. Brant et al. [24] also used a solvent exchange method that is widely accepted [25]. They used tetrahydrofuran to dissolve fullerene before mixing with water and, with this method, also had concentrations of 100 mg L^{-1} and mentioned a mean particle size of 160 nm after filtration. We were not able to reproduce these results.

Our observations may illustrate the general case that extensive particle interaction, both among nanoparticles and between nanoparticles and other materials in water, may be a main factor in explaining toxic effects of nanomaterials in the natural environment. In this light, our inability to observe differences in toxic effects between different particle sizes of PMMA nanoparticles should not be a surprise.

The question of whether stable colloidal suspensions should be expected in natural waters remains open. Our results suggest at least the possibility that under natural conditions, exposure concentrations of free, suspended nanoparticles may readily fall below levels at which no effects on organisms occur.

Our findings further suggest that environmental risk assessment of nanoparticles requires a nano-specific approach. In risk assessment of conventional chemical substances, dissolved concentrations in water often are predicted with models from emissions, assuming a tendency of molecules to partition among environmental phases according to thermodynamic solids-water partition coefficients. Because the behaviour of nanoparticles in water is driven largely by particle-particle interactions, concentrations of free nanoparticles in water are unlikely to be predictable by (partition) coefficients, the magnitude of which can be readily measured or even predicted from the physicochemical substance properties, such as the octanol-water partition coefficient. Instead, theoretical concepts to predict concentrations of free nanoparticles in water are to be found in classical theory of colloidal stability, possibly adapted to accommodate the much smaller sizes of nanoparticles as compared to the traditional micrometer sizes for which the DLVO theory [23] originally was derived.

A further issue to be addressed in environmental risk assessment of nanoparticles is the fate and ultimate availability of the agglomerated nanomaterials. Will the formation of larger aggregates and transport of aggregated nanomaterial to sediments lead to complete and irreversible loss of bioavailability? Would benthic organisms be able to disaggregate the larger particles in their intestines, and if so, would this lead to uptake of nanoparticles by benthic organisms? These questions remain open. Answers are needed for successful environmental risk assessment of nanoparticles.

6.5 Conclusion

In the ecotoxicity experiments, no effects were observed with an exposure to 100 mg L^{-1} of nanoparticles. The proposed reason for the (unexpected) absence of ecotoxic effects is low bio-active concentrations, caused by rapid aggregation and/or coagulation of the free nanoparticles. Dilution experiments show that formation of larger particles and settling of the larger particles under normal gravitation or centrifugation occurred to a greater extent in natural (pond) water than in ultrapure (Milli-Q) water.

Similar phenomena likely occur in natural waters. The environmental exposure modeling methods designed for conventional chemicals are expected to fail for nanoparticles. Prediction of bioactive concentrations of nanoparticles in water requires a nano-specific approach.

Acknowledgements

We thank Sylvia Speller and Joris Peters of Institute of Molecules and Materials (Radboud University Nijmegen) for performing AFM, Hans Hoogveld of The Netherlands Institute of Ecology (Nieuwersluis) for performing the flow cytometry, and Petra Krystek and Sjoerd Piso of the Laboratory for Environmental monitoring (National Institute of Public Health and the Environment) for performing the ICP-MS.

References

- [1] Dionysiou DD. 2004. Environmental applications and implications of nanotechnology and nanomaterials. *Journal of Environmental Engineering-Asce* 130:723-724.
- [2] Yuan GD. 2004. Environmental nanomaterials: Occurrence, syntheses, characterization, health effect, and potential applications. *Journal of Environmental Science and Health Part a-Toxic/Hazardous Substances & Environmental Engineering* 39:2545-2548.
- [3] Donaldson K, Stone V, Tran CL, Kreyling W, Borm PJA. 2004. Nanotoxicology. *Occupational and Environmental Medicine* 61:727-728.
- [4] Colvin VL. 2003. The potential environmental impact of engineered nanomaterials. *Nature Biotechnology* 21:1166-1170.
- [5] Wiesner MR, Lowry GV, Alvarez P, Dionysiou D, Biswas P. 2006. Assessing the risks of manufactured nanomaterials. *Environmental Science & Technology* 40:4336-4345.
- [6] Powell MC, Kanarek, M.S. 2006. Nanomaterial health effects - Part 1: Background and current knowledge. *Wisconsin Medical Journal* 115:16-20.
- [7] Oberdorster E. 2004. Manufactured nanomaterials (Fullerenes, C-60) induce oxidative stress in the brain of juvenile largemouth bass. *Environmental Health Perspectives* 112:1058-1062.
- [8] Oberdorster E. 2004. Toxicity of n-C60 fullerenes to two aquatic species: *Daphnia* and largemouth bass. *Abstracts, 227th American Chemical Society National Meeting, Anaheim, CA, March 27-April 1, IEC 21*
- [9] Hund-Rinke K, Simon M. 2006. Ecotoxic effect of photocatalytic active nanoparticles TiO₂ on algae and daphnids. *Environmental Science and Pollution Research* 13:225-232.
- [10] Shi JP, Evans DE, Khan AA, Harrison RM. 2001. Sources and concentration of nanoparticles (< 10 nm diameter) in the urban atmosphere. *Atmospheric Environment* 35:1193-1202.
- [11] Hoet P, Bruske-Hohlfeld I, Salata O. 2004. Nanoparticles - known and unknown health risks. *Journal of Nanobiotechnology* 2:12.
- [12] Borm P, Robbins D, Haubold S, Kuhlbusch T, Fissan H, Donaldson K, Schins R, Stone V, Kreyling W, Lademann J, Krutmann J, Warheit D, Oberdorster E. 2006. The potential risks of nanomaterials: a review carried out for ECETOC. *Particle and Fibre Toxicology* 3:11.
- [13] Yang L, Watts DJ. 2005. Particle surface characteristics may play an important role in phytotoxicity of alumina nanoparticles. *Toxicology Letters* 158:122-132.
- [14] Mackay CE, Johns M, Salatas JH, Bessinger B, Perri M. 2006. Stochastic probability modeling to predict the environmental stability of nanoparticles in aqueous suspension. *Integr Environ Assess Manag* 2:293-298.
- [15] Hyung H, Fortner JD, Hughes JB, Kim JH. 2007. Natural organic matter stabilizes carbon nanotubes in the aqueous phase. *Environmental Science & Technology* 41:179-184.
- [16] Powell MCK, M.S. 2006. Nanomaterial health effects - Part 2: Uncertainties and recommendations for the future. *Wisconsin Medical Journal* 105:18-23.
- [17] AZUR Environmental. 1998. *Microtox' Omni Manual*, Carlsbad, CA, USA.

- [18] Van Beusekom SAM, Admiraal, W., Sterkenburg, A., de Zwart, D. 1999. *Handleiding PAM-test*. National Institute of Public Health and the Environment, Bilthoven, The Netherlands.
- [19] van den Brandhof EJ. 2005. *Bepaling van de acute toxiciteit van oppervlaktewater concentraten op Chydorus sphaericus*. National Institute of Public Health and the Environment, Bilthoven, The Netherlands.
- [20] Schmitt H. 2005. The effects of veterinary antibiotics on soil microbial communities. PhD thesis, Utrecht University, Utrecht, The Netherlands.
- [21] Agilent Technologies. 2006. *ICP-MS: A Primer*, Santa Clara, CA, USA.
- [22] Lovern SB, Klaper R. 2006. Daphnia magna mortality when exposed to titanium dioxide and fullerene (C-60) nanoparticles. *Environmental Toxicology and Chemistry* 25:1132-1137.
- [23] Birdi KS, (ed). 2003. *Handbook of Surface and Colloid Chemistry*, 2nd ed. CRC Press, Boca Raton FL USA.
- [24] Brant J, Lecoanet H, Hotze M, Wiesner M. 2005. Comparison of electrokinetic properties of colloidal fullerenes (n-C-60) formed using two procedures. *Environmental Science & Technology* 39:6343-6351.
- [25] Deguchi S, Alargova RG, Tsujii K. 2001. Stable Dispersions of Fullerenes, C60 and C70, in Water. Preparation and Characterization. *Langmuir* 17:6013-6017.

Supporting Information

Colloidal particles in suspension move along the vertical as a result of gravitation and thermal motion. This results in a steady state in which the suspension concentration decreases exponentially from bottom to top, according to the well-known Boltzmann equation [14, 24]:

$$C_h = C_0 e^{-\frac{mgh}{kT}} \quad (\text{S6.1})$$

where C_h and C_0 (kg m^{-3}) represent the concentration of TiO_2 in suspension at a certain height h (m) and at the bottom, respectively, m (kg) is the mass of individual TiO_2 particles, g (9.8 m.s^{-2}) is the gravitational acceleration, k ($=1.38 \cdot 10^{-23} \text{ J K}^{-1}$) is the Boltzmann constant and T (K) is the temperature. The average concentration $\langle C \rangle$ in suspension follows from this by integration from the bottom ($h=0$) to the top ($h=H$):

$$\langle C \rangle = \frac{1}{H} \int_0^H C_0 e^{-\frac{mgh}{kT}} dh = \frac{C_0 kT}{mgH} \left(1 - e^{-\frac{mgH}{kT}} \right) \quad (\text{S6.2})$$

The concentration at the bottom cannot exceed the density of the solid phase C_s . If C_0 reaches that value, a deposit starts to form, so that the average concentration in suspension is limited to:

$$\langle C \rangle = C_s \frac{kT}{mgH} \left(1 - e^{-\frac{mgH}{kT}} \right) \quad (\text{S6.3})$$

This concentration $\langle C \rangle$ is smaller than that of the initially homogeneous suspension concentration C_{init} and the fraction of TiO_2 held in suspension under centrifugation F_{susp} can thus be quantified:

$$F_{susp} = \frac{\langle C \rangle}{C_{init}} = \frac{C_s}{C_{init}} \frac{kT}{mgH} \left(1 - e^{-\frac{mgH}{kT}} \right) \quad (\text{S6.4})$$

Chapter 7



Community effects of carbon nanotubes in aquatic environments



TiO₂ MWCNTs ZrO₂ TiO₂ CeO₂ MWCNTs CeO₂ SWCNTs SiO₂-Ag
SWCNTs PMMA Al₂O₃ PFOS PVP-Ag CeO₂ MWCNTs PVP-Ag SWCNTs
nano-PS C₆₀ micro-PE C₆₀ SiO₂-Ag TiO₂ C₆₀
Al₂O₃ SiO₂-Ag MWCNTs PVP-Ag CeO₂ PVP-Ag C₆₀ MWCNTs PFOS micro-PE
SiO₂-Ag PMMA PVP-Ag nano-PS C₆₀ MWCNTs PFOS micro-PE
PCBs SiO₂-Ag CeO₂ Al₂O₃ PVP-Ag nano-PS Al₂O₃ CeO₂ Al₂O₃
MWCNTs C₆₀ PCBs MWCNTs nano-PS CeO₂ ZrO₂ PVP-Ag TiO₂ PFOS
micro-PE C₆₀ Al₂O₃ CeO₂ PCBs CeO₂ SWCNTs nano-PS MWCNTs
nano-PS SWCNTs PCBs PFOS MWCNTs ZrO₂ micro-PE SiO₂-Ag PMMA
SiO₂-Ag ZrO₂ C₆₀ MWCNTs nano-PS ZrO₂ PMMA Al₂O₃ MWCNTs ZrO₂
C₆₀ PCBs SiO₂-Ag PFOS SiO₂-Ag PVP-Ag PMMA Al₂O₃ MWCNTs ZrO₂
ZrO₂ TiO₂ PCBs SiO₂-Ag MWCNTs TiO₂ PVP-Ag PCBs TiO₂ C₆₀
C₆₀ PCBs SiO₂-Ag PFOS SiO₂-Ag PVP-Ag PMMA Al₂O₃ MWCNTs ZrO₂
ZrO₂ TiO₂ C₆₀ MWCNTs PFOS TiO₂ MWCNTs ZrO₂ C₆₀ PMMA
CeO₂ MWCNTs SWCNTs ZrO₂ micro-PE SiO₂-Ag MWCNTs
micro-PE SiO₂-Ag nano-PS PFOS CeO₂ C₆₀ PFOS PMMA PVP-Ag
MWCNTs Al₂O₃ PFOS PVP-Ag SWCNTs PMMA TiO₂ CeO₂
TiO₂ MWCNTs micro-PE Al₂O₃ PFOS PVP-Ag SWCNTs PMMA nano-PS
PCBs micro-PE ZrO₂ C₆₀ PFOS PVP-Ag SWCNTs PMMA nano-PS

Published as: Velzeboer I, Kupryianchyk D, Peeters ETHM, Koelmans AA. 2011. Community effects of carbon nanotubes in aquatic sediments. *Environment International* 37:1126-1130.

Abstract

Aquatic sediments form an important sink for manufactured nanomaterials, like carbon nanotubes (CNT) and fullerenes, thus potentially causing adverse effects to the aquatic environment, especially to benthic organisms. To date, most nanoparticle effect studies used single species tests in the laboratory, which lacks ecological realism. Here, we studied the effects of multiwalled CNT (MWCNT) contaminated sediments on benthic macroinvertebrate communities. Sediment was taken from an unpolluted site, cleaned from invertebrates, mixed with increasing levels of MWCNTs (0, 0.002, 0.02, 0.2 and 2 g kg⁻¹ dry weight), transferred to trays and randomly relocated in the original unpolluted site, which now acted as a donor system for recolonization by benthic species. After three months of exposure, the trays were regained, organic (OC) and residual carbon (RC) were measured, and benthic organisms and aquatic macrophytes were identified. ANOVA revealed a significantly higher number of individuals with increasing MWCNT concentrations. The Shannon index showed no significant effect of MWCNT addition on biodiversity. Multivariate statistics applied to the complete macroinvertebrate dataset, did show effects on the community level. Principal component analysis (PCA) showed differences in taxa composition related to MWCNT levels indicating differences in sensitivity of the taxa. Redundancy analysis (RDA) revealed that MWCNT dose, presence of macrophytes, and spatial distribution explained 38.3% of the total variation in the data set, of which MWCNT dose contributed with 18.9%. Still, the net contribution of MWCNT dose was not statistically significant, indicating that negative community effects are not likely to occur at environmentally relevant future CNT concentrations in aquatic sediments.

7.1 Introduction

Understanding the safety, environmental and human health implications of nanotechnology-based products is of worldwide importance [1-4]. The production and use of manufactured nanoparticles is increasing, which makes the emission to environmental bodies probable [5]. Nanoparticles can be categorized in natural and anthropogenic particles, with the anthropogenic particles being further divided in unintentionally and intentionally produced nanoparticles [6]. Unintentionally produced nanoparticles, like atmospheric ultrafine particles (PM_{0.1}) originate from incomplete combustion of biomass and fossil fuels, such as soot and black carbon [7]. Intentionally produced nanoparticles are engineered or manufactured for a wide range of applications within many kinds of products and industries [1]. These manufactured particles can be classified as carbon-based nanoparticles, such as carbon black, polystyrene, fullerenes, single and multiwalled carbon nanotubes (MWCNTs), and inorganic nanoparticles such as titanium dioxide, zinc oxide, cerium oxide (metal oxides), colloidal silica, silver, alumina and metallic iron [5].

Nanoparticles can be transported to receiving waters through atmospheric deposition, surface run-off, open channels, wastewater treatment plants and direct input. Eventually, aquatic sediments are believed to form an important sink for nanoparticles [1, 6]. To our knowledge, no quantitative analytical methods are appropriate yet for measurements of engineered nanoparticles in environmental matrices at the low levels in which they are expected to occur in the environment [5, 6]. Consequently, concentrations of nanoparticles in the environment are estimated via model predictions. These predictions suggest low concentrations in aquatic sediments, i.e. 4×10^{-5} to 2×10^{-3} g kg⁻¹ d.w. in worst case scenarios, which however may increase if future emission scenarios are taken into account [6, 8, 9].

Amongst carbon-based nanoparticles, MWCNTs form an important group. Applications can be found in industrial sectors for materials, chemistry, medicine, life science, electronics, ICT and energy [10]. MWCNTs are also known to be formed during combustion processes, so that emission of natural soot particles may form an even larger source of MWCNTs to the environment [6, 11, 12]. CNTs without functionalizing surfactants are hydrophobic and will interact with other nanoparticles and organic matter. These interactions are known to cause stable suspensions but also aggregation followed by sedimentation [6, 13]. Consequently, exposure of carbon nanotubes to aquatic and benthic organisms is expected. Several earlier studies concerned the effects of nanoparticles on aquatic and benthic organisms [1, 5, 14, 15], but were restricted to single species tests in the laboratory. Such tests lack realism with respect to dynamic particle mixing, multiple exposure routes, aging or 'fouling' of nanoparticles, or ecological processes such as recolonization or community shifts. To our knowledge, no data on community effects or long term effects of carbon nanotubes exist, yet they are most relevant for overall risk assessments of nanoparticles. Effects of MWCNTs can be considered more relevant than those of single walled nanotubes (SWCNTs) or fullerenes, because recent reports show the emissions of the latter two particle types to be negligible compared to those of MWCNTs [16]. Because of these reasons, we studied the response of natural communities of benthic invertebrates to exposure to MWCNT contaminated sediments. Primary aim was to examine the influence of MWCNT contaminated sediment on the recolonization by benthic macroinvertebrates in a controlled and replicated field experiment. The range of MWCNT concentrations in the test was designed to cover the environmentally realistic but low concentration range predicted by several recent CNT-emission based fate and exposure models [6, 8], as well as the high but relatively unrealistic concentration range at which actual effects have been observed in invertebrate single species tests in the laboratory [6, 17-21].

7.2 Materials and methods

Community recolonization experiment

The field experiment was conducted in an uncontaminated ditch in “de Veenkampen”, an experimental field site of Wageningen University, The Netherlands (51°58′52″N, 5°37′25″E). This ditch has a width of about 2 to 3 m and a depth of about 1.5 m. It is a peaty area, mainly fed by deep groundwater and surrounded by extensive low productive grasslands. This study site has a diverse benthic macroinvertebrate community, characterized by the presence of Oligochaeta, Hirundinea, Bivalvia, Arachnida, Diptera, Gastropoda and Crustacea, which was determined prior to exposure. The upper 5 to 10 cm of the sediment was sampled from an area of 3 by 10 m in the ditch, using a 0.5 mm mesh size net, after which it was collected in 60 L buckets. The sediment was sieved using a 2 mm mesh stainless-steel screen to remove pebbles and large organic debris. Afterwards, the sediment was partly sieved with a 0.2 mm mesh copper sieve and partly with a 0.5 mm mesh copper sieve, collecting the part remained in the sieve to remove the excess water. The organic matter (OM) content was 20%, determined as loss on ignition (3h 550°C). Subsequently, the sediment was anaerobically stored at 20°C for two weeks in closed 26 L polyethylene (PE) buckets without headspace. This eliminated all macroinvertebrates, which was needed to prevent “false” colonization during the experiment. After anaerobic treatment, the sediment was homogenized and distributed evenly over five clean PE 26 L barrels. To these barrels, MWCNTs were added to obtain concentrations of 0, 0.002, 0.02, 0.2 and 2 g kg⁻¹ dry weight. This range includes levels of CNTs as anticipated from fate model predictions [6, 8, 9] as well as higher levels at which actual effects have been observed in earlier laboratory experiments with sediment exposure to benthic organisms [6, 17-21]. The MWCNTs were obtained from Cheaptubes (Brattleboro, VT, USA) and had an inner diameter of 5-10 nm, outer diameter of 20-30 nm, length of 10-30 µm and a purity of 95 wt%. Sediments with MWCNTs were thoroughly mixed for 6h using a rollerbank. After mixing, 20 open 30×20×15.5 cm polypropylene (PP) trays were filled with 5 cm of the five MWCNT-containing sediments, in order to obtain four replicates per MWCNT concentration. The trays were embedded randomly in a preselected grid in the unpolluted donor system “de Veenkampen”, where the sediment originally came from. First, the trays were carefully filled with water from the ditch, after which they were slowly placed into the donor-sediment, leaving about 5 cm of the wall of the tray emerging from the surrounding sediment surface. This was needed to prevent surrounding sediment from entering the trays. Finally, the trays were connected to wires spanning the surface of the ditch in order to prevent them from sinking too far in the sediment. At the start of the exposure, a sample from the donor system was taken with a standard dipnet (mesh size 0.5 mm) from a surface of 1 m², for determination of the community in the donor system at time zero. Exposure lasted for three months (June 2nd - September 30th, 2009). During exposure the ditch was monitored and checked for system failures. After exposure,

the trays were carefully lifted from the system. If present, macrophytes were carefully removed and collected for dry weight analysis. Sediment (30 mL) was sampled for chemical analysis and sieved in the field (mesh size 200 μm) to reduce the amount of material to be transported to the laboratory. Also three samples from the donor system were taken with a standard dipnet from a surface of 1 m^2 for determination of the community in the donor system after 3 months. A mixed sediment sample of each tray was taken to measure organic carbon (OC) and residual carbon (RC). RC is defined as the carbon content of sediment after heating at 375°C for 24 h. RC includes condensed or black carbon (BC), which has a constant background level in the ditch, as well as the dose dependent quantity of MWCNT carbon. OC and RC were measured using chemothermal oxidation (CTO-375 method) [22, 23] using a CHN analyzer (EA 1110 CHN Elemental Analyzer, CE Instruments, Milan, Italy). MWCNTs have been found to be resistant in the CTO-375 method [24], which supports its use as a proxy for MWCNT levels in aquatic sediments as long as BC related background responses are accounted for. Macroinvertebrates and macrophytes were carefully collected from the trays by rinsing the sediment with tap water using a 0.5 mm mesh sieve. Macrophytes were separated from retaining material, identified and weighed. The material retained in the sieve was preserved in 96% ethanol and stored at 4°C until identification of macro-benthos. Macroinvertebrates were selected from the sieved samples, identified to genus or family level using available keys and counted.

Data analysis

MWCNT effects on biodiversity were quantified using the Shannon diversity index, which describes the appearance as well as the homogeneity of the variance within the community:

$$H = -\sum(p_i \times \ln p_i) \quad (7.1)$$

in which H is the Shannon index, p_i is the fraction of total number of individuals of a taxon [25].

One-way ANOVA, with Tukey Post Hoc test, using SPSS (PASW Statistics 17.0, SPSS Inc., Chicago, IL, USA), was performed to test treatment effects on numbers of taxa and individuals, on the Shannon index and macrophyte density.

Furthermore, ordination techniques, were used to detect the patterns of variation in the macroinvertebrate data [26]. Prior to analysis, data were $\ln(x + 1)$ transformed. First, Principal Component Analysis (PCA), an indirect gradient analysis using information from taxa composition only, was applied to obtain an indication of the macroinvertebrate composition after 3 months of exposure to MWCNT containing sediments [27-30]. Second, Redundancy Analysis (RDA) with partitioning of the variance, a constrained linear ordination method, also called reduced rank regression, was performed to identify the variance (a) explained by all explanatory variables together, (b) for each explanatory variable without taking co-variance with

other variables into account, as well as (c) for each explanatory variable with the other variables as covariables, thus explicitly factoring out the influence of these other variables. [27-30]. The statistical significance of the percentages of explained variance was tested using the Monte Carlo permutation test [31].

The tested variables were; (a) MWCNT concentrations, (b) vegetation reported as the amount of dry weight of aquatic macrophytes present in the trays and (c) the spatial distribution of the trays in the ditch, expressed as coordinates, by numbering columns and rows in which the trays were placed. All multivariate analyses were performed with CANOCO 4.5 for Windows [26].

7.3 Results and discussion

Sediment characteristics, macroinvertebrate community and biodiversity

During exposure, no extreme weather circumstances, wind-induced resuspension or other incidents that could have interfered with the CNT level in the trays were observed. There was no visible flow and there were no signs of fresh sediment deposition. The water level fluctuated a bit but the trays stayed under the water level throughout the experiment.

In the control (0 g kg^{-1}) and highest MWCNT treatment (2 g kg^{-1}), OC contents were $26.95\% \pm 0.83$ and $22.37\% \pm 0.15$ respectively, thus reflecting some variability between the treatments. RC contents in control and highest MWCNT treatment were $1.77\% \pm 0.53$ and $2.15\% \pm 0.65$ respectively. The difference in RC content is consistent with the MWCNT amendment, but is not statistically significant because of the relatively large relative error of about 30%. This implies that this methodology may be suitable for much higher CNT concentrations, but not for the environmentally realistic concentration ranges applied in this experiment.

After three months, i.e. at the end of exposure, a total of 32 different macroinvertebrate taxa was identified in all trays together, most of them belonging to the taxonomic groups of Oligochaeta, Hirundinea, Bivalvia, Arachnida and Diptera. The donor system contained taxa from the same groups, but had a relatively larger number of taxa from Gastropoda and Crustacea than the sample trays. In the donor system a total of 30 different taxa was collected. The number of taxa per tray ranged from 3 to 13 and the number of individuals from 17 to 70 (Figure 7.1).

Comparing the number of individuals and taxa in the control trays to the data for the donor system at the end of exposure, approximately 30% of the individuals and roughly 50% of the taxa seemed to have recolonized the systems without MWCNTs. Remarkably, with increasing concentration of MWCNTs, the number of individuals and taxa also appeared to increase (Table 7.1). Differences between the MWCNT levels 0, 0.02, 0.2 and 2 g kg^{-1} were significant (One-way ANOVA with Tukey's Post Hoc test, $p < 0.05$). The 0.002 g kg^{-1} treatment differed significantly from the 0.02 g kg^{-1} treatment (Figure 7.1b).

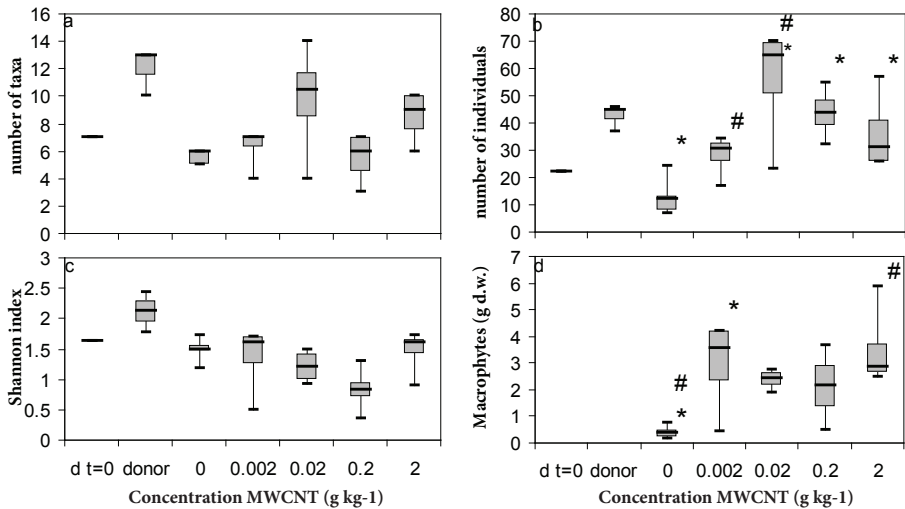


Figure 7.1 Number of taxa and individuals, Shannon index and macrophyte dry weight in the donor system at $t = 0$ ($dt=0$) and $t = 3$ months ($dt=3m$) and as a function of MWCNT concentrations. Boundaries of the box plots indicate the 25th and 75th percentile. Whiskers below and above indicate the minimum and maximum of the variables. The median is indicated with the black line. Boxes with identical associated symbol (*, #) relate to treatments that are significantly different from each other.

Shannon indices were calculated from species identities and abundance data and appeared to decrease slightly from 0 to 0.2 g kg⁻¹ MWCNT. This observation would be consistent with MWCNTs having negative effects on the community level, but the differences are too small to yield statistical rigor. Furthermore, the highest MWCNT level (2 g kg⁻¹) has the same Shannon index as the controls, indicating the MWCNT did not affect biodiversity (Table 7.1, Figure 7.1).

Table 7.1 Percentage of recolonization in the trays compared to the donor system, Shannon indices and macrophyte dry weight for each MWCNT level.

System or MWCNT treatment (g kg ⁻¹)	Recolonization		Shannon index (Eq. 7.1)	Macrophytes (g)
	Individuals (%)	Taxa (%)		
donor t = 0			1.63	
donor t = 3m			2.11	
0	31.7	46.7	1.49	0.41
0.002	68.7	54.2	1.36	2.93
0.02	136.7	79.2	1.19	2.38
0.2	107.7	45.8	0.82	2.11
2	89.7	72.9	1.47	3.51

Interestingly, macrophyte densities increased with increasing MWCNT level (Figure 7.1d). The controls, which had the lowest numbers of invertebrate individuals and taxa, had a macrophyte dry weight which was a factor 5 to 8 lower than in samples with MWCNTs. These differences in macrophyte dry weight were significant between the control (0 g kg^{-1}) and the 0.002 g kg^{-1} as well as the 2 g kg^{-1} MWCNT treatment (Figure 7.1d). Macrophyte taxa included *Chara sp.*, *Elodea nuttallii*, *Potamogeton obtusifolius*, *Glyceria sp.* and *Alisma plantago-aquatica*. *Chara sp.* occurred in all trays, *Elodea nuttallii* and *Potamogeton obtusifolius* were only found in a few trays, which contained lower numbers of macroinvertebrate taxa and individuals compared to replicates of the same MWCNT level. This difference in macrophyte composition probably contributes to the variability among replicates, which also suggests some relationship between macrophyte abundance and benthic species composition. However, the higher number of taxa and individuals in the 0.02 g kg^{-1} MWCNT level was not explained by the amount of macrophytes, because macrophyte abundance was comparable for the MWCNT levels. Consequently, other spatial differences in habitat, such as differences in flow, predation and substrate also explain small dissimilarities in species composition, even though there was not a clear relation between differences in number of taxa and individuals and spatial distribution [32].

Earlier laboratory studies showed negative effects of CNTs on growth and survival of benthic invertebrates [17-21] and therefore we expected a decrease in numbers of individuals and species with increasing MWCNT concentration. The fact that we now observe the opposite trend shows how results from field studies that cover ecologically realistic recolonization fluxes may deviate from results obtained in the laboratory.

Multivariate analysis of community data

The results of the PCA showed that 50.9% of the variation in the dataset was covered by the first 4 components. A biplot of the first two components of this PCA, explaining 30.4% of total variation summarizes the separation of taxa and samples (Figure 7.2). In Figure 7.2, samples and taxa that behave similarly are grouped together, whereas coincidence of taxa with samples relates to relatively higher abundances of these taxa in these samples. The strength of the correlations is indicated by the lengths of the taxa arrows. Consequently, *Corduliidae*, juvenile *Coleoptera*, *Corophidae*, *Glossiphonia* and *Haliplidae* appeared to be more abundant at the highest level of 2 g kg^{-1} MWCNTs (Figure 7.2, upper circle), whereas *Chaoboridae*, *Notonectidae*, *Aeschnidae*, *Hygrobiidae* and *Asellidae* were relatively abundant at lower MWCNT levels (lower left circle). Also *Lymnaea*, *Orthocladinae*, *Hemiclepsis*, *Valvata*, *Physa* and *Planorbidae* were relatively abundant at lower MWCNT levels (lower right circle).

species composition, because of small dissimilarities between the trays. Trays differed in their exact depth in the ditch. There also was a minor flow in the ditch, which may have been higher in the middle, whereas temperature and O₂ concentrations also may have been different to some extent. These differences may have contributed to differences in the community composition.

Table 7.2 Explained variation of species composition for MWCNT addition, macrophytes and spatial distribution with significance level for RDA.

Environment data	Co-variable data	Variation (%)	p-value
MWCNTs		25.2	0.002**
macrophytes		9.7	0.004**
spatial distr.		11.7	0.132
MWCNTs macrophytes		31.2	0.006**
MWCNTs spatial distr.		34.4	0.028*
macrophytes spatial distr.		19.4	0.022*
spatial distr. MWCNTs macrophytes		38.3	0.088*
MWCNTs	macrophytes	21.5	0.122
MWCNTs	spatial distr.	22.6	0.072*
macrophytes	MWCNTs	6.0	0.180
macrophytes	spatial distr.	7.7	0.016*
spatial distr.	MWCNTs	9.2	0.496
spatial distr.	macrophytes	9.7	0.384
MWCNTs spatial distr.	macrophytes	28.5	0.496
MWCNTs macrophytes	spatial distr.	26.5	0.180
macrophytes spatial distr.	MWCNTs	13.0	0.646
MWCNTs	spatial distr. macrophytes	18.9	0.544
macrophytes	spatial distr. MWCNTs	3.9	0.696
spatial distr.	MWCNTs macrophytes	7.1	0.888

** significant at $p < 0.05$

* significant at $0.05 < p < 0.1$

The explained percentages and their significance levels in RDA also reflect co-variation among variables. After excluding this effect, the percentages of explained variance remain considerable but the statistical significance levels were less (Table

7.2). For instance, when factoring out macrophytes and spatial distribution, 18.9% of the variation was still explained by the presence of MWCNTs, but this percentage was no longer statistically significant ($p = 0.544$, Table 7.2). This implies that effects of MWCNTs cannot be unambiguously identified from our experiments because of variability and co-variation with other environmental and ecological factors, in this case macrophyte biomass and spatial variability. As stated above, the known variables explained 38.3 %, which implies that 61.7% of the variation is explained from variables that were not or partly monitored in this work. Habitat characteristics, water (O_2 content, conductivity, pH, DOC) and sediment quality, sediment composition (grain size, OC and RC content), pollutants, temperature, depth, and macrophytes but also biological factors like competition, predation and food quantity and quality are known to contribute to the composition of aquatic macroinvertebrate communities [29], but these were beyond the scope of this work.

7.4 Conclusion

With increasing MWCNT levels in aquatic sediment, numbers of individuals and taxa increased, whereas loss of biodiversity was not indicated by the Shannon index. Thus, based on our data, no adverse effects of MWCNTs could be detected up to a very high level of 2 g MWCNTs per kg of sediment. Multivariate analysis of community shifts revealed some clear and statistically significant trends, and identified species that were more sensitive as well as species groups that were less sensitive to the factors that explained the community changes. The community responses reflected effects of multiple stressors or actors, which in this case were MWCNT levels, growth and presence of macrophytes and factors relating to the spatial distribution of the trays. Although the contribution of MWCNTs could be separated using multivariate techniques it was not statistically significant and therefore the multivariate analyses could not detect an effect of MWCNT dose on the community level. Because anticipated MWCNT concentrations as mentioned in the literature are much lower than the lowest concentrations used in this work, we conclude that community effects are not likely to occur at environmental relevant future MWCNT loadings in aquatic sediments, because of either negligible effects or sufficient recolonization potential of benthic communities.

Acknowledgements

We would like to thank Erik Reichman and John Beijer for their help and advice with sediment sampling, the placement and retrieving of the trays as well as their assistance and knowledge during species determination. We thank Frits Gillissen for his help with the OC and RC measurements.

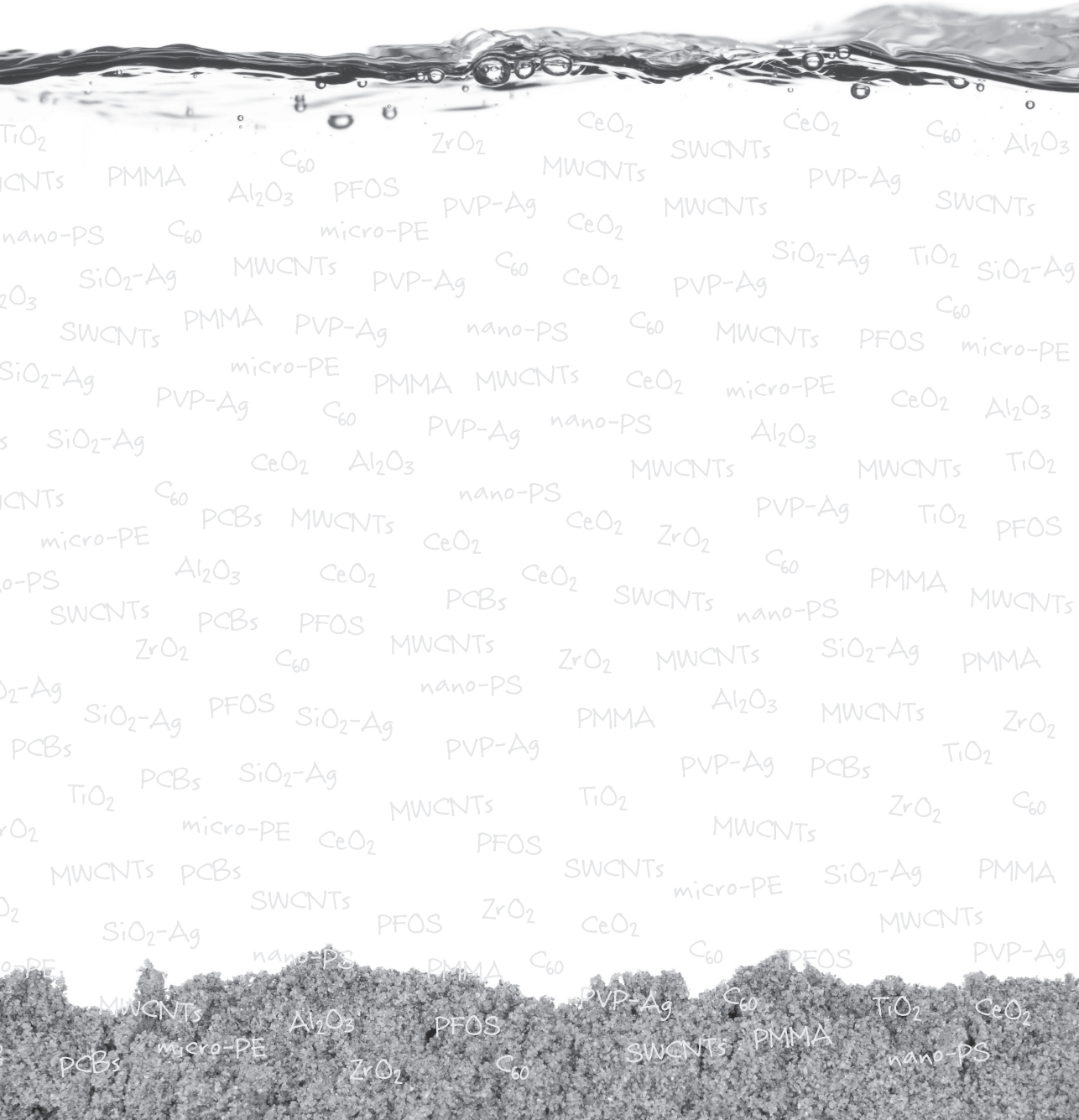
References

- [1] Klaine SJ, Alvarez PJJ, Batley GE, Fernandes TF, Handy RD, Lyon DY, Mahendra S, McLaughlin MJ, Lead JR. 2008. Nanomaterials in the environment: Behavior, fate, bioavailability, and effects. *Environmental Toxicology and Chemistry* 27:1825-1851.
- [2] Moore MN. 2006. Do nanoparticles present ecotoxicological risks for the health of the aquatic environment? *Environment International* 32:967-976.
- [3] Velzeboer I, Hendriks AJ, Ragas AMJ, Van de Meent D. 2008. Aquatic ecotoxicity tests of some nanomaterials. *Environmental Toxicology and Chemistry* 27:1942-1947.
- [4] Wiesner MR, Lowry GV, Alvarez P, Dionysiou D, Biswas P. 2006. Assessing the risks of manufactured nanomaterials. *Environmental Science & Technology* 40:4336-4345.
- [5] Nowack B, Bucheli TD. 2007. Occurrence, behavior and effects of nanoparticles in the environment. *Environmental Pollution* 150:5-22.
- [6] Koelmans AA, Nowack B, Wiesner MR. 2009. Comparison of manufactured and black carbon nanoparticle concentrations in aquatic sediments. *Environmental Pollution* 157:1110-1116.
- [7] Koelmans AA, Jonker MTO, Cornelissen G, Bucheli TD, Van Noort PCM, Gustafsson O. 2006. Black carbon: The reverse of its dark side. *Chemosphere* 63:365-377.
- [8] Gottschalk F, Sonderer T, Scholz RW, Nowack B. 2009. Modeled Environmental Concentrations of Engineered Nanomaterials (TiO₂, ZnO, Ag, CNT, Fullerenes) for Different Regions. *Environmental Science & Technology* 43:9216-9222.
- [9] Mueller NC, Nowack B. 2008. Exposure modeling of engineered nanoparticles in the environment. *Environmental Science & Technology* 42:4447-4453.
- [10] Köhler AR, Som C, Helland A, Gottschalk F. 2008. Studying the potential release of carbon nanotubes throughout the application life cycle. *Journal of Cleaner Production* 16:927-937.
- [11] Murr L, Garza K, Soto K, Carrasco A, Powell T, Ramirez D, Guerrero P, Lopez D, Venzor J. 2005. Cytotoxicity Assessment of Some Carbon Nanotubes and Related Carbon Nanoparticle Aggregates and the Implications for Anthropogenic Carbon Nanotube Aggregates in the Environment. *International Journal of Environmental Research and Public Health* 2:31-42.
- [12] Murr LE, Bang JJ, Esquivel EV, Guerrero PA, Lopez A. 2004. Carbon nanotubes, nanocrystal forms, and complex nanoparticle aggregates in common fuel-gas combustion sources and the ambient air. *Journal of Nanoparticle Research* 6:241-251.
- [13] Hyung H, Fortner JD, Hughes JB, Kim JH. 2007. Natural organic matter stabilizes carbon nanotubes in the aqueous phase. *Environmental Science & Technology* 41:179-184.
- [14] Farre M, Gajda-Schrantz K, Kantiani L, Barcelo D. 2009. Ecotoxicity and analysis of nanomaterials in the aquatic environment. *Analytical and Bioanalytical Chemistry* 393:81-95.
- [15] Handy RD, von der Kammer F, Lead JR, Hasselov M, Owen R, Crane M. 2008. The ecotoxicology and chemistry of manufactured nanoparticles. *Ecotoxicology* 17:287-314.

- [16] Engineering TRSTRAo. 2004. Nanoscience and nanotechnologies: opportunities and uncertainties. The Royal Society & The Royal Academy of Engineering, London.
- [17] Kennedy AJ, Hull MS, Steevens JA, Dontsova KM, Chappell MA, Gunter JC, Weiss Jr. CA. 2008. Factors influencing the partitioning and toxicity of nanotubes in the aquatic environment. *Environmental Toxicology and Chemistry*:1932–1941
- [18] Klaper R, Crago J, Barr J, Arndt D, Setyowati K, Chen J. 2009. Toxicity biomarker expression in daphnids exposed to manufactured nanoparticles: Changes in toxicity with functionalization. *Environmental Pollution* 157:1152-1156.
- [19] Liu XY, Vinson D, Abt D, Hurt RH, Rand DM. 2009. Differential Toxicity of Carbon Nanomaterials in Drosophila: Larval Dietary Uptake Is Benign, but Adult Exposure Causes Locomotor Impairment and Mortality. *Environmental Science & Technology* 43:6357-6363.
- [20] Oberdorster E, Zhu SQ, Blickley TM, McClellan-Green P, Haasch ML. 2006. Ecotoxicology of carbon-based engineered nanoparticles: Effects of fullerene (C-60) on aquatic organisms. *Carbon* 44:1112-1120.
- [21] Zhu XS, Zhu L, Chen YS, Tian SY. 2009. Acute toxicities of six manufactured nanomaterial suspensions to *Daphnia magna*. *Journal of Nanoparticle Research* 11:67-75.
- [22] Gustafsson O, Haghseta F, Chan C, MacFarlane J, Gschwend PM. 1997. Quantification of the dilute sedimentary soot phase: Implications for PAH speciation and bioavailability. *Environmental Science & Technology* 31:203-209.
- [23] Jonker MTO, Koelmans AA. 2002. Sorption of polycyclic aromatic hydrocarbons and polychlorinated biphenyls to soot and soot-like materials in the aqueous environment mechanistic considerations. *Environmental Science & Technology* 36:3725-3734.
- [24] Sobek A, Bucheli TD. 2009. Testing the resistance of single- and multi-walled carbon nanotubes to chemothermal oxidation used to isolate soots from environmental samples. *Environmental Pollution* 157:1065-1071.
- [25] Magurran AE. 1988. *Ecological diversity and its measurement*. University Press, Cambridge, U.K.
- [26] Ter Braak CJF, Smilauer, P. 2002. *CANOCO reference manual and CanoDraw for Windows user's guide: software for canonical community ordination (version 4.5)*. Ithaca Microcomputer Power, New York, USA.
- [27] Peeters ETHM, Dewitte A, Koelmans AA, van der Velden JA, den Besten PJ. 2001. Evaluation of bioassays versus contaminant concentrations in explaining the macroinvertebrate community structure in the Rhine-Meuse delta, the Netherlands. *Environmental Toxicology and Chemistry* 20:2883-2891.
- [28] Peeters ETHM, Gardeniers JJP, Koelmans AA. 2000. Contribution of trace metals in structuring in situ macroinvertebrate community composition along a salinity gradient. *Environmental Toxicology and Chemistry* 19:1002-1010.
- [29] Peeters ETHM, Gylstra R, Vos JH. 2004. Benthic macroinvertebrate community structure in relation to food and environmental variables. *Hydrobiologia* 519:103-115.
- [30] van Griethuysen C, van Baren J, Peeters ETHM, Koelmans AA. 2004. Trace metal availability and effects on benthic community structure in floodplain lakes. *Environmental Toxicology and Chemistry* 23:668-681.

- [31] Ter Braak CJF. 1990. *Update notes: CANOCO version 3.1*. Agricultural Mathematics Group, Wageningen, The Netherlands.
- [32] Lillie RA, Budd J. 1992. Habitat Architecture of *Myriophyllum-Spicatum* L as an Index to Habitat Quality for Fish and Macroinvertebrates. *Journal of Freshwater Ecology* 7:113-125.

Chapter 8



Multiwalled carbon nanotubes at environmentally relevant concentrations affect the composition of benthic communities



TiO₂ MWCNTs ZrO₂ TiO₂ CeO₂ MWCNTs CeO₂ SWCNTs SiO₂-Ag
SWCNTs PMMA Al₂O₃ PFOS PVP-Ag CeO₂ MWCNTs PVP-Ag SWCNTs
nano-PS C₆₀ micro-PE C₆₀ SiO₂-Ag TiO₂ C₆₀
Al₂O₃ SiO₂-Ag MWCNTs PVP-Ag CeO₂ PVP-Ag C₆₀ MWCNTs PFOS micro-PE
SiO₂-Ag PMMA PVP-Ag nano-PS C₆₀ MWCNTs PFOS micro-PE
PCBs SiO₂-Ag CeO₂ Al₂O₃ PVP-Ag nano-PS Al₂O₃ CeO₂ Al₂O₃
MWCNTs C₆₀ nano-PS MWCNTs CeO₂ micro-PE CeO₂ Al₂O₃ MWCNTs
micro-PE PCBs MWCNTs CeO₂ CeO₂ ZrO₂ PVP-Ag TiO₂ PFOS
nano-PS Al₂O₃ CeO₂ PCBs CeO₂ SWCNTs C₆₀ PMMA MWCNTs
SiO₂-Ag SWCNTs PCBs PFOS MWCNTs nano-PS SiO₂-Ag PMMA
SiO₂-Ag ZrO₂ C₆₀ MWCNTs ZrO₂ micro-PE SiO₂-Ag PMMA
C₆₀ PCBs SiO₂-Ag PFOS SiO₂-Ag nano-PS PMMA Al₂O₃ MWCNTs ZrO₂
ZrO₂ TiO₂ PCBs SiO₂-Ag PVP-Ag PMMA Al₂O₃ MWCNTs ZrO₂ C₆₀
TiO₂ MWCNTs TiO₂ ZrO₂ C₆₀ PMMA
CeO₂ MWCNTs SWCNTs ZrO₂ micro-PE SiO₂-Ag MWCNTs
micro-PE SiO₂-Ag nano-PS PFOS CeO₂ C₆₀ PFOS PMMA PVP-Ag
MWCNTs Al₂O₃ PFOS PVP-Ag SWCNTs PMMA TiO₂ CeO₂
TiO₂ MWCNTs micro-PE Al₂O₃ PFOS PVP-Ag SWCNTs PMMA nano-PS
PCBs micro-PE ZrO₂ C₆₀ nano-PS

Published as: Velzeboer I, Peeters E, Koelmans AA. 2013. Multiwalled Carbon Nanotubes at Environmentally Relevant Concentrations Affect the Composition of Benthic Communities. *Environmental Science & Technology* 47:7475-7482.

Abstract

To date, chronic effect studies with manufactured nanomaterials under field conditions are scarce. Here, we report *in situ* effects of 0, 0.002, 0.02, 0.2 and 2 g kg⁻¹ multiwalled carbon nanotubes (MWCNTs) in sediment on the benthic community composition after 15 months of exposure. Effects observed after 15 months were compared to those observed after 3 months and to community effects of another carbonaceous material (activated carbon; AC), which was simultaneously tested in a parallel study. Redundancy analysis with variance partitioning revealed a total explained variance of 51.7% of the variation in community composition after 15 months, of which MWCNT dose explained a statistically significant 9.9%. By stepwise excluding the highest MWCNT concentrations in the statistical analyses, MWCNT effects were shown to be statistically significant already at the lowest dose investigated, which can be considered environmentally relevant. We conclude that despite prolonged aging, encapsulation and burial, MWCNTs can affect the structure of natural benthic communities in the field. This effect was similar to that of AC observed in a parallel experiment, which however was applied at a fifty times higher maximum dose. This suggests that the benthic community was more sensitive to MWCNTs than to the bulk carbon material AC.

8.1 Introduction

In the last years, there has been an increase in efforts to assess the fate and effects of engineered nanoparticles (ENPs) in the environment [1, 2]. These efforts have largely focused on nanoparticles in water but have also increasingly included aquatic sediments, which are argued to be an important sink for nanoparticles [3-6]. For traditional pollutants, effect assessment has evolved from single species standard toxicity testing on laboratory scale to chronic and *in situ* effect studies, including endpoints on the population and community level [7]. For ENPs, however, assessment of *in situ* effects still is in its infancy. Most ENP ecotoxicity studies focus on the development of single species laboratory tests and use ENP doses far above environmentally relevant concentrations [2-4, 8-10]. Such tests are crucial to derive dose-response relationships in the framework of hazard assessment, and to identify mechanisms of toxicity on the species level [2]. However, they are less realistic with respect to multiple exposure routes, dynamic particle mixing, effects of fouling and aging of ENPs, or ecological processes on the community level like competition, predation, reproduction or recolonization. Alterations of ENPs on the particle scale depend on the exposure pathway and environmental history of the particles in the field and are likely to alter their ultimate behaviour and toxicity [11]. Timescales for the expression of ENP toxicity thus may exceed those of standard laboratory tests and may include species-specific sub-lethal or behavioural endpoints, which may only become visible in long

term multi-generation community assessments [12]. Consequently, assessment of *in situ* effects is urgently needed because laboratory studies may be expected to be poor predictors of effects under field conditions [1]. This may be true especially for ENPs for the reasons stated, but also because exposure assessment in current ENP toxicity tests is much less well controlled than for traditional chemicals [2].

The aim of the present study was to assess long-term macroinvertebrate community effects of multiwalled carbon nanotubes (MWCNTs) in sediment, including doses that can be considered environmentally relevant. MWCNTs constitute an important category of the carbon-based nanoparticles, used in all kinds of products [13], and suggested as a sorbent for the remediation treatment of contaminated sediments or waste waters [13-15]. Like all carbon nanotubes, MWCNTs are mostly hydrophobic and have been shown to aggregate with organic matter, other nanoparticles or suspended solids in aquatic systems [13], after which they are rapidly removed from the water column by sedimentation [5, 16, 17]. Consequently, exposure of benthic organisms to MWCNTs is plausible. Whereas previous work addressed community effects after relatively short exposure times of 3 months [18], the present study focussed on the influence of MWCNT-contaminated sediment on the recolonization of benthic communities in a controlled and replicated field experiment that lasted 15 months. MWCNT treatment effects after 15 months were also quantitatively compared to community composition after 3 months. Furthermore, these MWCNT effects were compared to community effects caused by another carbonaceous material (activated carbon; AC) which was applied simultaneously in parallel systems in the framework of another study [19]. By combining the current data on 15 month exposure to MWCNTs with those of 3 month exposure and those of the AC treatments, the effects of exposure time and carbon type could be assessed, in addition to MWCNT effects alone.

8.2 Materials and methods

Community experiment

The recolonization field experiment followed previously published procedures [18, 19]. Briefly, the experiment consisted of collecting sediment from the experimental site, elimination of invertebrates from the sediments, thorough mixing of MWCNTs into the sediments, transferring the MWCNT-amended sediments into trays, placing the trays with treated sediment back into the original site and monitoring the trays for colonization of species originating from the surrounding (continuous) donor system. The field experiment was performed in an uncontaminated ditch (2-3 m width, 1.5 m depth) at the “Veenkampen”, which is an experimental field site of Wageningen University in the Netherlands (51°58'52"N, 5°37'25"E). Organic contaminants, total organic carbon (TOC) and native black carbon (BC) concentrations in the sediment were measured in the framework of an earlier study,[19] and are provided as Supporting Information (Table S8.1). Additionally, organic matter (OM) content was determined

as loss on ignition (3 h, 550°C) and was 20% (SD 0.24). Prior to exposure, the benthic macroinvertebrate community of the study site was investigated and contained mostly Oligochaeta, Hirundinea, Gastropoda, Bivalvia, Arachnida, Crustacea, and Insecta.

In May 2009, the upper 5 to 10 cm of the sediment in an area of 3 by 10 m was sampled using a 0.5 mm mesh size net. The sediment was sieved with a 2 mm mesh stainless steel screen to remove pebbles and large organic debris. Macroinvertebrates were eliminated from the sediment by creating anoxic conditions to prevent false colonization during the experiment. This was done by storing the sediment for 2 weeks at 20°C in closed 26 L polyethylene barrels without headspace. Powdered MWCNTs with an inner diameter of 5-10 nm, outer diameter of 20-30 nm, length of 10-30 µm and a purity of 95 wt.% were obtained from Cheaptubes (Brattleboro VT, USA). Details on metal concentrations and on MWCNT characterisation by transmission electron microscopy (TEM images) are provided as Supporting Information (Table S8.2 and Figure S8.1). Sediment concentrations of MWCNT associated metals were far below toxicity thresholds and thus were too low to cause effects on the community (see Table S8.2). The MWCNTs were added to the sediment as a powder and thoroughly mixed on a roller bank for 6 hours to obtain final concentrations of 0, 0.002, 0.02, 0.2 and 2 g kg⁻¹ dry weight as described in Velzeboer et al. [18]. This range covers low but environmentally realistic concentrations anticipated from fate model predictions [5, 20, 21], as well as higher levels at which actual effects have been observed in invertebrate single species laboratory tests [5, 13, 22-27]. Open polypropylene trays (30×15.5×20 cm) were filled with 2 L MWCNT treated sediment each, to obtain 4 replicates per MWCNT concentration and 5 replicates for the control. The trays were embedded randomly in a preselected grid in the unpolluted donor system where the sediment originally came from. The trays were carefully filled with water from the ditch before inserting them 15 cm into the donor sediment. The top of the tray walls emerged 5 cm above the sediment level to prevent surrounding sediment from entering the trays. Previous work has shown that the tray walls did not prevent recolonization for any of the species originally present [18, 19]. To prevent the trays from sinking too far in the sediment, they were connected to wires spanning the surface of the ditch. Exposure lasted for 15 months (June 2009 till October 2010), after which the trays were carefully retrieved. Similarly, samples had been taken after 3 months for a short term MWCNT community effect study in the same system [18]. After retrieval, representative sediment subsamples (30 mL) were taken from the trays, combined per treatment and analysed for organic carbon (OC) and residual carbon (RC). OC and RC were measured by chemothermal oxidation (CTO-375 method) [28, 29] using a CHN analyser (EA 110 CHN Elemental Analyser, CE Instruments, Milan, Italy). To improve comparability of the 3 months and 15 months OC and RC data, original samples taken after 3 months and preserved by cooling, were reanalysed for OC and RC.

Macroinvertebrates and macrophytes were collected from the trays using a 0.5 mm mesh sieve and rinsing the sediment with tap water. Macrophytes were identified

and dry weight was measured. Macroinvertebrates were preserved in 80% ethanol and stored at 4°C until identification to genus or family level using available keys [30-32].

At time zero and after 15 months, 0.3 m² samples from the donor system outside the trays were taken with a standard dipnet (mesh size 0.5 mm) for determination of the community composition. To eliminate any chance of cross-contamination with the treated trays, the donor system samples were taken at a safe distance of at least 10 m from the MWCNT-treated trays.

Data analysis

Data analysis followed previously published procedures [18, 19] and focused on (a) long term MWCNT effects (15 months of exposure), (b) the effect of recolonization time, i.e. differences between 0, 3 and 15 months post treatment, and (c) differences between MWCNT and AC community effects. Data for 3 month exposure [18] were reanalysed and original data for 3 and 15 months of exposure to AC were kindly provided by Kupryianchyk et al. [19]. Previous 3 month MWCNT and AC data [18, 19] and current 15 month MWCNT data were obtained from simultaneous exposures in the same donor system, and therefore are directly comparable. Effects of MWCNTs on the benthic community were quantified using univariate as well as multivariate community measures. Univariate endpoints were number of individuals, number of taxa and the Shannon diversity index (H), describing the appearance as well as the homogeneity of the variance within the community:

$$H = - \sum_{i=1}^n (p_i \ln p_i) \quad (8.1)$$

where p_i is the fraction of the total number of individuals of taxon i and n is the number of taxa in the community [33]. Normality of the data was tested using the Shapiro-Wilk test. Statistical significance of effects was tested using one-way ANOVA with Tukey's Post Hoc test. To test the differences of the univariate endpoints between 3 and 15 months of exposure, an independent t test was used for each treatment. All analyses were performed using SPSS (IBM SPSS Statistics 19.0, IBM, Amonk, NY, USA) with $p < 0.05$ as criterion for significance.

Multivariate analysis included redundancy analysis (RDA) with partitioning of the variance to detect patterns and origins of variation in the macroinvertebrate data [19, 34-38]. Prior to multivariate analysis, the data were $\log(\text{abundance} + 1)$ transformed. First, RDA was performed to quantify the variance explained by the explanatory variables MWCNT concentration, duration of exposure, macrophyte biomass and spatial distribution in the ditch together. Spatial distribution was expressed as coordinates, by numbering columns and rows in which the trays are placed. Then, the explanatory power and significance of each variable was determined through a series of single constrained RDAs [34-37], followed by Monte Carlo permutation tests with 499 permutations, for testing statistical significance [39]. These analyses provide

percentages of variances explained by each of the explanatory variables and the significance level for each of the percentages. Furthermore, the percentage of variance that remains unexplained was calculated. The multivariate analyses were performed with CANOCO 4.5 for Windows [40].

8.3 Results and discussion

System characteristics

During exposure there was no visible flow in the ditch. The water level was regulated, so the trays maintained under water throughout the experiment. There were no extreme weather conditions, i.e. wind-induced resuspension or other incidents that could have interfered with the MWCNT level in the trays. OC after 3 and 15 months of exposure varied slightly among treatments; from 7.8 ± 2.6 to $10.8 \pm 2.8\%$ d.w. and from 6.4 ± 1.4 to $9.4 \pm 1.9\%$ d.w. respectively (Figure 8.1a), thus showing some random variability between the treatments as well as between time points. Similarly, RC content in the trays ranged from 0.41 ± 0.02 to $0.61 \pm 0.15\%$ d.w. after 3 months of exposure, and from 0.21 ± 0.01 to $0.39 \pm 0.04\%$ d.w., after 15 months of exposure (Figure 8.1b). Note that the presented errors relate to analytical error of the OC and RC determinations on the mixed samples, not to variation among replicate systems in the field. The observed RC percentages may be explained from the presence of natural kerogens or natural BC [41]. Theoretically, MWCNTs may also contribute to RC because carbon nanotubes have been reported to partly contribute to RC as measured by chemothermal oxidation [42]. The highest nominal MWCNT dose of 0.2% comes close to the measured 0.24% RC after 15 months (Figure 8.1b). However, the MWCNTs cannot explain the higher RC percentage at the much lower MWCNT doses, which therefore have to relate to background natural kerogens or BC. The same background kerogens and/or BC concentrations would also occur in the 0.2% MWCNT dose. Therefore, it is unlikely that MWCNTs contributed substantially to RC in any of the treatments.

Overall, the average RC content per treatment decreased in time. The observed differences are not to be considered large, given the natural temporal variability of sediment composition. We have no conclusive explanation for the decrease, but this may relate to local inhomogeneities in the sediment or local dilution with fresh organic matter. A similar dilution after 15 months was observed simultaneously for AC at the same study site [19], which may imply a common mechanism.

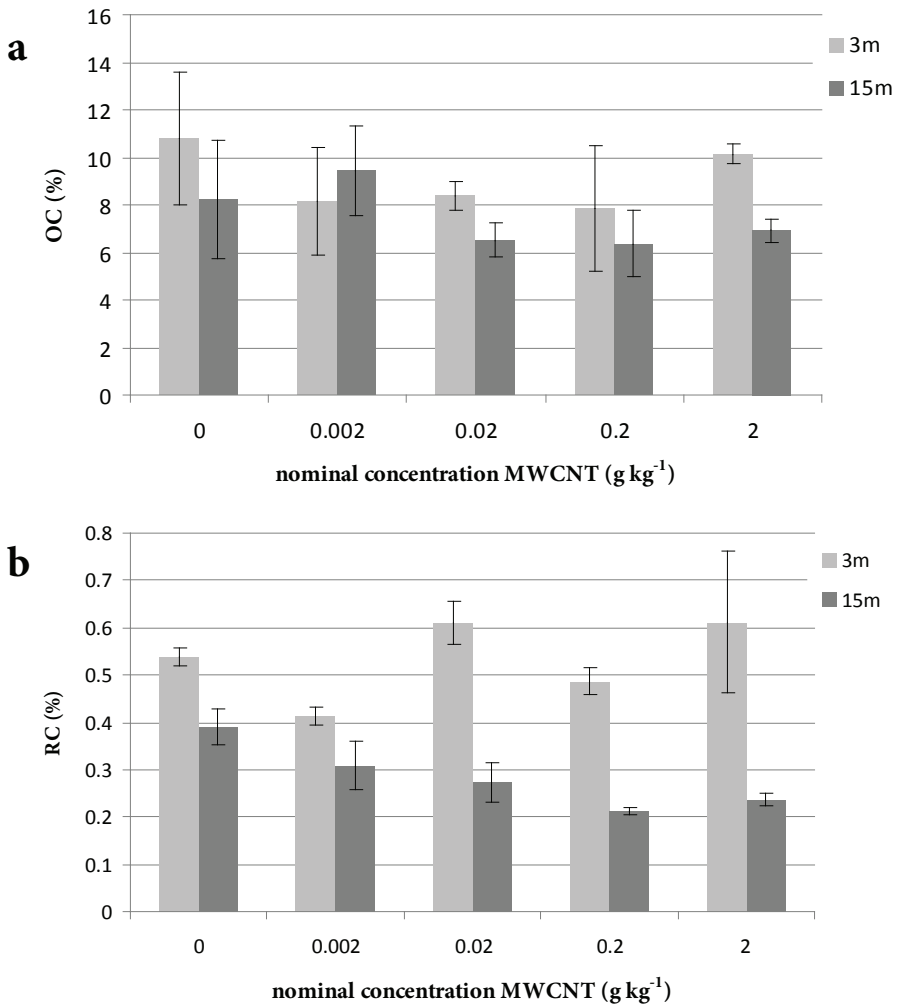


Figure 8.1 Organic carbon (OC) (a) and residual carbon (RC) (b), measured with chemothermal oxidation (CTO375) in sediment samples after 3 months (white bars) and 15 months (black bars) of exposure. SD's ($n=3$) do not relate to variability among replicates in the field, but to analytical variability among repeated measures on mixed samples per treatment.

Univariate analysis of community effects

After 15 months, approximately all taxa returned in their original abundance in the control trays (Table S8.4, Table S8.5), which shows that 15 months is long enough for this benthic community to recover. Our previously published data after 3 months, showed that only 30% of the individuals and 50% of the taxa had returned in the control trays [18]. This indicates that in 15 months, full recovery of the community

in terms of individuals and taxa was achieved. We explain the difference between the time points from the way natural recolonization occurs. After 3 months, recolonization probably was dominated by active or passive migration of individuals from the donor system to the trays, whereas after 15 months not only migration but also reproduction contributed to the observed community composition [43].

After 15 months a total of 26 different taxa was identified, ranging from 5 to 12 taxa per tray (Figure S8.2). This is comparable to the previous results for 3 months with 32 taxa ranging from 3 to 14 taxa per tray [18]. After 15 months, no effect of the MWCNT treatment on the number of taxa was detected (one-way ANOVA, $F(4,16) = 1.341$, $p = 0.298$; Figure S8.2), a lack of effect also observed in the data after 3 months (one-way ANOVA, $F(4,16) = 2.914$, $p = 0.055$ [18]). The number of taxa increased between the 3 and 15 month exposure period for the control and the lowest dose of 0.002 g kg^{-1} MWCNTs (independent t -test; 0 g kg^{-1} : $t = -4.417$, $p = 0.002$; 0.002 g kg^{-1} : $t = -5.058$, $p = 0.002$).

The number of individuals was $638\text{--}5236$ per m^2 after 15 months, compared to a much lower $154\text{--}1540$ per m^2 after 3 months (Figure S8.3). Therefore, total abundance increased between 3 and 15 month exposure, which was statistically significant for 3 levels of MWCNTs (independent t -test; 0 g kg^{-1} : $t = -4.746$, $p = 0.010$; 0.002 g kg^{-1} : $t = -3.545$, $p = 0.012$; 2 g kg^{-1} : $t = -2.443$, $p = 0.050$). After 3 months, the number of individuals increased with increasing MWCNT dose (one-way ANOVA, $F(4,16) = 6.737$, $p = 0.002$) [18], but this was not the case after 15 months (one-way ANOVA, $F(4,16) = 0.951$, $p = 0.461$). This may be explained by assuming that after 15 months a new stable situation was reached, whereas after 3 months the systems were not fully recolonized, which may cause larger differences between the systems.

Biodiversity in the trays as quantified with the Shannon index increased slightly in time from on average 1.28 ± 0.42 (3 months) [18] to 1.58 ± 0.20 (15 months) (Figure S8.4). For both time points, differences among MWCNT treatments were not statistically different (3 months: one-way ANOVA, $F(4,16) = 2.204$, $p = 0.115$ [18]; 15 months: one-way ANOVA, $F(4,16) = 1.035$, $p = 0.420$). The Shannon indices between the time points increased significantly only for the 0.2 g kg^{-1} MWCNT level (independent t -test; $t = -3.686$, $p = 0.010$).

Most abundant taxa in the 15 month systems were Erpobdella, Chironomidae, Lumbriculidae and Sphaeriidae. They were also the most abundant taxa in the 3 month systems, except for Chironomidae. In general, these species are also recognized to be less sensitive for pollution [30, 34]. The differences in absolute abundance among the MWCNT treatments were not statistically significant for these dominant species after 3 nor after 15 months of exposure (one-way ANOVA), except for Sphaeriidae abundance, which increased with MWCNT concentration after 3 months (one-way ANOVA, $F(4,16) = 7.287$, $p = 0.020$). For Erpobdella, the higher abundance after 15 months compared to the 3 month exposure was statistically significant for the 0 and 2 g kg^{-1} MWCNT levels (independent t -test; 0 g kg^{-1} : $t = -3.859$, $p = 0.005$; 2 g kg^{-1} : $t = -2.988$, $p = 0.024$). For Chironomidae, the increase of the absolute abundance

was shown to be statistically significant for all MWCNT treatments after 15 months, compared to 3 months. The abundance of Lumbriculidae was higher after 15 than after 3 months exposure, which was statistically significant for the 0 and 0.2 g kg⁻¹ MWCNT concentrations (independent *t*-test; 0 g kg⁻¹: $t = -2.806$, $p = 0.023$; 0.2 g kg⁻¹: $t = -3.693$, $p = 0.010$). Lumbriculidae thus developed over time, which contrasts to results from simultaneously exposed parallel trays amended with up to 10% AC, where the abundance of this taxon decreased [19]. The difference is probably explained by the much higher AC dose used. For Sphaeriidae only the 0.2 g kg⁻¹ MWCNT concentration was significantly lower after 15 months compared to the 3 months exposure (independent *t*-test; 0.2 g kg⁻¹: $t = 2.691$, $p = 0.036$). In contrast to the other dominant species, the abundance of Sphaeriidae decreased in time. This could be a direct negative effect of MWCNTs in time, but also the macrophyte abundance after 15 months was lower. This difference in habitat could also play a role in the abundance of Sphaeriidae. The abundance of Sphaeriidae can be compared to Pisiidiidae in the parallel AC treatments [19], as both taxa are small freshwater clams from the same Sphaeriidae family. For all doses of 0, 2, 4, 6 and 10% AC [19], the abundance of these clams decreased significantly between 3 and 15 months, whereas for the MWCNTs, the decrease was only significant for the 0.2 g kg⁻¹ dose.

After 15 months, macrophyte abundance varied considerably among MWCNT treatments and replicates, ranging from 0.68 ± 0.71 to 2.33 ± 2.15 g d.w. (Figure S8.5). The differences between treatments were not statistically significant (one-way ANOVA, $F(4,16) = 0.950$, $p = 0.461$). Macrophyte taxa included *Chara sp*, *Elodea nuttallii*, *Potamogeton obtusifolius*, *Alisma plantago-aquatica* and *Fontinalis sp* and one tray contained *Eleocharis palustris*. Interestingly, the number of macroinvertebrate individuals increased with increasing macrophyte abundance (Pearson's correlation, $r(21) = 0.550$, $p = 0.010$) as could be expected since macrophytes offer food, habitat and places to shelter for a variety of macroinvertebrate taxa. After 3 months, the macrophyte abundance was reported to increase with increasing MWCNT concentration (one-way ANOVA, $F(4,16) = 4.394$, $p = 0.014$; Figure S8.4) [18]. The difference of the macrophyte abundance between 3 and 15 months was not statistically significant. This is similar to results reported by Kupryanchyk et al. [19], showing that the variation in macrophyte abundance between AC treatments was significant after 3 months but not anymore after 15 months.

Multivariate analysis of community data

Data from both time points and all MWCNT treatments were analysed together to assess the effects of MWCNTs and other potential explanatory variables on the community composition. Detrended correspondence analysis (DCA) showed a gradient length of 2.024, indicating that a linear response model fitted best to this dataset [44]. RDA with partitioning of the variance showed that 51.7% of the variation ($p = 0.002$) in the dataset was explained by the variables MWCNT dose, exposure time, macrophyte biomass and spatial distribution (Table 8.1). General sediment

characteristics like OC and RC were not explicitly included because they were assumed identical in the homogeneously mixed sediments embedded randomly at the same site. After correction for co-variation among explanatory variables, the net variation explained by MWCNT treatments, time, and macrophytes was substantial and highly significant (Table 8.1). Most importantly, MWCNT treatments explained 9.9% of the variation in the benthic community composition ($p = 0.012$). Exposure time explained 35.0% of the variation ($p = 0.002$) and macrophyte abundance explained another 5.2% ($p = 0.004$).

Table 8.1 Explained variation of community structure for MWCNT addition, macrophyte abundance and spatial distribution with significance level for redundancy analysis (RDA).

MWCNT doses considered	Explanatory Variables	Variation explained by explanatory variable (%)	Significance of explained variation (p value) ^a
0 – 2 g kg ⁻¹	MWCNTs	9.9	0.012*
	macrophytes	5.2	0.004**
	spatial distr.	2.2	0.760
	time	35.0	0.002**
	unexplained	48.3	-
0 – 0.2 g kg ⁻¹	MWCNTs	10.6	0.002**
	macrophytes	6.2	0.004**
	spatial distr.	2.8	0.840
	time	36.7	0.002**
	unexplained	45.8	-
0 – 0.02 g kg ⁻¹	MWCNTs	17.9	0.002**
	macrophytes	4.9	0.022*
	spatial distr.	3.4	0.726
	time	39.2	0.002**
	unexplained	38.4	-
0 – 0.002 g kg ⁻¹	MWCNTs	7.1	0.020*
	macrophytes	6.2	0.056
	spatial distr.	7.3	0.244
	time	44.3	0.002**
	unexplained	36.1	-
0.002 – 2 g kg ⁻¹	MWCNTs	6.7	0.392
	macrophytes	4.1	0.054
	spatial distr.	4.7	0.350
	time	28.8	0.002**
	unexplained	51.0	-

^a statistical significance was tested using Monte Carlo permutation test with 499 permutations.

* Significant at $p < 0.05$

** Significant at $p < 0.01$

The importance of time can be understood primarily from the fact that the experiment was a recolonization experiment. At start there was no community at all, which explains the importance of time in rebuilding the community. However, also small changes in sediment composition (eg., RC) theoretically may have contributed to the significance of the variability explained by time. The influence of macrophytes is well understood, because the presence of macrophytes can change the composition of the sediment by rooting, by providing refuge for invertebrates against predation or by reducing the incidence of light on the sediment. Spatial distribution appeared not to be statistically significant (2.2% of the variation; $p = 0.760$), which confirms that random positioning of the trays in the ditch did not influence the community composition caused by dissimilarities between trays. This includes the absence of effects from small spatial dissimilarities in sediment characteristics (OC, RC), if any.

The first two axes of the variation in samples and species data revealed by RDA explained 38.4% and 5.5%, respectively. The first axis shows a separation of the samples based on exposure time. Samples retrieved after 3 months are on the left-hand side of the plot, whereas the trays exposed for 15 months are on the right-hand side of Figure 8.2a. The second axis relates to the MWCNT level and macrophyte content. A clear separation between the controls (C0) in the lower part of the figure and the contaminated samples (C1, C2 and C4) and the macrophyte content in the upper part

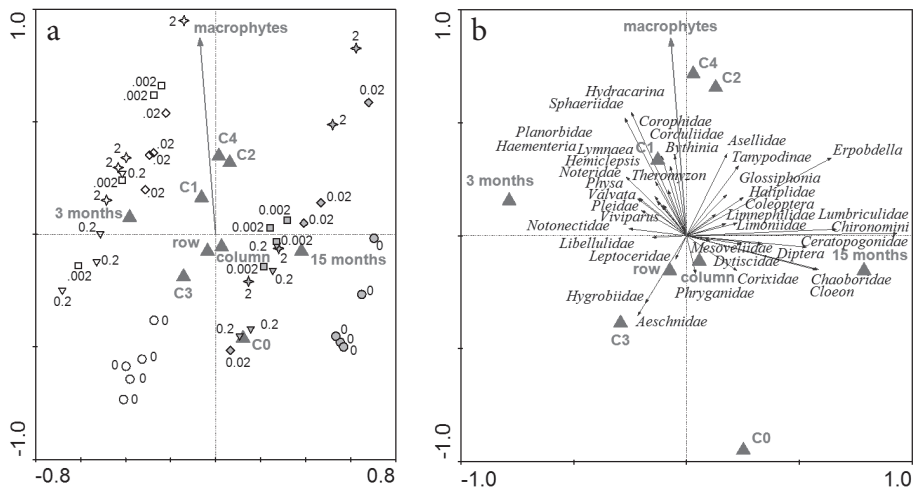


Figure 8.2 Samples scores (a) and macroinvertebrate scores (b) of the first two axes of a redundancy analysis (RDA) of the benthic community from the recolonization study performed in the Veenkampen with sediment contaminated with 0 (circles, C0), 0.002 (squares, C1), 0.02 (diamonds, C2), 0.2 (triangles, C3) and 2 (stars, C4) g kg^{-1} MWCNTs after 3 (open symbols) and 15 months (grey symbols). Environmental data are indicated with triangles. Samples and taxa grouped in the same part of the biplot are related to one another. The lengths of the taxa arrows indicate the strength of the relationship.

of the figure is visible. This difference between the controls and the MWCNT dosed samples indicates an effect on the community structure.

Taxa that were located in the centre of the ordination plot (i.e. with short arrows) can be defined as being hardly affected by MWCNT treatment or exposure time (Figure 8.2b). Taxa in the left part of the diagram show a relatively strong relation with the 3 month samples. However, the abundance of most of these taxa was low, so that the absence of these taxa after 15 months should not be interpreted as a MWCNT treatment effect. The abundance of Sphaeriidae and Hydracarina was high after 3 months, but these taxa had also a strong relation with the macrophyte content. Dominant species, e.g. Lumbriculidae, Erpobdella, Sphaeriidae and Chironomidae increased between 3 and 15 month exposure time despite MWCNT treatments, which again suggests that time is the main factor in the recolonization process.

MWCNT treatments and taxa were not explicitly grouped or separated (Figure 8.2b). The higher amount of macroinvertebrates after 15 months compared to 3 months of exposure suggests that time and natural circumstances have a higher effect on the community composition than the MWCNT sediment treatments. Nevertheless, the controls (C0) are clearly separated from the rest, which confirm the influence of MWCNTs on the community structure.

Interestingly, the statistical analysis revealed a significant effect of a dose of up to 2 g kg^{-1} MWCNTs on the invertebrate community. To our knowledge this is the first report of significant community effects of carbon nanomaterials under long term field conditions. Although the MWCNTs were added to the sediment in their pristine state, 15 months of aging in the sediment must have altered their aggregation state and possible transformation [5, 13] such that they more closely resemble an environmentally realistic state than those in current shorter term laboratory tests. Current MWCNT characterization methodologies are insufficient to assess the exact MWCNT state and concentration in sediments [13, 45], but the observed effects can be assumed to relate to the aged and aggregated MWCNTs, rather than to the primary particles. However, the exposure concentration of up to 2 g kg^{-1} is at least three orders of magnitude higher than exposure concentrations that can be expected in natural sediments [5, 20]. To test whether effects would still be significant at lower MWCNT doses, we re-analysed the data four times, each time excluding the highest dose (Table 8.1). The results show that despite the reduced statistical rigour due to the smaller dataset, the effect of MWCNTs remains statistically significant, even when only the data for the controls and the lowest treatment concentrations of 0.002 g kg^{-1} are used. At this low dose, MWCNTs still explained 7.1% of the community composition, a percentage that was significant ($p = 0.020$). These data thus indicate that even the lowest MWCNT dose that was tested (0.002 g kg^{-1}), seems to show significant chronic effects on the benthic community structure after 15 months. We argue that this dose can be considered environmentally relevant because model studies showed that given current emission rates, these concentrations can be reached within decades [5, 20], or earlier on locations subject to emission from local point sources.

Although our study design could detect community effects and patterns of sensitivities of species towards MWCNTs (Figure 8.2, discussed earlier), it was not fit to detect toxicity mechanisms for individual species. One reason for this is the current lack of methods to characterize the *in situ* state of MWCNTs in the sediment after 15 months [13, 45]. Therefore MWCNT state, i.e. level of aggregation, transformation and degradation, and concentration remained unknown and nominal concentrations had to be used. Still, some general inferences can be made from the data and the literature. When RDA is performed using data from MWCNT treated systems only, i.e. excluding the controls, the effect of MWCNT dose was not significant anymore (Table 8.1). Furthermore, there was no clear trend in the percentage explained, between systems that differed by orders of magnitude in MWCNT concentration (Table 8.1). This suggests that the nanoparticles trigger an effect on (certain) species, which apparently is independent on dose. Dose-independent bioaccumulation and effects of C₆₀ have recently been reported for earthworms [46]. Petersen et al. [13] reviewed MWCNT aquatic toxicity studies and reported minimal effects, i.e. effect ranges of 0.3 – 300 g kg⁻¹ for various benthic invertebrates and endpoints in 10 – 28 d sediment toxicity tests. The observed toxicity was ascribed to MWCNT disturbances on epithelial surfaces, oxidative stress, or blockage of the gastro intestinal tract. In our previous study, no effects of 0.002 – 2 g kg⁻¹ MWCNTs on community composition were detected after 3 months [18]. The main difference of the present study with all these previous studies is that exposure time was much longer. Long exposure and use of community composition as an endpoint for effect may increase the role of sub-lethal and behavioural effect mechanisms on the fitness of species. It has been observed that certain benthic invertebrates sense and avoid contaminated sediment, which is a common ecological mechanism [47]. After 15 months the role of reproduction in the observed community shifts must have been larger. We thus hypothesise that effects on reproduction of invertebrates may have contributed to the observed community shifts. Whereas 51.7% of the variation was explained by known variables, 48.3% of the variation remained unexplained. Theoretically, this percentage can be explained by variables not explicitly included in this study, like water (pH, conductivity, DOC, temperature, O₂ content) and sediment quality, sediment structure (OC and RC content, grain size), depth, habitat characteristics and traditional pollutants (if any), but also biological factors like food quality and quantity, competition and predation. These factors are known to affect community composition [36], but were beyond the scope of this work. Again, however, most of these variables were similar for all trays and therefore hardly will have affected the detected trends.

MWCNT versus AC impacts on benthic community structure

The observed impacts of MWCNTs on the benthic community structure can be compared directly to those of AC in our recently published study, which was performed simultaneously in parallel systems in the “Veenkampen” [19]. Kupryianchyk et al. [19] reported an effect of 100 g kg⁻¹ (i.e. 10%) AC of 9.0% ($p = 0.008$) [19], which is

very similar to the present effect observed for MWCNTs (9.9%, $p = 0.012$). However, although these components have a comparable impact, the highest concentration of MWCNTs was about fifty times lower than the highest AC concentration. This would imply that the MWCNTs are about 50 times more potent in structuring the benthic community than AC. In contrast, Kennedy et al. [22] reported a 10-20 times lower toxicity of high levels of MWCNTs compared to AC. However, their test conditions, species and endpoints were very different from those in the present study, rendering the data difficult to compare. Other recent studies propose the use of AC as well as nanomaterials for *in situ* remediation [14, 48]. Our findings suggest that further research on the state, persistence, bioavailability and ecological safety of MWCNT amendments to sediments is highly needed.

8.4 Implications

Whereas literature on short term laboratory tests shows relatively high effect thresholds for MWCNTs [13], our present data suggest that they may be much lower in the long term in the field. For MWCNTs, the observed effect threshold approaches concentrations anticipated to occur in natural sediments. This illustrates the relevance of long term *in situ* effect assessment of nanomaterials to natural communities. Although effect mechanisms are hard to identify from field studies, the main benefit is that many naturally occurring factors that are not covered in short term laboratory tests are accounted for, and therefore automatically are incorporated in the observed dose effect relationship. The present results also show that multivariate endpoints may be more sensitive to community changes than univariate endpoints such as the Shannon index, in which part of the community information is lost. Detection of *in situ* effects of MWCNTs can have far reaching consequences for the risk assessment of nanomaterials. We emphasize that although significant MWCNT effects were detected, the current data primarily call for confirmation in follow-up field experiments.

Acknowledgements

We would like to thank Darya Kupryianchyk for her advice during the experiments and data analysis. John Beijer and Erik Reichmann are acknowledged for their help and advice with sediment sampling, placement and retrieving of the trays and species identification. We thank Frits Gillissen for his help with the OC and RC measurements. Three anonymous reviewers are acknowledged for their critical comments on the manuscript.

References

- [1] Klaine SJ, Koelmans AA, Horne N, Carley S, Handy RD, Kapustka L, Nowack B, von der Kammer F. 2012. Paradigms to assess the environmental impact of manufactured nanomaterials. *Environmental Toxicology and Chemistry* 31:3-14.
- [2] Handy RD, Cornelis G, Fernandes T, Tsyusko O, Decho A, Sabo-Attwood T, Metcalfe C, Steevens JA, Klaine SJ, Koelmans AA, Horne N. 2012. Ecotoxicity test methods for engineered nanomaterials: Practical experiences and recommendations from the bench. *Environmental Toxicology and Chemistry* 31:15-31.
- [3] Nowack B, Bucheli TD. 2007. Occurrence, behavior and effects of nanoparticles in the environment. *Environmental Pollution* 150:5-22.
- [4] Klaine SJ, Alvarez PJJ, Batley GE, Fernandes TE, Handy RD, Lyon DY, Mahendra S, McLaughlin MJ, Lead JR. 2008. Nanomaterials in the environment: Behavior, fate, bioavailability, and effects. *Environmental Toxicology and Chemistry* 27:1825-1851.
- [5] Koelmans AA, Nowack B, Wiesner MR. 2009. Comparison of manufactured and black carbon nanoparticle concentrations in aquatic sediments. *Environmental Pollution* 157:1110-1116.
- [6] Money ES, Reckhow KH, Wiesner MR. 2012. The use of Bayesian networks for nanoparticle risk forecasting: Model formulation and baseline evaluation. *Science of The Total Environment* 426:436-445.
- [7] Diepens NJ, Arts GHP, Brock TCM, Smidt H, Van den Brink PJ, Van den Heuvel-Greve MJ, Koelmans AA. 2013. Sediment toxicity testing of organic chemicals in the context of prospective risk assessment: A review. *Critical Reviews in Environmental Science and Technology*:null-null.
- [8] Farre M, Gajda-Schrantz K, Kantiani L, Barcelo D. 2009. Ecotoxicity and analysis of nanomaterials in the aquatic environment. *Analytical and Bioanalytical Chemistry* 393:81-95.
- [9] Handy RD, von der Kammer F, Lead JR, Hasselov M, Owen R, Crane M. 2008. The ecotoxicology and chemistry of manufactured nanoparticles. *Ecotoxicology* 17:287-314.
- [10] Velzeboer I, Hendriks AJ, Ragas AMJ, Van de Meent D. 2008. Aquatic ecotoxicity tests of some nanomaterials. *Environmental Toxicology and Chemistry* 27:1942-1947.
- [11] Nowack B, Ranville JF, Diamond S, Gallego-Urrea JA, Metcalfe C, Rose J, Horne N, Koelmans AA, Klaine SJ. 2012. Potential scenarios for nanomaterial release and subsequent alteration in the environment. *Environmental Toxicology and Chemistry* 31:50-59.
- [12] Kulacki KJ, Cardinale BJ, Keller AA, Bier R, Dickson H. 2012. How do stream organisms respond to, and influence, the concentration of titanium dioxide nanoparticles? A mesocosm study with algae and herbivores. *Environmental Toxicology and Chemistry* 31:2414-2422.
- [13] Petersen EJ, Zhang L, Mattison NT, O'Carroll DM, Whelton AJ, Uddin N, Nguyen T, Huang Q, Henry TB, Holbrook RD, Chen KL. 2011. Potential Release Pathways, Environmental Fate, And Ecological Risks of Carbon Nanotubes. *Environmental Science & Technology* 45:9837-9856.

- [14] Karn B, Kuiken T, Otto M. 2009. Nanotechnology and in Situ Remediation: A Review of the Benefits and Potential Risks. *Environmental Health Perspectives* 117:1823-1831.
- [15] Theron J, Walker JA, Cloete TE. 2008. Nanotechnology and water treatment: Applications and emerging opportunities. *Critical Reviews in Microbiology* 34:43-69.
- [16] Hyung H, Kim JH. 2009. Dispersion of C-60 in natural water and removal by conventional drinking water treatment processes. *Water Research* 43:2463-2470.
- [17] Quik JTK, Velzeboer, I., Wouterse, M., Koelmans, A.A., van de Meent, D. May 2012. Sedimentation of nanomaterials in natural waters. *SETAC World congress*. Vol Abstract book p49, Berlin, Germany.
- [18] Velzeboer I, Kupryianchik D, Peeters ETHM, Koelmans AA. 2011. Community effects of carbon nanotubes in aquatic sediments. *Environment International* 37:1126-1130.
- [19] Kupryianchik D, Peeters ETHM, Rakowska MI, Reichman EP, Grotenhuis JTC, Koelmans AA. 2012. Long-Term Recovery of Benthic Communities in Sediments Amended with Activated Carbon. *Environmental Science & Technology* 46:10735-10742.
- [20] Gottschalk F, Sonderer T, Scholz RW, Nowack B. 2009. Modeled Environmental Concentrations of Engineered Nanomaterials (TiO₂, ZnO, Ag, CNT, Fullerenes) for Different Regions. *Environmental Science & Technology* 43:9216-9222.
- [21] Mueller NC, Nowack B. 2008. Exposure modeling of engineered nanoparticles in the environment. *Environmental Science & Technology* 42:4447-4453.
- [22] Kennedy AJ, Hull MS, Steevens JA, Dontsova KM, Chappell MA, Gunter JC, Weiss Jr. CA. 2008. Factors influencing the partitioning and toxicity of nanotubes in the aquatic environment. *Environmental Toxicology and Chemistry*:1932-1941
- [23] Klaper R, Crago J, Barr J, Arndt D, Setyowati K, Chen J. 2009. Toxicity biomarker expression in daphnids exposed to manufactured nanoparticles: Changes in toxicity with functionalization. *Environmental Pollution* 157:1152-1156.
- [24] Liu XY, Vinson D, Abt D, Hurt RH, Rand DM. 2009. Differential Toxicity of Carbon Nanomaterials in Drosophila: Larval Dietary Uptake Is Benign, but Adult Exposure Causes Locomotor Impairment and Mortality. *Environmental Science & Technology* 43:6357-6363.
- [25] Oberdorster E, Zhu SQ, Blickey TM, McClellan-Green P, Haasch ML. 2006. Ecotoxicology of carbon-based engineered nanoparticles: Effects of fullerene (C-60) on aquatic organisms. *Carbon* 44:1112-1120.
- [26] Zhu XS, Zhu L, Chen YS, Tian SY. 2009. Acute toxicities of six manufactured nanomaterial suspensions to *Daphnia magna*. *Journal of Nanoparticle Research* 11:67-75.
- [27] Mwangi JN, Wang N, Ingersoll CG, Hardesty DK, Brunson EL, Li H, Deng B. 2012. Toxicity of carbon nanotubes to freshwater aquatic invertebrates. *Environmental Toxicology and Chemistry* 31:1823-1830.
- [28] Gustafsson O, Haghseta F, Chan C, MacFarlane J, Gschwend PM. 1997. Quantification of the dilute sedimentary soot phase: Implications for PAH speciation and bioavailability. *Environmental Science & Technology* 31:203-209.

- [29] Jonker MTO, Koelmans AA. 2002. Sorption of polycyclic aromatic hydrocarbons and polychlorinated biphenyls to soot and soot-like materials in the aqueous environment mechanistic considerations. *Environmental Science & Technology* 36:3725-3734.
- [30] de Pauw N, Vannevel, R. . 1991. *Macro-invertebraten en waterkwaliteit. Determineersleutels voor zoetwatermacroinvertebraten en methoden ter bepaling van de waterkwaliteit*. Stichting Leefmilieu, Antwerpen.
- [31] Drost MBP, Cuppen, H.P.J.J., van Nieukerken, E.J., Schreijer, M. . 1992. *De waterkevers van Nederland*. Koninklijke Nederlandse Natuurhistorische Vereniging, Utrecht.
- [32] Keustermans K, Quanten, E.,. 2003. *Wateronderzoek PIME (Provinciaal Instituut voor Milieu Educatie)*. PIME, Lier, Vlaanderen, België.
- [33] Magurran AE. 1988. *Ecological diversity and its measurement*. University Press, Cambridge, U.K.
- [34] Peeters ETHM, Dewitte A, Koelmans AA, van der Velden JA, den Besten PJ. 2001. Evaluation of bioassays versus contaminant concentrations in explaining the macroinvertebrate community structure in the Rhine-Meuse delta, the Netherlands. *Environmental Toxicology and Chemistry* 20:2883-2891.
- [35] Peeters ETHM, Gardeniers JJP, Koelmans AA. 2000. Contribution of trace metals in structuring in situ macroinvertebrate community composition along a salinity gradient. *Environmental Toxicology and Chemistry* 19:1002-1010.
- [36] Peeters ETHM, Gylstra R, Vos JH. 2004. Benthic macroinvertebrate community structure in relation to food and environmental variables. *Hydrobiologia* 519:103-115.
- [37] van Griethuysen C, van Baren J, Peeters ETHM, Koelmans AA. 2004. Trace metal availability and effects on benthic community structure in floodplain lakes. *Environmental Toxicology and Chemistry* 23:668-681.
- [38] PinelAlloul B, Methot G, Lapierre L, Willsie A. 1996. Macroinvertebrate community as a biological indicator of ecological and toxicological factors in Lake Saint-Francois (Quebec). *Environmental Pollution* 91:65-87.
- [39] Ter Braak CJF. 1990. *Update notes: CANOCO version 3.1*. Agricultural Mathematics Group, Wageningen, The Netherlands.
- [40] Ter Braak CJF, Smilauer, P. 2002. *CANOCO reference manual and CanoDraw for Windows user's guide: software for canonical community ordination (version 4.5)*. Ithaca Microcomputer Power, New York, USA.
- [41] Koelmans AA, Jonker MTO, Cornelissen G, Bucheli TD, Van Noort PCM, Gustafsson O. 2006. Black carbon: The reverse of its dark side. *Chemosphere* 63:365-377.
- [42] Sobek A, Bucheli TD. 2009. Testing the resistance of single- and multi-walled carbon nanotubes to chemothermal oxidation used to isolate soots from environmental samples. *Environmental Pollution* 157:1065-1071.
- [43] Beukema JJ, Flach EC, Dekker R, Starink M. 1999. A long-term study of the recovery of the macrozoobenthos on large defaunated plots on a tidal flat in the Wadden Sea. *Journal of Sea Research* 42:235-254.

- [44] Leps J, Smilauer, P. 2003. *Multivariate Analysis of Ecological Data Using CANOCO*. Cambridge University Press, Cambridge, U.K.
- [45] von der Kammer F, Ferguson PL, Holden PA, Masion A, Rogers KR, Klaine SJ, Koelmans AA, Horne N, Unrine JM. 2012. Analysis of engineered nanomaterials in complex matrices (environment and biota): General considerations and conceptual case studies. *Environmental Toxicology and Chemistry* 31:32-49.
- [46] van der Ploeg M. 2013. Unravelling hazards of nanoparticles to earthworms, from gene to population. Ph.D Dissertation, Wageningen University, Wageningen.
- [47] De Lange HJ, Sperber V, Peeters ETHM. 2006. Avoidance of polycyclic aromatic hydrocarbon-contaminated sediments by the freshwater invertebrates *Gammarus pulex* and *Asellus aquaticus*. *Environmental Toxicology and Chemistry* 25:452-457.
- [48] Rakowska MI, Kupryianchuk D, Harmsen J, Grotenhuis T, Koelmans AA. 2012. In situ remediation of contaminated sediments using carbonaceous materials. *Environmental Toxicology and Chemistry* 31:693-704.

Supporting Information

Table S8.1 PAH and PCB concentration, Total Organic Carbon (TOC) and Black Carbon (BC) content in Veenkampen sediment [1].^a

PAHs	C (mg kg ⁻¹)	PCBs	C (µg kg ⁻¹)
Acenaphthylene	<LOD	CB-18	<LOD
Acenaphthene	<LOD	CB-20	<LOD
Anthracene	0.28 (0.01)	CB-28	<LOD
Benzo[a]anthracene	0.09 (0.003)	CB-29	<LOD
Benzo[a]pyrene	0.05 (0.002)	CB-44	<LOD
Benzo[b]fluoranthene	0.08 (0.003)	CB-52	1.4 (0.05)
Benzo[e]pyrene	0.12 (0.01)	CB-101	1.6 (0.01)
Benzo[ghi]perylene	0.04 (0.001)	CB-105	<LOD
Benzo[k]fluoranthene	<LOD	CB-118	1.2 (0.06)
Chrysene	0.25 (0.01)	CB-138	2.5 (0.09)
Dibenzo[a,h]anthracene	0.04 (0.001)	CB-149	<LOD
Fluoranthene	1.4 (0.03)	CB-153	1.7 (0.07)
Indeno[1,2,3-cd]pyrene	0.03 (0.001)	CB-155	<LOD
Naphthalene	<LOD	CB-180	0.91 (0.08)
Phenanthrene	0.81 (0.07)	CB-194	<LOD
Pyrene	1.5 (0.05)	CB-204	<LOD
		CB-209	<LOD
ΣPAH	4.7 (0.32)	ΣPCBs	9.3 (0.42)
Threshold concentration for intervention	40 [2]	Probable effect concentration	676 [3]
TOC, %	9.8 (0.41)	BC, %	1.8 (0.25)

^a SD between parenthesis. LOD = limit of detection

Table S8.2 Metal contents of MWCNTs, resulting metal concentrations on a sediment basis, and comparison with metal effect thresholds on a sediment basis.

Metal	MWCNT (mg kg ⁻¹)	In 2 g kg ⁻¹ MWCNTs (mg kg ⁻¹)	Probable effect concentration (mg kg ⁻¹ d.w.) [3]
Al	5.86E-04	1.17E-06	
As	3.76E-04	7.52E-07	33.0
B	>LOD		
Ba	1.44E-03	2.87E-06	
Be	1.94E-04	3.88E-07	
Co	3.69E-04	7.38E-07	
Cr	6.47E-04	1.29E-06	111
Cu	8.00E-05	1.60E-07	149
Fe	1.09E-02	2.18E-05	
Li	1.16E-03	2.32E-06	
Mg	>LOD		
Mn	8.17E-04	1.63E-06	
Ni	>LOD		48.6
P	3.44E-04	6.88E-07	
Pb	3.93E-04	7.86E-07	128
Sr	5.65E-03	1.13E-05	
Zn	1.04E-03	2.076E-06	459

Table S8.3 Recolonization^a, biodiversity and macrophyte density in relation to MWCNT treatment after 15 months^b.

MWCNT treatment (g kg ⁻¹)	Individuals (%)	Taxa (%)	Shannon index	Macrophytes (g d.w.)
0 ^c	160.6 (59.6)	96.0 (16.3)	1.39 (0.12)	1.34 (1.07)
0.002	91.3 (23.9)	107.5 (8.3)	1.74 (0.12)	1.08 (0.86)
0.02 ^d	182.4 (107.0)	96.7 (12.5)	1.65 (0.28)	1.29 (1.32)
0.2	71.5 (30.0)	72.5 (14.8)	1.65 (0.24)	0.68 (0.71)
2	129.9 (53.6)	87.5 (17.9)	1.54 (0.12)	2.32 (2.15)

^a Calculated as number in the trays divided by number in the donor system * 100%

^b Values are given as means (SD, n=4)

^c Values are given as means (SD, n=5)

^d Values are given as means (SD, n=3)

Table S8.4. Taxa abundance list of benthic macroinvertebrates.

Phylum	Class	Taxon	Average absolute abundance in the MWCNT treatments and donor system											
			3 months						15 months					
			0	0.002	0.02	0.2	2	Donor ^a	0	0.002	0.02	0.2	2	Donor ^a
Annelida	Oligochaeta	Lumbriculidae	2.40	2.00	2.00	2.50	3.00	-	36.60	14.75	51.33	12.50	26.75	0.67
		Hirundinea	1.00	0.25	1.50	1.25	2.25	0.67	2.00	1.50	1.33	0.75	1.00	0.33
		Haementeria	-	0.25	-	0.25	-	-	-	-	-	-	-	-
Mollusca	Gastropoda	Hemicleptis	-	-	0.25	-	-	-	-	-	-	-	-	-
		Theromyzon	-	-	1.50	-	-	-	-	-	-	-	-	-
		Erpobdella	1.20	1.75	3.25	1.75	3.00	1.67	5.60	8.75	7.00	4.50	10.75	2.33
Mollusca	Gastropoda	Viviparus	-	-	0.25	-	-	-	-	-	-	-	-	-
		Valvata	-	-	0.75	0.50	-	-	-	-	-	-	0.25	-
		Bythinia	-	-	0.75	-	1.25	-	-	-	0.33	0.50	-	-
Mollusca	Physa	Physa	-	-	0.25	0.25	-	1.67	-	-	-	-	-	-
		Lymnaea	-	-	0.50	-	-	-	-	-	-	-	-	-
		Planorbidae	0.20	0.75	0.75	1.50	0.25	9.33	-	-	-	-	-	-
Arthropoda	Arachnida	Sphaeriidae	5.40	14.50	38.50	34.00	20.00	3.67	5.00	19.00	13.67	15.00	22.00	3.00
		Hydracarina	0.20	3.00	0.50	-	2.25	-	-	0.75	-	-	0.25	-
		Corophidae	-	-	-	-	0.25	-	-	-	-	-	-	-
Arthropoda	Crustacea	Asellidae	0.20	1.00	1.00	0.25	0.25	8.00	0.80	0.75	2.00	-	0.75	1.00
		Decapoda	-	-	-	-	-	0.67	-	-	-	-	-	-
		Cloeon	-	-	-	0.25	0.25	5.67	3.60	1.25	0.67	0.25	1.75	8.00
Arthropoda	Insecta	Anisoptera	-	-	-	-	-	0.33	-	-	-	-	-	-
		Aeschnidae	0.40	-	-	-	-	-	-	-	-	-	-	-
		Corduliidae	-	-	0.25	-	0.25	-	-	-	-	-	-	-
Arthropoda	Libellulidae	Libellulidae	0.20	-	0.25	-	-	-	-	-	-	-	-	-

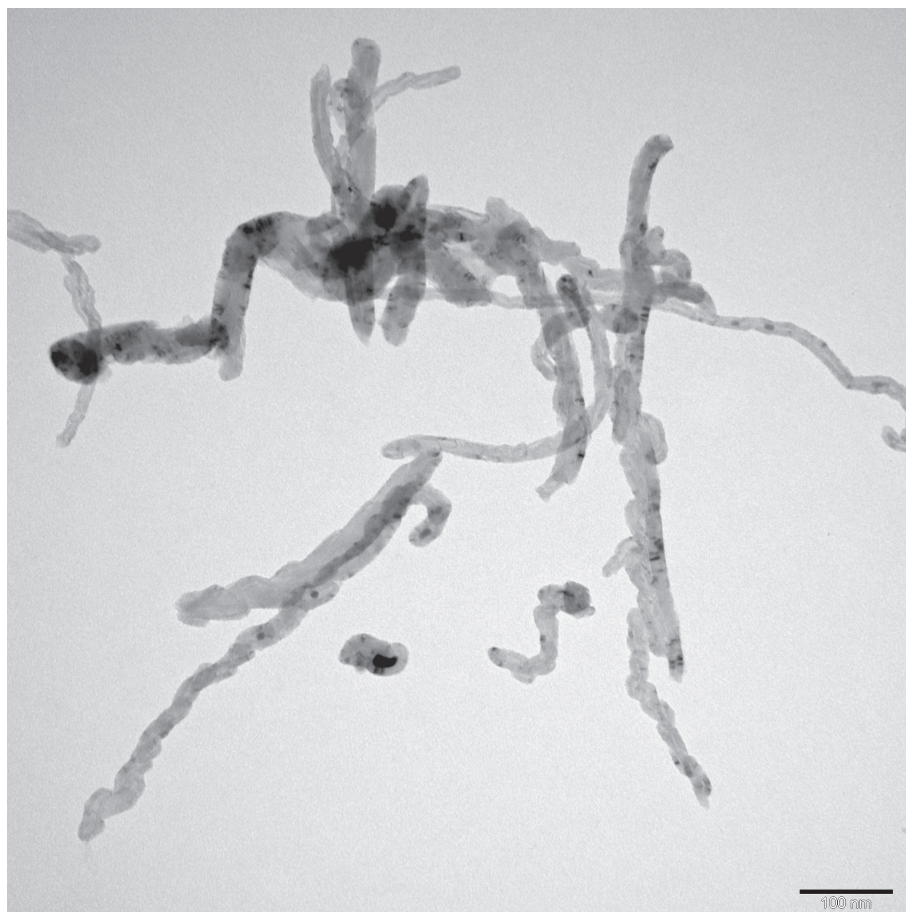


Figure S8.1 Transmission electron microscope (TEM; JEOL JEM1011) image of the used MWCNTs. Images were taken with a Veleta 2Kx2K camera (SIS). Quantified from the images, the diameter of the tubes ranged between 10 and 30 nm, which agrees with the information of the manufacturer (i.e. outer diameter: 20-30nm). The length of 10 to 30 μm as stated by the manufacturer was not observed in the images, the tubes ranged between 0.3 and 2 μm .

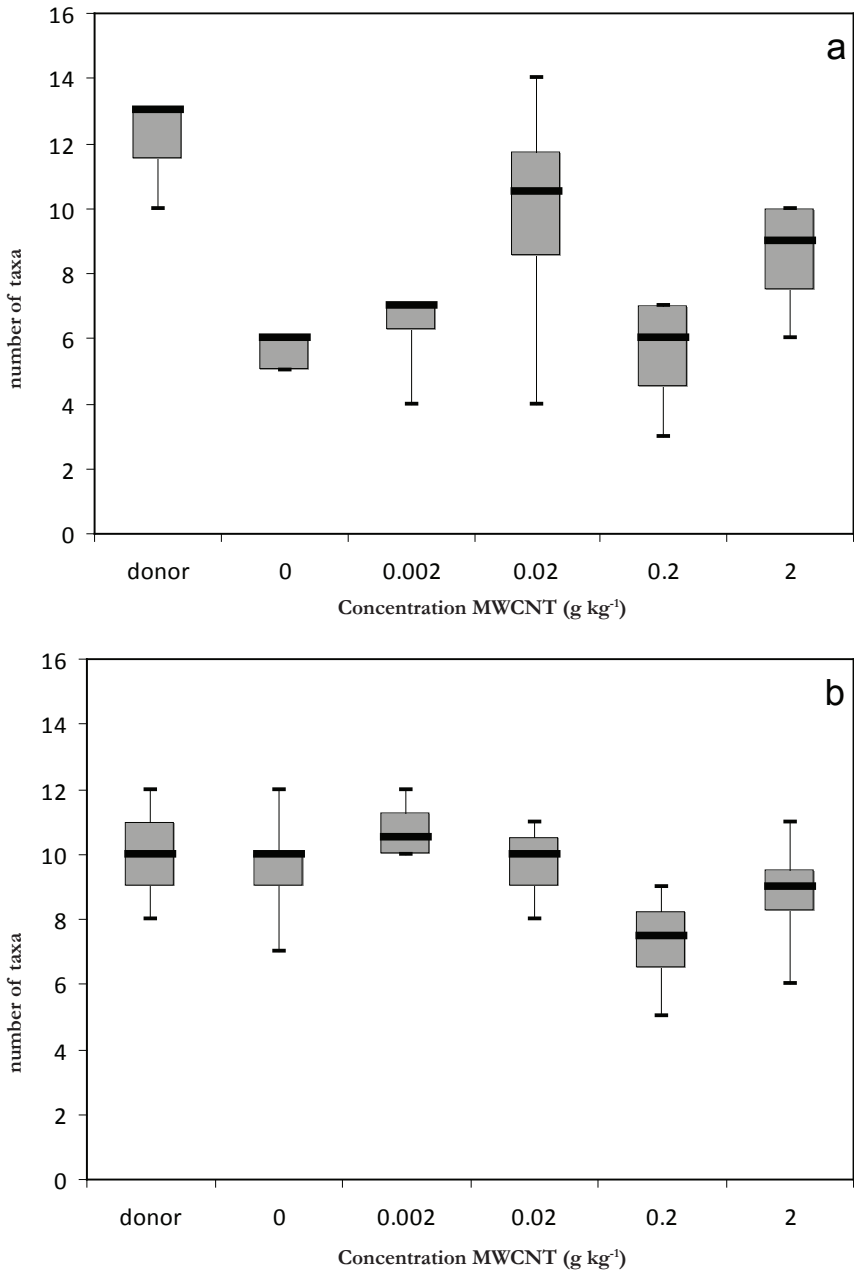


Figure S8.2 Number of taxa in the donor system and as a function of MWCNT concentration after (a) 3 months [4] and (b) 15 months exposure. Boundaries of the boxplots indicate the 25th and 75th percentile. Whiskers below and above indicate the minimum and maximum of the variables. The median is indicated with the black line.

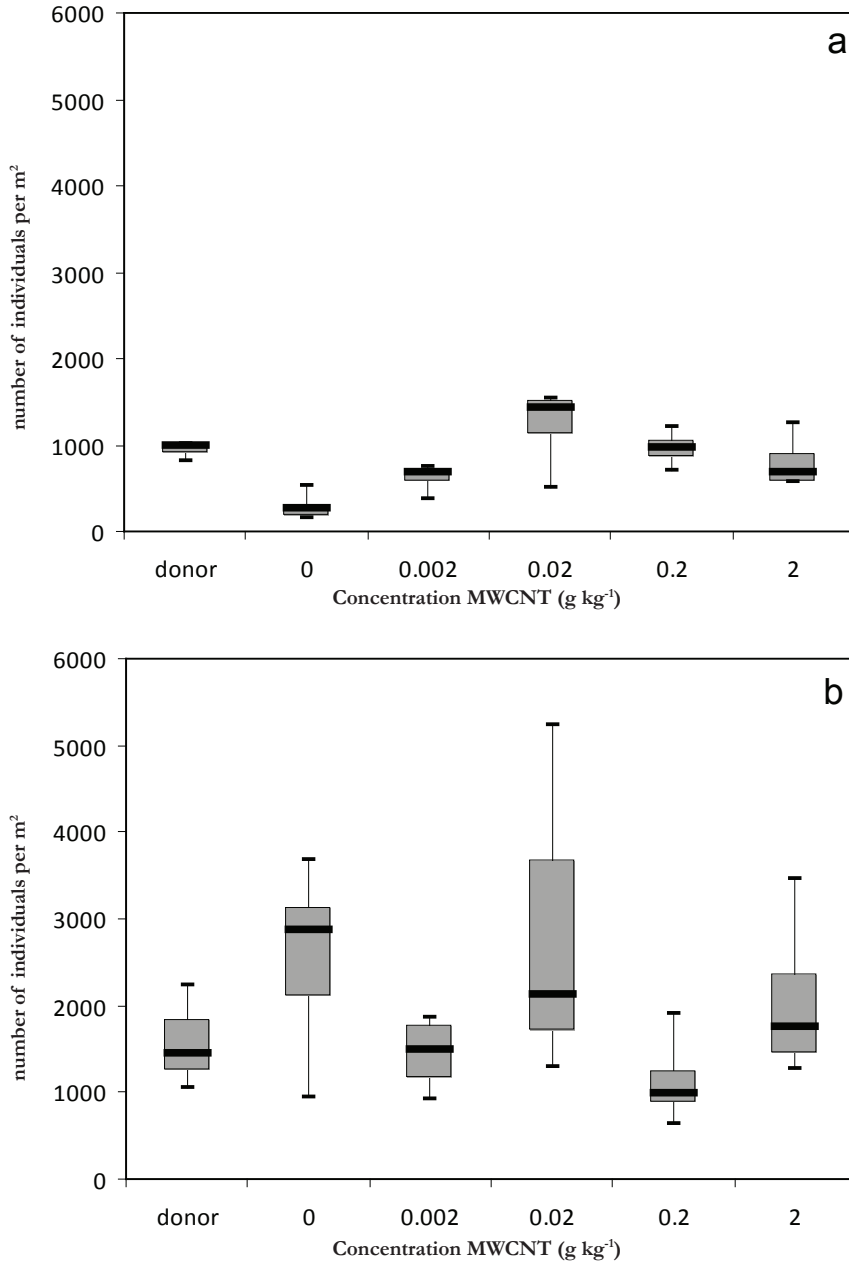


Figure S8.3 Number of individuals per m² in the donor system and as a function of MWCNT concentration after (a) 3 months [4] and (b) 15 months exposure. Boundaries of the boxplots indicate the 25th and 75th percentile. Whiskers below and above indicate the minimum and maximum of the variables. The median is indicated with the black line.

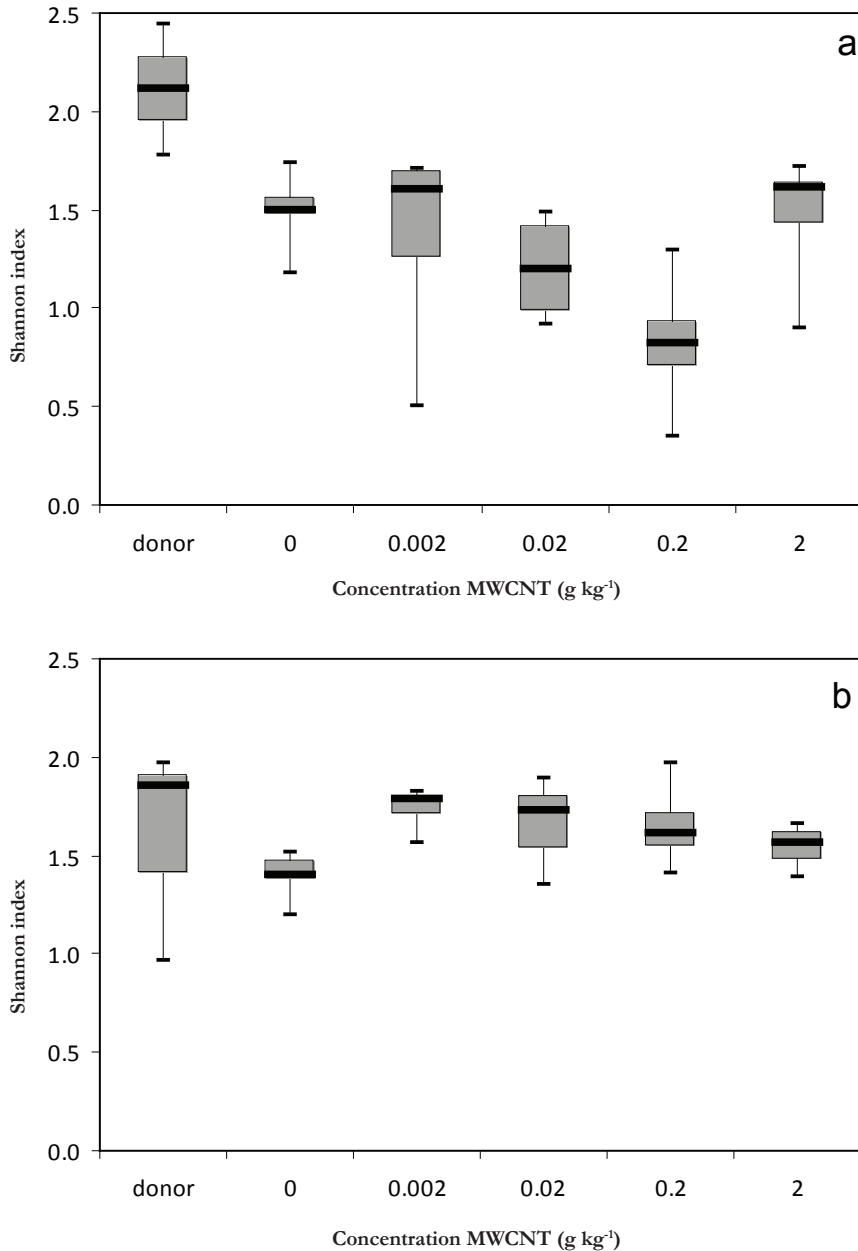


Figure S8.4. Shannon index in the donor system and as a function of MWCNT concentration after (a) 3 months [4] and (b) 15 months exposure. Boundaries of the boxplots indicate the 25th and 75th percentile. Whiskers below and above indicate the minimum and maximum of the variables. The median is indicated with the black line.

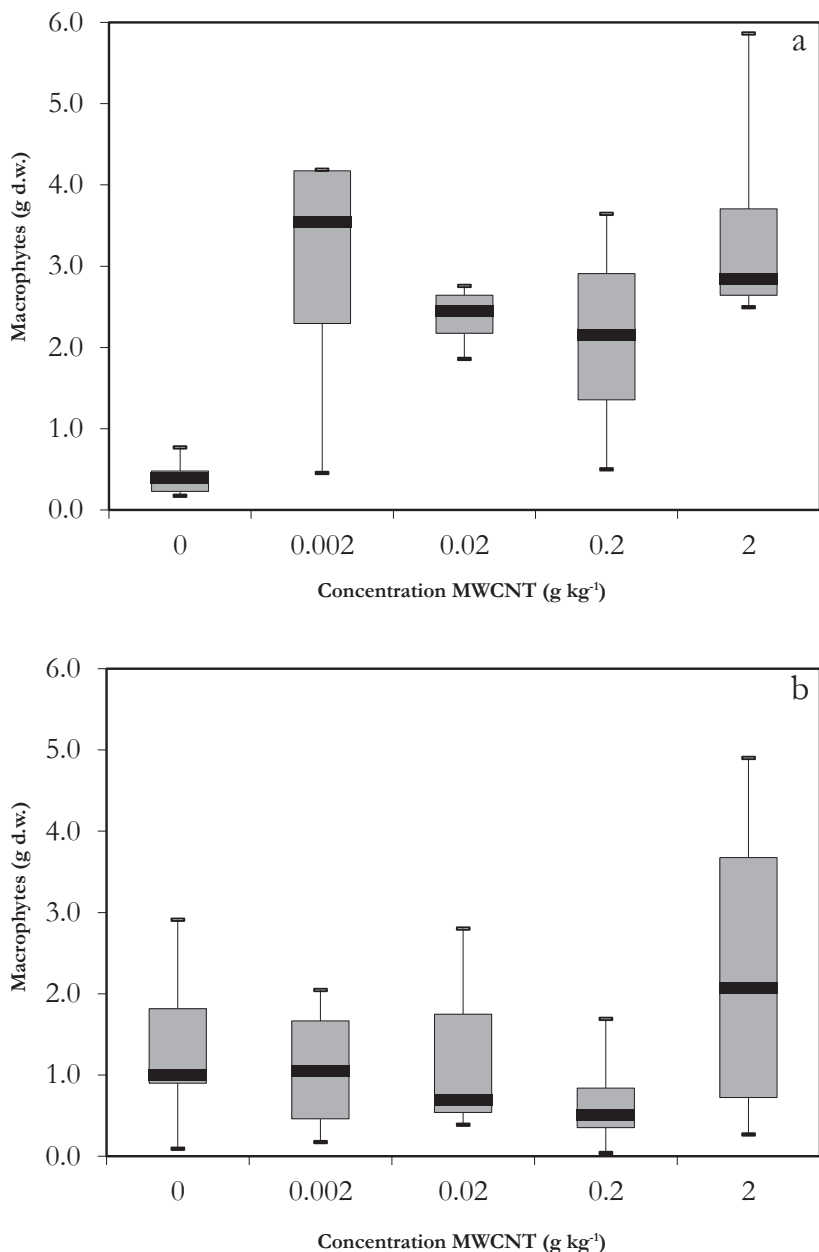


Figure S8.5 Macrophyte dry weight in the trays as a function of MWCNT concentration after (a) 3 months [4] and (b) 15 months exposure. Boundaries of the boxplots indicate the 25th and 75th percentile. Whiskers below and above indicate the minimum and maximum of the variables. The median is indicated with the black line.

References Supporting Information

- [1] Kupryianchyk D, Reichman EP, Rakowska MI, Peeters ETHM, Grotenhuis JTC, Koelmans AA. 2011. Ecotoxicological Effects of Activated Carbon Amendments on Macroinvertebrates in Nonpolluted and Polluted Sediments. *Environmental Science & Technology* 45:8567-8574.
- [2] Tweede Kamer T. 1994. Evaluatienota Water, Dutch standards for contaminated sediments.
- [3] MacDonald DD, Ingersoll CG, Berger TA. 2000. Development and evaluation of consensus-based sediment quality guidelines for freshwater ecosystems. *Archives of Environmental Contamination and Toxicology* 39:20-31.
- [4] Velzeboer I, Kupryianchyk D, Peeters ETHM, Koelmans AA. 2011. Community effects of carbon nanotubes in aquatic sediments. *Environment International* 37:1126-1130.

Implications of nanoparticles for the aquatic environment – general discussion



TiO₂ MWCNTs ZrO₂ TiO₂ CeO₂ MWCNTs CeO₂ SWCNTs SiO₂-Ag
SWCNTs PMMA Al₂O₃ PFOS PVP-Ag CeO₂ MWCNTs PVP-Ag SWCNTs
nano-PS C₆₀ micro-PE C₆₀ SiO₂-Ag TiO₂ C₆₀
Al₂O₃ SiO₂-Ag MWCNTs PVP-Ag CeO₂ PVP-Ag C₆₀ MWCNTs PFOS micro-PE
SiO₂-Ag PMMA PVP-Ag nano-PS C₆₀ MWCNTs PFOS micro-PE
PCBs SiO₂-Ag PVP-Ag C₆₀ PVP-Ag nano-PS Al₂O₃ CeO₂ Al₂O₃
MWCNTs C₆₀ nano-PS MWCNTs CeO₂ micro-PE CeO₂ Al₂O₃
micro-PE PCBs MWCNTs CeO₂ nano-PS CeO₂ ZrO₂ PVP-Ag TiO₂ PFOS
nano-PS Al₂O₃ CeO₂ PCBs CeO₂ SWCNTs C₆₀ PMMA MWCNTs
SiO₂-Ag SWCNTs PCBs PFOS MWCNTs nano-PS SiO₂-Ag PMMA
SiO₂-Ag ZrO₂ C₆₀ MWCNTs ZrO₂ micro-PE SiO₂-Ag PMMA
C₆₀ PCBs SiO₂-Ag PFOS SiO₂-Ag PMMA Al₂O₃ MWCNTs ZrO₂
ZrO₂ TiO₂ PCBs SiO₂-Ag PVP-Ag PMMA Al₂O₃ MWCNTs ZrO₂
ZrO₂ C₆₀ CeO₂ PFOS MWCNTs TiO₂ PVP-Ag PCBs TiO₂ C₆₀
CeO₂ MWCNTs PCBs SWCNTs ZrO₂ TiO₂ MWCNTs ZrO₂ C₆₀ PMMA
micro-PE SiO₂-Ag nano-PS PFOS PMMA PVP-Ag
TiO₂ MWCNTs PCBs SWCNTs ZrO₂ SWCNTs micro-PE SiO₂-Ag MWCNTs
CeO₂ SiO₂-Ag nano-PS PFOS C₆₀ PFOS PMMA PVP-Ag
MWCNTs Al₂O₃ C₆₀ PFOS PMMA PVP-Ag TiO₂ CeO₂
TiO₂ MWCNTs PCBs micro-PE Al₂O₃ PFOS PVP-Ag SWCNTs PMMA TiO₂ CeO₂
PCBs micro-PE ZrO₂ C₆₀ SWCNTs PMMA nano-PS

9.1 Introduction

The production of goods using nanotechnology is growing and the possibilities for applications of nanotechnology seem to be endless. Nanotechnology produces structures, devices and systems that have novel applications because of their nanoscale size [1, 2]. The inevitable emissions of engineered nanoparticles (ENPs) to the environment cause a potential hazard when exposure to organisms and ecosystems occurs [3, 4]. The implications of the presence of ENPs in water systems can be manifold. For instance, ENPs can cause (a) direct effects on species in the aquatic environment, (b) indirect effects on the community and/or food web level and (c) effects on the fate and risks of other chemicals in case of strong binding of these chemicals to ENPs [3-5]. For a safe continuous application of ENPs, understanding their impact on the receiving environment is required [5].

The aim of this Chapter is to evaluate the implications of ENPs in the aquatic environment from a risk perspective, by (a) integrating the information about the fate processes (**Chapter 2** and **3** [6, 7]) with simple concepts to calculate ENP retention in lakes, (b) calculating the effects of the presence of carbon-based ENPs on the retention of polychlorinated biphenyls (PCBs) and perfluorooctane sulfonate (PFOS) using the binding data presented in **Chapter 4** and **5** [8, 9], and (c) semi-quantitatively discussing the anticipated risks of ENPs in the aquatic environment using literature data and data from **Chapter 6, 7** and **8** [10-12]. To this end, this Chapter will give a concise overview of ENP relevant fate processes and an assessment of the anticipated ENP retention in lakes. Furthermore, an estimate of the extent of sorption of organic contaminants to ENPs and their influence on the retention of PCBs and PFOS in presence of ENPs in lakes will be provided. Then, an overview of effect studies focusing on aquatic and benthic species is given. Finally, current risk estimates are being discussed including the new insights on exposure and effects assessment.

9.2 Fate and exposure of ENPs in the aquatic environment: what needs to be known?

Factors defining ENP behaviour are on the one hand dependent on the nanoparticle characteristics such as the surface chemistry, composition, size, shape, presence of coatings and the potential of dissolution. On the other hand, when ENPs enter the environment, transformations and interactions including homo- and heteroaggregation, dissolution, surface transformation and degradation may occur in the receiving water. The composition of the water body, such as the amount of natural organic matter (dissolved or particulate), presence of microorganisms, oxidants and other pollutants and abiotic factors, such as salinity (ionic strength), light, pH and temperature will all affect ENP behaviour. These transformation processes modify ENP aggregation kinetics and affect the transport and exposure pathways [4, 5, 13-

15]. These possible transformations and interactions of ENPs in the complex aquatic environment and their presently low environmental concentrations make it difficult to measure these concentrations. This explains why the availability of empirical data presently is limited. Consequently, the expected environmental concentrations are mostly based on model predictions [16, 17]. Model predictions however, show considerable variations and uncertainties because of incomplete knowledge of the quantity of production and potential release into the environment, but also because of the often unknown physicochemical properties and fate process parameters of ENPs. Based on best educated models and model parameters, predicted environmental concentrations for TiO_2 , Ag, ZnO, CeO_2 , carbon nanotubes (CNT) and C_{60} ranged from 10^{-5} to $16 \mu\text{g L}^{-1}$ in surface water and from 10^{-2} to $10^4 \mu\text{g kg}^{-1}$ in sediments [16]. Using the predicted environmental concentrations from Gottschalk et al. [18] based on data from 2008, and using their predicted annual increase, the expected concentrations in surface water and sediment in 2025 and 2125 were calculated for Europe (Table 9.1).

Table 9.1 Predicted environmental concentrations of TiO_2 , Ag, ZnO, carbon nanotubes (CNT) and fullerenes for Europe, in 2008, 2025 and 2125 based on data from Gottschalk et al. [18].

ENP	Predicted environmental concentration					
	2008		2025		2125	
	surface water ($\mu\text{g L}^{-1}$)	sediment ($\mu\text{g kg}^{-1}$)	surface water ($\mu\text{g L}^{-1}$)	sediment ($\mu\text{g kg}^{-1}$)	surface water ($\mu\text{g L}^{-1}$)	sediment ($\mu\text{g kg}^{-1}$)
TiO_2	$1.50 \cdot 10^{-2}$	2864	$4.69 \cdot 10^{-2}$	8950	0.23	44750
Ag	$7.64 \cdot 10^{-4}$	7.62	$2.39 \cdot 10^{-3}$	23.80	$1.19 \cdot 10^{-2}$	119
ZnO	$1.00 \cdot 10^{-2}$	23.20	$3.13 \cdot 10^{-2}$	72.50	0.16	362.50
CNT	$4.00 \cdot 10^{-6}$	1.93	$1.25 \cdot 10^{-5}$	6.03	$6.25 \cdot 10^{-5}$	30.13
Fullerenes	$1.70 \cdot 10^{-5}$	0.14	$5.31 \cdot 10^{-5}$	0.43	$2.66 \cdot 10^{-4}$	2.14

These environmental concentrations (Table 9.1) are based on mass balance model calculations and do not explicitly take nano-specific processes such as aggregation into account. ENPs show behaviour similar to that of natural colloids, because colloids are defined as particles with a diameter between 1 nm and $1 \mu\text{m}$ and nanoparticles fit within this range [3, 4, 19]. The fate of colloids is dominated by aggregation resulting in particles large enough to settle. Pollutants, like for example metals, are known to be removed from surface waters by sorption onto natural colloids that aggregate and settle into the sediment. This behaviour may also be relevant to ENPs [3]. Therefore, ENP behaviour and transport are usually described using concepts of colloid chemistry, with aggregation and sedimentation as the most dominant processes [3, 14]. Attachment efficiency and collision frequency are important factors for aggregation. The attachment efficiency is the chance that collision of particles will cause them to aggregate and is dependent on electrostatic and Van der Waals forces, steric hindrance and magnetic and hydration forces [20]. The collision frequency is the

chance that particles collide, which is related to Brownian motion, fluid motion and differential settling [5, 21] (**Chapters 2 and 3** [6, 7]).

There is only very limited data on aggregation and sedimentation behaviour of ENPs in aquatic systems. This explains the relevance of experiments providing aggregation and sedimentation rates that can be used to improve model predictions [15, 22-24], like those performed in **Chapter 2 and 3** [6, 7]. In these Chapters sedimentation rates have been determined by measuring the total concentration of ENPs in the supernatant at different time points and by fitting the rates using simple models [23, 25]. The data provided by the sedimentation experiments were used to determine heteroaggregation rates, using a simplified Smoluchowski-Stokes equation. Sedimentation and heteroaggregation rates were determined from experiments including several types of nanoparticles and natural water. Quiescent settling of ceriumdioxide (CeO_2), polyvinylpyrrolidone coated silver (PVP-Ag), silica coated silver (SiO_2 -Ag) and fullerene (C_{60}) nanoparticles was measured in filtered and unfiltered natural waters, to calculate sedimentation rates and heteroaggregation rates for ENPs with NC (**Chapter 2** [6]). The natural waters included a coastal sea, tidal water, river, small stream, lake and a small acid pond. Rates for settling and heteroaggregation of CeO_2 , PVP-Ag and SiO_2 -Ag nanoparticles in the coastal seawater, tidal water and river water were also determined under turbulent conditions in the presence of suspended sediment (SS) (**Chapter 3** [7]). These experiments showed that heteroaggregation with NC to form settleable aggregates was more important than stabilizing effects of dissolved organic carbon (DOC). Resuspended sediment will also effectively form heteroaggregates with ENPs resulting in an even larger effect on the removal of ENPs from the water phase. These data suggest that ENPs ultimately will end up in the sediment. Note that this would not apply to natural systems only, but also to *in vivo* whole sediment toxicity test systems, where sediment, suspended solids and DOC are present which will similarly govern the bioavailability of the ENPs in such test systems.

9.3 Retention of nanoparticles in lakes

Lake retention of pollutants is an important endpoint used in water quality management [26]. Retention in a water body is dependent on transport processes like advective flow, sedimentation, resuspension, horizontal bed load transfer and burial in deep sediment [15]. Spatially and temporarily explicit transport models may provide realistic estimations of retention in aquatic reservoirs, yet may be too complex and challenging given the present understanding of ENP behaviour in natural waters [16, 17, 24]. Here, a simple concept of lake retention is used to illustrate the implications of the aggregation and settling rates determined for ENPs in **Chapter 2 and 3** [6, 7]. Lake retention estimations require system properties, such as lake morphometry as well as physicochemical properties of the chemical accountable for degradation, speciation,

sorption and settling behaviour. The removal of pollutants in a lake is dependent on the outflow through which the pollutant can leave the lake and the sedimentation rate through which the pollutant ends up in the receiving sediment. Assuming that settling is the main removal process, a mass balance for a completely mixed lake as generally applied for nutrients and organic chemicals in water quality models can be used [26, 27]:

$$V \frac{dC}{dt} = Q(C_{in} - C) - \frac{v_s}{H} V C \quad (9.1)$$

in which V is the volume of the lake (m^3), C is the suspended ENP concentration ($g\ m^{-3}$), Q is the water discharge in the lake ($m^3\ s^{-1}$), C_{in} is the incoming ENP concentration ($g\ m^{-3}$), v_s is the sedimentation rate ($m\ d^{-1}$) and H is the average depth of the lake (m). As shown in **Chapter 2** and **3** [6, 7], ENP settling in natural waters is governed by heteroaggregation with NC throughout the entire water column and by heteroaggregation with SS, due to resuspension in the lower part of the water column, close to the sediment. As both sedimentation regimes can be approximated by first order removal, they can be included in Equation 9.1, weighted by the relative height of the water column (H_i/H). With $Q = V/\tau$, this gives [26]:

$$\frac{dC}{dt} = \frac{(C_{in}-C)}{\tau} - \left(\frac{H_{NC}v_{s,NC}}{H^2} + \frac{H_{SS}v_{s,SS}}{H^2} \right) C \quad (9.2)$$

in which τ is the hydraulic detention time (d), H_{NC} is the height of the water column in which settling with NC dominates (m) and H_{SS} is the height of the water column in which settling with SS dominates (m) and $H = H_{NC} + H_{SS}$, $v_{s,NC}$ is the relatively slow ENP sedimentation rate in presence of NC ($m\ d^{-1}$) and $v_{s,SS}$ is the fast sedimentation rate in presence of SS ($m\ d^{-1}$). Lake morphometry can be expressed as the Inverse Areal Hydraulic Loading, $IAHL = \tau/H$ ($d\ m^{-1}$), which can be interpreted as the general tendency for sedimentation in a lake. Under steady state conditions, the retention fraction for ENPs can be describes as:

$$R_{ENP} = 1 - \frac{C}{C_{in}} = \frac{\tau}{\tau + \frac{H^2}{H_{NC}v_{s,NC} + H_{SS}v_{s,SS}}} = \frac{IAHL}{IAHL + \frac{H}{H_{NC}v_{s,NC} + H_{SS}v_{s,SS}}} \quad (9.3)$$

in which R_{ENP} is the lake retention (-) which indicates the amount of accumulation of ENPs in the sediment as fraction of the input. Lake retention for CeO_2 , PVP-Ag and SiO_2 -Ag ENPs as a function of $IAHL$ was calculated for 25 existing lakes (Figure 9.1). Morphometry of these lakes with a wide range of lake residence time, depth and areal hydraulic loadings was taken from Koelmans et al. [26] (Table S9.1). ENP sedimentation rates determined in presence of NC and SS in a fresh water river were taken from **Chapter 2** and **3** [6, 7] (Table 3.1). H_{SS} is set on 1 m, assuming that sediment resuspension occurred from the sediment-water interface till 1 m above the sediment. This is typical for shallow lakes, reflecting the importance of wind induced resuspension [28]. The H_{SS} of 1 m might be too high for deep lakes where

turbulence is lower and probably dominated by bioturbation [29]. However, because the relative height of SS settling would be negligible in deep lakes, this uncertainty can be considered unimportant.

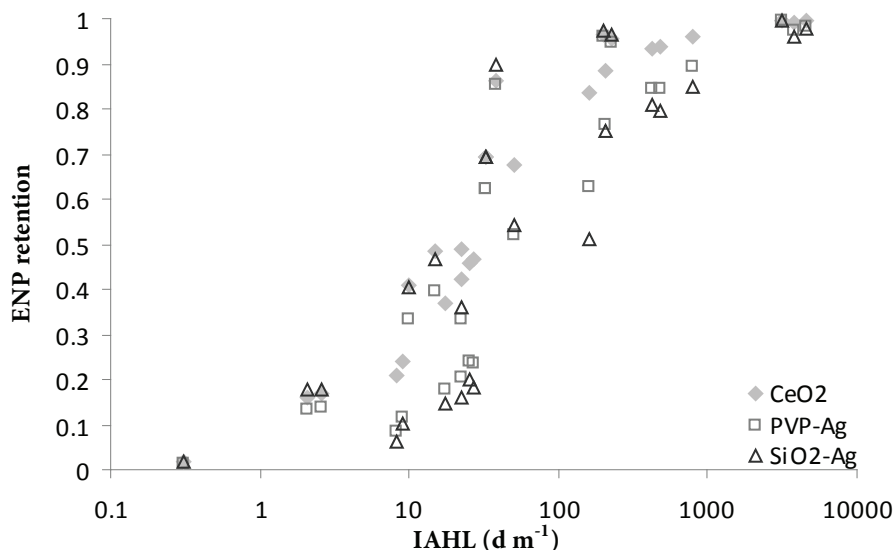


Figure 9.1 Retention CeO₂, PVP-Ag and SiO₂-Ag ENPs as function of IAHL for 25 world lakes (see Table S9.1). Retention is calculated using sedimentation rates from **Chapters 2 and 3** and actual morphometric data for 25 lakes [6, 7].

For lakes with $IAHL > 3000 \text{ d m}^{-1}$ (Table S9.1), the retention is close to 1 (i.e. 100%) for all three ENPs. This is the case for instance for lakes Columbia (USA), Tanganyika (Africa) and Titicaca (South America), but also for Lake Loosdrecht in the Netherlands. With an $IAHL$ of 197, retention would be between 96 and 97% in this lake. Retention in lakes with such high $IAHL$ is insensitive for differences in ENP sedimentation rates, even though the residence time and depth differ considerably between these lakes. The influence of ENP type is also negligible for lakes with an $IAHL < 1 \text{ d m}^{-1}$, as the ENPs already would have left the lake through the outflow before they could settle. The retention of CeO₂ is higher than or equal to the retention of the Ag ENPs, which can be explained by the higher sedimentation rate in presence of NC, especially for the deeper lakes where settling with NC is dominant. In general, the retention of PVP-Ag is higher than for SiO₂-Ag in deeper lakes, whereas in shallow lakes it is the other way around. This can be explained by the sedimentation rates with a higher $V_{s,NC}$ and lower $V_{s,SS}$ for PVP-Ag compared to SiO₂-Ag (**Chapter 2 and 3** [6, 7]). More specific ENP and lake morphometry data and spatially explicit detailed

system models accounting for stratification may provide more accurate predictions for heterogeneous lakes [30], yet the present method can be used more easily for screening a wide range of systems and ENP properties. When combining the ENP lake retention data with ENP emission data, the potential risks for benthic communities can be evaluated. With equal emissions, high retention relates to a higher exposure of benthic species, which are the lakes with a high *IAHL*. For lakes with a low *IAHL*, the main part of the ENPs leaves the lake through outflow. Note that the latter load however still may result in pollution with ENP downstream.

9.4 Implications for fate and exposure of ENP-associated toxicants

Another implication of ENPs in aquatic systems relates to their potential interactions with the cocktail of toxic hydrophobic compounds present in water systems. Depending on their chemical composition, ENPs can act as adsorbents for these compounds, which may reduce their bioavailability [5]. Here, the sorption of organic pollutants to carbon-based ENPs will be discussed, for which five types of interactions can be distinguished, i.e. hydrophobic binding, p-p bonding, hydrogen bonding, covalent bonding and electrostatic interactions. The structure and functional groups of the chemicals and the ENPs define the interactions and their strengths. The main surface of CNTs exists of hydrophobic graphene which is responsible for strong adsorption of organic chemicals. Interactions with polycyclic aromatic hydrocarbons (PAH) containing only aromatic rings may decrease the adsorption affinity for other organic chemicals, but not their adsorption capacity, while interactions with NOM could decrease both adsorption affinity and capacity [31]. The interaction with other chemicals is also dependent on the aggregation state of the CNT as the formation of aggregates will reduce the available surface area [31]. The number of studies on the interactions of ENPs and organic contaminants is growing. Most studies have addressed the sorption of PAH to carbon nanotubes (CNTs) (e.g. [31-37]). Sorption coefficients for PAHs to MWCNTs determined in different studies varied over a wide range [32, 33, 38]. These differences can be explained by differences in type of MWCNT, experimental set-up, aqueous concentration ranges, shape of the isotherm, type of sorption model used and the parameters used for these models. Sorption models that have been observed to provide good fits for aqueous sorption isotherms of organic chemicals to carbon-based ENPs are: linear, Freundlich, Langmuir, partition-adsorption and Polanyi isotherm models [31]. Detailed descriptions of these models are available in the literature (e.g. [39]).

Sorption behaviour of PFOS and PCBs to carbon-based ENPs was studied in **Chapter 4** and **5** [8, 9], respectively. For both PFOS and PCBs in artificial freshwater (near) linear sorption was observed for sediment, where sorption to MWCNTs in presence of sediment was highly non-linear, with Freundlich exponents (n) of 0.66

and on average 0.70 (0.39 – 1.06) for PFOS and PCBs respectively. Sorption of PCBs to MWCNTs without the presence of sediment, was also non-linear ($n = 0.65$), suggesting that the MWCNTs were the dominant factor in sorption behaviour. PCB sorption data were also obtained from experiments performed with natural seawater, where linear sorption was observed with average Freundlich exponents of 0.96 and 0.99 without and with the presence of sediment respectively. Interactions with dissolved organic matter (DOM) from the natural seawater, i.e. fouling, can explain this similarity with sorption to sediment and suggests that the influence of fouling and salinity was more dominant than the presence of MWCNTs. Salinity and the presence of sediment reduced the sorption coefficients for both PFOS and PCBs with MWCNTs. The higher sorption coefficients of PCBs to C_{60} compared to MWCNTs was explained by the higher total surface area of C_{60} . The experiments performed in **Chapter 4** and **5** [8, 9], illustrated the importance of competition mechanisms, fouling and characteristics of the receiving water system (e.g. pH, salinity and NOM content) for the interactions of ENPs and organic contaminants.

Because it is likely that ENPs will end up in the sediment (see above), a relevant question is whether their presence will affect bioaccumulation and toxicity of conventional chemicals for benthic species. Koelmans et al. [40] however, calculated that the extra binding to CNTs or C_{60} would be negligible with respect to that to natural nanoparticles e.g. soot particles, that are already present in almost all natural sediments. Ferguson et al. [41] saw a general decrease of bioaccumulation of PAHs, PCBs and polybrominated diphenyl ethers (PBDEs) in sediment-ingesting estuarine invertebrates when sediment was amended with 5 mg g⁻¹ singlewalled carbon nanotubes (SWCNTs) at levels similar to soot levels in highly contaminated harbour sediments. Petersen et al. [42] also observed a decrease of pyrene bioaccumulation in earthworms when 3 mg g⁻¹ SWCNTs or MWCNTs were added to soils. Baun et al. [43] observed increased toxicity to algae and crustaceans when C_{60} was associated with PAHs, which was explained by the ‘carrier effect’, suggesting that a part of the absorbed pollutant was still bioavailable. Xia et al. [44] supported the enhanced bioavailability of contaminants in presence of CNTs, dominated by mineralization of phenanthrene absorbed to MWCNTs instead of desorption. Hu et al. [45] also observed increased bioaccumulation in fish (medaka), but only for less hydrophobic organochlorine compounds associated to 5 mg L⁻¹ C_{60} in water. For small, highly hydrophobic compounds a decreased bioaccumulation was observed. All the above mentioned studies used relative high ENP concentrations, which were not environmentally relevant. Furthermore, from these studies it was not clear if avoidance of ENP-associated particles caused the reduction or that these organisms were not able to extract POPs from the ENPs, because uptake was not studied. When bioaccumulation of POPs was observed it was not clear whether there was uptake of the POP associated ENPs and if these organisms were able to extract POPs from the ENPs, because bioaccumulations of the ENPs was not observed. Schwab et al. [46] investigated uptake of CNTs by algae and reported that the tested algae did not uptake

CNTs. The observed enhanced bioavailability of contaminants in presence of CNTs was caused by attachment of the contaminated CNT on the surface of the algae. For perfluorinated compounds (PFCs), Xia et al [47] observed reduced bioaccumulation in *Chironomus plumosus* larvae up to 97% in sediment amended with 1.5% CNTs. This was caused by a reduction of aqueous phase concentration with increasing CNT concentration. For nanoplastics, Koelmans et al [48] calculated that ingestion would reduce bioaccumulation because non-digestible plastic would sorb POPs in the gut thus attenuating bioaccumulation. In summary, these laboratory studies show that at relatively high ENP concentrations, uptake and effects of conventional chemicals may be affected by the presence of ENPs. However, the studies are too diverse and fragmentary to see a general pattern in the data. Apart from these uncertainties of the effects of POP associated ENPs, it is important to know whether the contribution of ENP to the total concentration POPs in the sediment is sufficient to cause a substantial additional risk at environmentally realistic ENP concentrations [40, 46].

9.5 Retention of ENP-associated toxicants in lakes

The sorption of chemicals to carbon-based nanoparticles may influence the retention of these associated chemicals in lakes. An important question is whether this ENP related retention would be substantial. For instance, using the distribution coefficients for PCBs to MWCNTs and C_{60} in fresh water in the presence of sediment (**Chapter 5** [9]), the retention of PCBs due to ENPs can be estimated as:

$$R_{PCB} = R_{ENP} f_{PCB,ENP} = R_{ENP} \left(\frac{[ENP] K_d}{1 + [ENP] K_d} \right) \quad (9.4)$$

in which R_{PCB} is the retention of PCBs due to ENPs (-), $f_{PCB,ENP}$ is the fraction of the PCB concentration in the lake that is attached to ENPs (-), $[ENP]$ is the concentration ENPs in the lake (kg L^{-1}) and K_d is the apparent partition coefficient of the PCB to the ENP in the presence of sediment (L kg^{-1}). For the concentration ENPs in the lake ($[ENP]$), the predicted environmental concentrations (PEC) from Gottschalk et al. [18] were used (Table 9.1). For the calculation of the retention in 2008, the modeled concentrations from surface water in Europe were taken, with 0.004 and 0.017 ng L^{-1} for CNT and fullerenes respectively. Using the modeled annual increase based on annual production data [18], PEC values were extrapolated to 2025 and 2125, assuming that the ENP concentrations in 2000 were negligible and that the annual increase would remain the same. The partition coefficients of the PCBs to MWCNTs in the presence of sediment in fresh water were obtained from the $\log K_d - \log K_{ow}$ regression provided in **Chapter 5** [9]. The partition coefficients of PCBs to pristine C_{60} in freshwater were reduced with 4% to account for sorption attenuation by fouling with organic matter from the sediment. A 4% reduction was chosen because this was the average reduction observed in the sorption experiments with MWCNTs (**Chapter**

5 [9]). In order to assess the influence of lake morphometry, *IAHL* values of 1, 10, 100 and 1000 d m⁻¹ with associated *H* of 5, 50 100 and 250 m respectively, were used. H_{SS} was kept to 1 m, with $H_{NC} = H - H_{SS}$. For $v_{s,NC}$ the v_s of C_{60} of fresh water river (**Chapter 2** [6]), i.e. 0.136 m d⁻¹ was used and for $v_{s,SS}$ the average v_s of the turbulent systems in presence of sediment (**Chapter 3** [7]), i.e. 0.285 m d⁻¹ was used. This value was comparable for the different ENPs and close to the sedimentation rates of SS. To be able to compare retention due to sorption to ENPs with retention caused by sorption to natural suspended solids, retention by the latter solids (SS) was also determined. For these calculations the term $H_{NC} \times v_{s,NC}$ in Eq. 9.3 was set to zero, K_d values for PCB sorption to sediment as determined in **Chapter 5** [9] were used, and the value for the solid concentration [ENP] was replaced by that of [SS] with a value of 15 mg L⁻¹. Subsequently, the R_{PCB} for SS was used together with R_{PCB} for ENPs to quantify the percentage of the PCB retention caused by ENPs compared to that caused by the common suspended solids SS. It appears that the expected PCB retention caused by C_{60} and MWCNTs for 2008, 2025 and 2025 are highly dependent on $\log K_{ow}$ and *IAHL* (Figure 9.2; Table 9.1). The contribution of C_{60} on the total retention of PCBs by C_{60} and SS increased from 0.09 – 1.2% in 2008 to 0.27 – 3.9% in 2025 and 1.4 – 19.1% in 2125. The contribution of MWCNTs to lake retention is negligible and increased from $2.0 \cdot 10^{-4}$ – $7.7 \cdot 10^{-3}$ % in 2008 to $6.1 \cdot 10^{-4}$ – $2.4 \cdot 10^{-2}$ % in 2025 and $3.1 \cdot 10^{-3}$ – 0.12% in 2125. The retention of PCBs is higher with increasing hydrophobicity due to the stronger binding of more hydrophobic PCBs to the carbon-based ENPs. The PCB retention caused by C_{60} is higher than for MWCNTs because of the higher K_d values and higher PEC for C_{60} [18]. With increasing *IAHL*, the retention of ENPs increased because of the increased residence times and lower lake depths associated with increasing *IAHL* (Figure 9.1). The *percentage* of PCB retention caused by ENPs was the highest at an *IAHL* of 10 d m⁻¹ and decreased with increasing *IAHL*, because of the difference in K_{ow} dependence between the K_d of ENPs and SS. $\log K_d$ of SS increased linear with $\log K_{ow}$ with a slope of 1, while $\log K_d$ of ENPs increased less. The R_{PCB} with the *IAHL* of 1 d m⁻¹ was between the *IAHL* of 100 and 1000 d m⁻¹, as the time to settle was not long enough so that removal was dominated by outflow.

A similar calculation for MWCNT and PFOS using the data from **Chapter 4** [8] also showed very low contributions to lake retention (i.e. $9.5 \cdot 10^{-7}$ – $7.2 \cdot 10^{-6}$ % in 2008; $3.0 \cdot 10^{-6}$ – $2.3 \cdot 10^{-5}$ % in 2025; $1.5 \cdot 10^{-5}$ – $1.1 \cdot 10^{-4}$ % in 2125), even lower than those of the MWCNTs for PCBs due to the lower binding strength of PFOS to MWCNTs compared to that of PCBs.

In summary, from these data we conclude that despite the expected increasing future emissions, the contribution of ENPs on the retention of PFOS and POPs like PCBs is generally negligible. An increase in retention, i.e. concentration in sediment of about 20% for C_{60} may be considered rather small in terms of relevance for the risk assessment of ENPs and associated chemicals. In the long run however, such percentages may be considered relevant for the long term fate processes of ENP fate in aquatic reservoirs.

9.6 Effects of ENPs in the aquatic environment

Due to the release and distribution of ENPs in the aquatic environment, exposure to organisms is inevitable, which may have effects on single species, populations, communities or entire food webs. To assess dose-response relationships and to identify

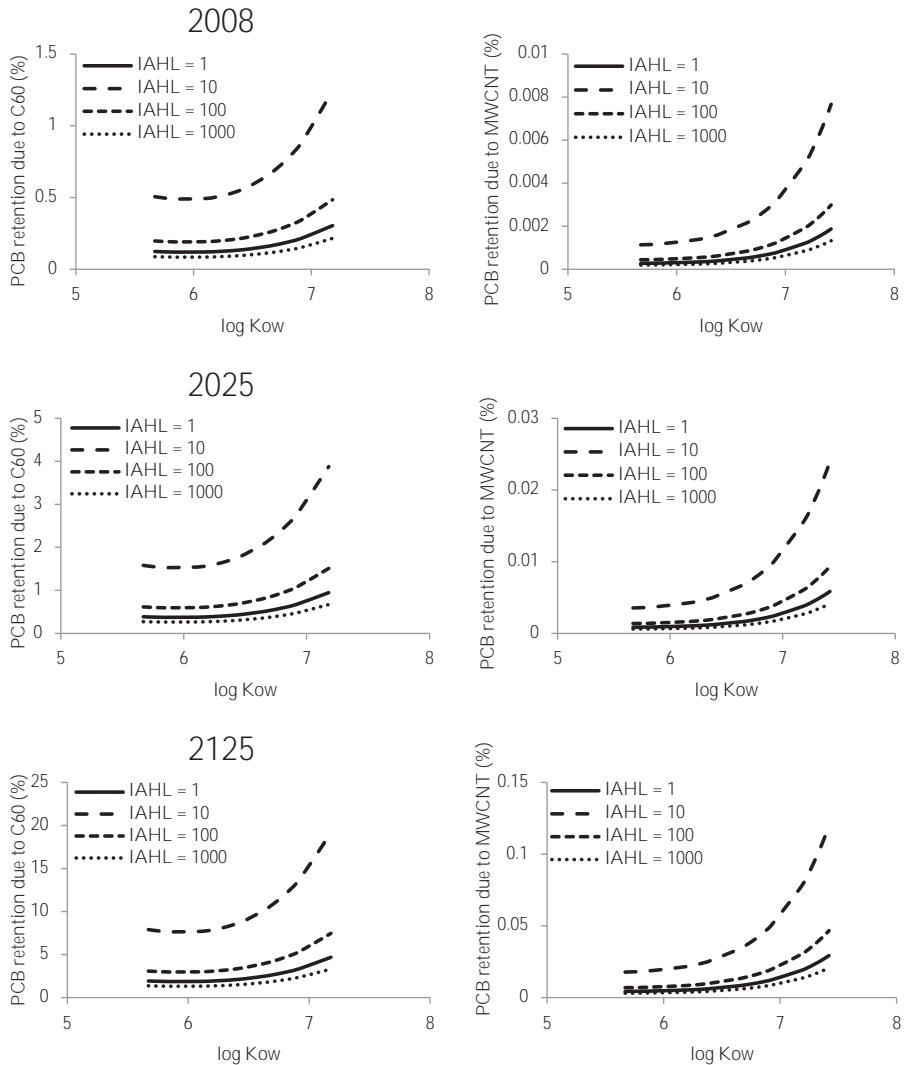


Figure 9.2 PCB retention caused by C₆₀ (left hand side panels) and MWCNTs (right hand side) calculated for 2008, 2025) and 2125 as a percentage of total retention due to settling of the ENPs and natural suspended solids present.

toxicity mechanisms, single species laboratory tests are available. However, these tests are still under development, because standard toxicity tests are not always suitable for ENPs (**Chapter 6**) [10, 49]. Gottschalk et al. [50] provided an overview of ENP effect thresholds in order to construct species sensitivity distributions (SSDs) for ENPs. Here we updated their list with data from four additional studies leading to a more extensive overview of ENP effect thresholds for a range of aquatic and benthic species tested with single species aquatic ecotoxicity tests (Table 9.2).

Table 9.2 Effect thresholds of ENPs on aquatic and benthic organisms.

ENP type	Organisms tested	Effect threshold (mg L ⁻¹)	Reference
C ₆₀	Alga (<i>Chlamydomonas reinhardtii</i>)	1	[50]
	Crustacean (<i>Daphnia magna</i>)	0.85	[3, 4, 50] ^a
	Amphipod (<i>Hyalella azteca</i>)	7	[4]
	Zebrafish (<i>Danio rerio</i>)	2.2	[3, 4, 50] ^a
	Goldfish (<i>Carassius auratus</i>)	0.04	[50]
	Largemouth bass (<i>Micropterus salmoides</i>)	0.5	[3, 4]
	Fathead minnow (<i>Pimephales promelas</i>)	0.5	[4]
CNT	Alga (<i>Dunaliella tertiolecta</i>)	0.82	[50]
	Alga (<i>Chlorella vulgaris</i>)	0.6	[50] ^a
	Alga (<i>Pseudokirchneriella subcapitata</i>)	2	[50] ^a
	Copepod (<i>Amphiascus tenuiremis</i>)	1.6	[50]
	Crustacean (<i>Ceriodaphnia dubia</i>)	78	[50] ^a
	Crustacean (<i>Daphnia magna</i>)	3.2	[3, 4, 50] ^a
	Amphipod (<i>Leptocheirus plumulosus</i>)	68 ^c	[51]
	Amphipod (<i>Hyalella azteca</i>)	264 ^c	[51]
	Oligochaete (<i>Lumbriculus variegatus</i>)	0.03 ^c	[51]
	Polychaete worm (<i>Arenicola marina</i>)	0.03 ^c	[51]
	Zebrafish (<i>Danio rerio</i>)	105	[3, 50] ^a
	Rainbow trout (<i>Oncorhynchus mykiss</i>)	0.2	[3, 4] ^a
	Cu	Zebrafish (<i>Danio rerio</i>)	1.5
CuO	Algae	2.8	[52]
	Crustaceans	2.1	[52]
	Fish	100	[52]
Ag	Alga (<i>Chlamydomonas reinhardtii</i>)	0.12	[50, 52] ^a
	Alga (<i>Pseudokirchneriella subcapitata</i>)	0.09	[50, 52] ^a
	Crustacean (<i>Ceriodaphnia dubia</i>)	0.006	[50, 52] ^a
	Crustacean (<i>Daphnia magna</i>)	0.013	[50, 52] ^a
	Nematode (<i>Ceanorhabditis elegans</i>)	3.34	[50, 52] ^a
	Zebrafish (<i>Danio rerio</i>)	0.8	[50, 52] ^a
	Fathead minnow (<i>Pimephales promelas</i>)	1	[50, 52] ^a
	Medaka (<i>Oryzias latipes</i>)	0.4	[50, 52] ^a

Table 9.2 Continued

ENP type	Organisms tested	Effect threshold (mg L ⁻¹)	Reference	
TiO ₂	Alga (<i>Chlorella sp.</i>)	16	[50] ^a	
	Alga (<i>Pseudokirchneriella subcapitata</i>)	26.3	[10, 50] ^{a,b}	
	Alga (<i>Scenedesmus subspicatus</i>)	21.2	[50]	
	Alga (<i>Desmodesmus subspicatus</i>)	44	[3, 50]	
	Cladoceran (<i>Chydorus sphaericus</i>)	100	[10] ^b	
	Crustacean (<i>Ceriodaphnia dubia</i>)	50.4	[50] ^a	
	Crustacean (<i>Daphnia magna</i>)	0.9	[3, 4, 50] ^a	
	Nematode (<i>Ceanorhabditis elegans</i>)	80	[50]	
	Zebrafish (<i>Danio rerio</i>)	124.5	[50]	
	Rainbow trout (<i>Oncorhynchus mykiss</i>)	1	[3, 4, 50]	
	Fathead minnow (<i>Pimephales promelas</i>)	500	[50]	
	ZnO	Alga (<i>Chlamydomonas reinhardtii</i>)	1	[50]
		Alga (<i>Pseudokirchneriella subcapitata</i>)	0.05	[3, 50, 52] ^a
Alga (<i>Chlorella sp.</i>)		5	[50]	
Alga (<i>Dunaliella tertiolecta</i>)		0.5	[50]	
Alga (<i>Isochrysis galbana</i>)		0.5	[50]	
Alga (<i>Skeletonema marinoi</i>)		0.5	[50]	
Alga (<i>Thalassiosira pseudonana</i>)		0.7	[50, 52] ^a	
Crustacean (<i>Daphnia magna</i>)		2.5	[50, 52] ^a	
Crustacean (<i>Thamnocephalus platyurus</i>)		0.3	[50] ^a	
Nematode (<i>Ceanorhabditis elegans</i>)		33.6	[50, 52] ^a	
Zebrafish (<i>Danio rerio</i>)		3.3	[50, 52] ^a	
ZrO ₂	Alga (<i>Pseudokirchneriella subcapitata</i>)	100	[10] ^b	
Al ₂ O ₃	Alga (<i>Pseudokirchneriella subcapitata</i>)	100	[10] ^b	
	Cladoceran (<i>Chydorus sphaericus</i>)	100	[10] ^b	
CeO ₂	Alga (<i>Pseudokirchneriella subcapitata</i>)	100	[10] ^b	
	Cladoceran (<i>Chydorus sphaericus</i>)	100	[10] ^b	
PMMA	Alga (<i>Pseudokirchneriella subcapitata</i>)	100	[10] ^b	
	Cladoceran (<i>Chydorus sphaericus</i>)	100	[10] ^b	

^a geometric mean of the different studies

^b this thesis, **Chapter 6**

^c for the benthic species, the unit is mg g⁻¹

For most ecotoxicity tests aquatic species were used. The benthic species that were used were all exposed to carbon based ENPs with effect thresholds in sediment between 0.03 and 264 mg g⁻¹ (Table 9.2) [51]. These thresholds were 4 to 8 orders of magnitude higher than the environmental concentrations in sediment estimated for 2008 (Table 9.1), and still 3 to 7 orders of magnitude higher compared to the estimated concentrations for 2125. For the pelagic aquatic species, effects were shown at concentrations of 0.006 mg L⁻¹ to 500 mg L⁻¹. In 2008, the highest environmental

concentration was assumed for TiO_2 , presuming a reasonable chance for hazards of TiO_2 . However, this concentration still was 4 orders of magnitude lower than the effect threshold from the single species toxicity tests for TiO_2 . An indication for future risk can be provided by dividing the predicted environmental concentration (PEC; Table 9.1) estimated for 2125 by the lowest measured effect threshold (Table 9.2), assumed as no effect concentration (NEC) and considered as a risk when higher than 1. PEC/NEC ratios of $3.0 \cdot 10^{-4}$ for TiO_2 , $2.0 \cdot 10^{-3}$ for Ag, $3.2 \cdot 10^{-3}$ for ZnO, $2.1 \cdot 10^{-3}$ for CNT and $6.7 \cdot 10^{-6}$ for fullerenes were calculated, suggesting that substantial risks of ENPs are not indicated for the near future when considering the single species toxicity data.

Considering ENP exposure concentrations separately might underestimate risks if different ENPs are present in mixtures and each of them would cause a similar effect on a species. When considering the sum of the ENP concentrations relative to their individual effect threshold and provisionally assuming effect addition, an overall risk of $7.5 \cdot 10^{-3}$ is anticipated, which still is not considered to represent a substantial risk.

For a risk assessment of ENPs, environmentally realistic toxicity tests are to be preferred. ENPs will most probably not enter water systems as pristine particles. If any 'pristine' or 'free' ENP enters an aquatic system it will probably soon be present associated with sediment, suspended solids and DOC at low environmentally relevant concentrations. Ideally, effect tests should include these natural components and processes that affect the bioavailability of ENPs, and they should also include chronic and multi-generation exposure. Furthermore, field studies are relevant to better approach ecologically relevant conditions concerning whole communities. Significant effects of MWCNT amended sediment on the composition of the benthic community were observed after exposure of 15 months already at the lowest test concentration of 0.002 mg g^{-1} (**Chapter 7 and 8** [11, 12]). This effect threshold concentration is 4 orders of magnitude lower than for example the observed LC_{50} of 68 mg g^{-1} for the amphipod *Leptocheirus plumulosus* (Table 9.2). It is difficult to identify effect mechanisms from field studies, but naturally occurring factors are automatically incorporated in the dose effects relationship observed *in situ*, which are not covered in short-term laboratory tests. The observed effects suggest that the effect thresholds in long term field tests may be much lower than expected from short term single species laboratory toxicity tests [53].

Gottschalk et al [50] used single species toxicity data for a probabilistic species sensitivity distribution (PSSD) together with predicted environmental concentrations for a risk estimation, where risk was expected when the PEC and the PSSD overlapped. When comparing the concentration of 0.002 mg g^{-1} , which was the lowest observed effect concentration (LOEC) on the benthic community (**Chapter 8** [12]) with the 2008 PEC for CNT of $1.93 \text{ } \mu\text{g kg}^{-1}$ (Table 9.1), the exposure concentrations are 3 orders of magnitude lower than the effect concentrations. Even when reducing the LOEC with a factor of 2 (e.g. 1 mg kg^{-1}) to transform to the no observed effect concentration (NOEC), as was done by Gottschalk et al. [50], and comparing this with the estimated

PEC for 2125 (e.g. 0.03 mg kg^{-1}), the PEC/NEC ratio is 0.03, suggesting that a potential risk is not indicated for the near future based on these data. However, the community experiments (**Chapter 8** [12]) detected effects at the lowest concentration tested, which therefore does not exclude the possibility of effects at even lower concentrations. Furthermore, the community experiments studied recolonization potential in rather small aquaria. It is plausible that the magnitude of effects on recolonization also relates to the size of these experimental units. For instance, after a year of exposure, Samuelsson [54] observed much more negative effects of activated carbon (AC) in recolonization experiments using 100 by 100 m exposure units than Kupryianchyk et al. [55] did, using the same small experimental units as those presently used for MWCNTs. This means that recolonization effect threshold concentrations for MWCNTs may also be lower for larger experimental units. Finally, mixture toxicity effects were not included in the present community experiments whereas ENPs obviously will be present as mixtures in the environment. This implies that long term larger scale community tests with ENP mixtures at realistic concentrations are required before more reliable conclusions on absence of effects can be drawn.

9.7 Concluding remarks and future perspectives

This thesis has provided sedimentation and heteroaggregation rates of ENPs in natural waters, which shows the importance of NC and SS on the fate of ENPs (**Chapter 2** and **3** [6, 7]). NC and SS are dominant in the removal of ENPs from the water phase as these particles form heteroaggregates with ENPs, enhance the sedimentation rates and contribute to the retention of ENPs in lakes (**Chapter 9**). The contribution of NC and SS is dependent on the type of water. SS play a dominant role in shallow lakes and rivers, whereas NC may be the dominant factor in deep lakes and oceans. The presented procedures for deriving sedimentation and aggregation rates may find further application in constraining parameter values for ENP fate models, or in the design of whole sediment ENP toxicity test set ups where understanding of fate processes is crucial to assess the actual bioavailability of ENPs for the organisms tested. To improve the fate and effect assessment, models should not use parameters for pristine ENPs because processes in natural waters affect these parameters (**Chapter 2** and **3** [6, 7]). The heteroaggregation and sedimentation rates and partition coefficients provided in this thesis are all derived from systems using natural waters and sediments and therefore are supposed to provide more realistic model predictions.

The sorption of PFOS and POPs like PCBs to carbon-based ENPs was determined and showed the importance of fouling and sorption competition mechanisms on their interactions (**Chapter 4** and **5** [8, 9]). The presence of sediment and DOC, but also salinity affected the sorption behaviour of these contaminants to carbon-based ENPs. Presence of ENPs in lakes or reservoirs will probably not substantially affect the fate or risk of these traditional chemicals because the contribution of ENP mediated retention

to total retention generally was small (**Chapter 9**). The strong association with carbon-based ENPs might however affect the bioaccumulation of POPs to aquatic organisms, due to transfer of POPs from nanoplastics, C₆₀ or CNTs nanoparticles in the gut or due to translocation of the particles with their associated toxicant load. It is important to further address the role of translocation and membrane transfer in nanoparticle mediated toxicity of traditional chemicals [56], or the combined effects of ENPs with these chemicals.

The single species toxicity tests and the long term community study showed that effect thresholds may be lower in the field than expected from laboratory tests (**Chapter 6, 7 and 8** [10-12]). Long-term *in situ* community effect assessments for ENPs incorporate many naturally occurring factors that may affect the toxicity of ENPs that are not covered in short-term laboratory tests. Obviously, effects on reproduction or early life stage development will be more important in chronic tests. The fact that effect thresholds observed in the long term community experiments were relatively low may be considered alarming and warrants more research under ecologically relevant conditions.

Based on the most recent predictions on environmental concentrations and effect thresholds of ENPs, a risk of ENPs is not yet clearly indicated for the near future. However, the environmental concentrations are still best educated estimates, based on the engineered part of the total nanosized fraction. These estimates are not yet validated by measured environmental concentrations [16]. Analytical methods for the complex environmental matrices are incomplete, and further development of methods to quantify actual bioavailable ENP concentrations in environmental media is required to validate model predictions.

References

- [1] Science Policy Council. 2007. U.S. Environmental Protection Agency Nanotechnology White Paper. EPA 100/B-07/001. U.S. Environmental Protection Agency, Washington, DC.
- [2] The Royal Society & The Royal Academy of Engineering. 2004. Nanoscience and nanotechnologies: opportunities and uncertainties. The Royal Society & The Royal Academy of Engineering, London.
- [3] Klaine SJ, Alvarez PJJ, Batley GE, Fernandes TF, Handy RD, Lyon DY, Mahendra S, McLaughlin MJ, Lead JR. 2008. Nanomaterials in the environment: Behavior, fate, bioavailability, and effects. *Environmental Toxicology and Chemistry* 27:1825-1851.
- [4] Handy RD, von der Kammer F, Lead JR, Hasselov M, Owen R, Crane M. 2008. The ecotoxicology and chemistry of manufactured nanoparticles. *Ecotoxicology* 17:287-314.
- [5] Nowack B, Bucheli TD. 2007. Occurrence, behavior and effects of nanoparticles in the environment. *Environmental Pollution* 150:5-22.
- [6] Quik JTK, Velzeboer I, Wouterse M, Koelmans AA, van de Meent D. 2014. Heteroaggregation and sedimentation rates for nanomaterials in natural waters. *Water Research* 48:269-279.
- [7] Velzeboer I, Quik, J.T.K., van de Meent, D., Koelmans, A.A. 2014. Rapid settling of nanoparticles due to heteroaggregation with suspended sediment. *Environmental Toxicology and Chemistry* submitted.
- [8] Kwadijk CJAF, Velzeboer I, Koelmans AA. 2013. Sorption of perfluorooctane sulfonate to carbon nanotubes in aquatic sediments. *Chemosphere* 90:1631-1636.
- [9] Velzeboer I, Kwadijk, C.J.A.F., Koelmans, A.A. 2014. Strong sorption of PCBs to nanoplastics, microplastics, carbon nanotubes and fullerenes. *Environmental Science & Technology* submitted.
- [10] Velzeboer I, Hendriks AJ, Ragas AMJ, Van de Meent D. 2008. Aquatic ecotoxicity tests of some nanomaterials. *Environmental Toxicology and Chemistry* 27:1942-1947.
- [11] Velzeboer I, Kupryianchuk D, Peeters ETHM, Koelmans AA. 2011. Community effects of carbon nanotubes in aquatic sediments. *Environment International* 37:1126-1130.
- [12] Velzeboer I, Peeters E, Koelmans AA. 2013. Multiwalled Carbon Nanotubes at Environmentally Relevant Concentrations Affect the Composition of Benthic Communities. *Environmental Science & Technology* 47:7475-7482.
- [13] Westerhoff P, Nowack B. 2013. Searching for Global Descriptors of Engineered Nanomaterial Fate and Transport in the Environment. *Accounts of Chemical Research* 46:844-853.
- [14] Wiesner MR, Lowry GV, Jones KL, Hochella MF, Di Giulio RT, Casman E, Bernhardt ES. 2009. Decreasing Uncertainties in Assessing Environmental Exposure, Risk, and Ecological Implications of Nanomaterials. *Environmental Science & Technology* 43:6458-6462.
- [15] Praetorius A, Scheringer M, Hungerbühler K. 2012. Development of Environmental Fate Models for Engineered Nanoparticles-A Case Study of TiO₂ Nanoparticles in the Rhine River. *Environmental Science & Technology* 46:6705-6713.

- [16] Gottschalk F, Sun T, Nowack B. 2013. Environmental concentrations of engineered nanomaterials: Review of modeling and analytical studies. *Environmental Pollution* 181:287-300.
- [17] Nowack B, Ranville JF, Diamond S, Gallego-Urrea JA, Metcalfe C, Rose J, Horne N, Koelmans AA, Klaine SJ. 2012. Potential scenarios for nanomaterial release and subsequent alteration in the environment. *Environmental Toxicology and Chemistry* 31:50-59.
- [18] Gottschalk F, Sonderer T, Scholz RW, Nowack B. 2009. Modeled Environmental Concentrations of Engineered Nanomaterials (TiO₂, ZnO, Ag, CNT, Fullerenes) for Different Regions. *Environmental Science & Technology* 43:9216-9222.
- [19] Christian P, Von der Kammer F, Baalousha M, Hofmann T. 2008. Nanoparticles: structure, properties, preparation and behaviour in environmental media. *Ecotoxicology* 17:326-343.
- [20] Petosa AR, Jaisi DP, Quevedo IR, Elimelech M, Tufenkji N. 2010. Aggregation and Deposition of Engineered Nanomaterials in Aquatic Environments: Role of Physicochemical Interactions. *Environmental Science & Technology* 44:6532-6549.
- [21] Arvidsson R, Molander S, Sanden BA, Hasselov M. 2011. Challenges in Exposure Modeling of Nanoparticles in Aquatic Environments. *Human and Ecological Risk Assessment* 17:245-262.
- [22] Quik JTK, Lynch I, Van Hoecke K, Miermans CJH, De Schamphelaere KAC, Janssen CR, Dawson KA, Stuart MAC, Van de Meent D. 2010. Effect of natural organic matter on cerium dioxide nanoparticles settling in model fresh water. *Chemosphere* 81:711-715.
- [23] Quik JTK, Stuart MC, Wouterse M, Peijnenburg W, Hendriks AJ, van de Meent D. 2012. Natural colloids are the dominant factor in the sedimentation of nanoparticles. *Environmental Toxicology and Chemistry* 31:1019-1022.
- [24] Praetorius A, Arvidsson R, Molander S, Scheringer M. 2013. Facing complexity through informed simplifications: a research agenda for aquatic exposure assessment of nanoparticles. *Environmental Science: Processes & Impacts* 15:161-168.
- [25] Newman KA, Morel FMM, Stolzenbach KD. 1990. Settling and coagulation characteristics of fluorescent particles determined by flow-cytometry and fluorometry *Environmental Science & Technology* 24:506-513.
- [26] Koelmans AA, Quik, J.T.K., Velzeboer, I., de Klein, J.J.M. 2014. Lake retention of manufactured nanoparticles. *Environmental Toxicology and Chemistry* in prep.
- [27] Lijklema L, Koelmans AA, Portielje R. 1993. Water-quality impacts of sediment pollution and the role of early diagenesis. *Water Science and Technology* 28:1-12.
- [28] Aalderink RH, Lijklema L, Breukelman J, Vanraaphorst W, Brinkman AG. 1985. Quantification of wind induced resuspension in a shallow lake. *Water Science and Technology* 17:903-914.
- [29] Stolzenbach KD, Newman KA, Wong CS. 1992. Aggregation of fine particles at the sediment-water interface. *Journal of Geophysical Research-Oceans* 97:17889-17898.
- [30] Quik JTK, De Klein J, Koelmans AA. 2014. Spatially explicit fate modelling of nanomaterials in water. In preparation
- [31] Yang K, Xing BS. 2010. Adsorption of Organic Compounds by Carbon Nanomaterials in Aqueous Phase: Polanyi Theory and Its Application. *Chemical Reviews* 110:5989-6008.

- [32] Kah M, Zhang X, Jonker MTO, Hofmann T. 2011. Measuring and Modeling Adsorption of PAHs to Carbon Nanotubes Over a Six Order of Magnitude Wide Concentration Range. *Environmental Science & Technology* 45:6011-6017.
- [33] Zhang X, Kah M, Jonker MTO, Hofmann T. 2012. Dispersion State and Humic Acids Concentration-Dependent Sorption of Pyrene to Carbon Nanotubes. *Environmental Science & Technology* 46:7166-7173.
- [34] Wang XL, Tao S, Xing BS. 2009. Sorption and Competition of Aromatic Compounds and Humic Acid on Multiwalled Carbon Nanotubes. *Environmental Science & Technology* 43:6214-6219.
- [35] Yang K, Wang X, Zhu L, Xing B. 2006. Competitive Sorption of Pyrene, Phenanthrene, and Naphthalene on Multiwalled Carbon Nanotubes. *Environmental Science & Technology* 40:5804-5810.
- [36] Yang K, Zhu L, Xing B. 2006. Adsorption of Polycyclic Aromatic Hydrocarbons by Carbon Nanomaterials. *Environmental Science & Technology* 40:1855-1861.
- [37] Yang K, Jing QF, Wu WH, Zhu LZ, Xing BS. 2010. Adsorption and Conformation of a Cationic Surfactant on Single-Walled Carbon Nanotubes and Their Influence on Naphthalene Sorption. *Environmental Science & Technology* 44:681-687.
- [38] Pan B, Xing BS. 2008. Adsorption Mechanisms of Organic Chemicals on Carbon Nanotubes. *Environmental Science & Technology* 42:9005-9013.
- [39] Allen-King RM, Grathwohl P, Ball WP. 2002. New modeling paradigms for the sorption of hydrophobic organic chemicals to heterogeneous carbonaceous matter in soils, sediments, and rocks. *Advances in Water Resources* 25:985-1016.
- [40] Koelmans AA, Nowack B, Wiesner MR. 2009. Comparison of manufactured and black carbon nanoparticle concentrations in aquatic sediments. *Environmental Pollution* 157:1110-1116.
- [41] Ferguson PL, Chandler GT, Templeton RC, Demarco A, Scrivens WA, Englehart BA. 2008. Influence of sediment-amendment with single-walled carbon nanotubes and diesel soot on bioaccumulation of hydrophobic organic contaminants by benthic invertebrates. *Environmental Science & Technology* 42:3879-3885.
- [42] Petersen EJ, Pinto RA, Landrum PF, Weber WJ. 2009. Influence of Carbon Nanotubes on Pyrene Bioaccumulation from Contaminated Soils by Earthworms. *Environmental Science & Technology* 43:4181-4187.
- [43] Baun A, Sørensen SN, Rasmussen RF, Hartmann NB, Koch CB. 2008. Toxicity and bioaccumulation of xenobiotic organic compounds in the presence of aqueous suspensions of aggregates of nano-C60. *Aquatic Toxicology* 86:379-387.
- [44] Xia X, Li Y, Zhou Z, Feng C. 2010. Bioavailability of adsorbed phenanthrene by black carbon and multi-walled carbon nanotubes to *Agrobacterium*. *Chemosphere* 78:1329-1336.
- [45] Hu X, Liu J, Zhou Q, Lu S, Liu R, Cui L, Yin D, Mayer P, Jiang G. 2010. Bioavailability of organochlorine compounds in aqueous suspensions of fullerene: Evaluated with medaka (*Oryzias latipes*) and negligible depletion solid-phase microextraction. *Chemosphere* 80:693-700.

- [46] Schwab F, Bucheli TD, Camenzuli L, Magrez A, Knauer K, Sigg L, Nowack B. 2012. Diuron Sorbed to Carbon Nanotubes Exhibits Enhanced Toxicity to *Chlorella vulgaris*. *Environmental Science & Technology* 47:7012-7019.
- [47] Xia X, Chen X, Zhao X, Chen H, Shen M. 2012. Effects of Carbon Nanotubes, Chars, and Ash on Bioaccumulation of Perfluorochemicals by *Chironomus plumosus* Larvae in Sediment. *Environmental Science & Technology* 46:12467-12475.
- [48] Koelmans AA, Besseling E, Wegner A, Foekema EM. 2013. Plastic as a Carrier of POPs to Aquatic Organisms: A Model Analysis. *Environmental Science & Technology* 47:7812-7820.
- [49] Handy RD, Cornelis G, Fernandes T, Tsyusko O, Decho A, Sabo-Attwood T, Metcalfe C, Steevens JA, Klaine SJ, Koelmans AA, Horne N. 2012. Ecotoxicity test methods for engineered nanomaterials: Practical experiences and recommendations from the bench. *Environmental Toxicology and Chemistry* 31:15-31.
- [50] Gottschalk F, Kost E, Nowack B. 2013. Engineered nanomaterials in water and soils: A risk quantification based on probabilistic exposure and effect modeling. *Environmental Toxicology and Chemistry* 32:1278-1287.
- [51] Petersen EJ, Zhang L, Mattison NT, O'Carroll DM, Whelton AJ, Uddin N, Nguyen T, Huang Q, Henry TB, Holbrook RD, Chen KL. 2011. Potential Release Pathways, Environmental Fate, And Ecological Risks of Carbon Nanotubes. *Environmental Science & Technology* 45:9837-9856.
- [52] Bondarenko O, Juganson K, Ivask A, Kasemets K, Mortimer M, Kahru A. 2013. Toxicity of Ag, CuO and ZnO nanoparticles to selected environmentally relevant test organisms and mammalian cells in vitro: a critical review. *Archives of Toxicology* 87:1181-1200.
- [53] Arndt DA, Moua M, Chen J, Klaper RD. 2013. Core Structure and Surface Functionalization of Carbon Nanomaterials Alter Impacts to Daphnid Mortality, Reproduction, and Growth: Acute Assays Do Not Predict Chronic Exposure Impacts. *Environmental Science & Technology* 47:9444-9452.
- [54] Samuelsson GS. 2013. In situ remediation of contaminated sediments using thin-layer capping: efficiency in contaminant retention and ecological implications. Ph.D Dissertation, Stockholm University, Stockholm.
- [55] Kupryianchyk D, Peeters ETHM, Rakowska MI, Reichman EP, Grotenhuis JTC, Koelmans AA. 2012. Long-Term Recovery of Benthic Communities in Sediments Amended with Activated Carbon. *Environmental Science & Technology* 46:10735-10742.
- [56] Rossi G, Barnoud J, Monticelli L. 2014. Polystyrene Nanoparticles Perturb Lipid Membranes. *Journal of Physical Chemistry Letters* 5:241-246.

Supporting Information

Table S9.1 Residence times, mean depths and inverse areal hydraulic loading (IAHL) of twenty-five world lakes, listed in the order of increasing IAHL (Koelmans et al. [26]).

Lake	Country	Residence Time (d)	Mean Depth (m)	IAHL τ/H (d m ⁻¹)
Wohlen	Switzerland	2.1	6.85	0.31
St Clair	Canada	7.0	3.4	2.06
Milton Pond	USA	11.1	4.3	2.58
Maggiore	Italy	1460	177.4	8.23
Zurich	Switzerland	440	49	8.98
Derwent	UK	55	5.5	10.0
Esthwaite	UK	95	6.4	14.8
Constance/Bodensee	GE, SW, AU, LIE	1570	90	17.4
Lugano	Switzerland, Italy	2993	134	22.3
Greifen	Switzerland	408	18	22.7
Ontario	Canada, USA	2190	86	25.5
Geneva	Switzerland, France	4161	154.4	27.0
IJssel	The Netherlands	182	5.5	33.1
Veluwe	The Netherlands	60	1.55	38.7
Erie	USA	949	19	50.0
Baikal	Russia	120450	744.4	161.8
Loosdrecht	The Netherlands	365	1.85	197.3
Victoria	Africa	8395	40	209.9
Balaton	Hungary	730	3.2	228.1
Michigan	USA	36135	85	425.1
Superior	USA	69715	147	474.3
Tahoe	USA	237250	300	790.8
Columbia	USA	17155	5.5	3119
Tanganyika	Africa	2190000	570	3842
Titicaca	S. America	490195	107	4581

Addendum



Summary
Samenvatting
Dankwoord
Curriculum vitae
List of publications
SENSE certificate



TiO₂ MWCNTs ZrO₂ TiO₂ CeO₂ MWCNTs CeO₂ SWCNTs SiO₂-Ag
SWCNTs PMMA Al₂O₃ PFOS PVP-Ag CeO₂ MWCNTs PVP-Ag SWCNTs
nano-PS C₆₀ micro-PE C₆₀ SiO₂-Ag TiO₂ C₆₀
Al₂O₃ SiO₂-Ag MWCNTs PVP-Ag CeO₂ PVP-Ag TiO₂ C₆₀
SiO₂-Ag SWCNTs PMMA PVP-Ag nano-PS C₆₀ MWCNTs PFOS micro-PE
PCBs SiO₂-Ag PVP-Ag C₆₀ PMMA MWCNTs CeO₂ micro-PE CeO₂ Al₂O₃
MWCNTs C₆₀ PVP-Ag nano-PS MWCNTs MWCNTs MWCNTs
micro-PE PCBs MWCNTs CeO₂ nano-PS CeO₂ ZrO₂ PVP-Ag TiO₂ PFOS
nano-PS Al₂O₃ CeO₂ PCBs CeO₂ CeO₂ C₆₀ PMMA MWCNTs
SWCNTs PCBs PFOS MWCNTs nano-PS SWCNTs nano-PS MWCNTs
SiO₂-Ag ZrO₂ C₆₀ MWCNTs ZrO₂ micro-PE SiO₂-Ag PMMA
C₆₀ PCBs SiO₂-Ag PFOS SiO₂-Ag PMMA Al₂O₃ MWCNTs ZrO₂
ZrO₂ TiO₂ PCBs SiO₂-Ag PVP-Ag PVP-Ag PCBs TiO₂ C₆₀
MWCNTs TiO₂ MWCNTs TiO₂ MWCNTs ZrO₂ C₆₀ PMMA
CeO₂ MWCNTs PCBs SWCNTs ZrO₂ SWCNTs micro-PE SiO₂-Ag MWCNTs
micro-PE SiO₂-Ag nano-PS PFOS CeO₂ C₆₀ PFOS PMMA PVP-Ag
MWCNTs Al₂O₃ PFOS PVP-Ag SWCNTs PMMA TiO₂ CeO₂
TiO₂ PCBs micro-PE Al₂O₃ PFOS ZrO₂ C₆₀ SWCNTs PMMA nano-PS

Summary

The production and use of engineered nanoparticles (ENPs) is growing, which causes extended emissions into the environment. This thesis focuses on the implications of ENPs in the aquatic environment, emphasising the sediment, because ENPs are primarily expected to end up in aquatic sediments. ENPs can have direct effects on species in the aquatic environment, indirect effects on the community level and/or food web and effects on the fate and risks of other chemicals. To identify the risks of ENPs, not only information about the hazard, i.e. the potential for an effect, but also about the potential for exposure is needed. In this thesis (a) fate processes of ENPs in natural waters, i.e. sedimentation and aggregation, (b) sorption of polychlorinated biphenyls (PCBs) and perfluorooctane sulfonate (PFOS) to ENPs and (c) effects of ENPs on single species and a benthic community were studied. This information was used for calculation of the retention of ENPs and associated contaminants in lakes and for an evaluation of the expected risks based on these insights.

To study fate processes of ENPs quiescent settling was measured in filtered and unfiltered water to determine sedimentation rates and heteroaggregation rates for ENPs with natural colloids (NC) (**Chapter 2**). These experiments were performed with 4 different ENPs (i.e. CeO₂, PVP-Ag, SiO₂-Ag and C₆₀) in 6 different natural waters including a coastal sea, tidal water, river, small stream, lake and a small acid pond. Sedimentation rates ranged from 0.0001 m d⁻¹ for SiO₂-Ag to 0.14 m d⁻¹ for C₆₀. The determination of heteroaggregation rates was based on a simplified Smoluchowski-Stokes equation and ranged from 0.007 to 0.6 L mg⁻¹ d⁻¹, with the highest values observed in seawater. Besides the quiescent settling experiments, also experiments under turbulent conditions in the presence of sediment were performed (**Chapter 3**). These experiments were performed with 3 different ENPs (i.e. CeO₂, PVP-Ag and SiO₂-Ag) in natural coastal seawater, brackish tidal water and fresh water from a river. Sedimentation rates ranged from 0.14 m d⁻¹ to 0.50 m d⁻¹ and were one to two orders of magnitude higher than in quiescent systems with NC. Heteroaggregation rates ranged between 0.151 and 0.547 L mg⁻¹ d⁻¹, which is up to 29 times higher than in quiescent systems with NC. The scavenging and settling of resuspended sediment was dominant for the settling of ENPs, resulting in minor variation in sedimentation rates among ENP type, salinity and aging time.

To study sorption behaviour of perfluorooctane sulfonate (PFOS), the effects of pH, Ca²⁺ concentration and aqueous PFOS concentration on the sorption of PFOS to sediment and to multiwalled carbon nanotubes (MWCNT) present in the sediment were determined (**Chapter 4**). Log K_d values for PFOS to MWCNTs were relatively low, i.e. 1.92 – 2.90 L kg⁻¹, because sediment organic matter (OM) fouling affected the interactions between PFOS and MWCNTs.

The sorption of 17 polychlorinated biphenyls (PCBs) to 10-180 μm polyethylene (micro-PE), 70 nm polystyrene (nano-PS), MWCNTs, C₆₀ and a natural sediment was studied (**Chapter 5**). Isotherms in fresh- and seawater with and without

the presence of sediment were measured to assess the effects of salinity and sediment organic matter on sorption. PCB sorption to sediment OM and micro-PE was linear, whereas sorption to nano-PS and MWCNTs was non-linear. Sorption to the latter sorbents and to C_{60} was much stronger than to OM and micro-PE. Especially for MWCNTs, presence of sediment reduced sorption, because of fouling with dissolved organic matter (DOM). Sorption of PCBs to sediment and MWCNTs decreased with increasing salinity, whereas it increased for micro-PE and nano-PS, suggesting a different influence on smooth polymer-based particles compared to heterogeneous surfaces of sediment and MWCNT aggregates.

Several standard ecotoxicity tests were performed for 7 types of ENPs i.e. TiO_2 , ZrO_2 , Al_2O_3 , CeO_2 , C_{60} , single-walled carbon nanotubes (SWCNTs) and polymethylmethacrylate (PMMA) (**Chapter 6**). Nominal concentration of up to 100 mg L^{-1} did not show any considerable effect. The rapid aggregation resulted in low free ENP concentrations, which explained that no effects were observed. Because ENPs are colloids, it was suggested that approaches based on the concepts of colloid chemistry should be applied instead of the bioavailability concepts used for convention chemicals.

For better ecological realism, a long term field experiment was performed to study the effects of MWCNT contaminated sediment on the recolonization of natural benthic macroinvertebrate communities (**Chapter 7 and 8**). The results after 3 months of exposure, showed no adverse effects up to 2 g kg^{-1} MWCNTs in the sediment (**Chapter 7**). After longer exposure however (**Chapter 8**) significant effects were observed already at the lowest dose of 0.002 g kg^{-1} , suggesting that in the long term MWCNTs can affect the composition of natural benthic communities at much lower concentrations than those detected using shorter term single species toxicity tests. A parallel experiment performed with activated carbon (AC) observed similar effects, but AC was applied at a 50 times higher maximum dose, suggesting that the benthic community was more sensitive to MWCNTs than to AC.

Several implications of ENPs for the aquatic environment were identified (**Chapter 9**). The sedimentation and heteroaggregation rates of ENPs in presence of NC and SS in different natural waters were used to estimate the retention of ENPs in lakes. Lakes with a high Inverse Areal Hydraulic Loading (IAHL; d m^{-1}), i.e. tendency for sedimentation, showed a higher retention for ENP. The data for PCB and PFOS sorption to the carbon-based ENPs were used to estimate the retention of PCBs and PFOS due to ENPs. This contribution of ENPs on the retention of these chemicals was shown to be generally negligible and will most likely not contribute to an increased risk. A summary of effect thresholds (PNEC) from single species toxicity tests was provided, which were compared with model-prediction based exposure concentrations (PEC). The resulting PEC/PNEC ratio was roughly estimated for 2125 ranging from $6.7 \cdot 10^{-6}$ for CNT to $3.2 \cdot 10^{-3}$ for Ag. Although this suggests that an actual potential risk for these ENPs is not expected in the near future, these results should be interpreted with care because of the large uncertainties in these PEC/PNEC ratios. Furthermore, the community study observed effects at much lower concentrations,

concentrations that can be considered environmentally relevant. It is recommended to further develop analytical methods, fate and exposure models and ecotoxicity tests for ENPs in the aquatic environment, with more emphasis on long term *in situ* effects on the community level.

Samenvatting

De productie en het gebruik van synthetische nanodeeltjes (ENPs) nemen toe en veroorzaken toenemende emissies naar het milieu. Dit proefschrift richt zich op de implicaties van ENPs in het aquatisch milieu, met de nadruk op het sediment, omdat er wordt verwacht dat ENPs hoofdzakelijk in het aquatisch sediment terecht zullen komen. ENPs kunnen directe effecten veroorzaken op organismen in het aquatisch milieu, indirecte effecten op het levensgemeenschap niveau en/of voedselweb en kunnen effecten op het gedrag en de risico's van andere contaminanten hebben. Om de risico's van ENPs vast te stellen, is niet alleen informatie nodig over het gevaar, oftewel de kans op een effect, maar ook over de kans op blootstelling. In dit proefschrift zijn (a) processen van het gedrag van ENPs in natuurlijk water, in dit geval sedimentatie en aggregatie, (b) sorptie van polychloorbifenylyls (PCBs) en perfluorocetaan sulfonaat (PFOS) aan ENPs en (c) effecten van ENPs op afzonderlijke soorten en een benthische levensgemeenschap bestudeerd. Deze informatie is gebruikt voor de berekening van de retentie van ENPs en hieraan gebonden contaminanten in meren en voor een evaluatie van de verwachte risico's gebaseerd op deze inzichten.

De gedragsprocessen van ENPs zijn onderzocht door de bezinking in stagnant water in gefiltreerd en ongefiltreerd water te meten. De sedimentatie- en heteroaggregatiesnelheden voor ENPs met natuurlijke colloïden (NC) zijn hiermee bepaald (**Hoofdstuk 2**). Deze experimenten zijn uitgevoerd met 4 verschillende ENPs (CeO_2 , PVP-Ag, SiO_2 -Ag en C_{60}) in 6 verschillende natuurlijke watertypes waaronder een zeewater, estuarien (brak) water, rivierwater, een beek, een meer en een kleine plas. Sedimentatiesnelheden varieerden van 0.0001 m d^{-1} voor SiO_2 -Ag tot 0.14 m d^{-1} voor C_{60} . De berekening van de heteroaggregatiesnelheden zijn gebaseerd op een vereenvoudigde Smoluchowski-Stokes formule en varieerde van 0.007 tot $0.6 \text{ L mg}^{-1} \text{ d}^{-1}$, met de hoogste waarden voor zeewater. Naast de experimenten met stilstaand water zijn er ook experimenten onder turbulente omstandigheden uitgevoerd in aanwezigheid van sediment (**Hoofdstuk 3**). Deze experimenten zijn uitgevoerd met 3 verschillende ENPs (CeO_2 , PVP-Ag en SiO_2 -Ag) in zeewater, estuarien (brak) water en zoet water afkomstig van een rivier. De sedimentatiesnelheden varieerden van 0.14 m d^{-1} tot 0.50 m d^{-1} en waren één tot twee ordes van grootte hoger dan in de stilstaande systemen met NC. Heteroaggregatie snelheden varieerden tussen 0.151 en $0.547 \text{ L mg}^{-1} \text{ d}^{-1}$, hetgeen tot 29 keer hoger was dan in de stilstaande systemen met NC. De bezinking van geresuspendeerd sediment was dominant voor de bezinking van ENPs, omdat de ENPs met het sediment mee uit het water werden verwijderd. Dit resulteerde in geringe variatie in sedimentatie snelheden tussen de ENP types, zoutgehalte en duur van de blootstelling.

Voor het onderzoek naar het sorptie gedrag van perfluorocetaan sulfonaat (PFOS), zijn de effecten bepaald van pH, Ca^{2+} concentratie en de PFOS concentratie in water op de sorptie van PFOS aan sediment en 'multiwalled' koolstof nanobuisjes (MWCNTs) aanwezig in het sediment (**Hoofdstuk 4**). $\log K_d$ waarden voor PFOS

aan MWCNTs waren relatief laag met $1.92 - 2.90 \text{ L kg}^{-1}$, omdat het organisch materiaal (OM) afkomstig van het sediment de interacties tussen PFOS en MWCNTs beïnvloedde.

De sorptie van 17 polychloorbifenylen (PCBs) aan 10-180 μm polyethyleen (micro-PE), 70 nm polystyreen (nano-PS), MWCNTs, C_{60} en een natuurlijk sediment was onderzocht (**Hoofdstuk 5**). Isothermen in zoet en zout water met en zonder de aanwezigheid van sediment zijn gemeten om het effect van zoutgehalte en sediment OM op de sorptie te bepalen. PCB sorptie aan sediment OM en micro-PE was lineair, terwijl de sorptie aan nano-PS en MWCNTs niet lineair was. Sorptie aan de laatste twee materialen en aan C_{60} was veel sterker dan aan OM en micro-PE. Vooral voor MWCNTs zorgde de aanwezigheid van sediment voor een verminderde sorptie vanwege de vervuiling van MWCNTs met opgelost organisch materiaal (DOM). De sorptie van PCBs aan sediment en MWCNTs nam af bij toenemende saliniteit, terwijl het toenam bij micro-PE en nano-PS. Dit suggereert dat de invloed op gladde polymeer deeltjes anders is vergeleken met de heterogene oppervlakken van sediment en MWCNT aggregaten.

Verschillende standaard ecotoxiciteitstesten zijn uitgevoerd voor 7 typen ENPs, namelijk TiO_2 , ZrO_2 , Al_2O_3 , CeO_2 , C_{60} , 'single walled' koolstof nanobuisjes (SWCNTs) en polymethylmethacrylaat (PMMA) (**Hoofdstuk 6**). Nominale concentraties tot 100 mg L^{-1} vertoonden geen noemenswaardige effecten. De snelle aggregatie resulteerde in lage vrije ENP concentraties waardoor geen effecten zijn waargenomen. Omdat ENPs colloïden zijn, is voorgesteld dat benaderingen gebaseerd op de concepten van de colloïd chemie zouden moeten worden toegepast in plaats van de concepten van biobeschikbaarheid die gebruikt worden voor conventionele contaminanten.

Voor een realistischere ecologische beeld, is een lange termijn veld experiment uitgevoerd om de effecten te bepalen van MWCNT gecontamineerd sediment op de rekolonisatie van een natuurlijke benthische macroinvertebraten levensgemeenschap (**Hoofdstuk 7 en 8**). Een blootstelling van 3 maanden liet geen nadelige effecten zien bij concentraties tot 2 g kg^{-1} MWCNTs in het sediment (**Hoofdstuk 7**). Na langere blootstelling (**Hoofdstuk 8**) zijn wel significante effecten waargenomen, al bij de laagste dosis van 0.002 g kg^{-1} . Dit geeft aan dat MWCNTs op lange termijn de samenstelling van natuurlijke bentische levensgemeenschappen kunnen beïnvloeden bij veel lagere concentraties dan die bij korte termijn bioassays voor soorten apart. Een parallel experiment, uitgevoerd met actieve kool (AC) liet vergelijkbare effecten zien, maar AC was toegepast bij een 50 keer hogere maximum dosis wat aangeeft dat de benthische levensgemeenschap veel gevoeliger was voor MWCNTs dan voor AC.

Verschillende implicaties van ENPs voor het aquatische milieu zijn geïdentificeerd (**Hoofdstuk 9**). De sedimentatie- en heteroaggregatiesnelheden van ENPs in aanwezigheid van NC en SS in verschillende natuurlijke wateren zijn gebruikt voor de bepaling van de retentie van ENPs in meren. Meren met een hoge 'inverse areal hydraulic loading' (IAHL; d m^{-1}), oftewel de neiging tot sedimentatie, vertonen een hogere retentie voor ENPs. De data van de PCB en PFOS sorptie aan de

koolstof gebaseerde ENPs zijn gebruikt voor de bepaling van de retentie van PCBs en PFOS veroorzaakt door de ENPs. Deze bijdrage van ENPs aan de retentie van deze stoffen was over het algemeen verwaarloosbaar en zal waarschijnlijk niet bijdragen aan een toenemend risico. Een samenvatting van de effect drempels (PNEC) van de single species toxiciteitstesten is weergegeven en de waarden zijn vergeleken met model voorspellingen die gebaseerd zijn op de blootstelling concentraties (PEC). De resulterende PEC/PNEC ratio was globaal geschat voor 2125 en varieerde van $6.7 \cdot 10^{-6}$ voor CNT tot $3.2 \cdot 10^{-3}$ voor Ag. Hoewel dit veronderstelt dat een werkelijk potentieel risico voor die ENPs niet wordt verwacht in de nabije toekomst, moeten deze resultaten zorgvuldig worden geïnterpreteerd vanwege de grote onzekerheden in de PEC/PNEC ratio's. Verder heeft de levensgemeenschap studie effecten waargenomen bij veel lagere concentraties, concentraties die kunnen worden beschouwd als milieu relevant. Een verdere ontwikkeling van analytische methoden, gedrags- en blootstellingsmodellen en ecotoxiciteitstesten voor ENPs in het aquatisch milieu wordt aanbevolen, met meer nadruk op lange termijn *in situ* effecten op het niveau van de levensgemeenschap.

Dankwoord

Met het schrijven van dit dankwoord komt er dan echt een einde aan dit promotie traject. Voor dat ik begon, had ik nooit gedacht dat ik zelf zou promoveren. Ik wilde iets praktisch doen, lekker bezig zijn in het lab, dus met veel plezier het HLO afgerond. Tijdens mijn stage op Texel, mocht ik onderzoek doen voor Micha, die toen AIO was (Micha, dank je wel dat ik via jouw onderzoek kennis heb mogen maken met de wetenschap). Toen ik na het HLO aan het werk wilde, bleek dat ik niet zomaar onderzoek mocht doen, de meeste baantjes waren routinebaantjes, dus toch maar naar de universiteit. Met een Bachelor thesis over nanodeeltjes en ervaring in het lab, mocht ik van Dik wel stage lopen bij het RIVM (Dik, heel erg bedankt voor deze kans). Toen daaruit een AIO plek ontstond, heb ik daar wel op gesolliciteerd, niet omdat ik zo graag wilde promoveren, maar omdat ik dan verder kon met 'mijn' onderzoek. Ze kozen voor Joris, maar gelukkig heb ik wel met hem samen mogen werken en mocht ik zijn paranimf zijn en is hij nu zelfs mijn paranimf. Via een open sollicitatie mocht ik bij John op gesprek komen. Zo ben ik bij Imares terechtgekomen als junior onderzoeker / projectleider. Na anderhalf jaar stelde Bart voor om te gaan promoveren. Zo kon ik alsnog verder met 'mijn' nano-onderzoek. Het was een inspirerende tijd, waarin ik allerlei nieuwe ervaringen heb opgedaan en héél veel heb geleerd. Het was soms zwaar, maar ook héél leuk.

Terugkijkend op deze periode zijn er heel veel mensen die op een of andere manier hebben bijgedragen aan dit proefschrift, die ik allemaal wil bedanken, een aantal zal ik hieronder in het bijzonder bedanken.

Allereerst wil ik mijn promotor Bart Koelmans bedanken. Bart, dank je wel voor de kans die je me gaf om te promoveren en voor je vertrouwen in mij. Je bent een geweldige promotor, die resultaat (= publicatie) gericht denkt en van al mijn twijfels en onzekerheden iets positiefs wist te maken. Het was en is nog steeds erg prettig samenwerken, je maakt altijd tijd om te helpen en reageert direct op je mail. Ik heb heel veel van je geleerd.

Zonder het Chemisch lab van Imares had ik het ook niet gekund, bedankt voor al jullie steun. Marion, mijn kamergenote vanaf het begin, jij hebt al mijn frustraties, maar ook successen meegemaakt, dank je wel voor al je steun. Michiel, fijn dat je altijd naar mijn presentaties wilde kijken en ook altijd nuttige tips had. Ook heel erg bedankt dat je mijn synthese wilde lezen en altijd in was om te sparren over nieuwe ideeën. Christiaan, jij was degene waar ik altijd terecht kon over praktische lab zaken over hoe ik het nu weer eens aan zou kunnen pakken. Het maakt niet uit waar het over gaat, je hebt er altijd wel een idee over. Ook heel fijn dat jij nu mijn paranimf wil zijn. Maadjieda, dank je wel voor al jouw hulp op het lab met de PFC's en PAK's en met bestellingen en je gezelligheid. Evert, bedankt voor al je hulp met LIMS en al die andere praktische zaken. Marco, bedankt voor je hulp op het lab en dat je zo je best hebt gedaan om me bij Imares te houden. Quy, bedankt voor je hulp op het lab

met o.a. de ASE en de GC-MS. Gerda, fijn dat jij het projectmanagement van IMAGE van mij overnam en leuk dat je nu met EU-projecten bezig mag zijn. Philip, je werkt niet meer bij Imares, maar ik wil jou ook bedanken voor al je hulp in het lab met o.a. droge stof bepalingen en ons boottochtje naar het Wolderwijd. Judith, ook jij werkt niet meer bij Imares, maar van jou heb ik ook veel geleerd over o.a. de GC-MS en GPC, bedankt daarvoor. John, ik wil jou bedanken voor de kans die je me gaf door mij in 2007 aan te nemen, voor het vertrouwen dat je al die jaren in mij had, je adviezen, dat je me introduceerde bij de sectie MCT en voor je mooie woorden tijdens mijn afscheidsborrel.

Naast alle steun van het Chemisch lab, was er ook nog een afdeling Milieu in Den Helder, met hele fijne collega's waar ik vóór en tijdens mijn promotie mee heb samen mogen werken, zoals Edwin, Diana, Pepijn, Klaas, Andrea, Jacqueline, Sander, Jan-Tjalling, maar ook de rest in Den Helder, bedankt allemaal. Dan zijn er ook nog al die andere collega's bij Imares, waar ik mee heb mogen samenwerken, zoals de OR, de Imares AIO's, de organisatie van de personeelsdagen en de Imares PhD dag en via projecten van de afdeling Visserij en Vis, teveel om allemaal persoonlijk te noemen, maar ook jullie bedankt voor alles wat ik van jullie heb geleerd en de fijne tijd die ik bij Imares heb gehad.

Ook was ik geregeld in Wageningen, bij de afdeling AEW, waar ook iedereen altijd bereid was te helpen. John, Frits, Wendy, Edwin en Erik, bedankt voor al jullie hulp bij de experimenten. Door jullie wist ik mijn weg te vinden in Wageningen.

Darya, jou wil ik ook speciaal bedanken (in het Nederlands, want dat begrijp je ook wel), het was leuk om met jou de community experimenten te kunnen doen, dat heeft mooie resultaten opgeleverd, bedankt voor deze mooie samenwerking. Ook bedankt voor je gastvrijheid, ik mocht altijd bij je slapen als ik in Wageningen moest zijn.

Joris, ik wil jou bedanken voor de samenwerking tijdens de sedimentatie experimenten en de mogelijkheden die ik daardoor bij het RIVM heb gehad. Het was heel fijn dat we ondanks dat jij de AIO plaats bij het RIVM had gekregen, toch leuke experimenten samen hebben kunnen doen, die ook erg mooie resultaten hebben opgeleverd. Extra leuk was dat onze samenwerking kon worden voortgezet toen je in Wageningen als postdoc verder mocht gaan met nano en heel fijn dat jij nu mijn paranimf wil zijn.

Dik, Jan en Ad, bedankt dat jullie mij de kansen gaven om al in 2006 kennis te mogen maken met nanodeeltjes, wat uiteindelijk heeft geleid tot mijn eerste nanopaper.

Rachel, jij heel erg bedankt voor het ontwerp en de lay-out van dit proefschrift.

Naast werken was er ook nog tijd om leuke dingen te doen (en te organiseren) met familie en vrienden, zoals weekendjes weg met de familie en met de "gang" en al die activiteiten met Stella Maris en RA13 en zelfs een buurtfeest. Bedankt voor jullie interesse en steun, zodat ik weer vol energie met het 'nano-onderzoek' verder kon.

Vooral in de laatste periode was het erg fijn dat Mama, Hans en Hermien (mijn lieve schoonouders) op Juno konden passen zodat ik nog even hard kon werken aan de laatste lootjes. Papa, jij ook bedankt voor je vertrouwen, ook al ben je nu in Sierra Leone en mis ik je enorm, ik weet dat je trots op me bent. Hans, ik wil je ook nog bedanken voor je inspiratie voor mijn laatste stelling. Als laatste wil ik mijn man Mathijs bedanken dat hij dit avontuur met mij aandurfde en voor zijn eindeloze geduld en steun en voor het allermooiste dat we samen hebben gekregen, onze zoon Juno! Mathijs, zonder jou was dit allemaal nooit gelukt. Juno, met jou erbij is dit resultaat extra bijzonder.

Curriculum vitae

Ilona Velzeboer was born on February 8, 1981 in Eindhoven, the Netherlands. She grew up in Helmond, where she finished high school (VWO) at the “Dr. Knipperbergcollege” in 1999. She did a Bachelor on Chemistry at the Fontys Hogeschool in Eindhoven. For her Bachelor study, she did an internship at the Royal NIOZ (Texel) on the influence of light on the iron binding ligands in seawater, resulting in co-authorship of two peer-reviewed publications. She did her graduation internship at Fortimedix (Nuth) on the chemical background of the electrochemical polishing process of stainless steel. After working as a chemical analyst in the Elkerliek hospital in Helmond, she started the Masters Environmental Sciences at the Radboud University in Nijmegen. For her Master, she did an internship at the RIVM in Bilthoven on the fate and effects of nanoparticles in the environment, which was the beginning of her nano-research. She did her graduation internship at TNO in Apeldoorn on the possibilities for passive sampling of ultrafine dust and analysis with Scanning Electron Microscopy (SEM) with Energy Dispersive X-ray detector (EDX). After her graduation, she started at IMARES in IJmuiden as project leader/junior researcher. After one and a half year she got the chance to start her PhD research at the Aquatic Ecology and Water Quality Management Group of Wageningen University. This research on the implications on nanoparticles in the aquatic environment was conducted primarily at IMARES. She was also active as board member of the IMARES PhD Council (2011-2012) and the section MCT (Environmental Chemistry and Toxicology) of the KNCV and NVT (from 2010) and co-organized the IMARES PhD day in 2011 and the MCT symposium in 2013. From 2009 to 2011 she was also involved in the co-management council of IMARES. During her doctoral research, Ilona got married to her husband Mathijs and got a son named Juno. At the moment Ilona is working as a researcher chemical water quality at the Waterlaboratorium in Haarlem.

List of publications

Papers

- **Velzeboer, I.**; Quik, J.T.K.; van de Meent, D.; Koelmans, A.A., Rapid settling of nanoparticles due to heteroaggregation with suspended sediment. *Environmental Toxicology and Chemistry* **2014**, DOI: 10.1002/etc2611
- **Velzeboer, I.**; Kwadijk, C.J.A.F.; Koelmans, A.A., Strong sorption of PCBs to nanoplastics, microplastics, carbon nanotubes and fullerenes. *Environmental Science & Technology* **2014**, DOI: 10.1021/es40572v
- **Velzeboer, I.**; Peeters, E.; Koelmans, A. A., Multiwalled Carbon Nanotubes at Environmentally Relevant Concentrations Affect the Composition of Benthic Communities. *Environmental Science & Technology* **2013**, *47*, (13), 7475-7482.
- **Velzeboer, I.**; Kupryianchyk, D.; Peeters, E. T. H. M.; Koelmans, A. A., Community effects of carbon nanotubes in aquatic sediments. *Environment International* **2011**, *37*, (6), 1126-1130.
- **Velzeboer, I.**; Hendriks, A. J.; Ragas, A. M. J.; Van de Meent, D., Aquatic ecotoxicity tests of some nanomaterials. *Environmental Toxicology and Chemistry* **2008**, *27*, (9), 1942-1947.
- Koelmans, A. A., Quik, J.T.K., **Velzeboer, I.**, de Klein, J.J.M., Lake retention of manufactured nanoparticles. *Environmental Toxicology and Chemistry* **2014**, *in prep.*
- Koelmans, A. A.; Poot, A.; De Lange, H. J.; **Velzeboer, I.**; Harmsen, J.; van Noort, P. C. M., Estimation of In Situ Sediment-to-Water Fluxes of Polycyclic Aromatic Hydrocarbons, Polychlorobiphenyls and Polybrominated Diphenylethers. *Environmental Science & Technology* **2010**, *44*, (8), 3014-3020.
- Quik, J. T. K.; **Velzeboer, I.**; Wouterse, M.; Koelmans, A. A.; van de Meent, D., Heteroaggregation and sedimentation rates for nanomaterials in natural waters. *Water Research* **2014**, *48*, 269-279.
- Kwadijk, C. J. A. F.; **Velzeboer, I.**; Koelmans, A. A., Sorption of perfluorooctane sulfonate to carbon nanotubes in aquatic sediments. *Chemosphere* **2013**, *90*, (5), 1631-1636.

- Rijkenberg, M. J. A.; Gerringa, L. J. A.; **Velzeboer, I.**; Timmermans, K. R.; Buma, A. G. J.; de Baar, H. J. W., Iron-binding ligands in Dutch estuaries are not affected by UV induced photochemical degradation. *Marine Chemistry* **2006**, *100*, (1-2), 11-23.
- Rijkenberg, M. J. A.; Gerringa, L. J. A.; Carolus, V. E.; **Velzeboer, I.**; de Baar, H. J. W., Enhancement and inhibition of iron photoreduction by individual ligands in open ocean seawater. *Geochimica Et Cosmochimica Acta* **2006**, *70*, (11), 2790-2805.

Conference proceedings

- **Velzeboer, I.**; Kwadijk, C.J.A.F.; Koelmans, A.A., Strong sorption of PCBs to nanoplastics, microplastics, carbon nanotubes and fullerenes. In Abstract book, SETAC Europe, 24th annual meeting, 11-15 May 2014, Basel, Switzerland.
- **Velzeboer, I.**; Peeters, E.; Koelmans, A. A., Multiwalled Carbon Nanotubes at Environmentally Relevant Concentrations Affect the Composition of Benthic Communities. In Abstract book, SETAC Europe, 23th annual meeting, 13-16 May 2013, Glasgow, UK.
- **Velzeboer, I.**; Quik, J.T.K.; van de Meent, D.; Koelmans, A.A., Rapid settling of nanoparticles due to heteroaggregation with suspended sediment. In Abstract book, SETAC North America, 33th annual meeting, 12-15 November 2012, Long Beach, CA, USA.
- **Velzeboer, I.**; Koelmans, A. A., Extremely strong Sorption of PCBs to Fullerene C₆₀ seems not to be attenuated by Organic Matter Fouling – A Pilot Study. In 5th International Conference on the Environmental Effects of Nanoparticles and Nanomaterials, 23-26 July 2010, Clemson, SC, USA
- **Velzeboer, I.**; Kupryianchyk, D.; Peeters, E. T. H. M.; Koelmans, A. A., Community effects of carbon-based nanoparticles. In Abstract book, SETAC Europe, 20th annual meeting, 25-28 May 2010, Seville, Spain
- **Velzeboer, I.**; Hendriks, A. J.; Ragas, A. M. J.; Van de Meent, D., Aquatic ecotoxicity tests of some nanomaterials. In Abstract book, SETAC Europe, 16th annual meeting, 13-16 May 2006, the Hague, the Netherlands.



Netherlands Research School for the
Socio-Economic and Natural Sciences of the Environment

C E R T I F I C A T E

The Netherlands Research School for the
Socio-Economic and Natural Sciences of the Environment
(SENSE), declares that

Ilona Velzeboer

born on 8 February 1981 in Eindhoven, The Netherlands

has successfully fulfilled all requirements of the
Educational Programme of SENSE.

Wageningen, 18 June 2014

the Chairman of the SENSE board

Prof. dr. Rik Leemans

the SENSE Director of Education

Dr. Ad van Dommelen

The SENSE Research School has been accredited by the Royal Netherlands Academy of Arts and Sciences (KNAW)



K O N I N K L I J K E N E D E R L A N D S E
A K A D E M I E V A N W E T E N S C H A P P E N



The SENSE Research School declares that **Ms. Ilona Velzeboer** has successfully fulfilled all requirements of the Educational PhD Programme of SENSE with a work load of 52 ECTS, including the following activities:

SENSE PhD Courses

- Speciation and Bioavailability (2010)
- Environmental Research in Context (2010)
- Environmental Risk Assessment of Chemicals (2010)
- Research Context Activity: Organizing Imares PhD day: 'Bottom-Up: life from small > big > ecology > society' (25 November 2011)
- Basic Statistics (2012)

Other PhD Courses

- Modelling comparative risk of toxics on humans and ecosystems (2008)
- Nanoparticles: Characterization and Environmental Risk Assessment (2009)
- PhD Competence Assessment (2009)
- Presentation Skills (2012)

Management and Didactic Skills Training

- Teaching and Supervising Thesis Students Course (2009)
- Member co-management council Imares (2009-2011)
- Supervision internship student Chemistry (HBO) (2010-2011)
- Boardmember section MilieuChemTox (KNCV/NVT) (2010-present)
- Member Imares PhD council (2011-2012)
- Co-organising MilieuChemTox Symposium 2013: Think BIG, Act NANO (2013)

Oral Presentations

- *Settling of nanomaterials in dynamic sediment-water systems.* nanoSENSE workshop, 27 October 2011, Amsterdam, Netherlands
- *Fate of nanoparticles in natural water systems.* Imares PhD day, 25 November 2011, Texel, Netherlands
- *Rapid settling of nanoparticles: heteroaggregation with suspended sediment.* SETAC North America, 12-15 November 2012, Longbeach, United States
- *Multiwalled carbon nanotubes at environmentally relevant concentrations affect the composition of benthic communities.* SETAC Europe, 13-16 May 2013, Glasgow, United Kingdom
- *Strong sorption of PCBs to carbon nanotubes, fullerenes, nanoplastics and microplastics. Effects of salinity and sediment organic matter.* SETAC Europe, 15-11 May 2014, Basel, Switzerland

SENSE Coordinator PhD Education

Dr. ing. Monique Gulickx

Colofon

Graphic design cover and inside:

Rachel van Esschoten, DivingDuck Design (www.divingduckdesign.nl)

Photography:

Photo's cover: iStock (www.istockphoto.com)

Printed by:

CPI Koninklijke Wöhrmann, Zutphen (www.wps.nl)

Financial support from Wageningen University and IMARES for printing this thesis is gratefully acknowledged.